

## **INFORMATION TO USERS**

**This manuscript has been reproduced from the microfilm master. UMI films the text directly from the original or copy submitted. Thus, some thesis and dissertation copies are in typewriter face, while others may be from any type of computer printer.**

**The quality of this reproduction is dependent upon the quality of the copy submitted. Broken or indistinct print, colored or poor quality illustrations and photographs, print bleedthrough, substandard margins, and improper alignment can adversely affect reproduction.**

**In the unlikely event that the author did not send UMI a complete manuscript and there are missing pages, these will be noted. Also, if unauthorized copyright material had to be removed, a note will indicate the deletion.**

**Oversize materials (e.g., maps, drawings, charts) are reproduced by sectioning the original, beginning at the upper left-hand corner and continuing from left to right in equal sections with small overlaps. Each original is also photographed in one exposure and is included in reduced form at the back of the book.**

**Photographs included in the original manuscript have been reproduced xerographically in this copy. Higher quality 6" x 9" black and white photographic prints are available for any photographs or illustrations appearing in this copy for an additional charge. Contact UMI directly to order.**

# **UMI**

**A Bell & Howell Information Company  
300 North Zeeb Road, Ann Arbor MI 48106-1346 USA  
313/761-4700 800/521-0600**



**University of Alberta**

**The Organometallic Chemistry of Heterobinuclear  
Complexes of Group 8 and Group 9 Metals**

by

**Brian Thomas Sterenberg**



**A thesis submitted to the Faculty of Graduate Studies and Research in partial fulfillment  
of the requirements for the degree of Doctor of Philosophy**

**Department of Chemistry**

**Edmonton, Alberta  
Fall, 1997**



National Library  
of Canada

Acquisitions and  
Bibliographic Services

395 Wellington Street  
Ottawa ON K1A 0N4  
Canada

Bibliothèque nationale  
du Canada

Acquisitions et  
services bibliographiques

395, rue Wellington  
Ottawa ON K1A 0N4  
Canada

*Your file Votre référence*

*Our file Notre référence*

The author has granted a non-exclusive licence allowing the National Library of Canada to reproduce, loan, distribute or sell copies of this thesis in microform, paper or electronic formats.

The author retains ownership of the copyright in this thesis. Neither the thesis nor substantial extracts from it may be printed or otherwise reproduced without the author's permission.

L'auteur a accordé une licence non exclusive permettant à la Bibliothèque nationale du Canada de reproduire, prêter, distribuer ou vendre des copies de cette thèse sous la forme de microfiche/film, de reproduction sur papier ou sur format électronique.

L'auteur conserve la propriété du droit d'auteur qui protège cette thèse. Ni la thèse ni des extraits substantiels de celle-ci ne doivent être imprimés ou autrement reproduits sans son autorisation.

0-612-23074-0

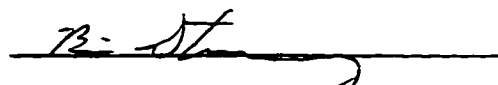
**University of Alberta**

**Library Release Form**

**Name of Author:** Brian Thomas Sterenberg  
**Title of Thesis:** The Organometallic Chemistry of Heterobinuclear  
Complexes of Group 8 and Group 9 Metals  
**Degree:** Doctor of Philosophy  
**Year Degree Granted:** 1997

Permission is hereby granted to the University of Alberta Library to reproduce single copies of this thesis and to lend or sell such copies for private, scholarly, or scientific research purposes only.

The author reserves all other publication and other rights in association with the copyright in the thesis, and except as hereinbefore provided, neither the thesis nor any substantial portion thereof may be printed or otherwise reproduced in any material form whatever without the author's prior written permission.

  
\_\_\_\_\_  
**Brian Thomas Sterenberg**

2670 Princeton Road RR4  
Duncan, British Columbia  
V5L 3W8

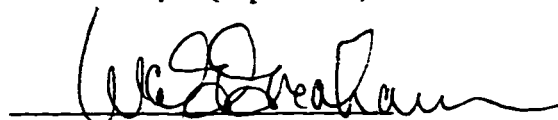
Date 28 May, 1997

**University of Alberta**

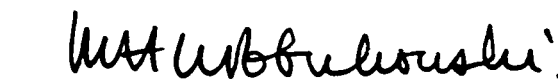
**Faculty of Graduate Studies and Research**

The undersigned certify that they have read, and recommend to the Faculty of Graduate Studies and Research for acceptance, a thesis entitled **The Organometallic Chemistry of Heterobinuclear Complexes of Group 8 and Group 9 Metals** submitted by Brian Thomas Sterenberg in partial fulfillment of the requirements for the degree of Doctor of Philosophy

  
M. Cowie (supervisor)

  
W. A. G. Graham

  
S. H. Bergens

  
M. A. Klobukowski

  
M. C. Williams

  
J. R. Norton  
(external examiner)

Date 27 May, 1997

## Abstract

Heterobinuclear RhOs complexes of the form  $[\text{RhOsR}(\text{CO})_3(\text{dppm})_2]$  ( $\text{R} = \text{CH}_3$ ,  $\text{CH}_2\text{CN}$ ,  $\text{C}\equiv\text{CH}$ ), have been prepared. In all of the compounds, the organic fragment is terminally bound to the Rh, while three carbonyls are bound to Os, one of which forms a semibridging interaction to Rh. Compounds **8** ( $\text{R} = \text{CH}_2\text{CN}$ ) and **11** ( $\text{R} = \text{CH}_3$ ) have been structurally characterized by X-ray crystallography. Upon protonation, **11** yields  $[\text{RhOs}(\text{CO})_3(\mu\text{-H})-(\mu^2\text{-}\eta^3\text{-}(o\text{-C}_6\text{H}_4)\text{PhPCH}_2\text{PPh}_2)(\text{dppm})]^\dagger$  (**14**) via methane loss and orthometallation at Os, while methylation of **11** yields  $[\text{RhOs}(\text{CH}_3)_2(\text{CO})_3(\text{dppm})_2]^\dagger$  (**17**). If the protonation reaction is carried out at  $-80^\circ\text{C}$  and slowly warmed, three hydrido methyl intermediates are observed at different temperatures, yielding information about the rearrangements leading to reductive elimination from these heterobinuclear species, which appears to occur from the Os center.

Reaction of the hydride complex  $[\text{RhOs}(\text{H})(\text{CO})_3(\text{dppm})_2]$  (**1**) with alkynes and allenes yields compounds of the form  $[\text{RhOs}(\text{R})(\text{CO})_3(\text{dppm})_2]$  ( $\text{R} = \text{C}(\text{CH}_3)=\text{CH}_2$ ), **18**;  $\text{R} = \text{C}(\text{CH}_3)=\text{C}(\text{CH}_3)_2$ ), **20**;  $\text{R} = \text{C}(\text{CO}_2\text{Me})=\text{C}(\text{H})\text{CO}_2\text{Me}$ ), **21**). Compound **18** has been structurally characterized. The  $\eta^3$ -allyl complex  $[\text{RhOs}(\eta^3\text{-C}_3\text{H}_5)(\text{CO})_3(\text{dppm})_2]$  (**19**) was formed as a minor product in the allene reaction and in addition was independently synthesized. Reaction of **18** with CO leads to the isopropenoyl complex  $[\text{RhOs}(\text{C}(\text{O})\text{C}(\text{CH}_3)=\text{CH}_2)(\text{CO})_3(\text{dppm})_2]$  (**23**). The vinyl compounds react with the electrophiles  $\text{CH}_3\text{SO}_3\text{CF}_3$  and  $\text{HBF}_4\cdot\text{Me}_2\text{O}$ , to form vinyl/alkyl and vinyl/hydride complexes of the form  $[\text{RhOs}(\text{R})(\text{R}')(\text{CO})_3(\text{dppm})_2]^\dagger$  ( $\text{R} = \text{alkenyl}$ ,  $\text{R}' = \text{CH}_3$ , H), of which compound **23** ( $\text{R} = \text{C}(\text{CH}_3)=\text{C}(\text{CH}_3)_2$ ,  $\text{R}' = \text{CH}_3$ ) has been structurally

characterized. Reductive elimination of alkenes occurs from the vinyl/hydride compounds under CO.

Reaction of  $[\text{RhOs}(\text{CO})_4(\text{dppm})_2]^+$  with excess  $\text{CH}_2\text{N}_2$  led to  $[\text{RhOs}(\eta^1\text{-CH}_2\text{CH}=\text{CH}_2)(\text{CH}_3)(\text{CO})_3(\text{dppm})_2]^+$  (**35**), which was independently synthesized by the reaction of **19** with methyl triflate. Carbene complexes of the form  $[\text{RhOs}(=\text{C}(\text{CH}_3)_2)(\text{R})(\text{CO})_3(\text{dppm})_2]^{2+}$  ( $\text{R} = \text{H}$ , **37**;  $\text{CH}_3$ , **38**) were formed via protonation of isopropenyl complexes, while protonation of the isopropenoyl complex **23** led to the carbene complex  $[\text{RhOs}(=\text{C}(\text{OH})(\text{C}(\text{CH}_3)=\text{CH}_2)(\text{CO})_3(\mu\text{-H})(\text{dppm})_2]^{2+}$  (**39**).

The RhRu methyl complexes  $[\text{RhRu}(\text{CH}_3)(\text{CO})_3(\text{dppm})_2]$  (**42**) and  $[\text{RhRu}(\text{CH}_3)_2(\text{CO})_3(\text{dppm})_2]^+$  (**44**) have been prepared and the latter has been structurally characterized. The dimethyl complex **44** reductively eliminates acetone in the presence of CO. Reaction of the RhRu hydride complex **40** with allene or dimethylallene leads to the allyl complexes  $[\text{RhRu}(\eta^3\text{-C}_3\text{H}_5)(\text{CO})_3(\text{dppm})_2]$  (**45**) and  $[\text{RhRu}(\eta^1\text{-CH}_2\text{CH}=\text{C}(\text{CH}_3)_2)(\text{CO})_3(\text{dppm})_2]$  (**46**), respectively.

## **Acknowledgments**

There are many people who deserve acknowledgment for their help over the years. Firstly, I would like to thank Dr. Marty Cowie, my supervisor, for all his assistance throughout my graduate career, for always being so cheerful, and for his superior taste in beer. It is a luxury to have a boss to whom you can always speak your mind. I'd also like to thank Gail Cowie, who also has good taste in beer but lousy taste in music, for her kind hospitality over the years. Next, I thank all the people currently serving time in the Cowie group, in particular, Todd for many bike repairs and for keeping a steady stream of women flowing through the lab, Darren for making me look stable and well adjusted, Jeff for always having a good supply of equipment for me to steal, and Steve, ahhh, I'll have to think about that one. Maybe eventually I'll come up with something for which to thank Steve. Just kidding. I thank Steve for taking endless abuse without ever turning violent. As well several past members of this group deserve thanks. First, all the other people involved with this project: Rob Hilts, the eternal optimist who started it all and taught me a lot of experimental chemistry; Giovanni Moro, who grew thin while he was away from his mother's pasta; Oliver the mad midnight cyclist; and Liz, who helped me with the carbene chemistry. Other former group members I must mention are Angela the crazy Spanish chick; Fred, the friendliest guy on the planet; and Li-Sheng the Chinese Californian.

There are many people in the department who were always friendly and helpful, and made this a great place to work. I wish to acknowledge the NMR staff, particularly Glen and Tom (thanks for fixing my computer, Tom); the spectral services and elemental analysis people; all the people in the general office, mail room and purchasing office,

especially Jeannette for many years of cheerful abuse; and Tony, without whom the department would fall to pieces.

I'd also like to thank Mike the supreme dictator of the universe for letting me be one of his cronies, Liz (wow, look Liz, you get mentioned twice!) for the X-files and for helping me relearn all my physics and calculus, Jeff Stryker for some great music and helpful chemistry discussions, Joe Takats for teaching me a lot about organometallic chemistry, Bob for being another computer geek (there is a distinct lack of them in this group) and for lots of help with crystallography, Anna Jordan for friendship and support, Judy, Colin, Aura, Jean Pearson (I think I've recovered from that ride now), and my family.

Finally, I want to thank some of the people and organizations that help to preserve my sanity and make life worth living. In no particular order: Leonard Cohen, Miles Davis, J. R. R. Tolkien, Rory McLeod, the Big Rock Brewery, Bill Bourne, John Prine, Ray Bradbury, Jasper National Park, NRBQ (who provided accompaniment for much of the final stages of writing this thing), D. Johnston & Co., Dumbarton and a myriad of other small Scottish distilleries, W. O. Mitchell, Bill Bruford, Fred Eaglesmith, Orson Scott Card, and many, many others that I haven't mentioned.

## **Table of Contents**

<b>Chapter 1 Introduction.....</b>	<b>1</b>
References.....	12
<b>Chapter 2 Hydrido, Alkyl, and Related Complexes of Rh/Os .....</b>	<b>18</b>
Introduction.....	18
Experimental Section .....	19
Preparation of the Compounds.....	20
X-Ray Data Collection.....	30
Structure Solution and Refinement.....	34
Results and Compound Characterization.....	35
(a) Mono-alkyl and Related Species.....	35
(b) Hydrido-Methyl Complexes and Reductive Elimination of CH <sub>4</sub> .....	57
Discussion.....	61
References.....	65
<b>Chapter 3 Vinyl, Allyl and Related Complexes of Rh/Os .....</b>	<b>69</b>
Introduction.....	69
Experimental Section .....	70
Preparation of the Compounds.....	70
Reactions.....	81

X-ray Data Collection.....	82
Structure Solution and Refinement.....	86
<b>Results and Compound Characterization.....</b>	<b>91</b>
(a) Preparation of Vinyl Complexes.....	91
(b) Reactivity of Vinyl Complexes.....	103
Discussion.....	120
References.....	129
<b>Chapter 4 Carbene Complexes of the Rh/Os System.....</b>	<b>134</b>
Introduction.....	134
Experimental Section.....	135
Preparation of Compounds.....	135
X-ray Data Collection.....	140
Structure Solution and Refinement.....	143
Results and Compound Characterization.....	144
Carbene complexes from Protonation Reactions.....	153
Discussion.....	157
References.....	164
<b>Chapter 5 Organometallic Chemistry of the Rh/Ru System.....</b>	<b>167</b>
Introduction.....	167
Experimental Section.....	168
Preparation of Compounds.....	168

<b>X-ray Data Collection</b> .....	173
<b>Structure Solution and Refinement</b> .....	175
<b>Results and Compound Characterization</b> .....	178
<b>(a) Preparation and Reactivity of methyl complexes</b> .....	178
<b>(b) Preparation and Reactivity of Allyl and Vinyl Complexes</b> .....	185
<b>Discussion</b> .....	189
<b>References</b> .....	194
<b>Chapter 6 Conclusions</b> .....	196
<b>References</b> .....	205

## List of Tables

### Chapter 2

<b>Table 2.1.</b> Spectroscopic Parameters for the Compounds.	21
<b>Table 2.2.</b> Crystallographic Experimental Details.	32
<b>Table 2.3.</b> Atomic Coordinates and Equivalent Isotropic Displacement Parameters for Selected Atoms of $[\text{RhOs}(\text{CH}_2\text{CN})(\text{CO})_3(\text{dppm})_2]$ ( <b>8</b> ).	36
<b>Table 2.4.</b> Atomic Coordinates and Equivalent Isotropic Displacement Parameters for Selected Atoms of $[\text{RhOs}(\text{CH}_3)(\text{CO})_3(\text{dppm})_2]$ ( <b>11</b> ).	37
<b>Table 2.5.</b> Selected Distances ( $\text{\AA}$ ) and Angles ( $^\circ$ ) in $[\text{RhOs}(\text{CH}_2\text{CN})(\text{CO})_3(\text{dppm})_2]$ ( <b>8</b> ).	48
<b>Table 2.6.</b> Selected Distances ( $\text{\AA}$ ) and Angles ( $^\circ$ ) in $[\text{OsRh}(\text{CO})_3(\text{CH}_3)(\text{dppm})_2]$ ( <b>11</b> ).	56

### Chapter 3

<b>Table 3.1.</b> Spectroscopic Parameters for the Compounds.	71
<b>Table 3.2.</b> Crystallographic Experimental Details.	83
<b>Table 3.3.</b> Atomic Coordinates and Equivalent Isotropic Displacement Parameters for the Core Atoms of Compound <b>17</b> .	92
<b>Table 3.4.</b> Atomic Coordinates and Equivalent Isotropic Displacement Parameters for the Core Atoms of Compound <b>23</b> .	92
<b>Table 3.5.</b> Selected Interatomic Distances ( $\text{\AA}$ ) and Angles ( $^\circ$ ) for Compound <b>17</b> .	102
<b>Table 3.6.</b> Selected Interatomic Distances ( $\text{\AA}$ ) and Angles ( $^\circ$ ) for Compound <b>23</b> .	110

## **Chapter 4**

<b>Table 4.1. Spectroscopic Parameters for the Compounds.</b>	136
<b>Table 4.2. Crystallographic Experimental Details.</b>	142
<b>Table 4.3 Atomic Coordinates and Equivalent Isotropic Displacement Parameters for the Core Atoms of Compound 33.</b>	145
<b>Table 4.4. Selected Interatomic Distances (Å) and angles (°) for compound 33.</b>	150

## **Chapter 5**

<b>Table 5.1. Spectroscopic Parameters for the Compounds.</b>	169
<b>Table 5.2. Crystallographic Experimental Details.</b>	174
<b>Table 5.3. Atomic Coordinates and Equivalent Isotropic Displacement Parameters for Inner-sphere Atoms of 44.</b>	177
<b>Table 5.4. Selected Interatomic Distances (Å) and Angles (°) for Compound 44.</b>	183

## List of Figures and Schemes

### Chapter 1

<b>Scheme 1.1</b>	5
<b>Scheme 1.2</b>	7

### Chapter 2

<b>Scheme 2.1</b>	38
<b>Figure 2.1.</b> $^{31}\text{P}\{^1\text{H}\}$ NMR spectra of $[\text{RhOs}(\text{CO})_4(\text{dppm})_2][\text{BF}_4]$ (2) and $[\text{RhOs}(\text{CO})_3(\mu\text{-OH})\text{-}(\mu\text{-H})(\text{dppm})_2][\text{BF}_4]$ (6).	41
<b>Scheme 2.2</b>	44
<b>Figure 2.2.</b> Perspective view of $[\text{RhOs}(\text{CH}_2\text{CN})(\text{CO})_3(\text{dppm})_2]$ (8).	47
<b>Figure 2.3.</b> $^{31}\text{P}\{^1\text{H}\}$ NMR spectrum of Compound 9.	51
<b>Figure 2.4.</b> Perspective view of $[\text{RhOs}(\text{CH}_3)(\text{CO})_3(\text{dppm})_2]$ (11).	54
<b>Scheme 2.3</b>	59

### Chapter 3

<b>Figure 3.1.</b> A view of the equatorial plane of compound 18 showing both disordered molecules.	88
<b>Figure 3.2.</b> A view of the equatorial plane of the cation of compound 24 showing the disorder of the two trimethylvinyl groups.	90
<b>Scheme 3.1</b>	94
<b>Scheme 3.2</b>	99
<b>Figure 3.3.</b> Perspective view of $[\text{RhOs}(\text{C}(\text{CH}_3)=\text{CH}_2)(\text{CO})_3(\text{dppm})_2]$ (18).	101

<b>Scheme 3.3</b>	106
<b>Figure 3.4.</b> Perspective view of $[\text{RhOs}(\text{C}(\text{CH}_3)=\text{C}(\text{CH}_3)_2(\text{CH}_3)(\text{CO})_3(\text{dppm})_2)]^+$ , the cation of compound <b>24</b> .	109
<b>Scheme 3.4</b>	115
<b>Scheme 3.5</b>	119
 <b>Chapter 4</b>	
<b>Scheme 4.1</b>	147
<b>Figure 4.1.</b> Perspective view of the $[\text{RhOs}(\eta^2\text{-N}(\text{O})\text{N}(\text{CH}_3)\text{C}(\text{NNO}_2)\text{NH})(\text{CO})_3(\mu\text{-H})(\text{dppm})_2]^+$ cation of compound <b>34</b> .	149
<b>Scheme 4.2</b>	156
<b>Scheme 4.3</b>	159
 <b>Chapter 5</b>	
<b>Scheme 5.1</b>	179
<b>Figure 5.1.</b> $^{31}\text{P}\{^1\text{H}\}$ NMR spectrum of compound <b>44</b> .	181
<b>Figure 5.2.</b> Perspective view of the cation of $[\text{RhRu}(\text{CH}_3)_2(\text{CO})_3(\text{dppm})_2][\text{CF}_3\text{SO}_3]$ ( <b>44</b> ).	182
<b>Scheme 5.2</b>	187

### **List of Abbreviations and Symbols**

<b>anal</b>	<b>analysis</b>
<b>approx.</b>	<b>approximately</b>
<b>ca.</b>	<b>circa (approximately)</b>
<b>calcd</b>	<b>calculated</b>
<b>DMAD</b>	<b>dimethylacetylenedicarboxylate</b>
<b>dppm</b>	<b>bis(diphenylphosphinomethane)</b>
<b>equiv</b>	<b>equivalent</b>
<b>Et</b>	<b>ethyl</b>
<b>h</b>	<b>hour(s)</b>
<b>IR</b>	<b>infrared</b>
<b>Me</b>	<b>methyl</b>
<b>MeOH</b>	<b>methanol</b>
<b>mg</b>	<b>milligrams</b>
<b>min</b>	<b>minute(s)</b>
<b>mL</b>	<b>millilitres</b>
<b>mmol</b>	<b>millimoles</b>
<b>MHz</b>	<b>megahertz</b>
<b>NMR</b>	<b>nuclear magnetic resonance</b>
<b>Ph</b>	<b>phenyl, C<sub>6</sub>H<sub>5</sub>-</b>
<b>THF</b>	<b>tetrahydrofuran</b>
<b><sup>t</sup>Bu</b>	<b>tertiary butyl</b>
<b>μL</b>	<b>microlitres</b>

## **Crystallographic Abbreviations and Symbols**

$a, b, c$	lengths of the x, y, and z axes, respectively, of the unit cell
$B$	isotropic thermal parameter
deg (or °)	degrees
$F_c$	calculated structure factor
$F_o$	observed structure factor
$GOF$	goodness of fit
$h, k, l$	Miller indices defining lattice planes, where the plane intersects the unit cell axes at $1/h, 1/k, 1/l$ of the respective lengths a, b, and c.
$p$	experimental instability factor (used in the calculation of $\sigma(I)$ to downweight intense reflections)
$R$	residual index (a measure of agreement between calculated and observed structure factors)
$R_w$	weighted residual index
$V$	unit cell volume
$w$	weighting factor applied to structure factor
$Z$	number of molecules per unit cell
$\text{Å}$	Angstrom(s) ( $1\text{Å} = 10^{-10}$ metres)
$\alpha, \beta, \chi$	angles between b and c, a and c, and a and b axes, respectively, of unit cell
$\beta_{ij}$	anisotropic displacement parameters
$\lambda$	wavelength
$\rho$	density
$\sigma$	standard deviation

## **Chapter 1**

### **Introduction**

Currently, one of the most active areas of organometallic chemistry is the study of polymetallic transition metal complexes.<sup>1</sup> Interest in this field stems from the possibility that metals, working in conjunction may show reactivity that is unique from that of mononuclear complexes. The interaction between the metals that results in the modified reactivity is generally referred to as metal-metal cooperativity.<sup>2</sup>

Two or more metals can work cooperatively in several different ways. They can act together to stabilize otherwise unstable fragments. Carbide ligands, for example, are unknown in mononuclear transition metal complexes, but can be stabilized in the presence of more than one metal, as evidenced by the many cluster complexes that contain this fragment.<sup>3</sup> Ligands can have bridged bonding modes in polymetallic complexes that are not available in mononuclear complexes, and these bridging modes can enhance the activation of certain fragments as compared to terminal binding. For example, activation of CO by metal clusters can result in CO bond cleavage, which appears to require coordination of both ends of the carbonyl.<sup>4</sup> Bridging modes can also change the type of reactivity displayed by a ligand,<sup>5</sup> as with methylene complexes, where terminal methylenes are generally strongly nucleophilic (in neutral complexes),<sup>6</sup> while bridged methylene complexes often show remarkable stability toward electrophiles.<sup>7</sup> Different functional groups of a molecule can be activated simultaneously by two or more different

metals. This is particularly important in the activation of polar molecules, and is the goal of many researchers working on early-late heterobimetallic complexes, where the disparate properties of the two metals are ideal for activation of polar substrates.<sup>8</sup> A coordinatively unsaturated metal adjacent to a saturated metal can enhance the reactivity at the saturated metal by providing a site for a ligand to enter the complex. In  $[\text{RhRe}(\text{CO})_4(\text{dppm})_2]$ , in which the unsaturated Rh centre is adjacent to the saturated Re, reaction with  $\text{H}_2$  occurs at  $-80^\circ$  with loss of a carbonyl.<sup>9</sup> In contrast, the dirhenium analogue  $[\text{Re}_2(\text{CO})_6(\text{dppm})_2]$ , containing two saturated metals must be heated to  $172^\circ$  before reaction with  $\text{H}_2$  occurs.<sup>10</sup> Alternately, a coordinatively unsaturated metal can be stabilized via interaction with a ligand on an adjacent metal through a bridging interaction, alleviating coordinative unsaturation at that metal. In general, an adjacent metal can act as a source of or a sink for molecular fragments,<sup>11</sup> and it has been suggested that polymetallic catalysts can use adjacent metals to store fragments needed in the catalytic cycle.<sup>11b</sup> The adjacent metal can also act as a source of or a sink for electrons,<sup>12</sup> an example of which has been described in the transformation of  $[\text{RhOs}(\text{I})(\text{CO})_3(\mu\text{-DMAD})(\text{dppm})_2]$  to  $[\text{RhOs}(\text{I})(\text{CO})_2(\mu\text{-DMAD})(\text{dppm})_2]$ , where the coordinative unsaturation created by the loss of a carbonyl from Os is alleviated by the formation of a dative  $\text{Rh}\rightarrow\text{Os}$  bond.<sup>13</sup>

Organo-transition metal chemistry plays an important role in elucidating the functions of transition metals in catalytic processes, and many of the key steps in these processes have been modeled in organometallic systems.<sup>14</sup> Our understanding of

heterogeneous catalysis, in particular, benefits from the use of homogeneous complexes as models because of the great difficulty of direct examination of the heterogeneous systems. Polymetallic model complexes are particularly appropriate for heterogeneous catalysis, and it has been suggested that an ensemble of metals surrounded by ligands in a polymetallic complex can serve as a model for a small part of the surface of a heterogeneous catalyst with coordinated ligands.<sup>15</sup> The presence of more than one metal in the model complex allows for the possibility of metal-metal cooperativity, resulting in chemistry that may be very different from that observed in the corresponding monometallic systems. Cooperativity between two or more metals on a surface may be an important factor in catalysis because of the close proximity of adjacent metals in such systems.<sup>16</sup> Although the vast majority of catalytic processes are heterogeneous, there have also been some spectacular successes in homogeneously catalyzed processes such as methanol carbonylation, olefin metathesis, and hydrogenations.<sup>17</sup> Increasingly researchers are looking for homogeneous applications involving multinuclear systems, and the processes which involve multiple metal centres are generally poorly understood, making polynuclear organometallic complexes potentially valuable as model systems for these processes.<sup>18</sup>

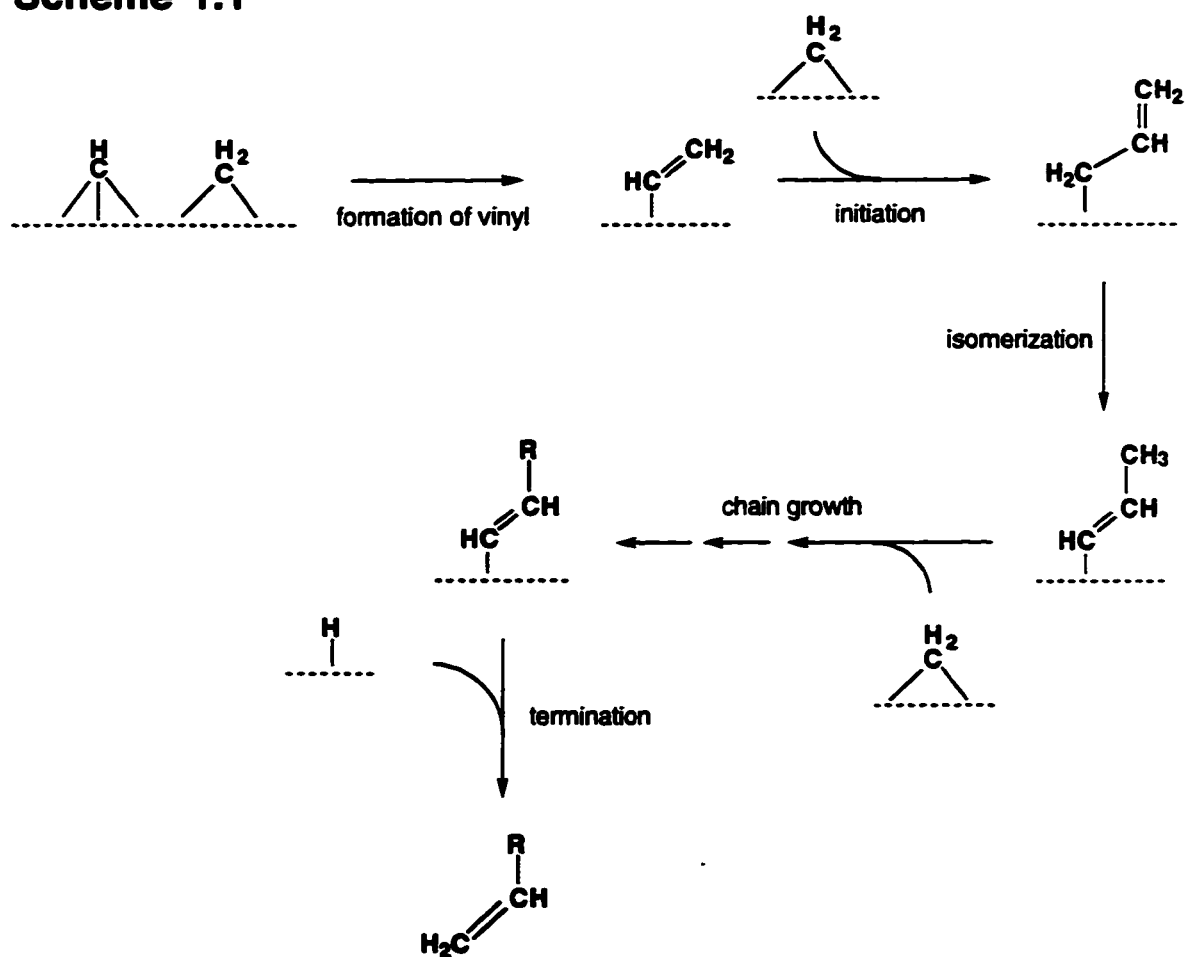
The Fischer-Tropsch reaction is a potentially important heterogeneously catalyzed reaction because it allows for the formation of valuable chemicals from inexpensive feedstocks.<sup>19</sup> In this reaction, CO and H<sub>2</sub> react in the presence of a catalyst to form long chain hydrocarbons and other organic products. The catalysts used in the Fischer-Tropsch process involve a wide range of transition metals, including Rh, Ru, Fe,

Zn/Cr, and Ni. As might be anticipated, the use of different catalysts and different reaction conditions leads to different products, including methane, medium- and long-chain hydrocarbons, ethanol, and acetic acid.<sup>19</sup> Most of these processes, however, suffer from a lack of selectivity and much work has been carried out to improve the catalysts.<sup>19,20</sup> An important part of this work is attempting to understand the reactions that occur on the metal surface. Studies on binuclear metal complexes have played an important role in developing mechanistic proposals for the Fischer-Tropsch reaction, including the original model by Pettit and more recently the Maitlis "vinyl mechanism".<sup>20,21a</sup>

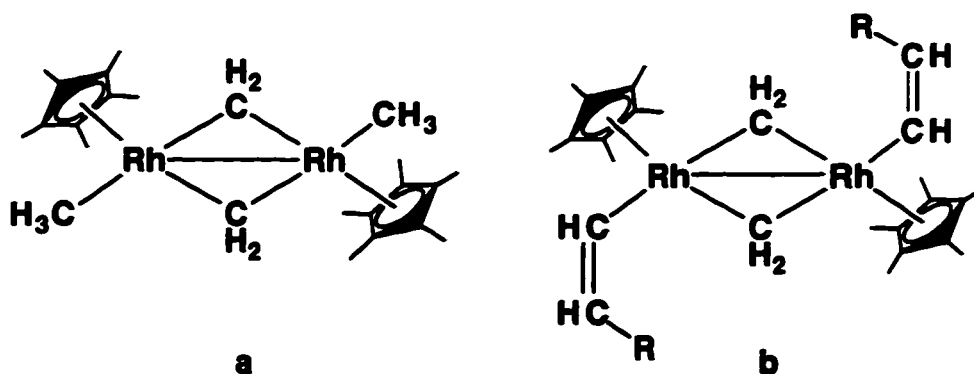
The initial steps of the Fischer-Tropsch reaction involve reduction of carbon monoxide by dihydrogen to organic fragments such as "C", "CH", "CH<sub>2</sub>", and "CH<sub>3</sub>" on the metal surface. All of these fragments have been observed as ligands in polymetallic homogeneous systems.<sup>20</sup> The next steps involve combination of these species on the metal surface to form hydrocarbon chains. There is some controversy over the mechanism of these reactions. Originally, the chain propagation steps were thought to involve methyl group migration onto a methylene fragment, followed by migration of the resulting alkyl fragment onto an additional methylene to form a longer alkyl chain.<sup>20</sup> The most recent proposal by Maitlis, however, suggests that CH and CH<sub>2</sub> fragments can combine to form vinyl groups, and that the vinyl groups then migrate to bridging methylene fragments to propagate the chain. It has been proposed that alkenyl groups combine more readily with methylenes than do alkyl groups because of the large kinetic barrier involved in orbital reorientation when combining two sp<sup>3</sup> hybridized carbons.<sup>22</sup>

One key step in the Maitlis mechanism is the isomerization of an  $\eta^1$ -allyl type species (which results from alkenyl migration to a methylene) to an  $\eta^1$ -alkenyl group (a substituted vinyl moiety) which can subsequently migrate to a  $\mu$ -CH<sub>2</sub> group to propagate the chain (see Scheme 1.1).

**Scheme 1.1**



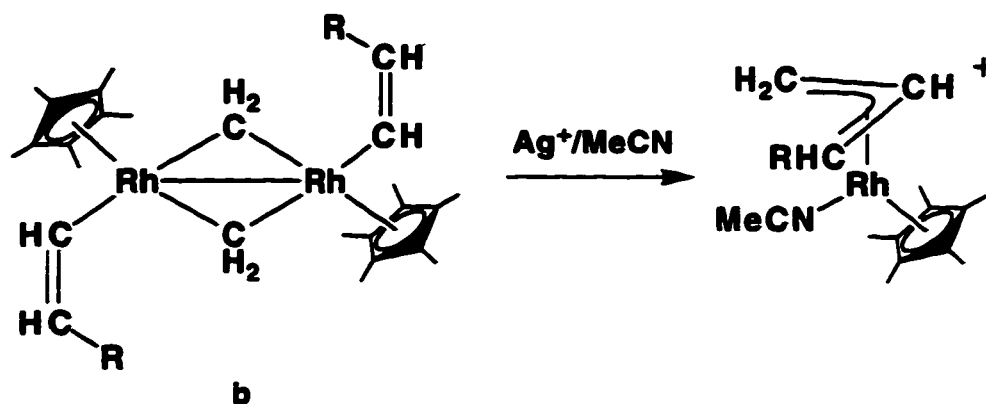
Organometallic model complexes that contain fragments such as alkyl, alkenyl, allyl, and methylene groups, similar to those proposed to exist on the Fischer-Tropsch catalyst surface, are therefore of interest in order to test the feasibility of the proposed steps in the above chain lengthening process. An example of the utility of organometallic complexes as model systems is seen in the dirhodium complexes shown.<sup>23</sup>



In these complexes, alkyl or alkenyl groups are adjacent to bridging methylene groups, similar to what is believed to be present on the surface of the catalyst. Thermal decomposition of compound **a** led to the formation of  $\text{CH}_2=\text{CHCH}_3$ . However, the isotope combinations obtained in experiments using  $^2\text{H}$  and  $^{13}\text{C}$  labeled material were inconsistent with direct coupling of the methyl and two methylene groups, and the authors suggested instead a pathway involving a vinyl intermediate which couples to a bridging methylene to form an allyl group, followed by reductive elimination of the allyl group as propene.<sup>21c</sup> This postulate was supported by the synthesis of compound **b**,

which reacts readily to form the allyl product via migration of the vinyl group onto the methylene group (see Scheme 1.2).

**Scheme 1.2**



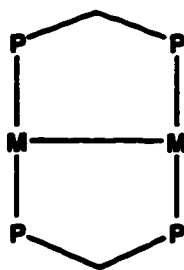
These modeling studies, along with other experiments, led to the mechanism described in Scheme 1.1.

Binuclear complexes are the simplest systems in which metals can display cooperativity effects, and they are attractive for a number of reasons. They are soluble in organic solvents, so they are conveniently studied using standard spectroscopic techniques. The presence of only two metals allows for metal-metal interactions, but the systems avoid many of the difficulties associated with larger clusters, such as difficult characterization due to the large number of ligands.

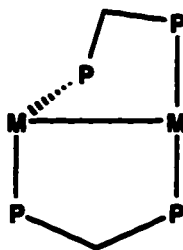
Metal-metal bonded bimetallic complexes unsupported by bridging ligands suffer from a tendency to dissociate, which is not surprising, considering that the metal-metal bond strengths are similar to metal-ligand bond strengths.<sup>24</sup> The tendency towards

dissociation makes it difficult to study metal-metal cooperativity effects. Because of this problem, much interest has been focused on complexes containing bridging ligands which will hold the metals together.<sup>25</sup> One of the most popular ligands has been dppm (bis(diphenylphosphino)methane), which appears to have the ideal bite angle to bridge two metals and forms many stable bimetallic complexes.<sup>26</sup> The bisphosphine ligand holds the two metals in close proximity, preventing fragmentation, and has the added advantage of having phosphorus nuclei which can serve as a  $^{31}\text{P}$  NMR spectroscopic probe which greatly assists in the characterization of the complexes.

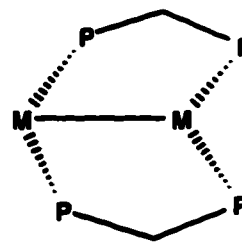
Although the primary function of the bridging dppm ligands is to hold the metals together, they are not completely innocent and can exert a number of influences. Owing to steric effects, two dppm ligands in a trans arrangement in a complex essentially restrict the chemistry to a horizontal plane perpendicular to the M-P bonds and between the phenyl groups of the two dppm ligands. However, the ligands can move into a cis arrangement at one or both metals, as shown below, to accommodate coordination geometries that are not possible with trans phosphines, such as perpendicularly bound alkynes, in which the alkyne is coordinated perpendicular to the metal-metal axis.<sup>27</sup>



trans



cis-trans



cis

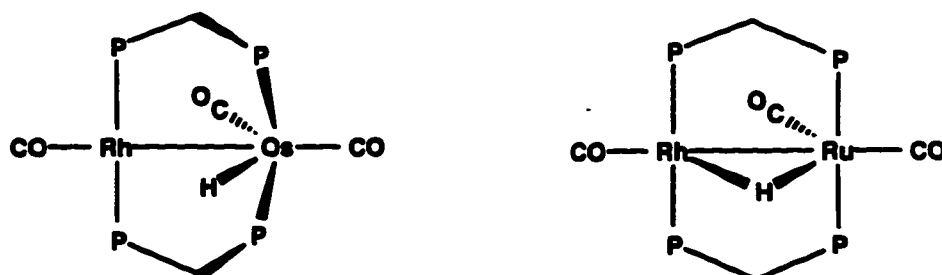
The dppm ligands themselves can also be involved in reactions. For example, the dppm methylene hydrogens are susceptible to deprotonation,<sup>28</sup> and orthometallations of the phenyl groups of dppm are also known.<sup>29</sup> The metal-phosphorous bond has also been shown to undergo insertion reactions in some cases,<sup>30</sup> and P-C bond cleavage has also been observed.<sup>31</sup>

Although most of the work on binuclear complexes has involved homobimetallic systems in which both of the metals are the same, there has recently been increasing interest in heterobinuclear systems.<sup>32</sup> Currently there is considerable interest in the development of heterogeneous catalysts that employ two or more different metals,<sup>33</sup> and these mixed-metal catalysts already find use in a wide range of industrial processes, including synthesis gas chemistry, coal hydrodesulfurization, methane or olefin oxidation and gasoline reforming. Heterobimetallic catalysts even find common use in automobile catalytic converters, which employ Group 9 and 10 combinations, such as Rh/Pt. In spite of extensive work in the development of these heterogeneous catalysts, little is understood about the functions of the different metals in the respective processes. The prospects of obtaining mechanistic information about processes occurring under heterogeneous conditions are difficult enough,<sup>34</sup> attempting to elucidate the functions of the different metals under these conditions is even more daunting. Soluble mixed-metal complexes are therefore valuable as model systems for these bimetallic catalysts.

Our interest in the group 8/9 combination of metals in particular was spurred by reports of the formation of ethylene glycol from synthesis gas using a mixed Rh/Ru catalyst system.<sup>35</sup> Rh and Ru catalysts individually are known to favour production of

$C_2$  oxygenates, however selectivity is poor in the homometallic systems. The mixed Rh/Ru system results in improved selectivity for ethylene glycol, the most valuable product, clearly pointing to a synergistic effect of the two different metals. In addition, recent reports have indicated that the carbonylation of methanol by Ir catalysts is promoted by the addition of a Ru complex.<sup>36</sup> It was of interest to us to bring together Rh, which typically has a 16 electron configuration in these systems, and a saturated group 8 metal and attempt to probe some of the organometallic chemistry of this metal combination.

Previous workers in this group have developed a general synthesis for dppm-bridged RhM complexes which involves displacement of chloride from  $RhCl(dppm)_2$  by metal carbonylate anions.<sup>37</sup> For the RhOs and RhRu systems, the anion used is  $HM(CO)_4^-$  and the products formed are  $[RhOs(H)(CO)_3(dppm)_2]$  and  $[RhRu(CO)_3(\mu-H)-(dppm)_2]$ . The structures of the two analogous compounds are different. The RhOs complex has a terminal hydride and cis phosphines at Os, while the RhRu complex has a bridging hydride and trans phosphines at Ru.<sup>29,37</sup>



The reason for the structural difference is not clear, although it may result from a stronger M-H bond to the third row metal Os, which may make a terminal bond to this metal

favourable. The chemistry of the RhOs system and its complexes with various small molecules and activated alkynes have been studied.<sup>38</sup> The goal of this thesis was to extend this chemistry to include alkyl, alkenyl, allyl, carbene and other organic groups and to develop the related chemistry of the RhRu system.

**References**

1. (a) Lotz, S.; van Rooyen, P. H.; Meyer, R.; *Adv. Organomet. Chem.* **1995**, *37*, 219.  
(b) Braga, D.; Dyson, P. J.; Grepioni, F.; Johnson, B. F. G. *Chem. Rev.* **1994**, *94*, 1585.
2. (a) Poilblanc, R. *Inorg. Chem. Acta.* **1982**, *62*, 75.  
(b) Werner, H.; Lippert, F.; Betz, P.; Kruger, C. *Chem. Ber.* **1992**, *125*, 337.  
(c) Baranger, A. M.; Bergman, R. G. *J. Am. Chem. Soc.* **1994**, *116*, 3822.
3. Tachikawa, M.; Geerts, R. L.; Mueterties, E. L. *J. Organomet. Chem.* **1981**, *213*, 11.
4. Hermann, W. A. *Angew. Chem. Int. Ed. Engl.* **1982**, *21*, 117.
5. Brown, M. P.; Fisher, J. R.; Franklin, S. J.; Puddephatt, R. J.; Thompson, M. A. in *Catalytic Aspects of Metal Phosphine Complexes*; Alyea, E. C.; Meek, D. W. eds.; ACS symp. ser. 196, 1982; p. 231.
6. Gallop, M. A.; Roper, W. R.; *Advances in Organometallic Chemistry* **1986**, *25*, 121.
7. (a) Hermann, W. A. *Advances in Organometallic Chemistry* **1982**, *20*, 159.  
(b) Collman, J.P.; Hegedus, L.S.; Norton, J. R.; Finke, R. G. *Principles and Applications of Organotransition Metal Chemistry*; University Science Books: Mill Valley, California, 1987, pp. 119-136.
8. (a) Stephan, D. W. *Coord. Chem. Rev.* **1989**, *95*, 41.

- (b) Hanna, T. A.; Baranger, A. M.; Bergman, R. G. *J. Am. Chem. Soc.* **1995**, *117*, 11363.
9. Antonelli, D. M.; Cowie, M. *Organometallics*, **1990**, *29*, 4039.
10. Lee, K.-W.; Brown, T. L. *Organometallics* **1985**, *4*, 1025.
11. (a) Roberts, D. A.; Geoffroy, G. L. in *Comprehensive Organometallic Chemistry*, Wilkinson, G.; Stone, F. G. A.; Abel, E. W. eds., Pergamon Press: Oxford, **1982**, *Vol. 8*, p763.
- (b) Gates, B. C. *Catalytic Chemistry*; John Wiley & Sons: New York, 1992. p. 118-123.
12. (a) Collman, J. P.; Denisevich, P.; Konai, P.; Marrocco, M.; Anson, F. C. *J. Am. Chem. Soc.* **1980**, *102*, 6027.
- (b) Balch, A. L. in *Homogeneous Catalysis with Metal Phosphine Complexes*, Plenum Press: New York and London, 1983. pp.167-169.
13. Hiltz, R. W.; Franchuk, R. A.; Cowie, M. *Organometallics* **1991**, *10*, 304.
14. Casey, C. P.; Audett, J. D. *Chem. Rev.* **1986**, *86*, 339.
15. Muetterties, E. L.; Rhodin, T. N.; Band, E.; Brucker, C. F.; Pretzer, W. R. *Chem. Rev.* **1979**, *79*, 91.
16. Gates, B. C. *Catalytic Chemistry*; John Wiley & Sons: New York, 1992. p.343-346.
17. (a) Parshall, G. W.; Ittel, S. D. *Homogeneous Catalysis* John Wiley & Sons Inc.: New York, 1992. pp. 10-47, 96-99.

- (b) Collman, J.P.; Hegedus, L.S.; Norton, J.R.; Finke, R.G. *Principles and Applications of Organotransition Metal Chemistry*; University Science Books: Mill Valley, California, 1987, pp. 523-571, 638.
18. Braunstein, P.; Rose, J. in *Comprehensive Organometallic Chemistry II*, Vol. 10, Abel, E. W.; Wilkinson, G.; Stone, F. G. A. (eds), Pergamon, Oxford, 1994. Chapt. 7.
19. Collman, J.P.; Hegedus, L.S.; Norton, J.R.; Finke, R.G. *Principles and Applications of Organotransition Metal Chemistry*; University Science Books: Mill Valley, California, 1987, pp. 653-660.
20. Herrman, W. A. *Angew. Chem. Int. Ed. Engl.* **1982**, *21*, 117.
21. (a) Maitlis, P. M.; Long, H. C.; Quayoum, R.; Turner, M. L.; Wang, Z-Q. *Chem. Commun.* **1996**, 1.
- (b) Muetterties, E. L.; Stein, J. *Chem. Rev.* **1979**, *79*, 479.
- (c) Maitlis, P. M.; Saez, I. M.; Meanwell, N. J.; Isobe, K.; Nutton, A.; Vaquez de Miguel, A.; Bruce, D. W.; Okeya, S.; Bailey, P. M.; Andrews, D. G.; Ashton, P. R.; Johnstone, I. R. *New J. Chem.*, **1989**, *13*, 419.
- (d) Brady, R. C.; Pettit, R. *J. Am. Chem. Soc.* **1980**, *102*, 6181.
22. Calhorda, M. J.; Brown, J. M.; Cooley, N. A. *Organometallics*, **1991**, *10*, 1431.
23. Martinex, J. M.; Adams, H.; Bailey, N. A.; Maitlis, P. M. *J. Chem. Soc., Chem. Commun.*, **1989**, 286.
24. Vahrenkamp, H. *Angew. Chem., Int. Ed. Engl.* **1978**, *17*, 379.
25. (a) Pringle, P.; Shaw, B.L. *J. Chem. Soc., Dalton Trans.* **1983**, 889.

- (b) Albinati, A.; Lehner, H.; Venanzi, L.M. *Inorg. Chem.* **1985**, *24*, 1483.
- (c) Horváth, I. *Organometallics* **1986**, *5*, 2333.
- (d) McDonald, R.; Cowie, M. *Inorg. Chem.* **1990**, *29*, 1564.
- (e) Elliot, D.J.; Ferguson, G.; Holah, D.G.; Hughes, A.N.; Jennings, M.C.; Magnuson, V.R.; Potter, D.; Puddephatt, R.J. *Organometallics* **1990**, *9*, 1336.
- (f) Garland, M.; Horváth, I.; Bor, G. *Organometallics* **1991**, *10*, 513.
- (g) Garland, M. *Organometallics* **1993**, *12*, 535.
26. (a) Puddephatt, R. J. *Chem. Soc. Rev.* **1983**, *12*, 99.
- (b) Balch, A. L. in *Homogeneous Catalysis with Metal Phosphine Complexes*; Pignolet, L. H., Ed: New York, 1983.
- (c) Chaudret, B.; Delvaux, B.; Poilblanc, R. *Coord. Chem. Rev.* **1988**, *86*, 191.
27. (a) George, D. S. A.; McDonald, R.; Cowie, M. *Can. J. Chem.*, **1996**, *74*, 2289.
- (b) Berry, D. H.; Eisenberg, R. *Organometallics*, **1987**, *6*, 1796.
- (c) Elliot, D. J.; Ferguson, G.; Holah, D. G.; Hughes, A. N.; Jennings, M. C.; Magnuson, V. R.; Potter, D.; Puddephatt, R. J. *Organometallics*, **1990**, *9*, 1336.
28. (a) Puddephatt, R. J. *Chem. Soc. Rev.*, **1983**, *12*, 99.
- (b) Sharp, P.R.; Ge, Y.-W. *J. Am. Chem. Soc.* **1987**, *109*, 3796.
- (c) Sharp, P.R.; Ge, Y.-W. *Inorg. Chem.* **1993**, *32*, 94.
29. Hiltz, R. W.; Franchuk, R. A.; Cowie, M. *Organometallics*, **1991**, *10*, 1297.
30. Antwi-Nsiah, F. H.; Oke, O.; Cowie, M. *Organometallics*, **1996**, *15*, 506.

31. Shiu, K-B; Jean, S-W.; Wang, H-J.; Wang, S-L.; Liao, F-L.; Wang, J-C.; Liou, L-S. *Organometallics*, **1997**, *16*, 114.
32. (a) Cullen, W.R.; Kim, T.-J.; Einstein, F.W.B.; Jones, T. *Organometallics* **1983**, *2*, 714.
- (b) Iggo, J.A.; Markham, D.P.; Shaw, B.L.; Thornton-Pett, M. *J. Chem. Soc., Chem. Commun.* **1985**, 432.
- (c) Turpin, R.; Dagnac, P.; Poilblanc, R. *J. Organometal. Chem.* **1987**, *319*, 247.
- (d) Arndt, L.W.; Bancroft, B.T.; Darenbourg, M.Y.; Janzen, C.P.; Kim, C.M.; Reibenspies, J.; Varner, K.E.; Youngdahl, K.D. *Organometallics* **1988**, *7*, 1302.
- (e) Mague, J.T. *Organometallics* **1991**, *10*, 513.
- (f) Hilts, R.W.; Franchuk, R.A.; Cowie, M. *Organometallics* **1991**, *10*, 1297.
- (g) Schiavo, S.L.; Rotondo, E.; Bruno, G.; Faraone, F. *Organometallics* **1991**, *10*, 1613.
- (h) Poulton, J.T.; Folting, K.; Caulton, K.G. *Organometallics* **1992**, *11*, 1364.
- (i) Fong, R.H.; Lin, C.-H.; Idmoumaz, H.; Hersh, W.H. *Organometallics* **1993**, *12*, 503.
- (j) Stang, P.J.; Cao, D. *Organometallics* **1993**, *12*, 996.
33. (a) Guzzi, L.; Solymosi, F.; Tétényi, P. Eds.; *New Frontiers in Catalysis*, Vol 75, Part C, Elsevier Science Publishers, Amsterdam 1993.
- (b) Dowden, D.A. *Catalysis*; Kemball, C.; Dowden, D.A., Eds.; Specialist Periodical Report. The Chemical Society: London, 1978, Vol 2, p1.

- (c) Sinfelt, J.H. *Bimetallic Catalysts: Discoveries, Concepts and Applications*; John Wiley and Sons: New York, 1983.
34. (a) Brown, R.K.; Williams, J.M.; Sivak, A.J.; Muetterties, E.L. *Inorg. Chem.* 1980, 19, 370.
- (b) Muetterties, E.L. *Angew. Chem., Int. Ed. Engl.* 1978, 17, 545.
- (c) Zaera, F. *Chem. Rev.* 1995, 95, 2651.
35. Dombek, B. D. *Organometallics*, 1985, 4, 1707.
36. Garland, C. S.; Giles, M. F.; Sunley, J. G. (BP Chemicals Ltd.) Eur. Pat. Appl. EP 643, 034.
37. Antonelli, D. M.; Cowie, M. *Organometallics*, 1990, 9, 1818.
38. Hilts, R. W.; Franchuk, R. A.; Cowie, M. *Organometallics*, 1991, 10, 304.

## **Chapter 2**

### **Hydrido, Alkyl, and Related Complexes of Rh/Os**

#### **Introduction**

Transition metal hydrido and alkyl complexes play a key role as models for intermediates in different catalytic processes.<sup>1</sup> Although the alkyl chemistry of many mononuclear systems is very well studied, their use as models for heterogeneous catalytic processes such as the Fischer-Tropsch reaction is limited by the presence of only one metal. A second metal in close proximity, such as occurs on a metal surface, can greatly alter the chemistry.<sup>2</sup> For this reason, the chemistry of bi- or polymetallic alkyl and hydrido complexes is important.

Studies in this group have focused on the alkyl chemistry of binuclear complexes bridged by dppm involving the group 9 metals<sup>3</sup> which were of particular interest because of their great importance as catalysts.<sup>4</sup> Reports of mixed-metal catalysts<sup>5</sup> have led us to extend our system to heterobinuclear alkyl complexes involving group 9 metals in combination with other groups including the metal combinations Rh/Re<sup>6</sup>, Ir/Re<sup>6</sup>, Rh/Mn<sup>7</sup>, and Rh/Mo<sup>8</sup>. Various aspects are of interest including the nature of the metal-alkyl interactions, the possibility of migratory insertion reactions, the ability of dialkyl or alkyl-hydride complexes to undergo binuclear reductive eliminations, and the roles of the different metals in these reactions. The mobility of the ligands over the bimetallic core is a key aspect and may be relevant to mobilities of fragments on a metal surface. The ultimate goal is to develop an understanding of the metal-metal cooperativity effects that are possible in these systems. This chapter reports the alkyl chemistry of the Rh/Os system.

are possible in these systems. This chapter reports the alkyl chemistry of the Rh/Os system.

### Experimental Section

**General Comments.** All solvents were dried and deoxygenated immediately before use. Sodium benzophenone was used as the drying agent for all of the solvents except dichloromethane, which was distilled over  $P_2O_5$ , and acetonitrile which was distilled over calcium hydride. The solvents were distilled under an atmosphere of prepurified nitrogen or argon. Rhodium(III) chloride trihydrate was purchased from Johnson Matthey Ltd.,  $Os_3(CO)_{12}$  was purchased from Sudtek, and  $Ph_2PCH_2PPh_2$  (dppm),  $HBf_4 \cdot Et_2O$ ,  $MeO_2CC \equiv CCO_2Me$  (DMAD), and  $[(Ph_3P)_2N]Cl$  were obtained from Aldrich as were THF solutions of  $CH_3MgCl$ ,  $CH_3MgI$  and  $CH_3Li$ . Sodium acetylide as an 18% slurry in a mixture of xylenes and light mineral oil was also purchased from Aldrich; this reagent was used shortly after receipt and was stored under dinitrogen. The 99% carbon-13-enriched carbon monoxide was purchased from Isotec Inc. The compounds  $[RhOsH(CO)_3(dppm)_2]$  (1),<sup>9</sup>  $[RhOs(CO)_4(dppm)_2][BF_4]$  (2)<sup>10a</sup>, and  $[RhOsCl(CO)_3-(dppm)_2]$ <sup>10b</sup> were prepared by published procedures.

The  $^1H$ ,  $^{31}P\{^1H\}$ , and  $^{13}C\{^1H\}$  NMR spectra were recorded on a Bruker AM-400 spectrometer operating at 400.1, 162.0 and 100.6 MHz for the respective nuclei. The internal deuterated solvent served as a lock for the spectrometer. All infrared spectra were run on a Nicolet 7199 Fourier transform interferometer as solids in Nujol or dichloromethane casts on KBr. The elemental analyses were performed by the

microanalytical service within the department. Spectroscopic data for all compounds are given in Table 2.1.

### Preparation of the Compounds.

(a) **[RhOs(CO)<sub>3</sub>(NCCH<sub>3</sub>)(μ-H)(dppm)<sub>2</sub>][BF<sub>4</sub>]<sub>2</sub>•CH<sub>3</sub>CN (3).** A solution of HBF<sub>4</sub>•Et<sub>2</sub>O (15 μL, 17 mg, 0.105 mmol) in 20 mL of acetonitrile was added dropwise over 1 h to a rapidly stirring solution of [RhOs(CO)<sub>4</sub>(dppm)<sub>2</sub>][BF<sub>4</sub>] (2) (100 mg, 0.079 mmol) in 20 mL of acetonitrile, causing the mixture to gradually change from yellow to orange. After all the acid had been added, the mixture was stirred for an additional hour and the solvent volume was reduced to *ca.* 1 mL under vacuum. The addition of 20 mL of diethyl ether to the solution caused the gradual formation of small orange crystals of 3 (83 mg, 0.059 mmol). Yield: 75%. Anal. Calcd. for C<sub>57</sub>H<sub>51</sub>N<sub>2</sub>B<sub>2</sub>F<sub>8</sub>O<sub>3</sub>OsP<sub>4</sub>Rh: C, 48.81; H, 3.67; N, 2.00. Found: C, 48.73; H, 3.59; N, 1.88.

(b) **[RhOs(CO)<sub>3</sub>(CN<sup>t</sup>Bu)(μ-H)(dppm)<sub>2</sub>][BF<sub>4</sub>]<sub>2</sub> (4).** A stirred solution of 3 (0.100g, 0.071 mmol) in 10 mL of CH<sub>2</sub>Cl<sub>2</sub> was charged with 9 μL of neat <sup>t</sup>BuNC (7 mg, 0.080 mmol), resulting in an immediate colour change from orange to pale yellow. After 1 h of stirring the solvent was removed under vacuum, leaving a pale yellow solid which was dissolved in 10 mL of THF and precipitated from solution through addition of 20 mL of Et<sub>2</sub>O and 20 mL of hexanes. Dissolution of the precipitate in 3 mL of CH<sub>2</sub>Cl<sub>2</sub>, followed by the slow addition of Et<sub>2</sub>O to the resulting solution afforded very pale yellow crystals of the desired product (0.071g, 0.051 mmol). Yield: 72%. Anal. Calcd. for

Table 2.1. Spectroscopic Parameters for the Compounds<sup>a</sup>

Compound	IR, cm <sup>-1b</sup>	NMR <sup>d</sup>	
		$\delta(^3\text{P}\{\text{H}\})$	$\delta(^1\text{C}\{\text{H}\})$
[RhOs(CO) <sub>3</sub> (NCCH <sub>3</sub> )(μ-H)- (dppm) <sub>2</sub> ][BF <sub>4</sub> ] <sub>2</sub> •CH <sub>3</sub> CN (3)	2078 (ss), 2004 (ss), 1819 (ss), 2321 (ws), ° 2292 (ws) <sup>6c</sup>	27.21 (RhP, <sup>1</sup> J <sub>RhP</sub> = 99 Hz); -7.05 (OsP)	OsCO: 174.27 (t, 1C, <sup>2</sup> J <sub>PC</sub> < 1 Hz); 176.82 (dt, 1C, <sup>2</sup> J <sub>CC</sub> = 27 Hz, <sup>2</sup> J <sub>PC</sub> = 9 Hz); 224.47 (ddt, 1C, <sup>2</sup> J <sub>CC</sub> = 27 Hz, <sup>1</sup> J <sub>RhC</sub> = 25 Hz, <sup>2</sup> J <sub>PC</sub> = 8 Hz)
	2083, 2015, 1822 (CH <sub>2</sub> Cl <sub>2</sub> sol'n)		PC <sub>H</sub> <sub>2</sub> P: (AB) 4.09 (dm, 2H), 3.88 (dm, 2H), <sup>2</sup> J <sub>HH</sub> = 14 Hz; Rh <sup>1</sup> H/Os: -15.18 (dt, 1H, <sup>1</sup> J <sub>RhH</sub> = 27 Hz, <sup>2</sup> J <sub>RhPH</sub> = 10 Hz, <sup>2</sup> J <sub>OsPH</sub> not resolved); NCC <sub>H</sub> <sub>3</sub> : 1.98 (s, 3H), 1.58 (s, 3H)
[RhOs(CO) <sub>3</sub> (CN <sup>t</sup> Bu)(μ-H)- (dppm) <sub>2</sub> ][BF <sub>4</sub> ] <sub>2</sub> (4)	2083 (ss), 2002 (sb), 1821 (mb), 2189 (ss) <sup>6c</sup>	27.71 (RhP, <sup>1</sup> J <sub>RhP</sub> = 100 Hz); -5.82 (OsP)	OsCO: 173.05 (t, 1C, <sup>2</sup> J <sub>PC</sub> < 1 Hz); 173.29 (dt, 1C, <sup>2</sup> J <sub>CC</sub> = 30 Hz, <sup>2</sup> J <sub>PC</sub> = 9 Hz); 211.56 (m, 1C, <sup>2</sup> J <sub>CC</sub> = 30 Hz)
	2088, 2022, 1831 (CH <sub>2</sub> Cl <sub>2</sub> sol'n)		PC <sub>H</sub> <sub>2</sub> P: (AB) 4.29 (dm, 2H), 4.05 (dm, 2H), <sup>2</sup> J <sub>HH</sub> = 14 Hz; Rh <sup>1</sup> H/Os: -11.09 (dt, 1H, <sup>1</sup> J <sub>RhH</sub> = 21 Hz, <sup>2</sup> J <sub>RhPH</sub> < 3 Hz, <sup>2</sup> J <sub>OsPH</sub> = 11 Hz); CNC(CH <sub>3</sub> ): 0.75 (s, 9H)
[RhOs(I)(CO) <sub>3</sub> (μ-H)- (dppm) <sub>2</sub> ][BF <sub>4</sub> ] <sub>2</sub> (5)	2066 (ss), 1993 (ss), 1793 (ss) <sup>c</sup>	20.08 (RhP, <sup>1</sup> J <sub>RhP</sub> = 104); -7.73 (OsP)	OsCO: 175.10 (m, 1C); 175.47 (m, 1C); 226.62 (bm, 1C)
	2060, 2000, 1798 (CH <sub>2</sub> Cl <sub>2</sub> sol'n)		PC <sub>H</sub> <sub>2</sub> P: (AB) 4.12 (dm, 2H), 3.83 (dm, 2H), <sup>2</sup> J <sub>HH</sub> = 14 Hz; Rh <sup>1</sup> H/Os: -11.17 (dt, 1H, <sup>1</sup> J <sub>RhH</sub> = 28 Hz, <sup>2</sup> J <sub>RhPH</sub> = 8 Hz, <sup>2</sup> J <sub>OsPH</sub> = 4 Hz)

Compound	IR, cm <sup>-1b</sup>	NMR <sup>d</sup>	
		$\delta(^1\text{P}\{\text{H}\})$	$\delta(^1\text{H})$ $\delta(^{13}\text{C}\{\text{H}\})$
[RhOs( $\mu$ -OH)(CO) <sub>2</sub> -( $\mu$ -H)(dppm) <sub>2</sub> ][BF <sub>4</sub> ] (6)	2036 (ss), 1946 (sb)	25.10 (RhP, <sup>1</sup> J <sub>RhP</sub> = 133 Hz); 1.83 (OsP)	PCl <sub>2</sub> P: (AB) 4.15 (dm, 2H), 3.20 Rh/Os: -2.83 (dt, 1H, <sup>1</sup> J <sub>RhH</sub> = 7 Hz, <sup>2</sup> J <sub>OsPH</sub> = 17 Hz) RhOH: 0.88 (s, 1H) OsCO: 177.61 (t, 1C, <sup>2</sup> J <sub>PC</sub> = 7 Hz); 179.15 (bs, 1C); RhCO: 189.99 (dt, <sup>1</sup> J <sub>RhC</sub> = 71 Hz, <sup>2</sup> J <sub>PC</sub> = 16 Hz)
[RhOs( $\eta^1$ -C $\equiv$ CH)(CO) <sub>2</sub> -(dppm) <sub>2</sub> ] · 1/2CH <sub>2</sub> Cl <sub>2</sub> (7)	2014 (ws), <sup>b</sup> 1954 (ss), 1930 (sb), 1835 (w) <sup>c</sup>	31.94 (RhP, <sup>1</sup> J <sub>RhP</sub> = 131); 4.78 (OsP)	PCl <sub>2</sub> P: 3.49 (pq, 4H); RhC $\equiv$ CH: 1.73 (dt, 1H, <sup>3</sup> J <sub>RhH</sub> = <sup>4</sup> J <sub>RhPH</sub> = 4 Hz) OsCO: 191.04 (t, 1C, <sup>2</sup> J <sub>PC</sub> = 15 Hz); 218.85 (m, 2C)
[RhOs( $\eta^1$ -CH <sub>2</sub> CN)(CO) <sub>2</sub> -(dppm) <sub>2</sub> ] (8)	1945 (ss), 1927 (ss), 1746 (sh), 1731 (ss), 2190 (m) <sup>c</sup>	35.32 (RhP, <sup>1</sup> J <sub>RhP</sub> = 139); 2.65 (OsP)	PCl <sub>2</sub> P: 3.59 (pq, 4H); RhCH <sub>2</sub> CN: 0.58 (td, 2H, <sup>2</sup> J <sub>RhH</sub> = 3 Hz, <sup>3</sup> J <sub>RhPH</sub> = 8 Hz) OsCO: 192.55 (td, 1C, <sup>2</sup> J <sub>PC</sub> = 11 Hz, <sup>2</sup> J <sub>RhC</sub> = 3 Hz); 216.34 (m, 2C)
[RhOs(CO) <sub>4</sub> ( $\mu$ -dppm)-( $\mu$ -Ph <sub>2</sub> PCHPPH <sub>2</sub> )] (9)	1985 (sh), 1962 (ss), 1926 (ss), 1905 (ss) <sup>c</sup>	P <sub>A</sub> : 29.73, P <sub>C</sub> : -15.21, P <sub>B</sub> : 25.78, P <sub>D</sub> : -6.97 J(P <sub>A</sub> P <sub>B</sub> ) = 321, J(P <sub>A</sub> P <sub>C</sub> ) = 159, J(P <sub>A</sub> P <sub>D</sub> ) = 34, J(P <sub>B</sub> P <sub>C</sub> ) = 32, J(P <sub>B</sub> P <sub>D</sub> ) = 96, J(P <sub>C</sub> P <sub>D</sub> ) = 117, J(RhP <sub>A</sub> ) = 109, J(RhP <sub>B</sub> ) = 117	PCl <sub>2</sub> P: 4.16 (dd, 2H, <sup>2</sup> J <sub>P<sub>B</sub>H</sub> = <sup>2</sup> J <sub>P<sub>D</sub>H</sub> = 11 Hz); PCHP: 2.84 (bs, 1H) OsCO: 184.90 (t, 1C, <sup>2</sup> J <sub>PC</sub> = 10 Hz); 197.14 (t, 2C, <sup>2</sup> J <sub>PC</sub> < 2 Hz); RhCO: 184.61 (dt, <sup>1</sup> J <sub>RhC</sub> = 77 Hz, <sup>2</sup> J <sub>PC</sub> = 14 Hz)

Compound	IR, cm <sup>-1b</sup>	NMR <sup>d</sup>		
		$\delta(^3\text{P}\{^1\text{H}\})$	$\delta(^{13}\text{C}\{^1\text{H}\})$	
[RhOs(CO) <sub>4</sub> (μ-dppm)- (μ-Ph <sub>2</sub> PCH(CH <sub>3</sub> )PPh <sub>2</sub> ) [CF <sub>3</sub> SO <sub>3</sub> ](10)	1984 (ss), 1952 (ss), 1915 (ss) <sup>c</sup>	P <sub>A</sub> : 35.80, P <sub>C</sub> : 5.10, P <sub>B</sub> : 28.48, P <sub>D</sub> : -6.23 J(P <sub>A</sub> P <sub>B</sub> ) = 326, J(P <sub>A</sub> P <sub>C</sub> ) = 86, J(P <sub>A</sub> P <sub>D</sub> ) = 26, J(P <sub>B</sub> P <sub>C</sub> ) = 26, J(P <sub>B</sub> P <sub>D</sub> ) = 84, J(P <sub>C</sub> P <sub>D</sub> ) = 179, J(RhP <sub>A</sub> ) = 119, J(RhP <sub>B</sub> ) = 119	PCH <sub>2</sub> P: (AB) 4.44 (dddd, 1H, <sup>2</sup> J <sub>P<sub>B</sub>H</sub> = <sup>2</sup> J <sub>P<sub>D</sub>H</sub> = 11 Hz), 4.03 (ddd, 1H, <sup>2</sup> J <sub>P<sub>B</sub>H</sub> = <sup>2</sup> J <sub>P<sub>D</sub>H</sub> = 11 Hz), <sup>2</sup> J <sub>H<sub>1</sub>H</sub> = 15 Hz; PCH(CH <sub>3</sub> )P: 3.77 (ddq, 1H, <sup>2</sup> J <sub>P<sub>A</sub>H</sub> = <sup>2</sup> J <sub>P<sub>C</sub>H</sub> = <sup>3</sup> J <sub>CH<sub>3</sub>H</sub> = 7 Hz) PCH(CH <sub>3</sub> )P: 1.34 (ddd, 3H, <sup>3</sup> J <sub>CH<sub>3</sub>H</sub> = 7 Hz, <sup>3</sup> J <sub>P<sub>A</sub>H</sub> = <sup>3</sup> J <sub>P<sub>C</sub>H</sub> = 10 Hz),	OsCO: 179.94 (t, 1C, <sup>2</sup> J <sub>PC</sub> = 10 Hz); 193.39 (m, 1C); 195.87 (m, 1C) RhCO: 181.79 (dt, <sup>1</sup> J <sub>RhC</sub> = 74 Hz, <sup>2</sup> J <sub>PC</sub> = 11 Hz) PCH(CH <sub>3</sub> )P: 14.58 (1C, bs); PCH(CH <sub>3</sub> )P: 48.80 (1C, dd, <sup>1</sup> J <sub>PC</sub> = 14, <sup>2</sup> J <sub>PC</sub> = 15, <sup>3</sup> J <sub>PC</sub> = 30 Hz)
[RhOsCH <sub>3</sub> (CO) <sub>3</sub> (dppm) <sub>2</sub> ] (11)	1911 (ss), 1858 (ss), 1723 (ss) 1910, 1869, 1740 (CH <sub>2</sub> Cl <sub>2</sub> sol'n)	38.46 (RhP, <sup>1</sup> J <sub>RhP</sub> = 150 Hz); 8.3 (m)	PCH <sub>2</sub> P: 3.5 (bs, 4H) CH <sub>3</sub> : -0.35 (td, <sup>2</sup> J <sub>RhH</sub> = 2 Hz, <sup>3</sup> J <sub>H<sub>1</sub>H</sub> = 7 Hz)	OsCO: 197.5 (m, 1C), 220.2 (m, 2C, <sup>1</sup> J <sub>RhC</sub> = 13Hz, <sup>2</sup> J <sub>PRhC</sub> not resolved)
[RhOs(CH <sub>3</sub> )(CO) <sub>3</sub> (μ-H)- (dppm) <sub>2</sub> ][X] <sup>3</sup> 12a X = SO <sub>3</sub> CF <sub>3</sub> 12b X = BF <sub>4</sub>		22.74 (RhP, <sup>1</sup> J <sub>RhP</sub> = 112 Hz) -3.32 (OsP)	PCH <sub>2</sub> P: (AB) 4.3 (dm, 2H), 4.05 (dm, 2H); OsCH <sub>3</sub> : -0.43 (t, 3H, <sup>3</sup> J <sub>POH</sub> = 7.5 Hz) RhHOs: -12.90 (bm)	OsCO: 181.67 (bs); 179.25 (bs); RhCO: 184.32 (dt, <sup>1</sup> J <sub>RhC</sub> = 75 Hz, <sup>2</sup> J <sub>PC</sub> = 15 Hz)
[RhOs(CO) <sub>3</sub> (μ-H)(μ <sup>2</sup> -η <sup>3</sup> - (o-C <sub>6</sub> H <sub>4</sub> )PhPCH <sub>2</sub> PPh <sub>2</sub> )- (μ-dppm)][X] • Et <sub>2</sub> O 13a X = SO <sub>3</sub> CF <sub>3</sub> 13b X = BF <sub>4</sub>	2038 (ss), 2004 (ss), 1914 (ss) <sup>c</sup>	P <sub>A</sub> : 25.43, P <sub>C</sub> : -4.73, P <sub>B</sub> : 22.53, P <sub>D</sub> : -20.24 J(P <sub>A</sub> P <sub>B</sub> ) = 302, J(P <sub>A</sub> P <sub>C</sub> ) = 46, J(P <sub>A</sub> P <sub>D</sub> ) = 31, J(P <sub>B</sub> P <sub>C</sub> ) = 9, J(P <sub>B</sub> P <sub>D</sub> ) = 67, J(P <sub>C</sub> P <sub>D</sub> ) = 227, J(RhP <sub>A</sub> ) = 107, J(RhP <sub>B</sub> ) = 112	PCH <sub>2</sub> P: 5.06 (dm, 1H, <sup>2</sup> J <sub>H<sub>1</sub>H</sub> = 15 Hz), 4.89 (dm, 1H, <sup>2</sup> J <sub>H<sub>1</sub>H</sub> = 15 Hz), 4.44 (dm, 1H, <sup>2</sup> J <sub>H<sub>1</sub>H</sub> = 15 Hz), 4.14 (dm, 1H, <sup>2</sup> J <sub>H<sub>1</sub>H</sub> = 15 Hz) RhHOs: -15.18 (dm, 1H, <sup>1</sup> J <sub>RhH</sub> = 21 Hz, <sup>2</sup> J <sub>RhPH</sub> = 10 Hz, <sup>2</sup> J <sub>OPH</sub> not resolved)	OsCO: 177.86 (bs), 178.48 (bs); RhCO: 187.56 (dt, <sup>1</sup> J <sub>RhC</sub> = 78 Hz, <sup>2</sup> J <sub>PC</sub> = 12 Hz)

Compound	IR, cm <sup>-1b</sup>	NMR <sup>d</sup>	
		$\delta(^1\text{P}\{\text{H}\})$	$\delta(^1\text{H})$
$[\text{CH}_3\text{RhOs}(\text{H})(\text{CO})_2(\text{dpppm})_2][\text{BF}_4]$ (14)		31.6 (RhP, $^1J_{\text{RhP}} = 139$ Hz) -0.59 (OsP)	PCH <sub>2</sub> P: (AB) 3.4 (dm, 2H), 3.0 (dm, 2H) RhCH <sub>3</sub> : 0.51 (t, $^3J_{\text{PH}} = 8$ Hz) OsH: -7.0 (t, $^2J_{\text{PH}} = 21$ Hz)
$[\text{CH}_3\text{RhOs}(\text{CO})_3(\mu\text{-H})(\text{dpppm})_2][\text{BF}_4]$ (15)		31.3 (RhP, $^1J_{\text{RhP}} = 141$ Hz) -4.5 (OsP)	PCH <sub>2</sub> P: (AB) 3.6 (dm, 2H), 3.4 (dm, 2H) RhCH <sub>3</sub> : 0.20 (t, $^3J_{\text{PH}} = 8$ Hz) RhHOS: -8.95 (bm)
$[\text{RhOs}(\text{CO})_3(\mu\text{-HC}\equiv\text{CH})(\text{dpppm})_2][\text{CF}_3\text{SO}_3]$ (16)		27.9 (RhP, $^1J_{\text{RhP}} = 112$ Hz) -5.5 (OsP)	HC≡CH: (AB) 4.18 (ddm, 1H, $^3J_{\text{RH}} = 3$ Hz) 4.47 (ddm, 1H, $^3J_{\text{RH}} = 5$ Hz) $J_{\text{AB}} = 12$ Hz PCH <sub>2</sub> P: (AB) 4.10 (dm, 2H), 3.78 (dm, 2H)
$[\text{RhOs}(\text{CH}_3)_2(\text{CO})_3(\text{dpppm})_2][\text{CF}_3\text{SO}_3]$ (17)	2037 (ss), 1805 (ss)	31.2 (RhP, $^1J_{\text{RhP}} = 141$ Hz) -5.0 (OsP)	RhCH <sub>3</sub> : 0.73 (dt, $^3J_{\text{PH}} = 6$ Hz, $^2J_{\text{RH}} = 2$ Hz) OsCH <sub>3</sub> : -0.15 (t, $^3J_{\text{PH}} = 6$ Hz)

a. abbreviations used: IR: ss = strong sharp, ms = medium sharp, ws = weak sharp, sb = strong broad, mb = medium broad, sh = shoulder, m = medium. NMR: t = triplet, dt = doublet of triplets, ddt = doublet of doublets of triplets, m = multiplet, td = triplet of doublets, bs = broad singlet, dd = doublet of doublets, dm = doublet of multiplets, dnt = doublet of triplets of triplets, s = singlet, pq = pseudo quintet, ddd = doublet of doublets of doublets of doublets, ddd = doublet of doublets of quintets, ddd = doublet of doublets of doublets, bm = broad multiplet.

b. Nujol mull except as indicated. Values quoted are  $\nu(\text{CO})$  except as indicated. c. CH<sub>2</sub>Cl<sub>2</sub> cast. d.  $^1\text{P}\{\text{H}\}$  chemical shifts are referenced vs. external 85% H<sub>3</sub>PO<sub>4</sub> while  $^1\text{H}$  and  $^{13}\text{C}\{\text{H}\}$  are referenced vs. external TMS. Chemical shifts for the phenyl hydrogens are not given in the  $^1\text{H}$  NMR data. e.  $\nu(\text{CN})$  for cocrystallized CH<sub>3</sub>CN. f.  $\nu(\text{CN})$  for coordinated CH<sub>3</sub>CN. g.  $\nu(\text{CN})$  for 'BuNC. h.  $\nu(\text{C}\equiv\text{C})$ . i.  $\nu(\text{CN})$  for Rh-CH<sub>3</sub>CN. j. -40°C. k. -80°C. l. -60°C.

$C_{58}H_{54}NB_2F_8O_3OsP_4Rh$ : C, 49.63; H, 3.88; N, 1.00. Found: C, 49.60; H, 3.99; N, 0.89.

(c) **[RhOs(I)(CO)<sub>3</sub>(μ-H)(μ-dppm)<sub>2</sub>][BF<sub>4</sub>] (5)**. 20 mL of acetone was added directly to a flask containing NaI (11 mg, 0.0715 mmol) and compound **3** (100 mg, 0.0713 mmol). Both solids rapidly dissolved to form a yellow solution. After stirring for 2 h the solvent was removed in vacuo, leaving a yellow solid which was dissolved in 20 ml of CH<sub>2</sub>Cl<sub>2</sub> and filtered. The solvent was removed in vacuo and the residue was recrystallized from CH<sub>2</sub>Cl<sub>2</sub>/Et<sub>2</sub>O to give a yellow crystalline solid (67 mg), yield 69%. Anal. Calcd. for  $C_{53}H_{45}BF_4IO_3OsP_4Rh$ : C, 46.78; H, 3.33; I, 9.33. Found: C, 46.89; H, 3.43; I, 9.72.

(d) **[RhOs (CO)<sub>3</sub>(μ-OH)(μ-H)(dppm)<sub>2</sub>][BF<sub>4</sub>] (6)**. Compound **3** (30 mg, 0.0356 mmol) was dissolved in 20 mL of THF. 1.6 mL of a 0.225 M solution of NaOH in water (0.036 mmol NaOH) was added via syringe and the solution was stirred for 2 h. The solvent was removed in vacuo and the residue was redissolved in 2 mL of THF and filtered to remove NaBF<sub>4</sub>. The THF was removed in vacuo and the residue was redissolved in 1 mL of CH<sub>2</sub>Cl<sub>2</sub> and crystallized by slow addition of Et<sub>2</sub>O to form a yellow microcrystalline solid, which was washed with 2x10 mL of Et<sub>2</sub>O and dried in vacuo. Yield: 17 mg, 64%.

(e) **Reaction of [RhOs(μ-OH)(CO)<sub>3</sub>(μ-H)(dppm)<sub>2</sub>][BF<sub>4</sub>] (6) with CO**. Compound **6** (10 mg, 0.080 mmol) was dissolved in 0.5 mL of CD<sub>2</sub>Cl<sub>2</sub> in an NMR tube. The tube was evacuated and refilled with CO. <sup>31</sup>P NMR showed that there was no reaction after 1 h, but after 24 h <sup>31</sup>P NMR showed a mixture of [RhOs(CO)<sub>3</sub>(μ-H)<sub>2</sub>(dppm)<sub>2</sub>][BF<sub>4</sub>],<sup>10</sup> [RhOs(CO)<sub>4</sub>(dppm)<sub>2</sub>][BF<sub>4</sub>] (**2**) and starting material.

**(f) Reaction of [RhOs( $\mu$ -H)(NCMe)(CO)<sub>3</sub>(dppm)<sub>2</sub>][BF<sub>4</sub>]<sub>2</sub> (3) with NaOCH<sub>3</sub>.**

Compound 3 (57 mg, 0.048) and NaOCH<sub>3</sub> (2.6 mg, 0.048 mmol) were dissolved in 15 mL of THF, forming a cloudy orange solution. The mixture was stirred for 20 h, filtered and the solvent was removed in vacuo. <sup>31</sup>P NMR showed the residue to be [RhOs(CO)<sub>3</sub>( $\mu$ -H)<sub>2</sub>(dppm)<sub>2</sub>][BF<sub>4</sub>].

**(g) Reaction of 3 with NaC $\equiv$ CH.** 40  $\mu$ L of a 0.18g/mL (7 mg, 0.146 mmol) suspension of NaC $\equiv$ CH in xylenes and mineral oil was added via syringe to a stirred, yellow solution of 3 (100 mg, 0.0713 mmol) in 20 mL of acetonitrile causing an immediate change in colour to orange-red, and finally to yellow-brown. After 1 h of stirring, the solvent was removed in vacuo, leaving a yellow-brown residue. 15 mL of CH<sub>2</sub>Cl<sub>2</sub> was added forming a cloudy orange solution which was filtered. Evaporation of the filtrate gave an orange-brown oil which was washed with 2x20 mL of hexanes and kept under vacuum for 6 h. Recrystallization of the residue from a 20:1 mixture of Et<sub>2</sub>O/CH<sub>2</sub>Cl<sub>2</sub> afforded 31 mg of yellow-brown crystalline solid which proved to be a 1:1 mixture of [RhOs( $\eta^1$ -C $\equiv$ CH)(CO)<sub>3</sub>(dppm)<sub>2</sub>] $\cdot$ 1/2CH<sub>2</sub>Cl<sub>2</sub> (7) and [RhOs( $\eta^1$ -CH<sub>2</sub>CN)(CO)<sub>3</sub>(dppm)<sub>2</sub>] (8). Essentially pure samples of 8 were obtained in yields ranging from 50 to 70% when 4 equiv of NaC $\equiv$ CH were used in the above procedure. Compound 8 is orange in the crystalline state. Anal. Calcd. for C<sub>55</sub>H<sub>46</sub>NO<sub>3</sub>OsP<sub>4</sub>Rh: C, 55.70; H, 3.91; N, 1.18. Found: C, 55.65; H, 3.94; N, 0.76.

Compound 7 was obtained as the predominant product (>90%) when 10 equiv of NaC $\equiv$ CH were added to acetonitrile solutions of 3 having concentrations greater than 0.02 g/mL. Yellow crystals of 7 containing cocrystallized CH<sub>2</sub>Cl<sub>2</sub> were grown from

CH<sub>2</sub>Cl<sub>2</sub>/Et<sub>2</sub>O. Anal. Calcd. for C<sub>55.5</sub>H<sub>46</sub>ClO<sub>3</sub>OsP<sub>4</sub>Rh: C, 54.94; H, 3.82. Found: C, 54.90; H, 3.85.

(h) **[RhOs(CO)<sub>4</sub>(μ-Ph<sub>2</sub>PCHPh<sub>2</sub>)(μ-dppm)] (9)**. Method (i). To a stirred solution of **3** (100 mg, 0.0713 mmol) in 10 mL of acetonitrile under a stream of CO gas was added a suspension of NaC≡CH (7 mg, 0.146 mmol) in 40 μL of xylene, causing a slight change in colour from yellow to brighter yellow. The mixture was stirred with constant CO purge for 2 h, during which time a bright yellow solid precipitated from solution. NMR studies showed essentially quantitative conversion to compound **9**. The solid was allowed to settle, the pale yellow supernatant was discarded and 15 mL of dichloromethane was added, forming a cloudy yellow solution which was filtered. The solvent volume was reduced to 1 mL under vacuum and 60 mL of Et<sub>2</sub>O was added causing the gradual formation of yellow crystals (39 mg). Isolated Yield 47%. Anal. Calcd. for C<sub>54</sub>H<sub>43</sub>O<sub>4</sub>OsP<sub>4</sub>Rh: C, 55.30; H, 3.70. Found: C, 55.88; H, 3.94.

Method (ii). 50 mg (0.040 mmol) of compound **2** was dissolved in 30 mL of THF to which were added three 0.1-mL portions of 1.7 M <sup>t</sup>BuLi in pentane (0.51 mmol) at 2 h intervals. The resulting solution was stirred for 24 h and the solvent was removed in vacuo. The yellow residue was redissolved in 15 mL of CH<sub>2</sub>Cl<sub>2</sub> and filtered. The solvent was removed in vacuo and <sup>31</sup>P{<sup>1</sup>H} NMR spectra of the solid showed **9** as the only phosphorus-containing product. The residue was redissolved in *ca.* 1 mL of CH<sub>2</sub>Cl<sub>2</sub> and addition of 30 mL of hexanes caused precipitation of a yellow powder. Yield 22 mg (47%).

(i) **[RhOs(CO)<sub>4</sub>(dppm)(Ph<sub>2</sub>PCH(CH<sub>3</sub>)PPh<sub>2</sub>)] [SO<sub>3</sub>CF<sub>3</sub>]•1/2CH<sub>2</sub>Cl<sub>2</sub> (10)**.

Methyl triflate (8 μL, 0.071 mmol) was added by syringe to a stirred yellow solution of **9**

(80 mg, 0.068 mmol) in 10 mL of  $\text{CH}_2\text{Cl}_2$ . No colour change was observed. After 1 h of stirring, the solvent volume was reduced to 2 mL under vacuum and 20 mL of  $\text{Et}_2\text{O}$  was mixed into the yellow solution forming a slightly cloudy mixture. Over 12 h small orange crystals formed. The supernatant was removed and the crystals were dried under vacuum. Yield: 52 mg (65%). Anal. Calcd. for  $\text{C}_{56.5}\text{H}_{47}\text{O}_7\text{F}_3\text{ClP}_4\text{SRhOs}$ : C, 49.19; H, 3.43. Found: C, 49.33; H, 3.51.

**(j)  $[\text{RhOs}(\text{CH}_3)(\text{CO})_3(\text{dppm})_2]$  (11).** Method (i): The complex  $[\text{RhOsCl}(\text{CO})_3(\text{dppm})_2]$  (50 mg, 0.042 mmol) was dissolved in 15 mL of THF and the solvent was degassed with two freeze-pump-thaw cycles. A large excess of  $\text{CH}_3\text{MgCl}$  (approx. 0.5 mL of 3.0 M THF solution, 1.5 mmol) was added via cannula at  $-78^\circ\text{C}$ . The mixture was stirred for 1 h at  $-78^\circ\text{C}$  and then slowly warmed to room temperature. 15 mL of diethyl ether was added and the mixture was washed with 3x25 mL of degassed water. The solvent was removed in vacuo and the residue was recrystallized from THF/hexanes and washed with 2x15 mL of hexanes. Yield 17 mg (35%). Anal. Calcd. for  $\text{C}_{54}\text{H}_{47}\text{O}_3\text{OsP}_4\text{Rh}$ : C, 55.87; H, 4.08. Found: C, 55.03; H, 4.34.

Method (ii):  $[\text{RhOsCl}(\text{CO})_3(\text{dppm})_2]$  (80 mg, 0.0677 mmol) was suspended in 30 mL of THF and cooled to  $0^\circ\text{C}$ . A 0.14 M THF solution of  $\text{CH}_3\text{Li}$  (0.58 mL, 0.081 mmol) was added by syringe and within minutes the yellow suspension turned to an orange solution. After 4 h the solution was filtered and the solvent removed in vacuo. The yellow-orange residue was recrystallized from  $\text{CH}_2\text{Cl}_2/\text{Et}_2\text{O}$  to give 58 mg of yellow solid. The  $^{31}\text{P}$  NMR spectrum showed the solid to be a mixture of  $[\text{RhOsCl}(\text{CO})_3(\text{dppm})_2]$  (35%) and 11 (65%).

Method (iii): 0.1 mL of a 1.4 M THF solution of CH<sub>3</sub>Li in THF (0.14 mmol) was added to a suspension of **2** (50 mg, 0.0397 mmol) in 50 mL THF. Upon addition, the yellow crystals gradually dissolved to form a yellow solution. After 3 h stirring under a slow dinitrogen purge, the solvent was reduced to *ca.* 1 mL and 30 mL of hexanes were added, precipitating a bright yellow solid which was washed with 3x20 mL of hexane and dried in vacuo. The solid was then extracted into 5 mL of CH<sub>2</sub>Cl<sub>2</sub> and filtered. The solvent was reduced to *ca.* 0.5 mL and 10 mL of Et<sub>2</sub>O was slowly added, followed by 20 mL of hexane to precipitate bright yellow solid. Yield 25 mg (46%).

**(k)** [RhOsH(CO)<sub>3</sub>(μ<sup>2</sup>-η<sup>3</sup>-(*o*-C<sub>6</sub>H<sub>4</sub>)PhPCH<sub>2</sub>PPh<sub>2</sub>)(μ-dppm)][CF<sub>3</sub>SO<sub>3</sub>]•Et<sub>2</sub>O (**13a**). 20 μL (0.177 mmol) of neat methyl triflate was syringed directly into a stirred solution of **1** (200 mg, 0.174 mmol) in 15 mL of CH<sub>2</sub>Cl<sub>2</sub>. The solution gradually changed from orange-red to orange-yellow. After 1 h of stirring the solvent was removed in vacuo and the residue was redissolved in 2 mL of CH<sub>2</sub>Cl<sub>2</sub>. Slow addition of Et<sub>2</sub>O caused immediate precipitation of a bright yellow solid (0.172 g) which was washed with 2x20 mL of Et<sub>2</sub>O and dried in vacuo. Yield 72%, Anal. Calcd for C<sub>58</sub>H<sub>54</sub>F<sub>3</sub>O<sub>7</sub>OsP<sub>4</sub>RhS: C, 50.77; H, 3.97. Found: C, 50.90; H, 3.98. Variable temperature NMR in CD<sub>2</sub>Cl<sub>2</sub> showed that the initial product formed at -40°C is [RhOs(CH<sub>3</sub>)(CO)<sub>3</sub>(μ-H)-(dppm)<sub>2</sub>][SO<sub>3</sub>CF<sub>3</sub>] (**12a**). Above 0°C the final product forms.

**(l)** Reaction of **11** with HBF<sub>4</sub>•Et<sub>2</sub>O. Compound **11** (30 mg, 0.025 mmol) was dissolved in 0.5 mL of CD<sub>2</sub>Cl<sub>2</sub> to form a yellow solution. HBF<sub>4</sub>•OEt<sub>2</sub> (7 μL, 0.050 mmol) was added by syringe. <sup>31</sup>P and <sup>1</sup>H NMR showed quantitative conversion to **13**. Variable temperature NMR shows that the initial product at -80°C was [(CH<sub>3</sub>)RhOs(H)(CO)<sub>3</sub>(dppm)<sub>2</sub>][BF<sub>4</sub>] (**14**). At -80°C to -60°C [(CH<sub>3</sub>)RhOs(CO)<sub>3</sub>(μ-H)-

(dppm)<sub>2</sub>][BF<sub>4</sub>] (15) was formed. Above -50°C compound **12b** was observed and above 0°C the final product **13** was formed.

(m) [RhOs(CO)<sub>3</sub>(μ-HC≡CH)(dppm)<sub>2</sub>][CF<sub>3</sub>SO<sub>3</sub>] (16). Compound **1** (100 mg, 0.087 mmol) was dissolved in 10 mL of CH<sub>2</sub>Cl<sub>2</sub> and the flask was purged with HC≡CH. Methyl triflate (10 μL, 14.5 mg, 0.088 mmol) was added, causing a colour change over 15 min from yellow to brown and the formation of a fluffy brown precipitate. After 1 h of stirring, the solution was filtered, resulting in a dark orange/brown solution. The solvent was removed in vacuo and the residue was recrystallized from CH<sub>2</sub>Cl<sub>2</sub>/Et<sub>2</sub>O and dried in vacuo, yielding a brown powder. Yield: 41 mg, 35%.

(n) [RhOs(CH<sub>3</sub>)<sub>2</sub>(CO)<sub>2</sub>(dppm)<sub>2</sub>][CF<sub>3</sub>SO<sub>3</sub>] (17). Compound **11** (40 mg, 0.034 mmol) was dissolved in 5 mL of CH<sub>2</sub>Cl<sub>2</sub>. Methyl triflate (4.3 μL, 6.2 mg, 0.038 mmol) was added causing a colour change from yellow-orange to yellow. The solution was stirred for 1 h and the solvent was removed in vacuo. The pale yellow residue was redissolved in 1 mL of CH<sub>2</sub>Cl<sub>2</sub> and crystallized by slow addition of Et<sub>2</sub>O to form a pale yellow powder. Yield 30 mg, 67%.

#### X-Ray Data Collection.

(a) [RhOs(CH<sub>2</sub>CN)(CO)<sub>3</sub>(dppm)<sub>2</sub>] (**8**). An orange crystal of compound **8**, obtained by slow diffusion of Et<sub>2</sub>O into a concentrated CH<sub>2</sub>CH<sub>2</sub> solution of **8**, was mounted in a glass capillary under nitrogen and solvent vapor, to minimize the possibility of decomposition or solvent loss. Data were collected on an Enraf-Nonius CAD4 diffractometer with use of MoKα radiation. Unit cell parameters were obtained from a least-squares refinement of the setting angles of 24 reflections in the range 20° ≤ 2θ ≤

24°. The diffraction symmetry and the systematic absences indicated the space groups  $Cc'$  or  $C2/c$ ; the latter was established based on the successful refinement of the structure.

Intensity data were collected at 22°C with  $\theta/2\theta$  scans being employed, covering reflections having indices of the form  $+h, +k \pm l$ , to a maximum of 50° in  $2\theta$ . Peak backgrounds were measured by extending the scan range by 25% on either side of the scan region. Three reflections were chosen as intensity and orientation standards, and were remeasured after every 120 min of exposure time; no appreciable decay of these standards was observed. The data were processed in the usual way, with a value of 0.04 for  $p^{11}$  employed to downweight intense reflections; 2891 reflections were considered observed ( $I \leq 3\sigma(I)$ ) and were used in subsequent calculations.<sup>12</sup> The data were corrected for absorption by use of an empirical scheme based on the absorption surface (Fourier filtering) method of Walker and Stuart.<sup>13</sup> See Table 2.2 for crystal and data collection details for both compounds **8** and **11**.

(b)  $[\text{RhOs}(\text{CH}_3)(\text{CO})_3(\text{dppm})_2]$  (**11**). A yellow-orange crystal of **11** was obtained by slow diffusion of  $\text{Et}_2\text{O}$  into a  $\text{CH}_2\text{Cl}_2$  solution of **11**. Data collection for compound **11** proceeded in much the same manner as for **8**. The  $2\theta$  range for centring reflections was  $18^\circ < 2\theta < 26^\circ$ . In this case both space groups  $P1$  and  $\bar{P}1$  were possible, with the latter being confirmed by the successful refinement of the model. Indices of the form  $+h, \pm k, \pm l$  were collected and a linear decay of 14.5% was observed over the span of data collection; the data were corrected for this decay. A total of 3953 unique reflections were observed and used in subsequent calculations.

**Table 2.2.** Crystallographic Experimental Details*A. Crystal Data*

compound	[RhOs(CH <sub>2</sub> CN)(CO) <sub>3</sub> -(dppm) <sub>2</sub> ] ( <b>8</b> )	[RhOs(CH <sub>3</sub> )(CO) <sub>3</sub> -(dppm) <sub>2</sub> ] ( <b>11</b> )
formula	C <sub>55</sub> H <sub>46</sub> NO <sub>3</sub> OsP <sub>4</sub> Rh	C <sub>54</sub> H <sub>47</sub> O <sub>3</sub> OsP <sub>4</sub> Rh
formula weight	1185.99	1160.98
crystal dimensions (mm)	0.40 × 0.35 × 0.20	0.60 × 0.50 × 0.37
space group	C2/c (No. 15)	P $\bar{1}$ (No. 2)
unit cell parameters		
<i>a</i> (Å)	18.313 (3)	11.102 (2)
<i>b</i> (Å)	13.279 (2)	11.684 (3)
<i>c</i> (Å)	22.492 (5)	10.954 (3)
α (°)	90	111.79 (2)
β (°)	115.89 (1)	93.16 (2)
γ (°)	90	68.18 (2)
<i>V</i> (Å <sup>3</sup> )	4921 (3)	1219.2 (8)
<i>Z</i>	4	1
ρ (calcd) (g cm <sup>-3</sup> )	1.601	1.584
μ (cm <sup>-1</sup> )	30.842	31.156

*B. Data Collection and Refinement Conditions*

diffractometer	Enraf-Nonius CAD4 <sup>b</sup>	Enraf-Nonius CAD4 <sup>b</sup>
temperature (°C)	22	22
radiation (λ[Å])	Mo K <sub>α</sub> (0.71073)	Mo K <sub>α</sub> (0.71073)
scan type	θ-2θ	θ-2θ
scan rate (° min <sup>-1</sup> )	6.7–1.4	6.7–1.4
scan width (°)	0.60 + 0.347tanθ	0.60 + 0.347tanθ
maximum 2θ (°)	50.0	50.0
unique reflections measured	4527 ( <i>h k ± l</i> )	4257 ( <i>h ± k ± l</i> )
range of absorption corr. factors	0.7147-1.2214	0.7214-1.4355

(Table 2.2 cont.)

total observations (NO)	2891 ( $F_o^2 \geq 3\sigma(F_o^2)$ )	3953 ( $F_o^2 \geq 3\sigma(F_o^2)$ )
final no. params. varied (NV)	285	307
$R^a$	0.046	0.047
$R_w^b$	0.058	0.077
GOF <sup>c</sup>	1.846	3.019

<sup>a</sup> $R = \Sigma||F_o| - |F_c|| / \Sigma|F_o|$ . <sup>b</sup> $R_w = [\Sigma w(|F_o| - |F_c|)^2 / (\Sigma w F_o^2)]^{1/2}$ . <sup>c</sup>GOF =  $[\Sigma w(|F_o| - |F_c|)^2 / (\text{NO} - \text{NV})]^{1/2}$  where  $w = 4F_o^2 / \sigma^2(F_o^2)$ .

<sup>b</sup>Programs for diffractometer operation and data collection were those supplied by Enraf-Nonius.

### Structure Solution and Refinement.

(a)  $[\text{RhOs}(\text{CH}_2\text{CN})(\text{CO})_3(\text{dppm})_2]$  (**8**). With 4 molecules per unit cell, and no inversion symmetry in the molecule two solutions seemed possible; either space group Cc with one molecule per asymmetric unit or C2/c with the metals lying on the crystallographic 2-fold axes. The Patterson map ruled out the second option and refinement attempts ruled out Cc. Instead the molecule is found to be disordered about the inversion centres. The phosphine groups are well behaved so that only the metals and the  $\text{CH}_2\text{CN}$  and CO ligands in the equatorial plane are affected. In spite of the disorder the atom positions resolved well. After locating the disordered metals from the Patterson map, the atoms of the diphosphine ligands were immediately obvious, and the disordered equatorial ligands were also located without difficulty in subsequent difference Fourier maps. Refinement proceeded by full-matrix least-squares techniques minimizing the function  $\sum w(|F_o| - |F_c|)^2$ , with  $w = 4F_o^2/\sigma^2(F_o^2)$ . The neutral atom scattering factors<sup>14</sup> and anomalous dispersion terms<sup>15</sup> were taken from the usual tabulations. The hydrogen atoms were generated at idealized calculated positions by assuming a C-H bond length of 0.95Å and the appropriate  $\text{sp}^2$  or  $\text{sp}^3$  geometry at carbon. All hydrogens were included in the calculations with fixed, isotropic Gaussian displacement parameters of 1.2 times those of the attached atoms, and were constrained to "ride" on the attached atoms.

The final model with 285 parameters varied converged to  $R = 0.046$  and  $R_w = 0.058$ . In the final difference Fourier map the ten highest residuals (0.2–0.6  $\text{e}\text{\AA}^{-3}$ ) were located near the metal atoms and the CO and  $\text{CH}_2\text{CN}$  ligands, and were judged to be

without chemical significance (a typical carbon on earlier maps had a density of *ca.* 2.3 eÅ<sup>-3</sup>).

**(b) [RhOs(CH<sub>3</sub>)(CO)<sub>3</sub>(dppm)<sub>2</sub>] (11).** Solution and refinement of 11 proceeded in a manner similar to that for 8. In the space group  $P\bar{1}$  the molecule was again found to be disordered about an inversion centre. The orientations of all ligands, even including the orientations of the dppm phenyl groups were found to be very similar to those in 8. Refinement of 11 was handled in the same manner as described above for 8, and converged to  $R = 0.047$  and  $R_w = 0.077$  with 307 parameters varied. In the final difference Fourier map the 10 highest residuals (0.6–2.6 eÅ<sup>-3</sup>) were located near the CO and CH<sub>3</sub> ligands and the metals. A typical carbon on earlier maps had a density of *ca.* 5.1 eÅ<sup>-3</sup>. The positional and isotropic thermal parameters for compounds 8 and 11 are given in Tables 2.3 and 2.4, respectively.

## Results and Compound Characterization

### (a) Mono-alkyl and Related Species.

Our investigations into mono-alkyl, alkyl-hydrido, and dialkyl derivatives of heterobinuclear complexes of Rh and Os began with the acetonitrile hydrido complex, [RhOs(NCMe)(CO)<sub>3</sub>(μ-H)(dppm)<sub>2</sub>][BF<sub>4</sub>]<sub>2</sub> (3). This species is readily prepared from the known precursor [RhOs(CO)<sub>4</sub>(dppm)<sub>2</sub>][BF<sub>4</sub>] (2)<sup>10</sup> by protonation in acetonitrile, as shown in Scheme 2.1. Protonation of the complex leads to exchange of the strong π-acid CO for the good σ-donor CH<sub>3</sub>CN. The IR spectrum of a solid sample of 3 shows two terminal carbonyl bands at 2078 and 2004 cm<sup>-1</sup>, a lower frequency stretch at 1819 cm<sup>-1</sup> (suggesting

**Table 2.3.** Atomic Coordinates and Equivalent Isotropic Displacement Parameters for Selected Atoms of [RhOs(CH<sub>2</sub>CN)(CO)<sub>3</sub>(dppm)<sub>2</sub>] (**8**).<sup>a</sup>

Atom	x	y	z	B, Å <sup>2</sup>
Rh/Os <sup>b</sup>	0.25390(2)	0.16357(3)	-0.03123(2)	3.98(1) <sup>c</sup>
P(1)	0.3155(1)	0.2450(2)	-0.08707(9)	4.44(6) <sup>c</sup>
P(2)	0.3306(1)	0.4279(2)	-0.0026(1)	4.27(5) <sup>c</sup>
O(1) <sup>b</sup>	0.239(1)	-0.007(1)	-0.1193(8)	10.4(5)
O(2)	0.4014(4)	0.1696(6)	0.0930(3)	7.8(2)
N <sup>b</sup>	0.317(1)	0.499(2)	0.192(1)	12.3(7)
C(1) <sup>b</sup>	0.2339(9)	0.070(1)	-0.0902(8)	5.3(4)
C(2) <sup>b</sup>	0.3481(8)	0.160(1)	0.0440(7)	4.3(3)
C(3) <sup>b</sup>	0.1729(8)	0.280(1)	-0.0563(6)	4.1(3)
C(4) <sup>b</sup>	0.2292(9)	0.490(1)	0.0722(7)	4.7(3)
C(5) <sup>b</sup>	0.2841(8)	0.493(1)	0.1371(7)	4.4(3)
C(6)	0.3807(4)	0.3488(6)	-0.0393(4)	5.0(2) <sup>c</sup>

<sup>a</sup>Numbers in parentheses are estimated standard deviations in the least significant digits for quantities in this and subsequent tables. Parameters for phenyl carbon atoms are given in the supplementary material. <sup>b</sup>Atom Rh/Os is half-occupancy in each of Os and Rh, and atoms O(1), N, C(1), C(2), C(3), C(4) and C(5) are half-occupancy owing to disorder. <sup>c</sup>Indicates an atom refined anisotropically. Displacement parameters for the anisotropically refined atoms are given in the form of the equivalent isotropic Gaussian displacement parameter,  $B_{\text{eq}}$ , defined as  $\frac{1}{3}[a^2\beta_{11} + b^2\beta_{22} + c^2\beta_{33} + ab(\cos \gamma)\beta_{12} + ac(\cos \beta)\beta_{13} + bc(\cos \alpha)\beta_{23}]$ .

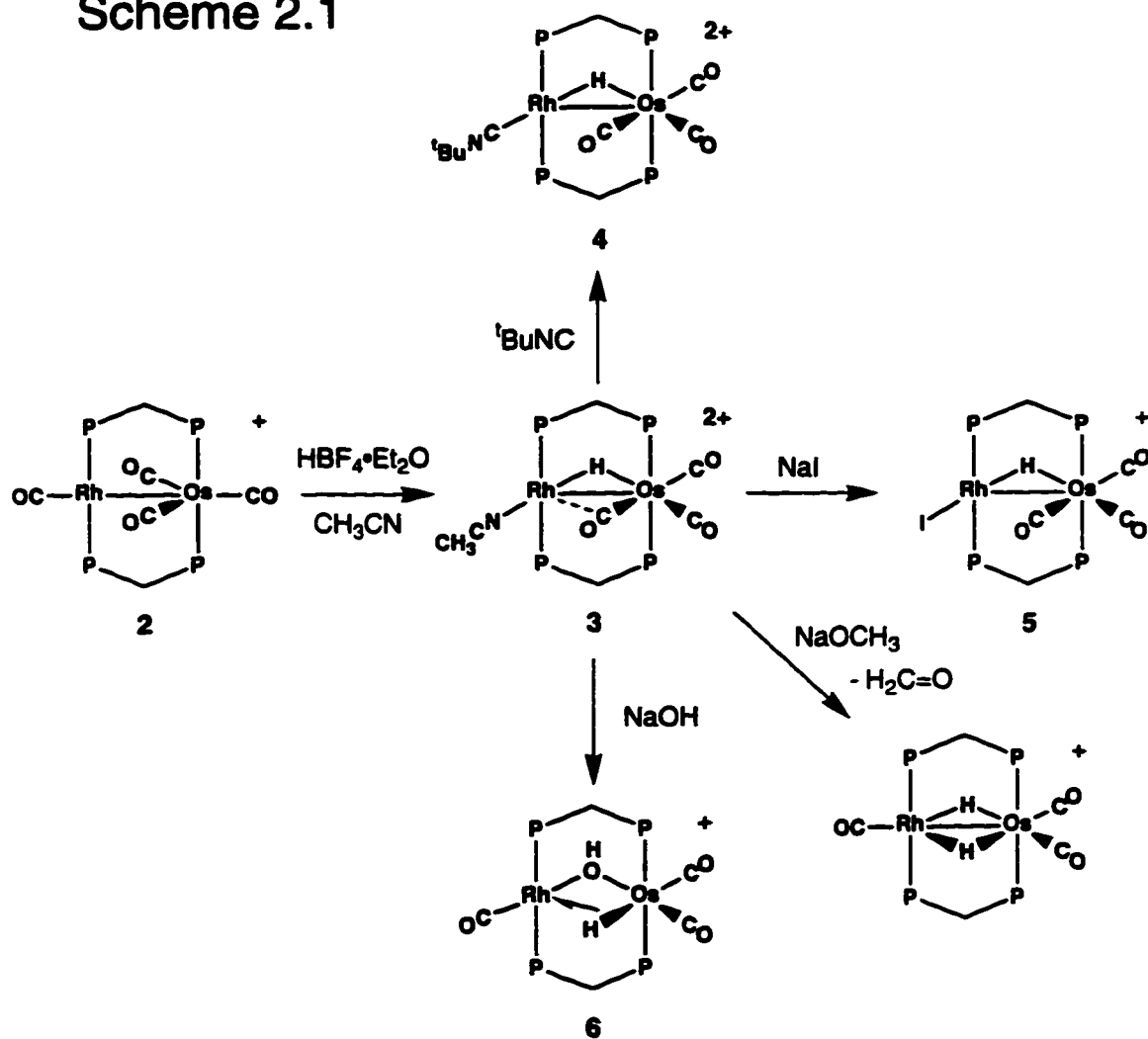
**Table 2.4.** Atomic Coordinates and Equivalent Isotropic Displacement Parameters for Selected Atoms of [RhOs(CH<sub>3</sub>)(CO)<sub>3</sub>(dppm)<sub>2</sub>] (11).<sup>a</sup>

Atom	<i>x</i>	<i>y</i>	<i>z</i>	<i>B</i> , Å <sup>2</sup>
Rh/Os <sup>b</sup>	0.07421(3)	-0.13306(3)	-0.06882(3)	3.413(9) <sup>c</sup>
P(1)	0.1517(2)	-0.1647(1)	0.1198(2)	3.73(4) <sup>c</sup>
P(2)	-0.0286(1)	0.1180(1)	0.2741(2)	3.35(4) <sup>c</sup>
O(1) <sup>b</sup>	0.2903(7)	-0.3952(7)	-0.2070(8)	3.3(2) <sup>c</sup>
O(2)	-0.1849(4)	-0.1085(5)	0.0234(6)	6.1(2) <sup>c</sup>
C(1) <sup>b</sup>	0.222(1)	-0.317(1)	-0.169(1)	5.1(3) <sup>c</sup>
C(2) <sup>b</sup>	-0.082(1)	-0.138(1)	-0.024(1)	3.8(3) <sup>c</sup>
C(3) <sup>b</sup>	0.118(1)	0.046(1)	-0.017(1)	3.4(3) <sup>c</sup>
C(4) <sup>b</sup>	-0.151(2)	0.347(1)	0.183(1)	4.7(4) <sup>c</sup>
C(5)	0.0372(5)	-0.0535(5)	0.2674(6)	3.6(2) <sup>c</sup>

<sup>a</sup>Parameters for phenyl carbon atoms are given in the supplementary material.

<sup>b</sup>Atom Rh/Os is half-occupancy in each of Os and Rh, and atoms O(1), C(1), C(2), C(3) and C(4) are half-occupancy owing to disorder. <sup>c</sup>Indicates an atom refined anisotropically. Displacement parameters for the anisotropically refined atoms are given in the form of the equivalent isotropic Gaussian displacement parameter,  $B_{\text{eq}}$ , defined as  $\frac{1}{3}[a^2\beta_{11} + b^2\beta_{22} + c^2\beta_{33} + ab(\cos \gamma)\beta_{12} + ac(\cos \beta)\beta_{13} + bc(\cos \alpha)\beta_{23}]$ .

Scheme 2.1



a bridging mode for this carbonyl) and two bands attributed to a coordinated ( $2292\text{ cm}^{-1}$ ) and a co-crystallized solvent acetonitrile ( $2321\text{ cm}^{-1}$ ). The solution spectrum was almost identical to the solid state spectrum. The  $^{13}\text{C}\{^1\text{H}\}$  NMR spectrum displays three carbonyl resonances at  $\delta 174.27$ ,  $176.82$  and  $224.47$ , and selective  $^{31}\text{P}$ -decoupling experiments establish that the former two signals correspond to carbonyls terminally bound to Os, whereas the low-field signal shows coupling to the Os-bound phosphorus nuclei and to Rh (25 Hz), confirming its position bridging the metals. Although the coupling of this carbonyl to Rh is substantial, it is somewhat less than the 30-35 Hz expected for a symmetrically bridged carbonyl,<sup>16</sup> and this together with the lack of coupling of this group to the Rh-bound phosphorus nuclei leads to its formulation as being more strongly bound to Os, either in an asymmetric or a semibridging mode.<sup>17</sup> This carbonyl also displays coupling (25 Hz) to one of the terminal CO groups (in the  $^{13}\text{C}$  labeled complex), consistent with a mutually trans arrangement. In the  $^1\text{H}$  NMR spectrum the hydride resonance at  $\delta -15.18$  displays coupling to all four phosphorus atoms and to Rh ( $^1J_{\text{Rh-H}} = 27\text{ Hz}$ ), confirming its bridged position.

Compound **3** appeared to be a potentially useful precursor for a variety of organometallic hydride complexes through displacement of the acetonitrile ligand by neutral or anionic organic groups. This reactivity was initially demonstrated by replacement of NCMe by  $^t\text{BuNC}$  and  $\Gamma$ , yielding  $[\text{RhOs}(^t\text{BuNC})(\text{CO})_3(\mu\text{-H})(\text{dppm})_2][\text{BF}_4]_2$  (**4**) and  $[\text{RhOsI}(\text{CO})_3(\mu\text{-H})(\text{dppm})_2][\text{BF}_4]$  (**5**), respectively. Both products are structurally analogous to the acetonitrile precursor, having very comparable spectroscopic parameters. The IR spectra of compounds **3-5** are closely comparable in both the solid and solution, suggesting no major structural difference in the

two states. Although the low carbonyl stretch in each compound ( $1821\text{ cm}^{-1}$  (4),  $1793\text{ cm}^{-1}$  (5)) again suggests a bridging interaction, the lack of resolvable  $^{103}\text{Rh}$ - $^{13}\text{C}$  coupling in the  $^{13}\text{C}$  NMR implies that the interaction with Rh is weaker than in 3, indicating a weak semi-bridging interaction. In 4 the CN stretch of the  $^t\text{BuNC}$  group ( $2189\text{ cm}^{-1}$ ) is at higher frequency than that of the free ligand ( $2125\text{ cm}^{-1}$ ), indicating that this group functions more as a  $\sigma$  donor than a  $\pi$  acceptor<sup>18</sup> in this dicationic complex.

Similarly, 3 reacts with NaOH to form the hydroxy species  $[\text{RhOs}(\mu\text{-OH})(\mu\text{-H})(\text{CO})_3(\text{dppm})_2][\text{BF}_4]$  (6). The  $^1\text{H}$  NMR for 6 shows an AB quartet with additional coupling to phosphorus for the dppm methylenes, as well as a singlet at  $-0.80$  for the hydroxide hydrogen and a doublet of triplets at  $\delta -2.83$  for the hydride. The hydride of 6, in contrast with those of 3, 4, and 5, shows strong coupling to the osmium-bound phosphines, but only weak coupling (7 Hz) to Rh, and no coupling to the Rh-bound phosphines. Unlike compounds 3-5, in which the hydride is apparently symmetrically bridging the two metals, as shown by the strong coupling to Rh and by coupling to all four  $^{31}\text{P}$  nuclei in the  $^1\text{H}$  NMR spectrum, the hydride in 6 appears to be only interacting weakly with Rh. The  $^{13}\text{C}$  NMR of the carbonyl region shows three resonances at  $\delta 177.61$ ,  $179.15$ , and  $189.99$ . The two high-field resonances correspond to terminal carbonyls on Os and the lowfield resonance is a terminal carbonyl on Rh, appearing as a doublet of triplets, showing coupling to the Rh (71 Hz) and to the Rh-bound phosphines (16 Hz). The IR spectrum is consistent with the  $^{13}\text{C}$  NMR spectrum, showing only terminal carbonyl bands at  $2036$  and  $1946\text{ cm}^{-1}$ . The  $^{31}\text{P}$  NMR spectrum of 6 also contrasts with those of the other complexes (see Figure 2.1). The different

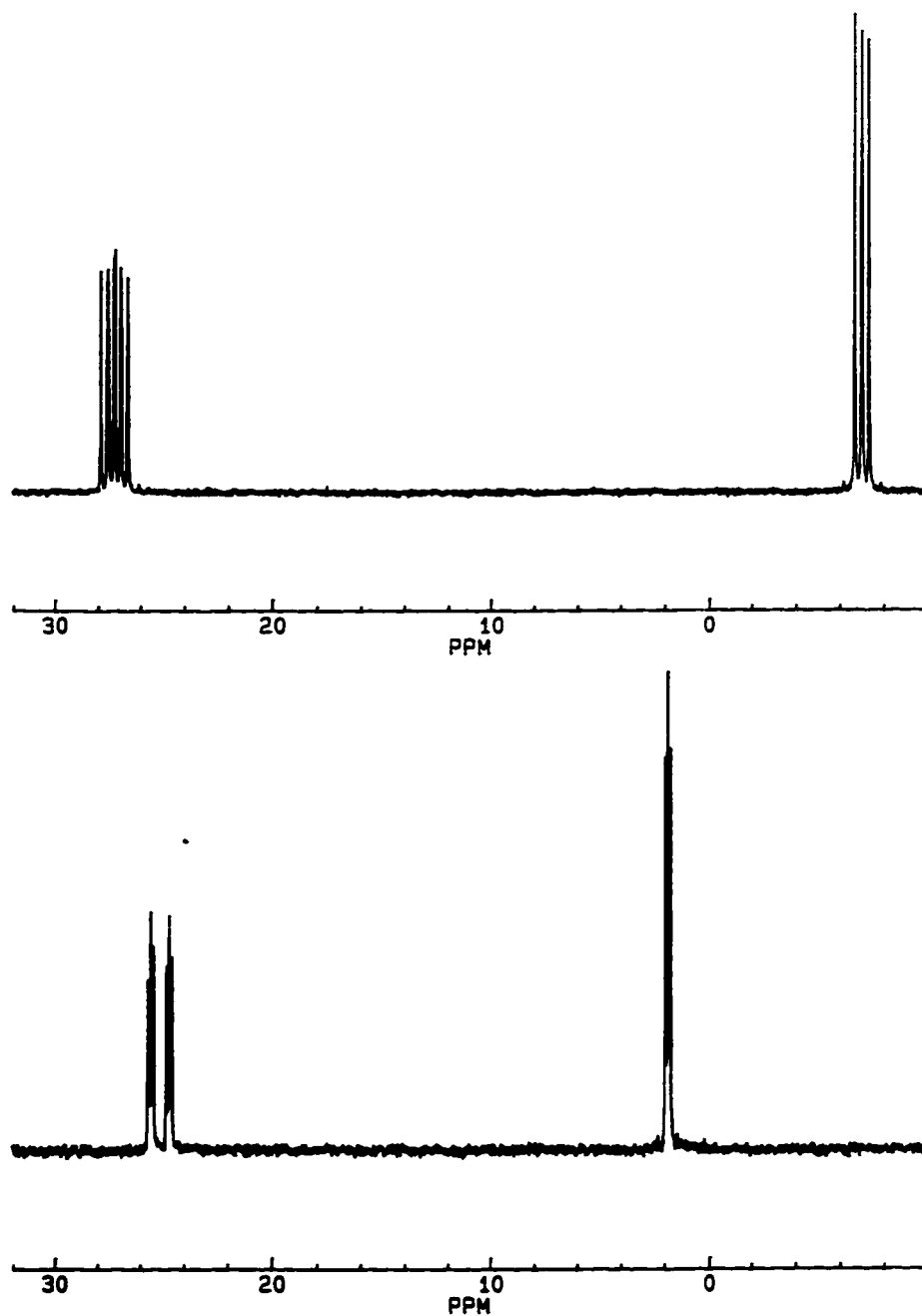


**Figure 2.1.**  $^{31}\text{P}\{^1\text{H}\}$  NMR of  $[\text{RhOs}(\text{CO})_4(\text{dppm})_2][\text{BF}_4]$  (**2**) (top) and  $[\text{RhOs}(\text{CO})_3(\mu\text{-OH})-(\mu\text{-H})(\text{dppm})_2][\text{BF}_4]$  (**6**) (bottom) showing the unusually small coupling constants for **6**.

appearance of the  $^{31}\text{P}$  NMR results from reduced P-P coupling across the dppm methylene. Although there are not enough lines in the spectrum to extract exact coupling constants, simulations using typical coupling constants for these complexes reveal that reducing the P-P coupling constants across the dppm ligands leads to patterns similar to that seen for **6**. The smaller P-P coupling constant is expected for a six-membered ring, as compared to a five membered ring.<sup>19</sup> Related complexes with bridging ligands and no metal-metal bonds that have been structural characterized show a similar pattern in the  $^{31}\text{P}\{^1\text{H}\}$  NMR spectrum.<sup>20</sup> The  $^{31}\text{P}\{^1\text{H}\}$  NMR spectrum, as well as the terminal carbonyl on Rh, suggest that the hydroxyl group occupies a bridging position. This structure results in the favoured 16e/18e count without a metal-metal bond, and a Rh(+1)/Os(+2) formulation.

Compound **3** also reacts with  $\text{NaOCH}_3$ , but in this case the presumed methoxide complex is unstable toward  $\beta$ -hydrogen elimination and the only product observed is the known dihydride complex,  $[\text{RhOs}(\text{CO})_3(\mu\text{-H})_2(\text{dppm})_2][\text{BF}_4]$ .<sup>10</sup>

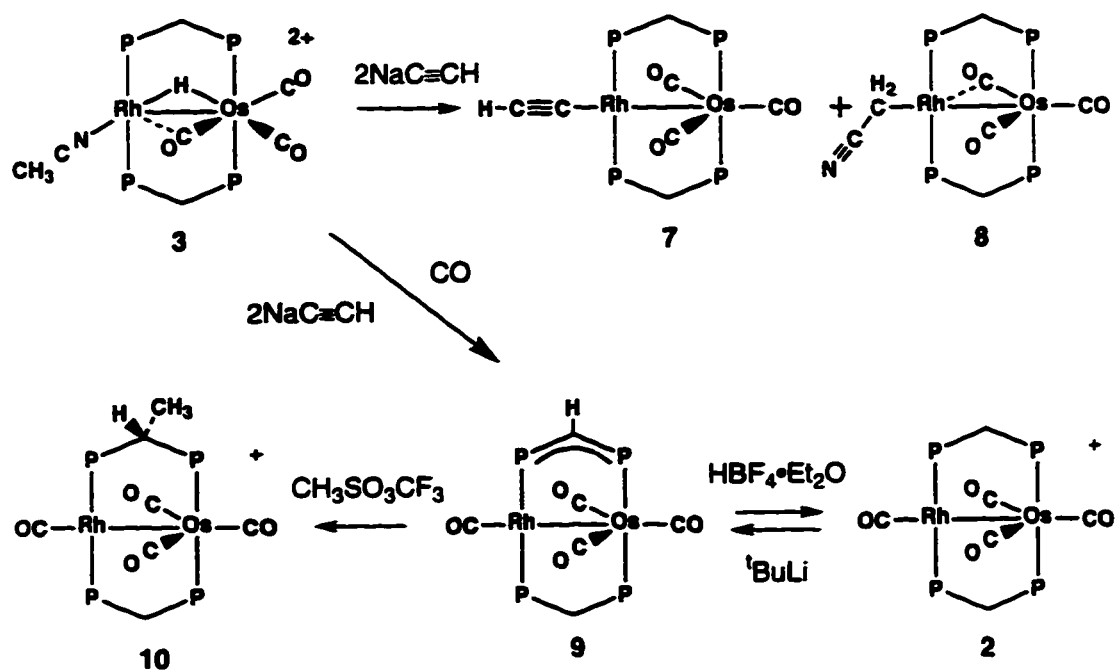
Compound **6** reacts slowly with CO over 24 h to form a mixture of the known complexes  $[\text{RhOs}(\text{CO})_3(\mu\text{-H})_2(\text{dppm})_2][\text{BF}_4]$  and  $[\text{RhOs}(\text{CO})_4(\text{dppm})_2][\text{BF}_4]$ . The dihydride complex likely results from a water-gas shift type reaction in which the hydroxide ligand reacts with CO to form  $\text{CO}_2$  and a hydride, and the tetracarbonyl complex presumably results from subsequent reaction of the dihydride with CO, giving rise to elimination of  $\text{H}_2$ .<sup>10</sup>

Attempts to obtain either an alkyne-hydrido complex or an alkenyl species resulting from alkyne insertion into the metal-hydrogen bond of **3** failed, as no reaction was observed with alkynes such as acetylene, diphenylacetylene, dimethyl

acetylenedicarboxylate or hexafluoro-2-butyne. Presumably, substitution of the  $\sigma$ -donor acetonitrile ligand by  $\pi$  acceptors is not favourable, a conclusion that is in line with the observation that  $t$ BuNC functions primarily as a  $\sigma$  donor in the related species **4** (vide supra). The acetonitrile ligand in **3** surprisingly is not very labile, showing no exchange of this ligand with  $CD_3CN$  solvent, even after several days.

Reaction of **3** with carbanions also occurs, but invariably these stronger bases result in deprotonation at one or more locations in the complex. With sodium acetylide, reaction of **3** in acetonitrile yields two products in a 1:1 ratio (in other solvents a large number of unidentified species resulted). The first product,  $[RhOs(\eta^1-C\equiv CH)(CO)_3(dppm)_2]$  (**7**), shown in Scheme 2.2, is an acetylide complex resulting from deprotonation at the metals and subsequent replacement of the neutral acetonitrile ligand by the second equiv of acetylide ion. The second product quite unexpectedly is the cyanomethyl complex  $[RhOs(CH_2CN)(CO)_3(dppm)_2]$  (**8**), which has apparently resulted from a double deprotonation, removing both the hydrido ligand (as  $H^+$ ) and a proton from the coordinated acetonitrile ligand. This latter deprotonation, although not anticipated, can be rationalized by the expected increase in the acidity of acetonitrile upon coordination to a dicationic species. The possibility that the reaction occurred by deprotonation of acetonitrile solvent followed by attack on **3** by the resulting acetonitrilide anion seems unlikely when the reaction of **3** with  $NaC\equiv CH$  in THF is considered. Although many decomposition products were obtained in this solvent, compound **8** was still obtained in up to 10% yield. Furthermore we saw no evidence of exchange of the coordinated acetonitrile ligand of **3** with solvent THF after 12 h. Further support for deprotonation of coordinated acetonitrile came from the

## Scheme 2.2



reaction of **3** with excess NaOH in acetonitrile which again gave **8** in approximately 10% yield together with decomposition products. NaOH is not a strong enough base to deprotonate free acetonitrile to an appreciable extent.<sup>21</sup> Labelling studies using CD<sub>3</sub>CN were not carried out owing to the large volumes of labeled solvent required. Both products (**7** and **8**) have NMR spectroscopic parameters that are very similar to those of the related methyl complex **11**, which is well characterized (*vide infra*). The acetylide hydrogen in **7** appears as a triplet of doublets at  $\delta$  1.73 in the <sup>1</sup>H NMR spectrum, displaying coupling to the Rh-bound P nuclei (4 Hz) and to Rh (4 Hz); although we have not seen reports of coupling between an acetylide hydrogen and Rh or Rh-bound phosphines, the chemical shift of this proton is in agreement with that reported for another Rh-acetylide complex.<sup>22</sup> Compounds **7** and **8** each display one resonance for the dppm methylene protons and have very similar <sup>13</sup>C NMR spectra, displaying a resonance for a single carbonyl bound to Os at *ca.*  $\delta$  192 and an unresolved multiplet at *ca.*  $\delta$  217, integrating as two carbonyls. Although no Rh coupling is obvious in the latter signal, a small coupling could be masked by the breadth of the peak. It is noteworthy that for compound **8** the unique carbonyl on Os, opposite the Rh-Os bond, shows weak coupling to Rh of 3 Hz. Coupling of this magnitude, through a metal-metal bond, has previously been observed in related systems.<sup>16a</sup> We suggest that both **7** and **8** have weak semibridging interactions much like that spectrally observed in a methyl analogue (**11**) (*vide infra*). The structure proposed for **7** is based on the structural determinations for **8** and **11** (*vide infra*); it appears that an exchange of bonding modes between the semibridging CO and the terminal one on the opposite face is occurring as proposed later for **11**. Compound **8** displays a triplet of doublets for the cyanomethyl group at  $\delta$  0.58

(2H) in the  $^1\text{H}$  NMR spectrum, and this resonance is closely comparable to those observed in a series of related alkyl complexes,<sup>16c,16b,8</sup> including **11** (vide infra). The  $\text{C}\equiv\text{N}$  stretch of this cyanomethyl group is observed at  $2190\text{ cm}^{-1}$  in the IR spectrum and compares favourably to values obtained for a number of cyano-alkyl complexes.<sup>23,24</sup>

Confirmation of this formulation comes from the X-ray structure determination. Although the structure of  $[\text{RhOs}(\text{CH}_2\text{CN})(\text{CO})_3(\text{dppm})_2]$  (**8**) is disordered about the inversion centre (see Experimental section), only the oxygen atoms of two disordered carbonyls and the metals were actually superimposed, so the other disordered atoms were readily resolved. The phosphines were not disordered and are well behaved. A perspective view of **8** is shown in Figure 2.2, while relevant parameters are given in Table 2.5. Whether the cyanomethyl and the carbonyl groups are bound to Rh or Os cannot be established crystallographically owing to the nature of the disorder; however, the connectivity shown is unambiguously established from the NMR studies (vide supra). Both diphosphines bridge the metals in the usual trans arrangement, perpendicular to the plane of the other ligands. The Os centre can be viewed as trigonal bipyramidal, having the three carbonyls in the equatorial plane, with all intercarbonyl angles of approximately  $120^\circ$ . This gives Os its favoured 18e configuration. Rh, with only three ligands attached, requires a dative bond from Os to give it a 16 electron configuration; the resulting Rh-Os distance ( $2.7272(4)\text{\AA}$ ) is normal. In addition, Rh also forms a semibridging interaction with one carbonyl (C(3)O(2')) which is  $\sigma$  bound to Os. Although the parameters involving C(3)O(2') seem to clearly indicate a semibridging geometry for this group, with it being primarily bound to Os (note the Os-C(3)-O(2') angle of  $156.4(9)^\circ$ ), we avoid any

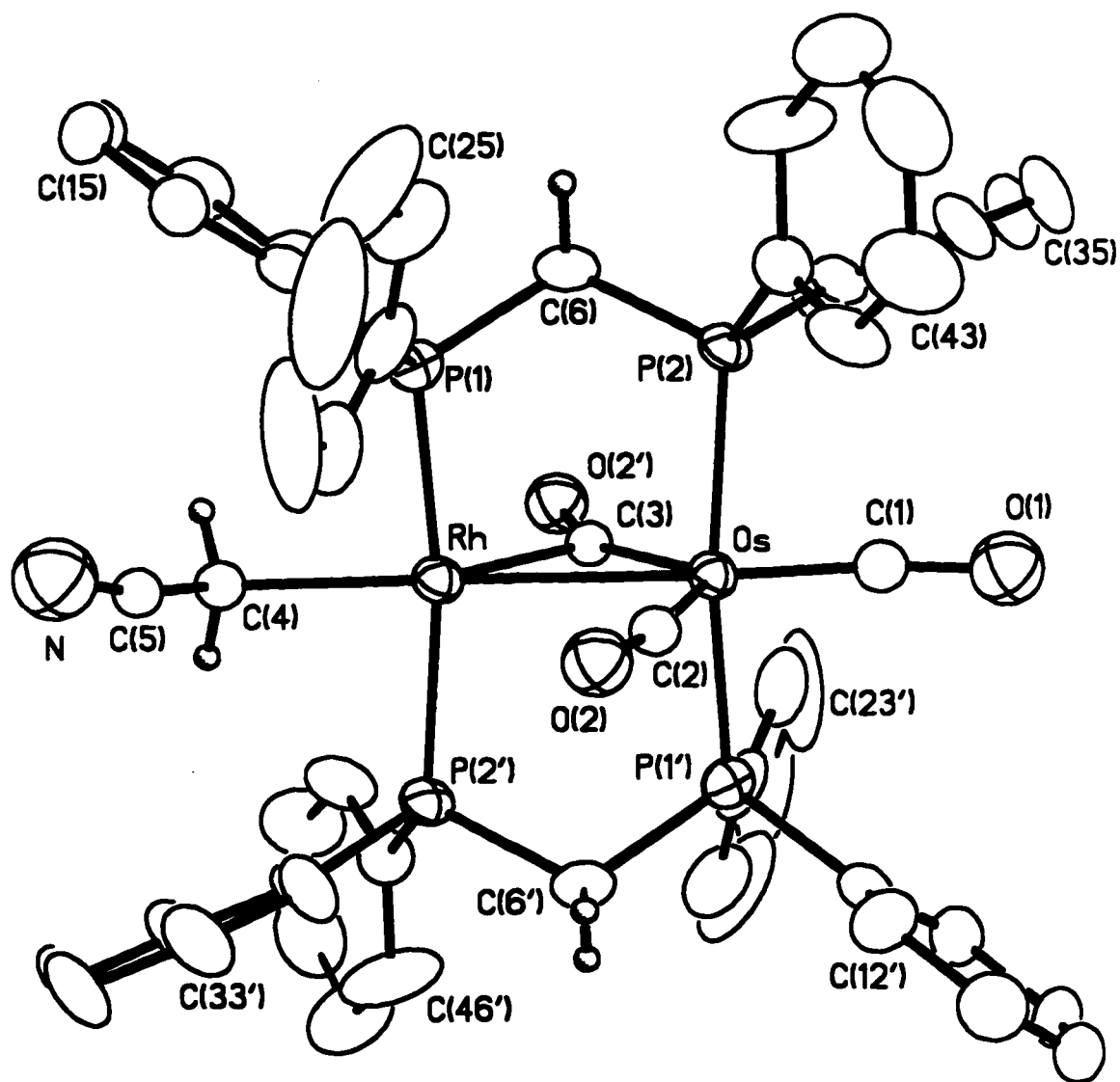


**Figure 2.2.** Perspective view of  $[\text{RhOs}(\text{CH}_2\text{CN})(\text{CO})_3(\text{dppm})_2]$  (8). Thermal ellipsoids are shown at the 20% level, except for hydrogens which are shown arbitrarily small. Phenyl hydrogens have been omitted. Phenyl carbons are numbered sequentially for each phenyl ring beginning with the ipso carbon. (eg C(x1)-C(x6) for x = 1-4)

**Table 2.5.** Selected Distances (Å) and Angles (°) in [RhOs(CH<sub>2</sub>CN)(CO)<sub>3</sub>(dppm)<sub>2</sub>] (8).

Atom1	Atom2	Distance	Atom1	Atom2	Distance
Os	Rh	2.7272 (4)	P(1)	C(6)	1.833 (7)
Os	P(1)	2.293 (2)	P(2)	C(6)	1.813 (7)
Os	P(2')	2.340 (2)	O(1)	C(1)	1.24 (2)
Os	C(1)	1.73 (2)	O(2)	C(2)	1.11 (1)
Os	C(2)	1.82 (1)	O(2')	C(3)	1.41 (1)
Os	C(3)	2.04 (1)	N	C(5)	1.11 (2)
Rh	C(3)	1.98 (1)	C(4)	C(5)	1.36 (2)
Rh	C(4)	2.31 (1)			

Atom1	Atom2	Atom3	Angle	Atom1	Atom2	Atom3	Angle
Rh	Os	P(1)	91.96 (5)	Os	Rh	C(4)	173.3 (3)
Rh	Os	P(2')	94.51 (5)	P(1)	Rh	C(3)	94.9 (3)
Rh	Os	C(1)	162.6 (5)	P(1)	Rh	C(4)	90.8 (3)
Rh	Os	C(2)	77.4 (4)	P(2)	Rh	C(3)	97.4 (3)
Rh	Os	C(3)	46.4 (3)	P(2)	Rh	C(4)	84.0 (3)
P(1)	Os	P(2')	167.47 (7)	C(3)	Rh	C(4)	125.4 (5)
P(1)	Os	C(1)	84.7 (5)	Os	P(1)	C(6)	112.5 (2)
P(1)	Os	C(2)	91.6 (4)	Rh	P(2)	C(6)	112.7 (2)
P(1)	Os	C(3)	87.9 (3)	Os	C(1)	O(1)	162 (2)
P(2')	Os	C(1)	86.0 (4)	Os	C(2)	O(2)	170 (1)
P(2')	Os	C(2)	100.3 (4)	Os	C(3)	Rh	85.2 (5)
P(2')	Os	C(3)	88.8 (3)	Os	C(3)	O(2')	156.4 (9)
C(1)	Os	C(2)	119.7 (7)	Rh	C(3)	O(2')	117.5 (8)
C(1)	Os	C(3)	116.3 (6)	Rh	C(4)	C(5)	107 (1)
C(2)	Os	C(3)	123.7 (5)	N	C(5)	C(4)	167 (2)
Os	Rh	C(3)	48.3 (4)	P(1)	C(6)	P(2)	111.9 (3)

detailed discussion of the bonding involving this carbonyl owing to the disorder. Therefore the abnormally long C(3)-O(2') distance of 1.41(1)Å is probably a consequence of this disorder. The semibridging nature of this interaction is supported however by the almost identical structure of **11**, for which clear evidence of this semibridging interaction also appears in the  $^{13}\text{C}\{^1\text{H}\}$  NMR spectra (vide infra).

The binding mode of the  $\text{CH}_2\text{CN}$  group is shown in Figure 2.2, and all parameters involving this group are as expected. In particular, the angle at C(4) of  $107(1)^\circ$  is close to the tetrahedral value and the essentially linear C(4)-C(5)-N linkage and the short C(5)-N bond (1.11(2)Å) are consistent with the presence of a  $\text{C}\equiv\text{N}$  triple bond.<sup>25,26</sup> The Rh-C(4) distance of 2.31(1)Å is slightly longer than expected for a Rh-alkyl bond; however, the disorder of the groups in the equatorial plane precludes an in-depth discussion of their parameters, since their positions are not accurately determined.

Although compounds **7** and **8** can be independently obtained in high yield by the above route through variations of the stoichiometries and experimental conditions (see Experimental section), attempts to obtain these products by more rational routes were unsuccessful. It appears that obtaining a cyanomethyl complex by deprotonation of a coordinated acetonitrile ligand is unusual; more conventional routes involve oxidative addition of an  $\alpha$ -halo acetonitrile to a metal,<sup>23</sup> halide displacement from  $\text{XCH}_2\text{CN}$  by anionic complexes,<sup>23,24</sup> or nucleophilic attack by cyanide ion on a methyldene complex.<sup>24</sup> There are also reports of formation of cyanomethyl complexes via C-H activation of acetonitrile.<sup>25</sup>

Under a CO atmosphere the reaction of **3** with sodium acetylide takes a very different and unexpected course, resulting in deprotonation of the metals and of one dppm

group, yielding  $[\text{RhOs}(\text{CO})_4(\text{dppm-H})(\text{dppm})]$  (**9**) (dppm-H = bis(diphenylphosphino)methanide). The  $^{31}\text{P}\{^1\text{H}\}$  NMR spectrum of **9** shown in Figure 2.3, displays a complex pattern of an ABCDX spin system in which all four phosphorus nuclei (ABCD) are chemically inequivalent. Simulation of the spectrum gives values of 321 and 117 Hz for the P-P coupling across Rh and Os, respectively, consistent with a trans arrangement of the phosphines at both metals. The much larger values of trans P-P coupling across Rh than Os appear typical.<sup>26</sup> In addition, the  $^2J_{\text{P-P}}$  value within the deprotonated dppm group (159 Hz) is greater than that within the normal dppm (96 Hz), consistent with  $\pi$  delocalization over the deprotonated group and  $\text{sp}^2$ , rather than  $\text{sp}^3$  hybridization of the central carbon. The methanide proton appears at higher field ( $\delta$  2.84) as a broad resonance compared to the dppm methylene signal, which is an apparent triplet at  $\delta$  4.16; such an upfield shift upon deprotonation has previously been observed.<sup>27,28</sup>

We assume that the different reactivity of **3** with sodium acetylide under CO results from substitution of NCMe by CO at some stage of the reaction, leaving the hydrido ligand and the dppm methylene groups as the only remaining acidic sites in the molecule. Although **9** was obtained in only *ca.* 50% isolated yield, spectroscopically monitoring the reaction indicated that conversion of **3** to **9** was essentially quantitative. Sodium acetylide also reacts with the cationic tetracarbonyl **2**, but surprisingly **9** is *not* obtained by deprotonation of a dppm methylene group; instead two other unidentified products result. This indicates that **2** is not an intermediate in the double deprotonation of **3** by  $\text{NaC}\equiv\text{CH}$  under CO. However, compound **9** can be obtained as the only observable species (by NMR) from **2** through the use of  $^t\text{BuLi}$  as the base. The latter route presents a more rational synthesis of **9** than the double deprotonation of **3** by sodium

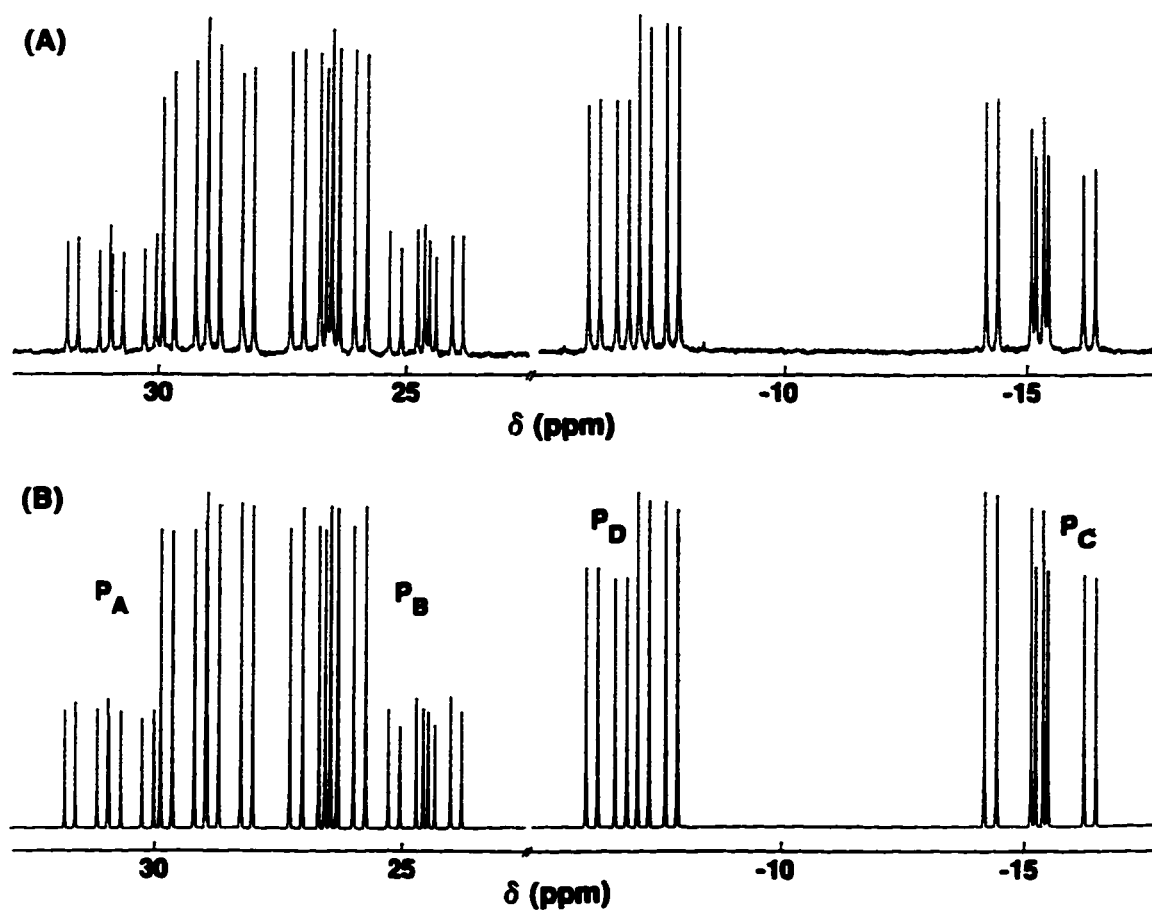


**Figure 2.3.** Experimental (top) and calculated (bottom)  $^{31}\text{P}\{^1\text{H}\}$  NMR spectrum of Compound 9 showing the ABCDX coupling pattern.

acetylide.

Compound **9** reacts with methyl triflate resulting in alkylation of the methanide carbon to give  $[\text{RhOs}(\text{CO})_4(\text{dppmMe})(\text{dppm})][\text{SO}_3\text{CF}_3]$  (**10**). This appears to be the only reported example of substitution of a methylene hydrogen of a *bridged* dppm group by an alkyl group. Prior synthesis of dppmMe and its subsequent coordination to metals has been described,<sup>29-33</sup> and direct alkylation of dppm bound to a single metal has also been reported.<sup>34-36</sup> Although in one report<sup>35</sup> the alkylation of bridging dppm was noted as under investigation, no report has appeared. Surprisingly, the related complex,  $[\text{Li}(\text{THF})_4][\text{Re}_2(\text{CO})_8(\mu\text{-dppm-H})]$ , was inert to alkylation of the methanide carbon,<sup>27</sup> and alkylation of a (dppm-H)-bridged dirhodium compound occurred at a bridging amido group and *not* at the methanide carbon of dppm-H.<sup>28b</sup> Apparently in **9** there is no site nucleophilic enough to compete with the methanide carbon.

The  $^{31}\text{P}\{^1\text{H}\}$  NMR spectrum of **10** appears as an ABCDX spin system and derived parameters (Table 1) are consistent with our formulation; in particular the intraligand P-P coupling within dppm and dppmMe are almost identical. In the  $^1\text{H}$  NMR spectrum the methyl signal appears at  $\delta$  1.34 and the three signals for the protons on the methylenic carbons appear at  $\delta$  4.44, 4.03 and 3.77. Owing to the front-back asymmetry in **10**, imposed by the methyl substituent, four distinct carbonyl resonances are also observed in the  $^{13}\text{C}$  NMR spectrum.

As anticipated, protonation of **9** occurs much like alkylation, with this electrophile again attacking the methanide carbon of dppm-H to regenerate compound **2**, together with the appropriate anion.

The iodo-hydrido complex **5** also appeared to be a potential precursor to hydrido alkyl complexes, via replacement of the iodo ligand by reaction with a Grignard reagent. Again, however, deprotonation occurs so readily that no hydride complex is obtained, although the neutral alkyl complex  $[\text{RhOs}(\text{CH}_3)(\text{CO})_3(\text{dppm})_2]$  (**11**), can be isolated in low yield in the reaction of **5** with MeMgI. The  $^1\text{H}$  NMR spectrum of **11** shows the methyl resonance as a triplet of doublets at  $\delta$  -0.35. The coupling of the methyl hydrogens to the adjacent phosphorus atoms ( $^3J_{\text{P-H}} = 7$  Hz) and to Rh ( $^2J_{\text{Rh-H}} = 2$  Hz) is typical for such species.<sup>16c,16b,8</sup> The spectroscopic properties involving the carbonyls in **11** are similar to those of compounds **7** and **8**, yet have important minor differences. In the IR spectrum **11** shows a very low carbonyl stretch at  $1723\text{ cm}^{-1}$  consistent with a bridging interaction of this group. In addition, the low-field  $^{13}\text{C}$  resonance ( $\delta$  220.2), corresponding to two carbonyl ligands, displays coupling to Rh of 13 Hz; this is clearly much less than expected for a symmetrically bridged CO and indicates a semibridging geometry having a weaker, although substantial, interaction with Rh. Although one resonance for two carbonyls implies that both are semibridging, the solid-state structure indicates that only one is semibridging (vide infra), and the solution IR spectrum is almost identical to that in the solid (apart from broader bands in the former), showing three carbonyl stretches, of which only one is at low frequency. It appears therefore that a fluxional process exchanges the semibridging CO with the terminal CO on the opposite face of the complex. This exchange is extremely facile since no change in the  $^{13}\text{C}$  NMR spectrum was obvious to  $-80^\circ\text{C}$ .

The X-ray structure determination of **11** confirms the structural assignment, as shown in Figure 2.4, and although this structure was also disordered, it was resolved

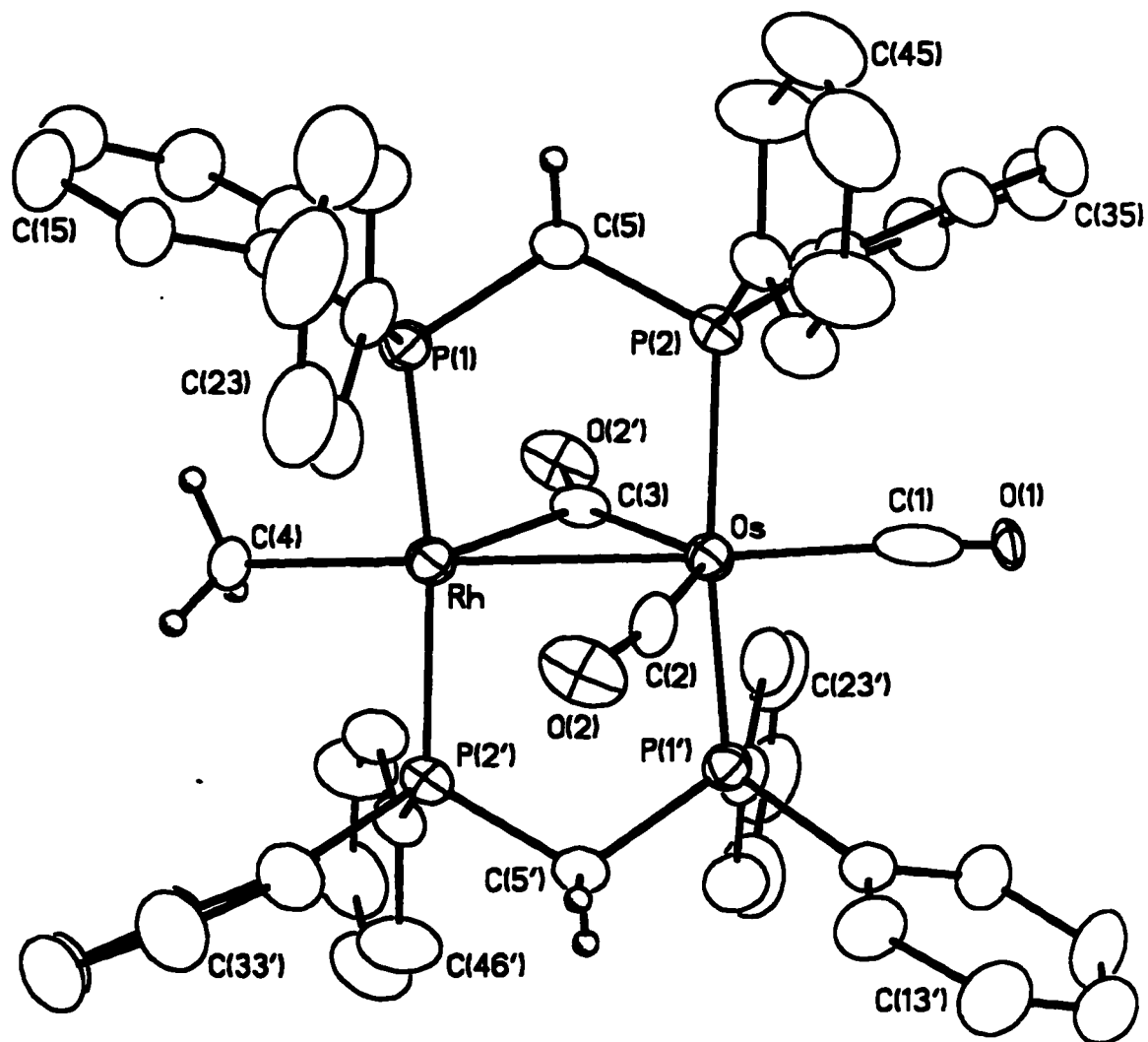


**Figure 2.4.** Perspective view of  $[\text{RhOs}(\text{CH}_3)(\text{CO})_3(\text{dppm})_2]$  (11). Thermal ellipsoids are shown at the 20% level, except for hydrogens which are shown arbitrarily small. Phenyl hydrogens have been omitted. Phenyl carbons are numbered sequentially for each phenyl ring, beginning with the ipso carbon.

satisfactorily, allowing a meaningful discussion of at least the important structural features. Important structural parameters are given in Table 2.6. At osmium, the geometry is that of a coordinatively saturated trigonal bipyramidal,  $\text{OsL}_2(\text{CO})_3$  moiety; the phosphines are essentially trans ( $171.25(4)^\circ$ ) and the angles between the equatorial carbonyl groups are all close to  $120^\circ$ . Having only a methyl group and two ends of the diphosphines bound to Rh leaves this metal with only 14 valence electrons, necessitating a dative bond from Os to give Rh an essentially square planar, 16e configuration. The observed Rh-Os separation of  $2.7643(9)\text{\AA}$  is clearly consistent with a significant metal-metal interaction associated with a single bond. Donation from Os to Rh in addition to the methyl group, which is also a good donor, and the two diphosphine ligands causes a buildup of electron density at Rh which is alleviated by the semi-bridging interaction with  $\text{C}(3)\text{O}(2)'$ . Surprisingly the shorter metal-C(3) distance ( $2.087(8)\text{\AA}$ ) is to Rh and not to Os ( $2.183(9)\text{\AA}$ ) (much as in **8**), even though this carbonyl is significantly more linear with respect to Os than Rh ( $\text{Os-C}(3)\text{-O}(2)' = 153.9(7)^\circ$ ,  $\text{Rh-C}(3)\text{-O}(2)' = 124.9(7)^\circ$ ), which indicates a stronger interaction with Os. The shorter Rh-C(3) distance may in part be due to the smaller radius of  $\text{Rh}^{+1}$  compared to that of  $\text{Os}^0$ ,<sup>37</sup> but may also be, in part, a consequence of the disorder. However we feel that this disorder has been satisfactorily resolved, so that these distances together with the  $^{103}\text{Rh}\text{-}^{13}\text{C}$  coupling for this CO in the  $^{13}\text{C}\{^1\text{H}\}$  NMR spectra, indicate substantial  $\pi$  donation from Rh to C(3). The structure also shows that exchange of the semibridging and one terminal carbonyl in solution (vide supra) would require movement of only the two carbonyl carbon atoms by *ca.*  $0.4\text{\AA}$ , indicating that very little change in the overall configuration of the molecule is required.<sup>39</sup> Although the positions of the disordered methyl and carbonyl ligands are for the most

**Table 2.6.** Selected Distances (Å) and Angles (°) in [OsRh(CO)<sub>3</sub>(CH<sub>3</sub>)(dppm)<sub>2</sub>] (11).

Atom1	Atom2	Distance	Atom1	Atom2	Distance
Os	Rh	2.7643 (9)	Rh	C(4)	2.183 (8)
Os	P(1)	2.298 (1)	P(1)	C(5)	1.832 (4)
Os	P(2')	2.333 (1)	P(2)	C(5)	1.834 (4)
Os	C(1)	2.08 (2)	O(1)	C(1)	0.91 (1)
Os	C(2)	1.859 (8)	O(2)	C(2)	1.151 (8)
Os	C(3)	2.183 (9)	O(2')	C(3)	1.244 (8)
Rh	C(3)	2.087 (8)			

Atom1	Atom2	Atom3	Angle	Atom1	Atom2	Atom3	Angle
Rh	Os	P(1)	92.64 (4)	Os	Rh	C(3)	51.2 (2)
Rh	Os	P(2')	93.26 (4)	Os	Rh	C(4)	167.7 (3)
Rh	Os	C(1)	166.2 (3)	P(1')	Rh	C(3)	91.3 (2)
Rh	Os	C(2)	77.5 (3)	P(1')	Rh	C(4)	91.6 (3)
Rh	Os	C(3)	48.2 (2)	P(2)	Rh	C(3)	97.4 (2)
P(1)	Os	P(2')	171.25 (4)	P(2)	Rh	C(4')	83.9 (3)
P(1)	Os	C(1)	85.3 (2)	C(3)	Rh	C(4)	117.2 (4)
P(1)	Os	C(2)	89.4 (3)	Os	P(1)	C(5)	113.1 (1)
P(1)	Os	C(3)	92.1 (2)	Rh	P(2)	C(5)	113.6 (1)
P(2')	Os	C(1)	87.5 (2)	Os	C(1)	O(1)	175.5 (9)
P(2')	Os	C(2)	98.2 (3)	Os	C(2)	O(2)	163.0 (7)
P(2')	Os	C(3)	87.0 (2)	Os	C(3)	Rh	80.7 (2)
C(1)	Os	C(2)	116.0 (4)	Os	C(3)	O(2')	153.9 (7)
C(1)	Os	C(3)	118.3 (4)	Rh	C(3)	O(2')	124.9 (7)
C(2)	Os	C(3)	125.6 (3)	P(1)	C(5)	P(2)	110.6 (2)

part well defined, that of C(1) is poorly defined as shown by the long Os-C(1) and short C(1)-O(1) distances, and by the elongated thermal ellipsoid of C(1) (see Figure 2.4). Although both compounds **8** and **11** show disorder of the alkyl and carbonyl ligands, limiting any structural interpretations, the structural parameters of the two compounds are closely comparable, giving us confidence in the gross structural features.

Superior routes for synthesizing **11** utilize either the analogous chloro complex,  $[\text{RhOsCl}(\text{CO})_3(\text{dppm})_2]$  or compound **2**. Compound **11** can be obtained in moderate yields (*ca.* 35%) in the reactions of  $[\text{RhOsCl}(\text{CO})_3(\text{dppm})_2]$  with either  $\text{MeMgCl}$  or  $\text{LiCH}_3$ . Of these two routes, that involving the Grignard is the better since we were never able to obtain the methyl compound **11** free from the starting chloride via the latter route. Even with the former method the Grignard must be destroyed with water immediately after the reaction to minimize reconversion of the methyl to the chloro compound. Another route to **11**, involving the reaction of **2** (as the  $\text{BF}_4^-$  salt) with  $\text{LiCH}_3$ , appears to be the best route and is the one currently used.

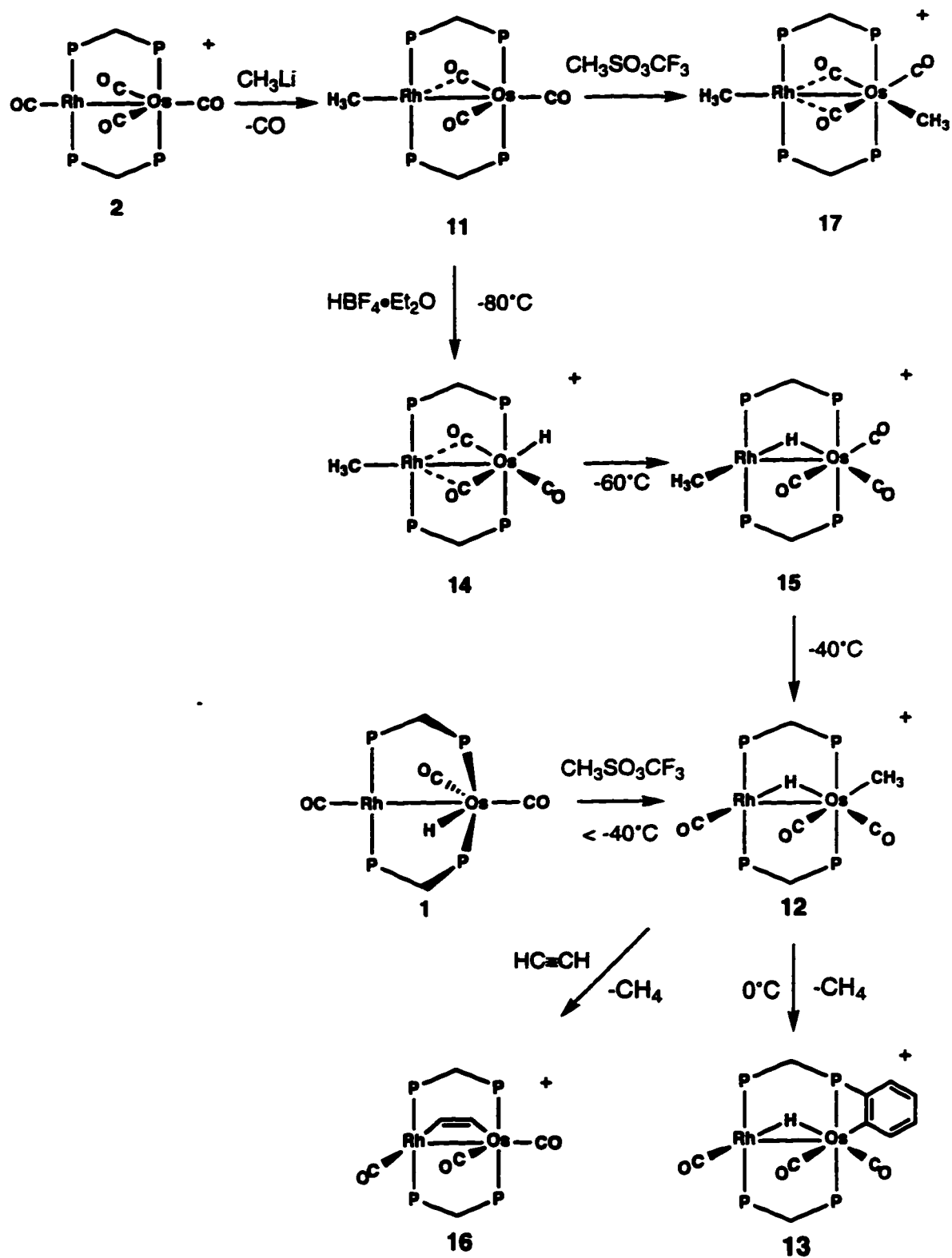
#### **(b) Hydrido-Methyl Complexes and Reductive Elimination of $\text{CH}_4$ .**

One of our original goals had been the synthesis of binuclear hydrido alkyl complexes to allow the investigation of the reductive elimination of the alkane fragment from the two metal centres. Two obvious routes to such a species involved alkylation (using a source of  $\text{CH}_3^+$ ) of the hydrido complex **1** (outlined in Scheme 2.3) or protonation of the alkyl complex **11**. At  $-40^\circ\text{C}$  alkylation of **1** yields a metastable hydrido alkyl complex  $[\text{RhOs}(\text{CH}_3)(\text{CO})_3(\mu\text{-H})(\text{dppm})_2][\text{SO}_3\text{CF}_3]$  (**12a**). At lower temperatures the reaction proceeded more slowly and did not occur appreciably at  $-80^\circ\text{C}$ .

Compound **12a** was the only observed product over the temperature range of  $-80^{\circ}$  to  $-40^{\circ}\text{C}$ . The  $^1\text{H}$  NMR spectrum of **12a** displays the hydride resonance at  $\delta$  -12.90 with coupling to all P nuclei and to Rh, indicating a bridged geometry, and the methyl resonance at  $\delta$  -0.43 with coupling to only the P nuclei on Os (as shown by selective  $^{31}\text{P}$  decoupling), indicating that it is terminally bound to this metal. One carbonyl in the  $^{13}\text{C}\{^1\text{H}\}$  NMR spectrum shows 75 Hz coupling to Rh, indicating its terminal coordination to this metal, and two carbonyls appear as broad singlets and are bound to Os, in agreement with the formulation shown on Scheme 2.3. Allowing a solution of **12a** to warm to ambient temperature results in methane evolution (as detected in the  $^1\text{H}$  NMR) to yield the orthometallated product,  $[\text{RhOs}(\text{CO})_3(\mu^2\text{-}\eta^3\text{-(o-C}_6\text{H}_4\text{)PPhCH}_2\text{PPh}_2\text{-(}\mu\text{-H)}(\text{dppm}))][\text{SO}_3\text{CF}_3]$  (**13a**). The  $^{31}\text{P}\{^1\text{H}\}$  NMR spectrum of this product shows a complex pattern for four chemically distinct  $^{31}\text{P}$  nuclei and simulation of this spectrum is consistent with a trans arrangement of phosphines at both metals. The IR,  $^1\text{H}$ , and  $^{13}\text{C}$  NMR spectra are also consistent with the structure shown on Scheme 2.3. Orthometallation is assumed to be at Os since both signals for the two Rh-bound  $^{31}\text{P}$  nuclei in the  $^{31}\text{P}$  NMR spectrum are near those in other  $\text{Rh}^{+1}$  systems reported in this paper, whereas the signals for the Os-bound  $^{31}\text{P}$  nuclei are widely separated with one at rather high field, consistent with the presence of a strained 4-membered ring<sup>19</sup> involving the orthometallated phenyl group.

Since the hydrido methyl intermediate **12a**, which preceded methane loss, contained a methyl group bound to Os, we undertook the preparation of this species via protonation of **11**, which has the methyl group bound to Rh. It was of interest to determine whether methane elimination from the Rh centre might occur in this case, or

## Scheme 2.3



whether rearrangement to **12** would precede methane loss. At  $-80^{\circ}\text{C}$  reaction of **11** with  $\text{HBF}_4\cdot\text{OEt}_2$  yields a new hydrido methyl complex  $[(\text{CH}_3)\text{RhOsH}(\text{CO})_3(\text{dppm})_2][\text{BF}_4]$  (**14**), which was shown by  $^1\text{H}$  and  $^1\text{H}\{^{31}\text{P}\}$  experiments to have the methyl group still bound to Rh while the hydrido ligand is terminally bound to Os. At  $-60^{\circ}\text{C}$  this species transforms to the isomer **15**, which still has the methyl group on Rh but now has the hydrido ligand bridging the metals. At  $-40^{\circ}\text{C}$  compound **15** undergoes another rearrangement to yield **12b**, which is identical to **12a** apart from the  $\text{BF}_4^-$  anion instead of  $\text{SO}_3\text{CF}_3^-$ . No other intermediates are observed when **12b** is warmed to give **13b**. The absence of resolvable coupling of the methyl protons to Rh in the  $^1\text{H}$  NMR spectra of both compounds **14** and **15** is not surprising considering that the line widths of these resonances at these temperatures were 4-5 Hz; as noted earlier, Rh-H coupling in methyl complexes such as **11** is generally only *ca.* 2 Hz.

Reaction of the deuterio analogue of **1**  $[\text{RhOsD}(\text{CO})_3(\text{dppm})_2]$  with  $\text{CH}_3^+$  in  $\text{CD}_2\text{Cl}_2$  or  $\text{CH}_2\text{Cl}_2$  at ambient temperature gives  $\text{CH}_3\text{D}$ , as observed in the  $^2\text{H}$  NMR, and compound **13**, in which no deuterium incorporation was observed. This reaction confirms that the hydrogen atom required for conversion of the methyl ligand to methane comes from the hydrido ligand and not from elsewhere, such as the dppm groups, and that the hydrido ligand in the orthometallated product **13** comes from dppm.

Reductive elimination of methane from compound **12** has the potential to serve as a method to generate a coordinatively unsaturated intermediate for reaction with substrate molecules. This reactivity was demonstrated by the reaction of **1** with methyl triflate in the presence of acetylene. In the presence of acetylene, the orthometallation reaction does not take place upon methane elimination. Instead the presumed unsaturated

intermediate reacts to form  $[\text{RhOs}(\text{CO})_3(\mu\text{-HC}\equiv\text{CH})(\text{dppm})_2][\text{CF}_3\text{SO}_3]$  (16), which was characterized by conventional means and contains a bridging acetylene group which is bound parallel to the metal-metal axis.

The methyl complex 11 also reacts with methyl triflate. Again, the site of electrophilic attack is at Os and results in the formation of  $[\text{RhOs}(\text{CH}_3)_2(\text{CO})_3(\text{dppm})_2][\text{CF}_3\text{SO}_3]$  (17). The  $^1\text{H}$  NMR spectrum of 17 shows a triplet at  $\delta$  -0.15 which is coupled to the Os-bound phosphines ( $^3J_{\text{PH}} = 6$ ), and a doublet of triplets at 0.73, which couples to Rh and to the Rh-bound phosphines ( $^3J_{\text{PH}} = 6$  Hz,  $^2J_{\text{RHH}} = 2$  Hz). The  $^{13}\text{C}$  NMR spectrum of 17 differs from those of the mono-alkyl complexes. In this case there are three sharp resonances for carbonyls at  $\delta$  179.59, 206.67, and 230.22. The two lower field resonances show coupling to Rh of 14 and 24 Hz, respectively. These peaks are sharp, suggesting that there is no exchange process as in 11, and that both the carbonyls are semibridging. This proposed structure is supported by the structure determinations of  $[\text{RhOs}(\text{C}(\text{CH}_3)=\text{C}(\text{CH}_3)_2(\text{CH}_3)(\text{CO})_3(\text{dppm})_2][\text{CF}_3\text{SO}_3]$  (23) (see Chapter 3) and  $[\text{RhRu}(\text{CH}_3)_2(\text{CO})_3(\text{dppm})_2][\text{CF}_3\text{SO}_3]$  (43) (see Chapter 5), which also have one organic group on each metal and an arrangement of carbonyl ligands as proposed for 17. In contrast to the methyl/hydride complexes, the dimethyl complex is unreactive towards reductive elimination, even when heated. Surprisingly, it is also unreactive towards CO and  $\text{H}_2$ .

## Discussion

Transition-metal hydrido complexes occupy a key position in organometallic chemistry. Their reactions with olefins, alkynes and other unsaturated substrates yield

alkyl, alkenyl and related species via insertions into the M-H bonds, and hydrido complexes also having  $\sigma$ -bound organic ligands present are important intermediates leading to organic products through the reductive elimination of these fragments from the metal. Clearly such species are pivotal in a variety of catalytic processes in which hydrogen transfer to an unsaturated substrate occurs.<sup>39</sup>

A series of alkyl and related species, of the form  $[\text{RhOsR}(\text{CO})_3(\text{dppm})_2]$  ( $\text{R} = \text{CH}_3, \text{CH}_2\text{CN}, \text{C}\equiv\text{CH}$ ), have been prepared. In all cases the organic group is  $\sigma$ -bound to Rh, in spite of our expectation that the Os-C bond is stronger than Rh-C.<sup>40</sup> The observed structures, having the alkyl group on Rh, give the metals a  $\text{Rh}^{+1}/\text{Os}^0$  formulation, whereas having the  $\sigma$ -bound organic group on Os would result in a  $\text{Rh}^0/\text{Os}^{+1}$  formulation. We suggest that the  $\text{Rh}^{+1}/\text{Os}^0$  combination is one important driving force favouring the structures obtained. Clearly however, this cannot be the sole factor since the analogous hydride species  $[\text{RhOsH}(\text{CO})_3(\text{dppm})_2]$  has the hydride on Os and a  $\text{Rh}^0/\text{Os}^{+1}$  formulation.

The X-ray studies on **8** and **11**, together with the spectroscopic data on related species, indicate that in most cases Rh is involved in one semibridging interaction with a carbonyl on Os in the solid state. In solution, the two carbonyls directed towards Rh exchange between bridging and terminal positions. It is suggested that this semibridging interaction stabilizes these species by removing the excess charge from Rh that results from the good donor ability of the alkyl group<sup>41</sup> and from the absence of another  $\pi$  acceptor on Rh. In addition, the Os $\rightarrow$ Rh dative bond, required to give Rh a 16e configuration also gives rise to a charge build-up on Rh. The presence of at least one

accompanying semibridging carbonyl group is typical of these A-frame-like alkyls.<sup>16b,16c,21</sup>

The extent of carbonyl semibridging appears to correlate well with the  $\sigma$ -donor ability of the group on Rh. The absence of a strong semibridging carbonyl (as indicated by significant  $^{103}\text{Rh}$ - $^{13}\text{C}$  coupling, and the IR stretches) in either **7** or **8** is understandable in view of the acetylide and cyanomethyl groups in the respective compounds being poorer net donors to Rh than  $\text{CH}_3$ , resulting in less  $\pi$  back donation to the semibridging CO groups.<sup>42</sup> Although we suggest a weaker semibridging interaction in **8** than in **11**, on the basis of NMR studies, it should be recalled that the comparable solid-state structures suggest substantial interactions for both compounds.

Addition of an electrophile to Os to form cationic dialkyl complexes results in the formation of a second semibridging carbonyl interaction. There are two factors that favour bridging of both carbonyls. First, the geometry at Os is now pseudo-octahedral, rather than trigonal-bipyramidal, allowing both carbonyls to form semibridging interactions without large distortions. Secondly, the carbonyls are now bound to a cationic  $\text{Os}^{+2}$  centre instead of a neutral  $\text{Os}^0$  centre. Less electron density is available from Os, making back donation from Rh more favourable. It is clear from the Rh-C coupling constants that one semi-bridging interaction is substantially stronger than the other (24 vs 14 Hz). It is suggested that the stronger interaction is with the bridging carbonyl trans to the carbonyl that is terminally bound to osmium. This  $\mu$ -carbonyl receives less back-donation from Os, since it competes with a trans carbonyl, and thus can accept more electron density from Rh. The carbonyl trans to the methyl group is more tightly bound to Os.

Reductive elimination of methane from methyl-hydride species has been shown to be site specific; even when the methyl group is initially on Rh, reductive elimination occurs from the Os centre. This is not the result expected on the basis of bond strengths<sup>40</sup> or kinetic labilities,<sup>43</sup> which should favour elimination from the second row element (Rh). We assume that reductive elimination from Rh is inhibited by the trans arrangement of the hydride and methyl groups in the appropriate intermediate, and by the unfavourable, highly coordinatively unsaturated 14e Rh centre which would result, having only two phosphines coordinated. Analogous diplatinum complexes having a trans arrangement of terminal methyl and bridging hydride ligands have been shown to be remarkably inert towards methane elimination.<sup>44</sup> Instead, reductive elimination of methane occurs from the pseudo-octahedral Os<sup>+2</sup> centre, in which we assume a cis arrangement of H and CH<sub>3</sub> groups. The reductive elimination of methane from Os yields an unstable, coordinatively unsaturated Os<sup>0</sup> centre which rapidly leads to orthometallation of one of the dppm phenyl rings to give a saturated Os<sup>+2</sup> centre. Facile oxidative addition to a 16e Os<sup>0</sup> centre is well known.<sup>45</sup> The reactions in which a hydride is transferred from a terminal site to a bridging site, and a methyl group transfers from Rh to Os are not straightforward, and it is not clear how these transformations occur.

**References**

1. (a) Atwood, J. D. *Coord. Chem. Rev.* **1988**, *83*, 93.  
(b) Collman, J.P.; Hegedus, L.S.; Norton, J.R.; Finke, R.G. *Principles and Applications of Organotransition Metal Chemistry*; University Science Books: Mill Valley, California, 1987, Chapter 12.
2. (a) *Comprehensive Organometallic Chemistry*, Vol. 10, Abel, E. W.; Wilkinson, G., Stone, F.G.A., (eds), Pergamon, Oxford, 1994.  
(b) Chaudret, B.; Delvaux, B.; Poilblanc, R. *Coord. Chem. Rev.* **1988**, *86*, 191.
3. (a) Antwi-Nsiah, F.; Cowie, M. *Organometallics* **1992**, *11*, 3157.  
(b) Antwi-Nsiah, F.H.; Oke, O.; Cowie, M. *Organometallics* **1996**, *15*, 506.  
(c) Antwi-Nsiah, F.H.; Oke, O.; Cowie, M. *Organometallics* **1996**, *15*, 1042.
4. (a) Parshall, G. W.; Ittel, S. D. *Homogeneous Catalysis*; John Wiley & Sons: New York, 1992.  
(b) Gates, B. C. *Catalytic Chemistry*; John Wiley & Sons: New York, 1992.
5. (a) Dombek, B.D. *Organometallics* **1985**, *4*, 1707; and references therein.  
(b) Braunstein, P.; Rose, J. in *Comprehensive Organometallic Chemistry II*, Vol. 10, Wilkinson, G., Stone, F.G.A. (eds), Pergamon, Oxford, 1994, Chapt. 7.
6. Antonelli, D. M.; Cowie, M. *Organometallics*, **1992**, *10*, 1297.
7. Wang, L.-S., Cowie, M. *Can. J. Chem.*, **1995**, *73*, 1058.
8. Graham, T.; Van Gastel, F.; Cowie, M., manuscript in preparation, describing alkyl complexes of RhMo.
9. Antonelli, D.M.; Cowie, M. *Organometallics* **1990**, *9*, 1818.
10. (a) Hilts, R.W.; Franchuk, R.A.; Cowie, M. *Organometallics* **1991**, *10*, 304.

- (b) Sterenberg, B. T.; Hiltz, R. W.; Moro, G.; McDonald, R.; Cowie, M. *J. Am. Chem. Soc.* **1995**, *117*, 245.
11. Doedens, R.J.; Ibers, J.A. *Inorg. Chem.* **1967**, *6*, 204.
12. Programs used were those of the Enraf-Nonius Structure Determination Package by B.A. Frenz, in addition to local programs by R.G. Ball.
13. Walker, N.; Stuart, D. *Acta Crystallogr., Sect. A: Found. Crystallogr.* **1983**, *A39*, 158.
14. (a) Cromer, D.T.; Waber, J.T. *International Tables for Crystallography*; Kynoch Press: Birmingham, England, 1974; Vol. IV, Table 2.2A.  
(b) Stewart, R.F.; Davidson, E.R.; Simpson, W.T. *J. Chem. Phys.* **1965**, *42*, 3175.
15. Cromer, D.T.; Liberman, D. *J. Chem. Phys* **1970**, *53*, 1891
16. (a) Jenkins, J.A.; Cowie, M. *Organometallics* **1992**, *11*, 2767.  
(b) Antwi-Nsiah, F.; Cowie, M. *Organometallics* **1992**, *11*, 3157.  
(c) Antonelli, D.M.; Cowie, M. *Organometallics* **1991**, *10*, 2550.
17. Colton, R.; McCormick, M.J. *Coord. Chem. Rev.* **1980**, *31*, 1.
18. Treichel, P.M. *Adv. Organometal. Chem.* **1973**, *11*, 21.
19. (a) Garrou, P.E. *Inorg. Chem.* **1975**, *14*, 1435.  
(b) Garrou, P.E. *Chem. Rev.* **1981**, *81*, 229.
20. Wang, L-S.; McDonald, R.; Cowie, M. *Inorganic Chemistry*, **1994**, *33*, 3735.
21. March, J. *Advanced Organic Chemistry*; John Wiley & Sons: New York, 1992; Chapter 8.
22. Stang, P.J.; Crittall, C.M. *Organometallics* **1990**, *9*, 3191.

23. Porta, F.; Ragaini, F.; Cenini, S.; Demartin, F. *Organometallics* **1990**, *9*, 929.
24. Crocco, G.L.; Lee, K.E.; Gladysz, J.A. *Organometallics* **1990**, *9*, 2819.
25. (a) English, A.D.; Herskovitz, T. *J. Am. Chem. Soc.* **1977**, *99*, 1648.  
(b) Ittel, S.D.; Tolman, C.A.; English, A.D.; Jesson, J.P. *J. Am. Chem. Soc.* **1978**, *100*, 7577.
26. (a) Jenkins, J.A. M.Sc. Thesis, Dalhousie University, 1984.  
(b) Hilts, R.W., Cowie, M. Unpublished results.
27. Dominguez, R.; Lynch, T.J.; Wang, F. *J. Organometal Chem.* **1988**, *338*, C7.
28. (a) Sharp, P.R.; Ge, Y.-W. *J. Am. Chem. Soc.* **1987**, *109*, 3796.  
(b) Sharp, P.R.; Ge, Y.-W. *Inorg. Chem.* **1993**, *32*, 94.
29. Kraihanzel, C.S.; Maples, P.K. *J. Organometal. Chem.* **1976**, *117*, 159.
30. van der Ploeg, A.M.J.; van Koten, G. *Inorg. Chim. Acta* **1981**, *51*, 225.
31. Sommer, K. *Z. Anorg. Chem.* **1970**, *376*, 37.
32. Dean, P.A.W.; Srivastava, R.S. *Can. J. Chem.* **1985**, *63*, 2829.
33. Lee, C.-L.; Yang, Y.-P.; Rettig, S.J.; James, B.R.; Nelson, D.A.; Lilga, M.A. *Organometallics* **1986**, *5*, 2220.
34. Al-Jibori, S.; Shaw, B.L. *J. Chem. Soc., Chem. Commun.* **1982**, 286.
35. Al-Jibori, S.; Shaw, B.L. *Inorg. Chem. Acta* **1982**, *65*, L123.
36. Al-Jibori, S.; Shaw, B.L. *Inorg. Chem. Acta* **1983**, *74*, 235.
37. The radii for the metals are, Rh (1.34), Os (1.35) (see: Wells, A.F. "*Structural Inorganic Chemistry*", Oxford University Press, London, 1975, p. 1020) so that for  $\text{Rh}^{+1}$  will be even smaller than that of Os.

38. This distance was calculated by leaving O(2') in its observed position and moving C(3) to a position to give a linear Os-C(3)-O(2') unit.
39. (a) Pruetz, R.L. *Adv. Organometal. Chem.* **1979**, *17*, 1.  
(b) James, B.R. *Adv. Organometal. Chem.* **1979**, *17*, 319.  
(c) Speier, J.L. *Adv. Organometal. Chem.* **1979**, *17*, 407.  
(d) Parshall, G.W. "Homogeneous Catalysis"; John Wiley & Sons: New York, 1980; Chapters 3, 4, 8.  
(e) Halpern, J.A. *Inorg. Chim. Acta* **1981**, *50*, 11.
40. (a) Ziegler, T.; Tschinke, V. *Bonding Energetics in Organometallic Compounds*; American Chemical Society: Washington, DC 1990, T.J. Marks, ed.; Chapter 19.  
(b) Ziegler, T.; Tschinke, V.; Ursenbach, B. *J. Am. Chem. Soc.* **1987**, *109*, 4825.  
(c) Armentrout, P.B. *Bonding Energetics in Organometallic Compounds*; American Chemical Society: Washington, DC 1990, T.J. Marks, ed.; Chapter 2.
41. Rees, W.M.; Churchill, M.R.; Li, Y.-J.; Atwood, J.D. *Organometallics* **1985**, *4*, 1162.
42. Lichtenberger, D.L.; Renshaw, S.K.; Bullock, R.M. *J. Am. Chem. Soc.* **1993**, *115*, 3276.
43. Shen, J.-K.; Tucker, D.S.; Basolo, F.; Hughes, R.P. *J. Am. Chem. Soc.* **1993**, *115*, 11312; and references therein.
44. (a) Brown, M.P.; Cooper, S.J.; Frew, A.A.; Muir, K.W.; Puddephatt, R.J.; Thompson, M.A. *J. Chem. Soc., Dalton Trans.* **1982**, 299.  
(b) Azam, K.A.; Puddephatt, R.J. *Organometallics* **1983**, *2*, 1396.
45. Collman, J.P.; Roper, W.R. *Adv. Organometal. Chem.* **1968**, *7*, 53.

## Chapter 3

### Vinyl, Allyl and Related Complexes of Rh/Os From Alkynes and Allenes

#### Introduction

In this chapter we extend the organometallic chemistry of our previously studied “Rh/Os” systems<sup>1</sup> to include  $\sigma$ -bound organic groups having unsaturation within their framework. Two such groups are the vinyl ( $-\text{CH}=\text{CH}_2$ ) and allyl ( $-\text{CH}_2\text{CH}=\text{CH}_2$ ) moieties and their substituted analogues. The unsaturation in these groups means that, in addition to being  $\sigma$ -bound to one metal, simultaneous  $\pi$ -donation to an adjacent metal is also possible. How this  $\mu,\eta^1:\eta^2$ -interaction can modify the reactivity of the group, or its ability to influence the chemistry at a metal by stabilizing coordinatively unsaturated intermediates, was of interest to us.

The proposed involvement of vinyl groups in Fischer-Tropsch chemistry<sup>2</sup> has permitted an explanation of the propagation steps that successfully accounts, not only for the lower than expected amounts of  $\text{C}_2$  products obtained, but also for the formation of small amounts of branched-chain hydrocarbons. A key part of this proposal involves the isomerization of substituted allyl groups to the corresponding vinyl groups on the metal surface. An investigation of allyl and vinyl ligands in the presence of our mixed Rh/Os system was therefore of interest to us, particularly as it relates to C-C bond formation,<sup>3</sup> and is reported herein. Related studies on binuclear Ru complexes had previously shown

and is reported herein. Related studies on binuclear Ru complexes had previously shown an extensive chemistry of bridging vinyl groups,<sup>4</sup> suggesting tremendous potential for our heterobinuclear species.

## Experimental Section

**General Comments.** 3-methyl-1,2-butadiene, dimethyl acetylenedicarboxylate, and allyl magnesium chloride (2.0 M solution in THF) were purchased from Aldrich, and allene was obtained from Matheson. Dioxane was distilled over sodium benzophenone under an atmosphere of prepurified nitrogen. Spectroscopic data for all compounds are given in Table 3.1.

### Preparation of the Compounds.

(a)  $[\text{RhOs}(\text{C}(\text{CH}_3)=\text{CH}_2)(\text{CO})_3(\text{dppm})_2]$  (**18**). Allene or propyne was passed over a solution of  $[\text{RhOs}(\text{H})(\text{CO})_3(\text{dppm})_2]$  (**1**; 200 mg, 0.174 mmol) in 20 mL of  $\text{CH}_2\text{Cl}_2$  for 3 min causing an immediate colour change from yellow-orange to orange. The solution was then stirred under allene or propyne for 30 min and the solvent was removed in vacuo. The dark orange residue was recrystallized from  $\text{CH}_2\text{Cl}_2/\text{Et}_2\text{O}$ , washed with 3x20 mL of  $\text{Et}_2\text{O}$  and dried in vacuo, yielding a bright orange powder. Yield: 0.155g, 0.131 mmol, 75%. Anal. Calcd. for  $\text{C}_{56}\text{H}_{59}\text{O}_3\text{OsP}_4\text{Rh}$ : C, 56.67; H, 4.16. Found: C, 56.41; H, 3.93. If the allene reaction was carried out without recrystallization, the sample was found to contain approx. 10% of compound **19**.

Table 3.1. Spectroscopic Parameters for the Compounds<sup>a</sup>

compound	IR, $\text{cm}^{-1}$	NMR <sup>d</sup>	
		$\delta(\text{P}\{\text{H}\})$	$\delta(\text{H})$
$[\text{RhOs}(\text{C}(\text{CH}_3)=\text{CH}_2)-(\text{CO})_2(\text{dppm})_2] (\mathbf{18})$	1910 (ss), 1861 (ss), 1725 (ss)	RhP: 31.23 ( $J_{\text{RhP}} = 158$ Hz) OsP: 5.54	PCH <sub>2</sub> P (25°): 3.44 (b, 4H) (0°): 3.25 (m, 2H), 3.19 (m, 2H) (75°): 3.46 (pq, 4H, J = 5 Hz) <sup>d</sup> RhC=CH <sub>2</sub> : 3.73 (bs), 4.77 (bs) RhC-CH <sub>2</sub> : 0.76 (s, 3H)
$[\text{RhOs}(\text{CH}_2\text{CH}=\text{CH}_2)(\text{CO})_2(\text{dppm})_2] (\mathbf{19})^e$	1910 (sb), 1852 (sb), 1715 (sb)	RhP: 27.34 (vb) OsP: 1.32	OsCO: 226.5 (bs, 2C); 189.6 (bs, 1C)
(b) -80°C		P <sub>A</sub> : 36.80; P <sub>B</sub> : 9.80; P <sub>C</sub> : 4.73; P <sub>D</sub> : -5.20 J(P <sub>A</sub> P <sub>B</sub> ) = 22 Hz J(P <sub>A</sub> P <sub>C</sub> ) = 112 Hz J(P <sub>A</sub> P <sub>D</sub> ) = 35 Hz J(P <sub>B</sub> P <sub>C</sub> ) = 28 Hz J(P <sub>B</sub> P <sub>D</sub> ) = 119 Hz J(P <sub>C</sub> P <sub>D</sub> ) = 242 Hz J(RhP <sub>A</sub> ) = 157 Hz J(RhP <sub>B</sub> ) = 125 Hz	CH <sub>C</sub> : 5.55 PCH <sub>2</sub> P: 4.46, 4.12, 3.85, 3.07 CH <sub>S</sub> : 2.53, 1.30 CH <sub>A</sub> : 0.99, 0.22 OsCO: 188.3 (bs); 204.7 (bs); 253.4 (bs)

compound	IR, $\text{cm}^{-1}$	NMR <sup>d</sup>	
		$\delta(^1\text{P}\{\text{H}\})$	$\delta(^1\text{C}\{\text{H}\})$
$[\text{RhOs}(\text{C}(\text{CH}_3)=\text{C}(\text{CH}_3)_2)(\text{CO})_2(\text{dppm})_2]$ (20)	1924 (ss), 1875(ss), 1707(ss)	RhP: 28.52 ( $^1J_{\text{RhP}} = 160$ Hz) OsP: 4.79	PC $\text{H}_2$ P: 3.4 (m, 2H) 3.5 (m, 2H) RhC-CH $_3$ : 0.95 (s, 3H) RhC=C(CH $_3$ ) $_2$ : 0.80 (bs, 3H), 0.40 (bs, 3H) OsCO: 196.7 (tm, $^2J_{\text{OsC}} = 15$ Hz); 216.7 (bm); 228.2 (bs)
$[\text{RhOs}(\text{CH}_3\text{O}_2\text{CC}=\text{C}(\text{H})\text{CO}_2\text{CH}_3)(\text{CO})_2(\text{dppm})_2]$ (21)	1950, 1921, 1895	32.46 (RhP, $^1J_{\text{RhP}} = 143$ Hz) 0.81 (OsP)	OsCO: 190.35 (t, 1C, $^2J_{\text{OsC}} = 14$ Hz), 210.6 (bs, 1C), 225.1 (bs, 1C) RhC=C $\text{H}$ : 4.12 (dt, 1H, $^3J_{\text{RhH}} = 2$ Hz, $^4J_{\text{H}} = 1$ Hz) PC $\text{H}_2$ P: (AB) 3.8 (dm, 2H), 3.05 (dm, 2H) C $\text{H}_3$ : 3.0 (s, 3H), 2.8 (s, 3H)
$[\text{RhOs}(\text{C}(\text{O})\text{C}(\text{CH}_3)=\text{CH}_2)(\text{CO})_2(\text{dppm})_2]$ (22)	1934(m), 1882(ss), 1720(m), 1555(ms) <sup>c</sup>	RhP: 27.20 ( $^1J_{\text{RhP}} = 164$ Hz) OsP: 4.56	OsCO: 194.10 (m); 206.38 (bs); 230.47 (bs) RhCO: 271.93 (dt, $^1J_{\text{RhC}} = 31$ Hz, $^2J_{\text{RhC}} = 5$ Hz) OsCO: 179.4 (m); 201.9 (s); 230 (m)
$[\text{RhOs}(\text{C}(\text{CH}_3)=\text{CH}_2)(\text{CH}_3)(\text{CO})_2(\text{dppm})_2][\text{CF}_3\text{SO}_3]$ (23a)	2032 (sb), 1840 (mb), 1805 (sb) (both isomers)	RhP: 21.74 ( $^1J_{\text{RhP}} = 150$ Hz) OsP: -5.07	PC $\text{H}_2$ P: 3.38(m, 2H), 3.26(m, 2H) RhC=C $\text{H}_2$ : 5.11 (s, 1H), 4.18 (s, 1H) RhC-CH $_3$ : 1.05 (s, 3H) OsCH $_3$ : -0.23 (t, 3H, $^3J_{\text{OsPH}} = 6.5$ Hz)
(23b)		RhP: 22.24 ( $^1J_{\text{RhP}} = 158$ Hz) OsP: -5.93	OsCO: 179.4 (m); 203.5 (s); 230 (m)

compound	IR, $\text{cm}^{-1}$	NMR <sup>a</sup>	
		$\delta(^1\text{P}\{\text{H}\})$	$\delta(^1\text{C}\{\text{H}\})$
$[\text{RhOs}(\text{C}(\text{CH}_3)=\text{C}(\text{CH}_3)_2)-(\text{CH}_3)_2(\text{CO})_2(\text{dppm})_2]-[\text{CF}_3\text{SO}_3]$ (24a)	2041 (ss), 1860 (w), 1808 (ss)	RhP: 19.31 ( $^1J_{\text{RhP}} = 154$ Hz) OsP: -4.79	OsCO: 180.8 (m); 204.4 (t, $^3J_{\text{OsPC}} = 5$ Hz); 231.5 (bm)  PCH <sub>2</sub> P: 3.35 (m, 4H) RhC-CH <sub>3</sub> : 1.15 (s, 3H) RhC=C(CH <sub>3</sub> ) <sub>2</sub> : 0.90 (bs, 3H), 0.40 (bs, 3H) OsCH <sub>3</sub> : -0.3 (t, 3H) $^3J_{\text{OsPH}} = 6.5$ Hz
(24b)	2032 (sh), 1832 (w), 1789 (ms)	RhP: 19.80 ( $^1J_{\text{RhP}} = 152$ Hz) OsP: -6.29	OsCO: 180.1 (m); 201.6 (bm); 233.0 (m)  PCH <sub>2</sub> P: 3.44 (m, 4H) RhC-CH <sub>3</sub> : 1.05 (s, 3H) RhC=C(CH <sub>3</sub> ) <sub>2</sub> : 0.90 (bs), 0.50 (bs) OsCH <sub>3</sub> : -0.1 (t, $^3J_{\text{OsPH}} = 7$ Hz)
$[\text{RhOs}(\text{CH}_3\text{O}_2\text{CC}=\text{C}(\text{H})-\text{CO}_2\text{CH}_3)(\text{CH}_3)(\text{CO})_2-(\text{dppm})_2][\text{SO}_3\text{CF}_3]$ (25)	2055 (ss) 1955 (ss) 1920 (sh)	23.49 (RhP, $^1J_{\text{RhP}} = 129$ Hz) -3.03 (OsP)	OsCO: 180.1 (bs, 1C), 192.6 (bs, 1C), 224.2 (bs, 1C)  RhC=CH: 4.73 (dt, 1H, $^3J_{\text{RhH}} = 3$ Hz, $^1J_{\text{PH}} = 1$ Hz) PCH <sub>2</sub> P: (AB) 3.59 (dm, 2H), 3.2 (dm, 2H); CH <sub>3</sub> : 3.1 (s, 3H), 3.05 (s, 3H) OsCH <sub>3</sub> : -0.6 (t, 3H, $^3J_{\text{OsPH}} = 7$ Hz)
$[\text{RhOs}(\text{C}(\text{CH}_3)=\text{CH}_2)(\text{H})-(\text{CO})_2(\text{dppm})_2][\text{BF}_4]$ (26a)	2033(ms), 1984(ss), 1942(ms), 1799(mb), 1770(sb) (both isomers)	RhP: 22.88 ( $^1J_{\text{RhP}} = 149$ Hz) OsP: -1.24	OsCO: 180.1 (bs, 1C), 192.6 (bs, 1C), 224.2 (bs, 1C)  PCH <sub>2</sub> P: 3.3 (m, 4H), RhC=CH <sub>2</sub> : 5.2 (s, 1H), 4.55 (s, 1H) RhC-CH <sub>3</sub> : 0.75 (s, 3H) OsH: -6.8 (t, 1H, $^3J_{\text{OsPH}} = 18$ Hz)
(26b)		RhP: 24.40 ( $^1J_{\text{RhP}} = 149$ Hz) OsP: -1.24	OsCO: 180.1 (bs, 1C), 192.6 (bs, 1C), 224.2 (bs, 1C)  PCH <sub>2</sub> P: 3.4 (m, 4H), RhC=CH <sub>2</sub> : 5.1 (s, 1H), 3.9 (s, 1H) RhC-CH <sub>3</sub> : 1.15 (s, 3H) OsH: -6.7 (t, 1H, $^3J_{\text{OsPH}} = 18$ Hz)

compound	IR, $\text{cm}^{-1}$	NMR <sup>d</sup>	
		$\delta(^1\text{P}\{\text{H}\})$	$\delta(^1\text{C}\{\text{H}\})$
$[\text{RhOs}(\text{C}(\text{CH}_3)=\text{C}(\text{CH}_3)_2)(\text{H})(\text{CO})_2(\text{dppm})_2][\text{BF}_4]$ (27a)	2027 (ss), 1859 (w), 1815 (mb)	RhP: 21.19 ( $^1J_{\text{RhP}} = 153$ Hz) OsP: -1.70	OsCO: 178.6 (dm, $^1J_{\text{CC}} = 24$ Hz); 208.5 (dm, $^1J_{\text{RNC}} = 13$ Hz); 223.7 (ddm, $^1J_{\text{RNC}} = 25$ Hz, $^2J_{\text{CC}} = 24$ Hz)
(27b)	2044 (ms), 1888 (w), 1793 (ms)	RhP: 20.49 ( $^1J_{\text{RhP}} = 132$ Hz) OsP: -1.57	OsCO: 178.1 (dm, $^1J_{\text{CC}} = 24$ Hz); 203.7 (dm, $^1J_{\text{RNC}} = 8$ Hz); 224.5 (ddm, $^1J_{\text{RNC}} = 29$ Hz, $^2J_{\text{CC}} = 24$ Hz)
$[\text{RhOs}(\text{CH}_3\text{O}_2\text{CC}=\text{C}(\text{H})-\text{CO}_2\text{CH}_3)(\text{CO})_2(\mu\text{-H})(\text{dppm})_2][\text{BF}_4]$ (28)	2052 (ss), 1997 (ss), 1959 (sh)	24.8 (RhP, $^1J_{\text{RhP}} = 124$ Hz) -6.85 (OsP)	OsCO: 175.6 (bs, 1C), 180.48 (bs, 1C), 225.6 (bs, 1C)
$[\text{RhOs}(\text{H})(\text{CH}_3\text{O}_2\text{CC}=\text{C}(\text{H})-\text{CO}_2\text{CH}_3)(\text{CO})_2(\text{dppm})_2][\text{BF}_4]$ (29a)		26.84 (RhP, $^1J_{\text{RhP}} = 120$ Hz) -4.23 (OsP)	
$[\text{RhOs}(\text{H})(\text{H})(\text{CH}_3\text{O}_2\text{CC}=\text{C}(\text{H})-\text{CO}_2\text{CH}_3)(\text{CO})_2(\text{dppm})_2][\text{BF}_4]$ (29b)		25.63 (RhP, $^1J_{\text{RhP}} = 128$ Hz) -2.56 (OsP)	

compound	IR, $\text{cm}^{-1}$	$\delta(^1\text{P}\{\text{H}\})$	NMR <sup>a</sup> $\delta(^1\text{H})$	$\delta(^{13}\text{C}\{\text{H}\})$
$[\text{RhOs}(\text{C}(\text{O})\text{C}(\text{CH}_3)=\text{CH}_2)-(\mu\text{-H})(\text{CO})_2(\text{dpppm})_2][\text{BF}_4]$ (30)	2044 (ss), 1981 (ss), 1755 (ss), 1587 (ss) <sup>c</sup>	RhP: 17.33 ( $^1J_{\text{RhP}} = 153$ Hz) OsP: -3.89	PCH <sub>2</sub> P: 3.34(m, 2H), 3.07(m, 2H) RhC=CH <sub>2</sub> : 5.88 (s, 1H), 4.95 (s, 1H) RhC-CH <sub>3</sub> : 0.52 (s, 3H) OsHRh: -8.82 (bm)	OsCO: 174.17 (s); 179.97 (dt, $^2J_{\text{CC}} = 22$ Hz, $^2J_{\text{PC}} = 9$ Hz); 234.26 (dd, $^2J_{\text{CC}} = ^1J_{\text{RhC}} = 22$ Hz) RhCO: 254.05 (d, $^1J_{\text{RhC}} = 31$ Hz)
$[\text{RhOs}(\text{C}(\text{CH}_3)=\text{CH}_2)-(\mu\text{-H})(\text{CO})_2(\text{dpppm})_2][\text{BF}_4]$ (31a,b)		RhP: 26.23 ( $^1J_{\text{RhP}} = 149$ Hz) OsP: -4.64	PCH <sub>2</sub> P: 3.34(m, 2H), 3.07(m, 2H) RhC=CH <sub>2</sub> : 5.84 (bs, 1H), 4.64 (m, 1H) RhC-CH <sub>3</sub> : 1.58 (s, 3H) OsHRh: -8.90 (bm)	
(31b)		RhP: 24.47 ( $^1J_{\text{RhP}} = 114$ Hz) OsP: -5.75	PCH <sub>2</sub> P: 3.34(m, 2H), 3.07(m, 2H) RhC=CH <sub>2</sub> : 6.59 (bs, 1H), 5.02 (m, 1H) RhC-CH <sub>3</sub> : 1.15 (s, 3H) OsHRh: -12.41 (bm)	
$[\text{RhOs}(\text{C}(\text{CH}_3)=\text{C}(\text{CH}_3)_2)-(\mu\text{-H})(\text{CO})_2(\text{dpppm})_2][\text{BF}_4]$ (32a,b)		RhP: 23.59 ( $^1J_{\text{RhP}} = 153$ Hz) OsP: -5.96	PCH <sub>2</sub> P: 3.4 (bm) RhC-CH <sub>3</sub> : 1.67 (t, 3H, $^1J_{\text{RhP-H}} < 2$ Hz) RhC=C(CH <sub>3</sub> ) <sub>2</sub> : 1.60 (s, 3H), 1.01 (s, 3H) OsHRh: -8.38 (bm)	OsCO: 175.1 (s); 180.6 (m); 233.7 (dm, $^1J_{\text{RhC}} = 35$ Hz)
(32b)		RhP: 23.5 ( $^1J_{\text{RhP}} = 153$ Hz) OsP: -6.25	PCH <sub>2</sub> P: 3.4 (bm) RhC-CH <sub>3</sub> : 0.77 (t, 3H, $^1J_{\text{RhP-H}} = 2$ Hz) RhC=C(CH <sub>3</sub> ) <sub>2</sub> : 0.86 (s, 3H), 0.57 (s, 3H) OsHRh: -8.8 (bm)	OsCO: 175.5 (s); 179.9 (m); 233.7 (dm, $^1J_{\text{RhC}} = 23$ Hz)

<sup>a</sup> IR abbreviations: ss = strong sharp, ms = medium sharp, ws = weak sharp, sb = strong broad, mb = medium broad, wb = weak broad, m = medium, w = weak, sh = shoulder. NMR abbreviations: s = singlet, d = doublet, t = triplet, m = multiplet, dd = doublet of doublets, dt = doublet of triplets, dm = doublet of multiplets, ddm = doublet of doublets of multiplets, tm = triplet of multiplets, bs = broad singlet, bm = broad multiplet. <sup>b</sup> Nujol mull. Values quoted are  $\nu(\text{CO})$  except as indicated. <sup>c</sup>  $\nu(\text{C}=\text{C})$  chemical shifts are referenced vs external 85% H<sub>3</sub>PO<sub>4</sub>, while <sup>1</sup>H and <sup>13</sup>C (<sup>1</sup>H) are referenced vs external TMS. Chemical shifts for the phenyl hydrogens are not given in the <sup>1</sup>H NMR data. Spectra were recorded in CD<sub>2</sub>Cl<sub>2</sub>, except as indicated. <sup>d</sup> Spectra recorded in THF-d<sub>6</sub>. <sup>e</sup> Recorded in CH<sub>2</sub>Cl<sub>2</sub> solution. <sup>f</sup> Recorded in benzene-d<sub>6</sub>. <sup>g</sup> Recorded at -40 C. <sup>h</sup> DMAD methyl groups and dppm methylene groups could not be assigned due to the number of species present in solution.

**(b)  $[\text{RhOs}(\eta^3\text{-C}_3\text{H}_5)(\text{CO})_3(\text{dppm})_2]$  (19).** Diallylmagnesium was prepared by addition of 1 mL of 2.0 M allylmagnesium chloride to 9 mL of dioxane. Five millilitres of the resulting solution (0.5 mmol) was filtered and added to  $[\text{RhOs}(\text{CO})_4(\text{dppm})_2][\text{BF}_4]$  (**2**; 95 mg, 0.075 mmol), suspended in 100 mL of THF, causing gradual dissolution of the yellow crystals and a colour change to orange. After stirring for 2.5 h, the solvent was removed in vacuo and the residue washed with 2 times 10 mL of pentane and then extracted into THF/Et<sub>2</sub>O (10 mL/20 mL) and filtered. The solvent was removed in vacuo and the bright orange residue was crystallized by slow addition of Et<sub>2</sub>O to a saturated THF solution to form a bright orange powder. Yield: 0.035 mg, 0.029 mmol, 39%. Satisfactory elemental analyses could not be obtained due to difficulties in removing Mg(BF<sub>4</sub>)<sub>2</sub>.

**(c)  $[\text{RhOs}(\text{C}(\text{CH}_3)=\text{C}(\text{CH}_3)_2)(\text{CO})_3(\text{dppm})_2]$  (20).** 3-methyl-1,2-butadiene (9.4 μL, 0.096 mmol) was added to a solution of **1** (110 mg, 0.096 mmol) in 5 mL of CH<sub>2</sub>Cl<sub>2</sub>, causing a darkening of the orange solution. After stirring for 2 h the solvent was reduced to 2 mL. Slow addition of 20 mL of Et<sub>2</sub>O resulted in the formation of a yellow-orange micro-crystalline solid. The pale orange supernatant was discarded and the solid was washed with 3x20 mL of Et<sub>2</sub>O and dried in vacuo. Yield 0.88 g, 0.072 mmol, 76%. Anal. Calcd. for C<sub>58</sub>H<sub>53</sub>O<sub>3</sub>OsP<sub>4</sub>Rh: C, 57.33; H, 4.40. Found: C, 57.15; H, 4.58.

**(d)  $[\text{RhOs}(\text{CH}_3\text{O}_2\text{CC}\equiv\text{C}(\text{H})\text{CO}_2\text{CH}_3)(\text{CO})_3(\text{dppm})_2]$  (21).** The complex **1** (100 mg, 0.0875 mmol) was dissolved in 5 ml of CH<sub>2</sub>Cl<sub>2</sub> and the solution was cooled to -78°C. Dimethyl acetylenedicarboxylate (10.8 μL, 0.0875 mmol) was then added, causing the

solution to turn immediately from yellow-orange to red. After 5 min of stirring the solution was warmed to room temperature. The solvent was then removed in vacuo and the resulting red residue was recrystallized from CH<sub>2</sub>Cl<sub>2</sub>/hexanes to give a dark-orange powder which was washed with 2x20 mL of hexanes and dried in vacuo. Yield: 92 mg, 82%. Anal. Calcd. for C<sub>59</sub>H<sub>51</sub>O<sub>7</sub>OsP<sub>4</sub>Rh: C, 54.98; H, 3.95. Found: C, 54.75; H, 4.07.

**(e) [RhOs(C(O)C(CH<sub>3</sub>)=CH<sub>2</sub>)(CO)<sub>3</sub>(dppm)<sub>2</sub>] (22).** [RhOs(C(CH<sub>3</sub>)=CH<sub>2</sub>)(CO)<sub>3</sub>-(dppm)<sub>2</sub>] (**28**; 150 mg, 0.126 mmol) was dissolved in 20 mL of CH<sub>2</sub>Cl<sub>2</sub> and CO gas was passed over the solution for 3 min, causing a darkening of the orange solution. The solution was stirred under CO for 1 h and the solvent was removed in vacuo. The dark orange residue was recrystallized from CH<sub>2</sub>Cl<sub>2</sub>/Et<sub>2</sub>O/hexanes to yield a dark orange powder. Yield: 118 mg, 0.097 mmol, 77%.

**(f) [RhOs(C(CH<sub>3</sub>)=CH<sub>2</sub>)(CH<sub>3</sub>)(CO)<sub>3</sub>(dppm)<sub>2</sub>][CF<sub>3</sub>SO<sub>3</sub>] (23a,b).** *Method (i):* Methyl triflate (4.8 μL, 6.9 mg, 0.042 mmol) was added to a stirred solution of [RhOs(C(CH<sub>3</sub>)=CH<sub>2</sub>)(CO)<sub>3</sub>(dppm)<sub>2</sub>] (**18**; 50 mg, 0.042 mmol) in 10 mL of CH<sub>2</sub>Cl<sub>2</sub> at -80°C. The solution was stirred at -80°C for 30 min and allowed to slowly warm to ambient temperature. The solvent was removed in vacuo and the residue was recrystallized from CH<sub>2</sub>Cl<sub>2</sub>/Et<sub>2</sub>O. Yield: 36 mg, 63%. *Method (ii):* Methyl triflate (12 μL, 17 mg, 0.104 mmol) was added to a solution of [RhOs(H)(CO)<sub>3</sub>(dppm)<sub>2</sub>] (**1**; 120 mg, 0.104 mmol) in 30 mL of CH<sub>2</sub>Cl<sub>2</sub> at -80°C and the solution was warmed to -40°C and stirred for 1 h. Allene gas was then passed over the solution for 2 min. The solution was stirred under allene and gradually allowed to return to ambient temperature. The solution

volume was then reduced to 5 mL, and 30 mL Et<sub>2</sub>O was added, causing precipitation of a fine, pale yellow powder, which was washed with 3x10 mL of Et<sub>2</sub>O and dried in vacuo. The residue was then recrystallized from CH<sub>2</sub>Cl<sub>2</sub>/Et<sub>2</sub>O. Yield: 70 mg, 50%. Anal. Calcd. for C<sub>58</sub>H<sub>52</sub>F<sub>3</sub>O<sub>6</sub>OsP<sub>4</sub>RhS: C, 51.56; H, 3.88. Found: C, 51.21; H, 3.91.

**(g) [RhOs(C(CH<sub>3</sub>)=C(CH<sub>3</sub>)<sub>2</sub>)(CH<sub>3</sub>)(CO)<sub>3</sub>(dppm)<sub>2</sub>][CF<sub>3</sub>SO<sub>3</sub>]<sub>2</sub>·2CH<sub>2</sub>Cl<sub>2</sub> (24a,b).**

Methyl triflate (3.5 μL, 5 mg, 0.031 mmol) was added to a cloudy, yellow-orange solution of [RhOs(C(CH<sub>3</sub>)=C(CH<sub>3</sub>)<sub>2</sub>)(CO)<sub>3</sub>(dppm)<sub>2</sub>] (**20**; 35 mg, 0.029 mmol) in 10 mL of CH<sub>2</sub>Cl<sub>2</sub>. Over 15 min the cloudiness disappeared and the colour changed to yellow. After 1 h of stirring the solvent was removed in vacuo and the residue was recrystallized from CH<sub>2</sub>Cl<sub>2</sub>/Et<sub>2</sub>O to give a yellow, microcrystalline solid. Yield: 25 mg, 0.018 mmol, 63%. Anal. Calcd. for C<sub>61.25</sub>H<sub>56.25</sub>Cl<sub>0.25</sub>F<sub>3</sub>O<sub>6</sub>OsP<sub>4</sub>RhS: C, 51.96; H, 4.08; Cl, 0.64. Found: C, 51.72; H, 3.71; Cl, 0.69. Note: The crystals desolvated rapidly. The analytical sample contained 0.125 mol equiv. of co-crystallized CH<sub>2</sub>Cl<sub>2</sub>.

**(h) [RhOs(CH<sub>3</sub>O<sub>2</sub>CC=C(H)CO<sub>2</sub>CH<sub>3</sub>)(CH<sub>3</sub>)(CO)<sub>3</sub>(dppm)<sub>2</sub>][SO<sub>3</sub>CF<sub>3</sub>] (25).**

Compound **21** (100 mg, 0.077 mmol) was dissolved in 10 mL of CH<sub>2</sub>Cl<sub>2</sub>, and CH<sub>3</sub>SO<sub>3</sub>CF<sub>3</sub> (8.7 μL, 0.077 mmol) was added by syringe. The red solution was stirred for 1 h, after which the CH<sub>2</sub>Cl<sub>2</sub> was removed in vacuo. The dark red residue was recrystallized from CH<sub>2</sub>Cl<sub>2</sub>/hexanes and the light-brown product obtained was washed 2x10 mL of hexanes and dried in vacuo. Yield: 95 mg, 85%. Anal. Calcd. for C<sub>61</sub>H<sub>55</sub>SF<sub>3</sub>O<sub>10</sub>OsP<sub>4</sub>Rh: C, 50.37; H, 3.78. Found: C, 49.94; H, 3.73.

(i) **[RhOs(C(CH<sub>3</sub>)=CH<sub>2</sub>)(H)(CO)<sub>3</sub>(dppm)<sub>2</sub>][BF<sub>4</sub>] (26a,b)**. HBF<sub>4</sub>·Et<sub>2</sub>O (4.5 μL, 5.34 mg, 0.33 mmol) was added to a stirred solution of **[RhOs(C(CH<sub>3</sub>)=CH<sub>2</sub>)(CO)<sub>3</sub>(dppm)<sub>2</sub>] (18; 39 mg, 0.033 mmol)** at -80°C, causing the colour to change from orange to yellow. The solution was stirred at -80°C for 30 min and then allowed to warm to ambient temperature. The solvent was removed in vacuo and the residue was recrystallized from CH<sub>2</sub>Cl<sub>2</sub>/Et<sub>2</sub>O and then washed with 3x10 mL of Et<sub>2</sub>O and dried in vacuo, resulting in a pale yellow powder. Yield: 25 mg, 0.020 mmol, 60%.

(j) **[RhOs(C(CH<sub>3</sub>)=C(CH<sub>3</sub>)<sub>2</sub>)(H)(CO)<sub>3</sub>(dppm)<sub>2</sub>][BF<sub>4</sub>] (27a,b)**. HBF<sub>4</sub>·Me<sub>2</sub>O (4.4 μL, 4.8 mg, 0.036 mmol) was added to a solution of **20** (44 mg, 0.036 mmol) in 15 mL of CH<sub>2</sub>Cl<sub>2</sub>, causing an immediate change from cloudy orange to clear yellow. After 1 h the solvent was removed in vacuo and the residue was recrystallized from CH<sub>2</sub>Cl<sub>2</sub>/Et<sub>2</sub>O, yielding a yellow microcrystalline solid. Yield: 33 mg, 0.025 mmol, 70%. Anal. Calcd. for C<sub>58</sub>H<sub>54</sub>BF<sub>4</sub>O<sub>3</sub>OsP<sub>4</sub>Rh: C, 53.47; H, 4.18. Found: C, 52.97; H, 4.18.

(k) **[RhOs(CH<sub>3</sub>O<sub>2</sub>CC≡C(H)CO<sub>2</sub>CH<sub>3</sub>)(CO)<sub>3</sub>(μ-H)(dppm)<sub>2</sub>][BF<sub>4</sub>] (28)**. The complex **21** (100 mg, 0.077 mmol) was dissolved in 10 mL of CH<sub>2</sub>Cl<sub>2</sub>, and HBF<sub>4</sub>·Et<sub>2</sub>O (11.0 μL, 0.077 mmol) was added by syringe. The solution turned a darker shade of red, was stirred for 5 min and the solvent was removed in vacuo. The dark red residue was recrystallized from CH<sub>2</sub>Cl<sub>2</sub>/hexanes to give a light-brown powder which was washed with 2x10 mL of hexanes and dried in vacuo. Yield: 87 mg (81%). Anal. Calcd. for C<sub>59</sub>H<sub>52</sub>BF<sub>4</sub>O<sub>7</sub>OsP<sub>4</sub>Rh: C, 51.45; H, 3.78. Found: C, 50.90; H, 4.15. Variable

temperature NMR spectra in  $\text{CD}_2\text{Cl}_2$  showed that the initial products formed at  $-80^\circ\text{C}$  were two isomers of  $[\text{RhOsH}(\text{CH}_3\text{O}_2\text{CC}=\text{C}(\text{H})\text{CO}_2\text{CH}_3)(\text{CO})_3(\text{dppm})_2][\text{BF}_4]$  (**29a**, **29b**). Above  $-20^\circ\text{C}$  the final product formed.

**(l)  $[\text{RhOs}(\text{C}(\text{O})\text{C}(\text{CH}_3)=\text{CH}_2)(\mu\text{-H})(\text{CO})_3(\text{dppm})_2][\text{BF}_4]$  (**30**).**  $\text{HBF}_4\cdot\text{Me}_2\text{O}$  (5.0  $\mu\text{L}$ , 5.5 mg, 0.041 mmol) was added to a stirred solution of **22** (50 mg, 0.041 mmol) in 10 mL of  $\text{CH}_2\text{Cl}_2$  at  $-80^\circ\text{C}$ , causing an immediate colour change from orange to yellow-orange. The solution was stirred at  $-80^\circ\text{C}$  for 30 min and then allowed to warm to ambient temperature. The solvent was removed in vacuo and the residue was recrystallized from  $\text{CH}_2\text{Cl}_2/\text{Et}_2\text{O}$  to give a pale yellow powder. Yield: 37 mg, 0.028 mmol, 69%.

### Reactions.

**(a) Reaction of  $[\text{RhOs}(\text{C}(\text{CH}_3)=\text{CH}_2)(\text{H})(\text{CO})_3(\text{dppm})_2][\text{BF}_4]$  (**26a,b**) with CO.** (i) Compound **26** (10 mg, 0.0078 mmol) was dissolved in 0.5 mL of  $\text{CD}_2\text{Cl}_2$  in an NMR tube which was then evacuated and refilled with  $^{13}\text{C}$ CO to approximately 1.2 atm.  $^1\text{H}$ ,  $^{31}\text{P}$  and  $^{13}\text{C}$  NMR showed complete conversion to two isomeric intermediates  $[\text{RhOs}(\text{C}(\text{CH}_3)=\text{CH}_2)(\mu\text{-H})(\text{CO})_3(\text{dppm})_2][\text{BF}_4]$  (**31a,b**). The intermediates ultimately yielded  $[\text{RhOs}(\text{CO})_4(\text{dppm})_2][\text{BF}_4]$  and  $\text{H}_2\text{C}=\text{C}(\text{H})\text{CH}_3$ , with **31a** reacting slowly, over a 20 h period, while **31b** disappeared within 2 h. (ii) Reaction was repeated as above, but the CO was removed by evacuating the tube and refilling with Ar after 2 min. NMR spectra showed complete conversion to **31a,b**. In the absence of CO, **31a,b** reacted slowly over 48 h to form a mixture of  $[\text{RhOs}(\text{CO})_4(\text{dppm})_2][\text{BF}_4]$  (**2**) and

$[\text{RhOs}(\text{CO})_3(\mu\text{-H})(\mu^2\text{-}\eta^3\text{-}\phi\text{-C}_6\text{H}_4)\text{PhPCH}_2\text{PPh}_2)(\text{dppm})][\text{BF}_4]$  (**12**), along with decomposition products.

**(b) Reaction of  $[\text{RhOs}(\text{C}(\text{CH}_3)=\text{C}(\text{CH}_3)_2)(\text{H})(\text{CO})_3(\text{dppm})_2][\text{BF}_4]$  (**27a,b**) with CO.** Compound **27** (10 mg, 0.0077 mmol) was dissolved in 0.5 mL  $\text{CD}_2\text{Cl}_2$  in an NMR tube, which was then evacuated and refilled with  $^{13}\text{C}$ CO to approximately 1.2 atm.  $^1\text{H}$ ,  $^{31}\text{P}$  and  $^{13}\text{C}$  NMR showed slow formation of two isomeric intermediates  $[\text{RhOs}(\text{C}(\text{CH}_3)=\text{C}(\text{CH}_3)_2)(\mu\text{-H})(\text{CO})_3(\text{dppm})_2][\text{BF}_4]$  (**32a,b**), with the starting materials completely disappearing in approximately 2 h. The intermediates ultimately yielded  $[\text{RhOs}(\text{CO})_4(\text{dppm})_2][\text{BF}_4]$  and  $(\text{CH}_3)_2\text{C}=\text{C}(\text{H})\text{CH}_3$ ; **32a** reacted slowly, persisting for days in solution, but **32b** disappeared within 1 h once the starting compounds were depleted.

#### **X-ray Data Collection.**

**(a)  $[\text{RhOs}(\text{C}(\text{CH}_3)=\text{CH}_2)(\text{CO})_3(\text{dppm})_2]$  (**18**).** Diffusion of ether into a concentrated  $\text{CH}_2\text{Cl}_2$  solution of complex **18** yielded deep red-orange crystals, which were mounted and flame-sealed in glass capillaries under  $\text{N}_2$  and solvent vapor to minimize decomposition and/or solvent loss. Data were collected on an Enraf-Nonius CAD4 diffractometer using Mo  $K\alpha$  radiation at 22°C. Unit cell parameters were obtained from a least-squares refinement of the setting angles of 25 reflections in the range  $17.3^\circ \leq 2\theta \leq 25.6^\circ$ . The cell parameters indicated a triclinic space group and the lack of systematic absences indicated either  $P1$  or  $\bar{P}1$  with  $Z = 1$ . The centrosymmetric space group  $\bar{P}1$  was confirmed as the correct choice by the successful solution and refinement of the structure

with the molecule being inversion disordered (*vide infra*). Intensity data were collected as outlined in Table 3.2. Three reflections were chosen as intensity standards and were remeasured every 120 min of X-ray exposure time; no decay was evident.

**(b)  $[\text{RhOs}(\text{C}(\text{CH}_3)=\text{C}(\text{CH}_3)_2)(\text{CH}_3)(\text{CO})_3(\text{dppm})_2][\text{CF}_3\text{SO}_3]\cdot 2\text{CH}_2\text{Cl}_2$  (24a,b).**

Yellow crystals of **24** were grown by slow diffusion of ether into a concentrated  $\text{CH}_2\text{Cl}_2$  solution, and mounted as for compound **18**. Data collection for compound **24** proceeded as for **18**, except at  $-50^\circ\text{C}$ . Unit cell parameters, obtained from 20 reflections in the range  $20^\circ \leq 2\theta \leq 25^\circ$ , and the systematic absences uniquely defined the space group as  $P2_1/c$ .

#### Structure Solution and Refinement.

**(a)  $[\text{RhOs}(\text{C}(\text{CH}_3)=\text{CH}_2)(\text{CO})_3(\text{dppm})_2]$  (**18**).** Initial attempts to solve and refine the structure of complex **18** in the space group  $P1$  were unsuccessful, however, solution in  $P\bar{1}$  proceeded well, with the molecule disordered about an inversion centre. Similar disorder had been observed in a number of related compounds.<sup>1b,5</sup> The position of the disordered Os/Rh atom was obtained through use of the direct-methods program *SHELXS-86*.<sup>6</sup> The remaining non-hydrogen atoms were located using successive difference Fourier maps. The positions of the atoms of the carbonyl and isopropenyl ligands were resolved without difficulty despite the disorder; the carbon atom C(1) (belonging to the osmium-bound carbonyl C(1)O(1)) and the isopropenyl ligand H3C(4)-C(1')=C(5)H2) and the oxygen atom O(2) (belonging to the carbonyl groups C(2)O(2) and C(3)O(2')) were included at full occupancy while the other atoms (O(1),

**Table 3.2.** Crystallographic Experimental Details*A. Crystal Data*

compound	[RhOs(C(CH <sub>3</sub> )=CH <sub>2</sub> )- (CO) <sub>3</sub> (dppm) <sub>2</sub> ] (18)	[RhOs(C(CH <sub>3</sub> )=C(CH <sub>3</sub> ) <sub>2</sub> - (CO) <sub>3</sub> (CH <sub>3</sub> ) (dppm) <sub>2</sub> ]- [CF <sub>3</sub> SO <sub>3</sub> ] <sub>2</sub> ·2CH <sub>2</sub> Cl <sub>2</sub> (24)
formula	C <sub>56</sub> H <sub>49</sub> O <sub>3</sub> OsP <sub>4</sub> Rh	C <sub>62</sub> H <sub>60</sub> Cl <sub>4</sub> F <sub>3</sub> O <sub>6</sub> OsP <sub>4</sub> RhS
formula weight	1186.94	1579.92
crystal dimensions (mm)	0.66 × 0.55 × 0.35	0.39 × 0.20 × 0.10
crystal system	triclinic	monoclinic
space group	$\bar{P}1$ (No. 2)	<i>P</i> 2 <sub>1</sub> / <i>c</i> (No. 14)
unit cell parameters <sup>a</sup>		
<i>a</i> (Å)	11.247 (2)	20.445(2)
<i>b</i> (Å)	11.737 (2)	10.3890(12)
<i>c</i> (Å)	11.061 (3)	29.300(3)
α (deg)	113.72 (2)	90
β (deg)	93.24 (2)	98.231(10)
γ (deg)	68.567 (15)	90
<i>V</i> (Å <sup>3</sup> )	1237.3 (4)	6159.3(11)
<i>Z</i>	1	4
ρ <sub>calcd</sub> (g cm <sup>-3</sup> )	1.593	1.704
μ (cm <sup>-1</sup> )	30.71	27.27

(Table 3.2 cont.)

**B. Data Collection and Refinement Conditions**

diffractometer	Enraf-Nonius CAD4 <sup>b</sup>	Enraf-Nonius CAD4 <sup>b</sup>
radiation ( $\lambda$ [Å])	Mo K $\alpha$ (0.71073)	Mo K $\alpha$ (0.71073)
monochromator	incident-beam, graphite crystal	incident-beam, graphite crystal
temperature (°C)	22	-50
scan type	$\theta$ - $2\theta$	$\theta$ - $2\theta$
data collection $2\theta$ limit (deg)	56.0	50
total data collected	6248 ( $-13 \leq h \leq 14$ , $0 \leq k \leq 15$ , $-14 \leq l \leq 13$ )	10991 ( $-24 \leq h \leq 24$ , $0 \leq k \leq 12$ , $0 \leq l \leq 34$ )
independent reflections	5959	10754
number of observations ( <i>NO</i> )	5367 ( $F_o^2 \geq 2\sigma(F_o^2)$ )	5757 ( $F_o^2 \geq 2\sigma(F_o^2)$ )
structure solution method	direct methods ( <i>SHELXS-86</i> <sup>c</sup> )	direct methods ( <i>SHELXS-86</i> <sup>c</sup> )
refinement method	full-matrix least-squares on $F^2$ ( <i>SHELXL-93</i> <sup>d</sup> )	full-matrix least-squares on $F^2$ ( <i>SHELXL-93</i> <sup>d</sup> )
absorption correction method	<i>DIFABS</i> <sup>e</sup>	<i>DIFABS</i> <sup>e</sup>
range of abs. corr. factors	1.195–0.835	1.084–0.853
data/restraints/parameters	5959 [ $F_o^2 \geq 3\sigma(F_o^2)$ ]/0/316	10738 [ $F_o^2 \geq 3\sigma(F_o^2)$ ]/1 <sup>f</sup> /753
goodness-of-fit ( <i>S</i> ) <sup>g</sup>	1.191 [ $F_o^2 \geq 3\sigma(F_o^2)$ ]	1.006 [ $F_o^2 \geq 3\sigma(F_o^2)$ ]
final <i>R</i> indices <sup>h</sup>		
$F_o^2 > 2s(F_o^2)$	$R_1 = 0.0300$ , $wR_2 = 0.0900$	$R_1 = 0.0556$ , $wR_2 = 0.0989$
all data	$R_1 = 0.0409$ , $wR_2 = 0.1073$	$R_1 = 0.1758$ , $wR_2 = 0.1321$
largest diff. peak and hole	1.281 and $-2.043$ e Å <sup>-3</sup>	1.604 and $-1.635$ Å <sup>-3</sup>

(Table 3.2 cont.)

<sup>a</sup>Obtained from least-squares refinement of 24 reflections with  $17.3^\circ < 2\theta < 25.6^\circ$  for **18**, and 20 reflections with  $20^\circ < 2\theta < 25^\circ$  for **24**.

<sup>b</sup>Programs for diffractometer operation and data collection were those supplied by Enraf-Nonius.

<sup>c</sup>Sheldrick, G. M. *Acta Crystallogr.* **1990**, *A46*, 467.

<sup>d</sup>Sheldrick, G. M. *SHELXL-93*, Program for crystal structure determination. University of Gottingen, 1993. Weighted  $R$ -factors  $wR_2$  and all goodnesses of fit  $S$  are based on  $F_o^2$ ; conventional  $R$ -factors  $R_1$  are based on  $F_o$ , with  $F_o$  set to zero for negative  $F_o^2$ . The observed criterion of  $F_o^2 > 2\sigma(F_o^2)$  is used only for calculating  $R_1$ , and is not relevant to the choice of reflections for refinement.  $R$ -factors based on  $F_o^2$  are statistically about twice as large as those based on  $F_o$ , and  $R$ -factors based on ALL data will be even larger.

<sup>e</sup>Walker, N.; Stuart, D. *Acta Crystallogr.* **1983**, *A39*, 158.

<sup>f</sup> $d(\text{Rh-C}(5'))$  was fixed at 2.05 Å.

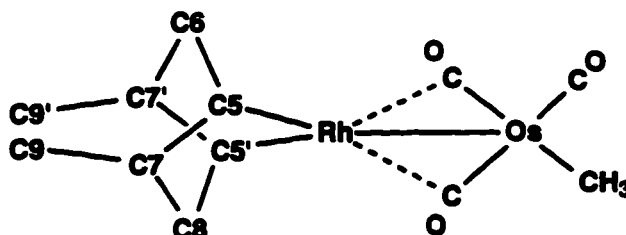
<sup>g</sup> $S = [\sum w(F_o^2 - F_c^2)^2 / (n - p)]^{1/2}$  ( $n$  = number of data;  $p$  = number of parameters varied;  $w = [s^2(F_o^2) + (a_1P)^2 + a_2P]^{-1}$  where  $P = [\text{Max}(F_o^2, 0) + 2F_c^2]/3$ ),  $a_1 = 0.0675$ ,  $a_2 = 0.3857$  for **18**, and  $a_1 = 0.0314$ ,  $a_2 = 40.2796$  for **24**.

<sup>h</sup> $R_1 = \sum ||F_o| - |F_c|| / \sum |F_o|$ ;  $wR_2 = [\sum w(F_o^2 - F_c^2)^2 / \sum w(F_o^4)]^{1/2}$ .

C(2), C(3), C(4) and C(5)) were refined at half occupancy. A view of the equatorial plane of the complex showing the atom positions corresponding to the two superimposed molecules is shown in Figure 3.1. Refinement was completed using the program *SHELXL-93*.<sup>7</sup> The diphosphine unit was well behaved. Hydrogen atom positions were calculated by assuming idealized  $sp^2$  or  $sp^3$  geometries about their attached carbons as appropriate; these hydrogens were given thermal parameters equal to 120% of the equivalent isotropic displacement parameters of their attached carbons. After all atoms had been located and the structure refined to convergence using isotropic displacement parameters, the data were corrected for absorption using the method of Walker and Stuart.<sup>8</sup> The structure was further refined with all non-hydrogen atoms having anisotropic thermal parameters. The final model for complex **3**, with 316 parameters varied, converged to a value of  $R_1 = 0.0300$ .

(b)  $[\text{RhOs}(\text{C}(\text{CH}_3)=\text{C}(\text{CH}_3)_2)(\text{CH}_3)(\text{CO})_3(\text{dppm})_2][\text{CF}_3\text{SO}_3] \cdot 2\text{CH}_2\text{Cl}_2$  (**24a,b**).

The structure of compound **24** was disordered due to the presence of two isomers in the crystal, resulting in the superposition of two differently oriented trimethylvinyl groups as shown (one ligand fragment consists of unprimed atoms while the other has primed atom labels; atoms C(6) and C(8) correspond to the superposition of methyl group positions from both isomers):



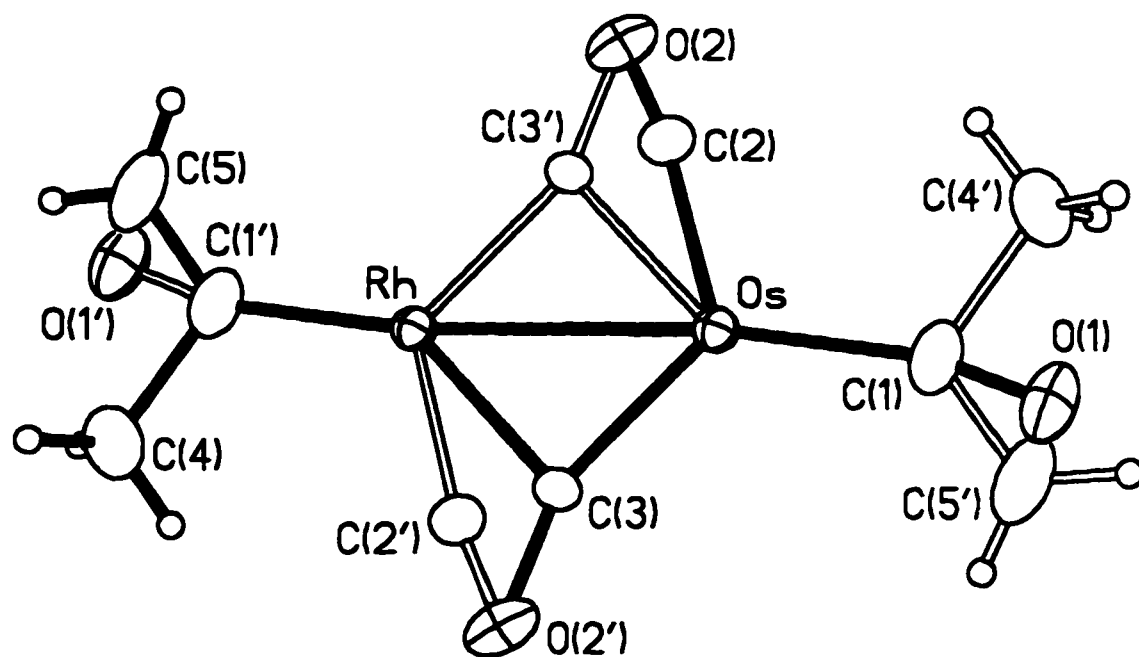


**Figure 3.1.** A view of the equatorial plane of compound **18** showing the positions of the disordered atoms. One disordered molecule is shown with dark bonds while the other has open bonds. The positions labeled Rh and Os actually contain a 50:50 occupancy of each.

The positions of the Rh and Os atoms were obtained through use of the direct-methods program *SHELXS-86*.<sup>7</sup> The remaining non-hydrogen atoms of the major isomer were located using successive difference Fourier maps. However, unusually large thermal parameters and severe elongation of the thermal ellipsoids for atoms C(5), C(7), and C(9) suggested the possibility of a disordered position for the vinyl group. Atoms C(5'), C(7'), and C(9') of the minor isomer were then located using electron density contour plots. The disorder between the C(5), C(7), C(9) and C(5'), C(7'), C(9') sets of positions did not follow an even 50:50 distribution; the most satisfactory results were obtained when C(5), C(7), and C(9) were given occupancy factors of 0.7 and C(5'), C(7') and C(9') were given occupancy factors of 0.3. Furthermore, the Rh-C(5') distance was fixed at 2.05 Å (as suggested by the Rh-C(5) distance) to allow C(5') to refine satisfactorily. Elongation of the thermal ellipsoid of C(4) (the Os-bound methyl carbon) suggested the possibility of disorder involving the superposition of the this group and carbonyl C(1)O(1). In addition, O(1') was located on the Fourier map and refined acceptably with an occupancy of 0.2. Attempts were made to refine the two disorder modes (the Rh-bound isopropenyl group and the Os-bound CO and Me groups) with the same occupancy but the results were unsatisfactory, indicating that the disorder modes are independent. The position O(1') could result from rotamers of either the major or the minor isomer. A view of the equatorial plane of the cation of **24**, showing the disorder of the trimethylvinyl ligand is given in Figure 3.2. Refinement was completed using the program *SHELXL-93*.<sup>7</sup> Hydrogen atom positions for the major isomer were calculated by assuming idealized  $sp^2$  or  $sp^3$  geometries about their attached carbons, and the methyl groups were allowed to

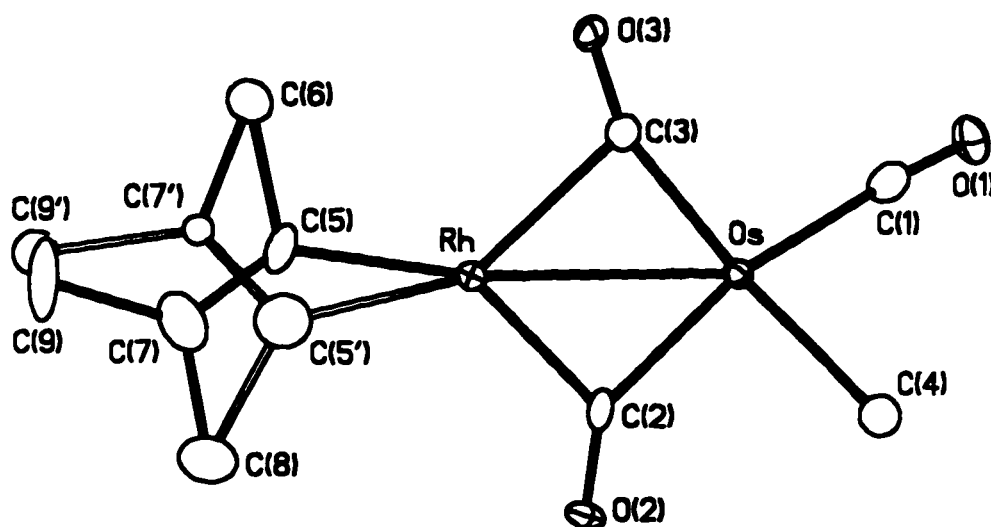


**Figure 3.2.** A view of the equatorial plane of the cation of compound 23 showing the positions of the disordered atoms of the trimethylvinyl group. The dark bonds show the predominant disordered group. The additional disorder involving the carbonyl C(1)O(1) and the methyl group carbon C(4) is not shown.

rotate freely. These hydrogens were given thermal parameters equal to 120% of the equivalent isotropic displacement parameters of their attached carbons. After all atoms had been located and the structure refined to convergence using isotropic displacement parameters, the data were corrected for absorption using the method of Walker and Stuart.<sup>8</sup> The structure was further refined with all non-hydrogen atoms of the major isomer having anisotropic thermal parameters. Atoms C(5'), C(7'), C(9') and O(5') were refined isotropically. The final model for complex **24**, with 753 parameters varied, converged to a value of  $R_1 = 0.0556$ . Atomic coordinates and displacement parameters for the non-hydrogen core atoms of **18** and **24** are given in Tables 3.3 and 3.4, respectively.

## Results and Compound Characterization

### (a) Preparation of Vinyl Complexes.

A number of routes can be used to generate vinyl complexes, including reactions with vinyl Grignard reagents or with vinyl lithium compounds.<sup>9</sup> They can also be obtained via reaction of metal hydrides with alkynes and their tautomers. Attempts to obtain a species,  $[\text{RhOs}(\text{CH}=\text{CH}_2)(\text{CO})_3(\text{dppm})_2]$ , containing the unsubstituted vinyl group by reaction of **1** with acetylene failed, resulting in complex mixtures of products over a range of reaction conditions. However, the analogous isopropenyl species,  $[\text{RhOs}(\text{C}(\text{CH}_3)=\text{CH}_2)(\text{CO})_3(\text{dppm})_2]$  (**18**), containing a mono-substituted vinyl group, is obtained in the reaction of **1** with propyne, as shown in Scheme 3.1. Compound **18** results from hydrogen transfer to the terminal carbon of the alkyne, with the metal ending

**Table 3.3.** Atomic Coordinates and Equivalent Isotropic Displacement Parameters for the Core Atoms of Compound 18.

Atom	<i>x</i>	<i>y</i>	<i>z</i>	$U_{eq}, \text{\AA}^2$
Os/Rh	-0.06608(2)	0.13618(2)	0.08369(2)	0.03876(8)*
P(1)	-0.26646(9)	0.12360(10)	0.03974(10)	0.0408(2)*
P(2)	-0.12282(10)	-0.16227(10)	-0.15889(10)	0.0422(2)*
O(1) <sup>a</sup>	-0.2075(16)	0.4052(17)	0.3068(15)	0.090(4)*
O(2)	0.0229(4)	0.1094(5)	-0.1759(4)	0.0796(11)*
C(1)	-0.1556(5)	0.3179(6)	0.2180(6)	0.0712(14)*
C(2) <sup>a</sup>	-0.0172(9)	0.1308(11)	-0.0783(9)	0.052(2)*
C(3) <sup>a</sup>	-0.0200(7)	-0.0357(9)	0.1105(8)	0.0411(14)*
C(4) <sup>a</sup>	0.1841(12)	-0.4405(12)	-0.1717(16)	0.089(4)*
C(5) <sup>a</sup>	0.1848(25)	-0.3673(27)	-0.3483(22)	0.101(8)*
C(6)	-0.2628(4)	-0.0478(4)	-0.0345(4)	0.0461(8)*

Anisotropically-refined atoms are marked with an asterisk (\*). The form of the anisotropic displacement parameter is:  $\exp[-2\pi^2(h^2a^{*2}U_{11} + k^2b^{*2}U_{22} + l^2c^{*2}U_{33} + 2klb^*c^*U_{23} + 2hla^*c^*U_{13} + 2hka^*b^*U_{12})]$ . <sup>a</sup>Refined with an occupancy factor of 0.5.

**Table 3.4.** Atomic Coordinates and Equivalent Isotropic Displacement Parameters for the Core Atoms of Compound 24.

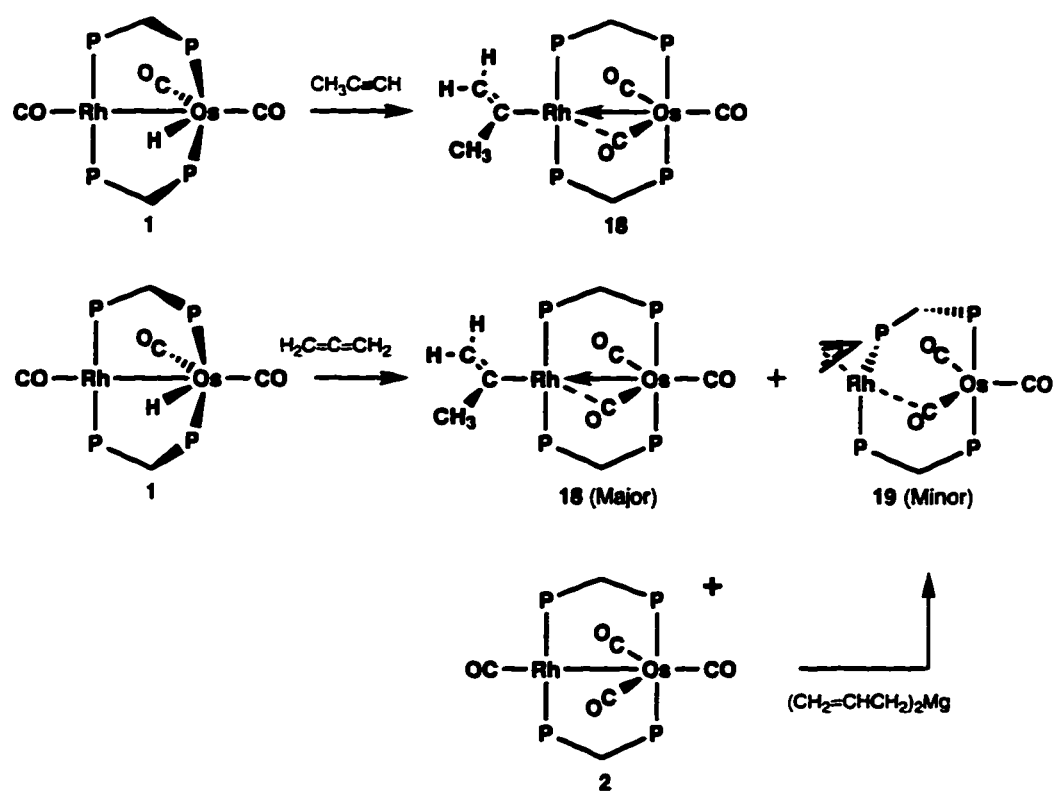
Atom	<i>x</i>	<i>y</i>	<i>z</i>	$U_{eq}, \text{\AA}^2$
Os	0.83456(2)	0.26983(4)	0.18160(2)	0.02257(12)*
Rh	0.69433(4)	0.24842(8)	0.16212(3)	0.0230(2)*
P(1)	0.83987(14)	0.3506(3)	0.10583(10)	0.0223(7)*
P(2)	0.68956(14)	0.3369(3)	0.08756(10)	0.0234(7)*
P(3)	0.83214(14)	0.1831(3)	0.25673(10)	0.0243(7)*
P(4)	0.68141(14)	0.1692(3)	0.23504(11)	0.0245(7)*

(Table 3.4 cont.)

O(1) <sup>a</sup>	0.9729(5)	0.1509(11)	0.1844(4)	0.049(3)*
O(1') <sup>b</sup>	0.9388(21)	0.4778(42)	0.2212(15)	0.046(12)
O(2)	0.7411(4)	0.4812(7)	0.2108(3)	0.034(2)*
O(3)	0.7711(3)	0.0338(7)	0.1297(3)	0.033(2)*
C(1)	0.9231(6)	0.1900(11)	0.1817(4)	0.038(3)*
C(2)	0.7549(5)	0.3863(12)	0.1931(4)	0.027(3)*
C(3)	0.7825(5)	0.1277(11)	0.1497(4)	0.030(3)*
C(4)	0.9004(6)	0.4223(12)	0.2114(4)	0.040(3)*
C(5) <sup>c</sup>	0.5968(8)	0.2032(19)	0.1455(6)	0.039(5)*
C(5') <sup>d</sup>	0.59509(4)	0.28770(8)	0.14700(3)	0.079(22)
C(6)	0.5887(6)	0.0625(12)	0.1199(5)	0.050(4)*
C(7) <sup>c</sup>	0.5440(10)	0.2666(27)	0.1482(7)	0.063(6)*
C(7') <sup>d</sup>	0.5565(23)	0.1819(39)	0.1351(14)	0.024(9)
C(8)	0.5502(7)	0.3991(14)	0.1703(5)	0.069(5)*
C(9) <sup>c</sup>	0.4749(8)	0.2200(24)	0.1287(15)	0.096(15)*
C(9') <sup>d</sup>	0.4711(14)	0.1891(24)	0.1271(32)	0.055(23)
C(10)	0.7674(5)	0.3050(10)	0.0652(3)	0.022(3)
C(20)	0.7537(5)	0.2144(11)	0.2772(3)	0.027(3)

Anisotropically-refined atoms are marked with an asterisk (\*). The form of the anisotropic displacement parameter is:  $\exp[-2\pi^2(h^2a^{*2}U_{11} + k^2b^{*2}U_{22} + l^2c^{*2}U_{33} + 2klb^*c^*U_{23} + 2hla^*c^*U_{13} + 2hka^*b^*U_{12})]$ . <sup>a</sup>Refined with an occupancy factor of 0.8. <sup>b</sup>Refined with an occupancy factor of 0.2. <sup>c</sup>Refined with an occupancy factor of 0.7. <sup>d</sup>Refined with an occupancy factor of 0.3.

### Scheme 3.1



up in the 2-position. No evidence of the other isomer, the n-propenyl species, was observed.

The  $^1\text{H}$  NMR spectrum of **18** shows singlets for the methyl group and the olefinic hydrogens of the isopropenyl group. The methylene groups of the bridging dppm ligands appear as an AB quartet, with additional  $^{31}\text{P}$  coupling at temperatures below  $0^\circ\text{C}$ , indicating asymmetry on either side of the  $\text{RhOsP}_4$  plane in the molecule resulting from the orientation of the vinyl group. Above  $0^\circ\text{C}$ , the peaks broaden and coalesce, becoming a sharp quintet at  $75^\circ\text{C}$ , indicating an average front-back symmetry of the molecule, presumably resulting from rotation of the vinyl group about the Rh-C bond. The  $^{13}\text{C}\{^1\text{H}\}$  NMR spectrum at ambient temperature shows three unique carbonyl resonances at  $\delta$  195.46, 212.24, and 229.41; the high-field signal appears as a triplet, showing coupling of 14 Hz to the osmium-bound phosphines, while the other two resonances are broad, showing no resolvable coupling. The lack of observed coupling to rhodium rules out a terminal carbonyl on rhodium, however, the breadth of the two lower-field resonances (ca. 40 Hz linewidths at half height) could mask substantial Rh coupling, so the possibility of semi-bridging interactions cannot be ruled out. In fact, the low frequency IR stretch at  $1725\text{ cm}^{-1}$ , as well as the low-field  $^{13}\text{C}$  resonance, suggests the involvement of a bridging carbonyl. The  $\alpha$ -carbon of the vinyl group appears as a doublet of triplets at  $\delta$  181.31, showing coupling to Rh (29 Hz) and to the Rh-bound phosphines, clearly indicating that the vinyl group is bound to Rh. The chemical shift is as expected for Rh-bound vinyl groups.<sup>10</sup> The methyl carbon and the vinyl  $\beta$ -carbon appear at  $\delta$  31.02 and  $\delta$

115.29, respectively. Both are triplets, showing coupling to the Rh-bound phosphines. The broadness of the carbonyl resonances in **18** suggests an exchange process in which the two carbonyls on opposite faces of the molecule move back and forth from bridging to terminal positions. This behavior parallels that of the methyl analogue  $[\text{RhOs}(\text{CH}_3)(\text{CO})_3(\text{dppm})_2]$  (**11**), which has a semi-bridging carbonyl on one face and a terminal carbonyl on the opposite face in the solid state, but two equivalent carbonyls in solution, as discussed in Chapter 2. In the case of compound **18**, the carbonyls do not become equivalent at ambient temperature owing to the orientation of the isopropenyl group, having the methyl substituent on one side of the  $\text{RhOsP}_4$  plane and the vinylic moiety on the other side, but the exchange causes broadening. At  $-80^\circ\text{C}$ , the carbonyl resonances sharpen significantly, but are still broad enough to mask any coupling. The presence of a semi-bridging carbonyl, which acts as a  $\pi$  acceptor from the electron-rich rhodium centre, is typical of these types of complexes<sup>1b,5</sup> and appears to be necessary because of the absence of another good  $\pi$  acceptor on rhodium.

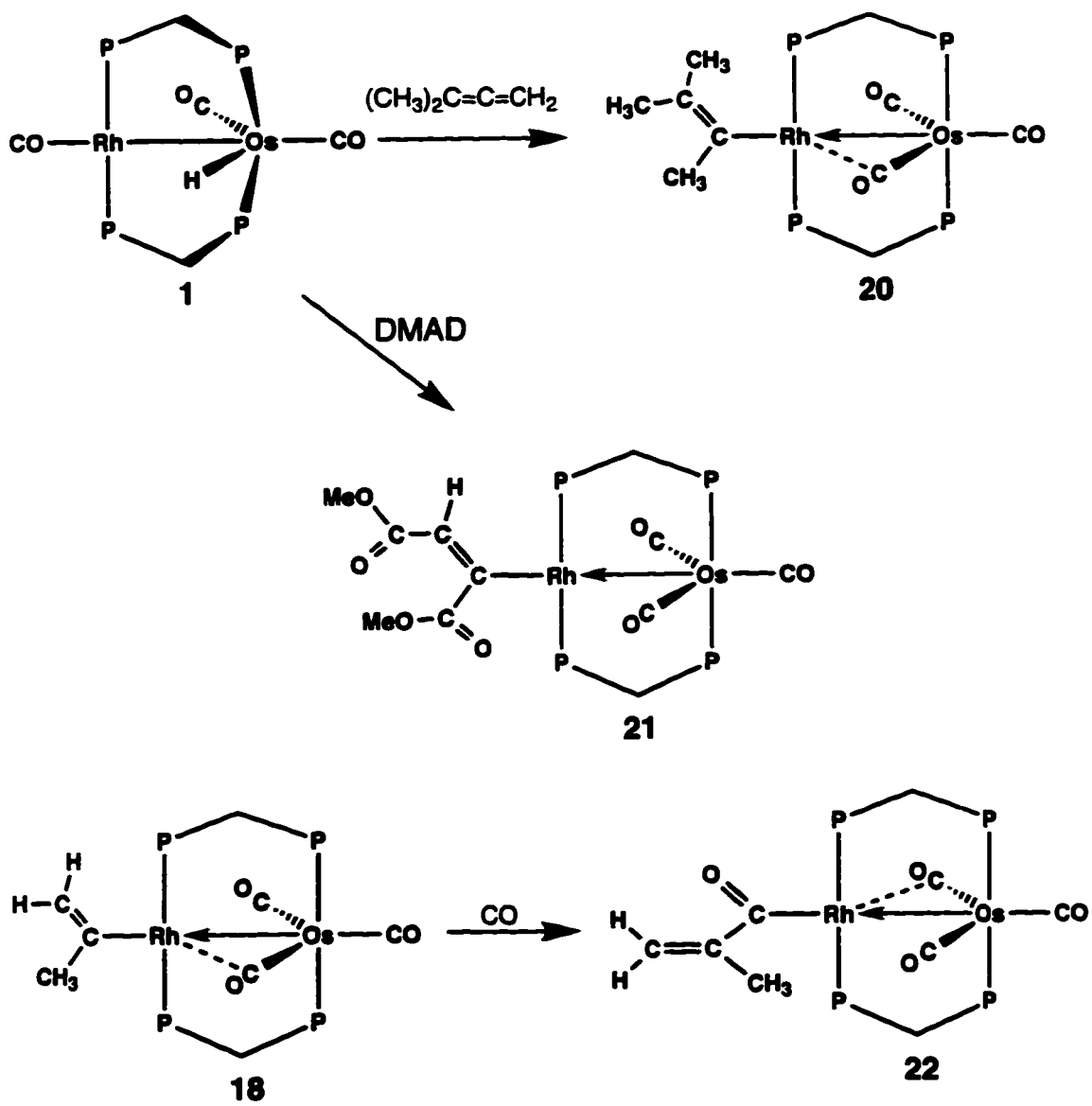
The same isopropenyl complex **18** can also be obtained by the reaction of **1** with allene, as shown in Scheme 3.1. In this reaction a small amount (approx. 10% by  $^{31}\text{P}$  NMR) of  $[\text{RhOs}(\eta^3\text{-C}_3\text{H}_5)(\text{CO})_3(\text{dppm})_2]$  (**19**) is also obtained. This  $\eta^3$ -allyl product has been independently synthesized by reaction of  $[\text{RhOs}(\text{CO})_4(\text{dppm})_2][\text{BF}_4]$  (**2**) with diallylmagnesium. At ambient temperature, the  $^{31}\text{P}$  NMR spectrum of **19** consists of two resonances, a multiplet for the osmium-bound phosphines, and a very broad resonance for the rhodium-bound phosphines. At  $-80^\circ\text{C}$ , the spectrum shows four unique phosphorus

resonances. The coupling constant between the osmium-bound phosphines is 242 Hz, indicating a trans arrangement of the phosphines on this metal, whereas the P-P coupling at Rh is only 22 Hz, indicating that the phosphines are cis. At ambient temperature, the  $^1\text{H}$  NMR shows only a broad singlet for the dppm methylene hydrogens. At  $-80^\circ\text{C}$ , the  $^1\text{H}$  NMR spectrum displays nine unique resonances, four for the dppm methylene hydrogens and five for the allyl ligand. Unfortunately, all resonances are broad, even at  $-110^\circ\text{C}$ , so the coupling information could not be obtained. The chemical shifts of two of the allyl hydrogens are at unusually high field ( $\delta$  1.30 (syn),  $\delta$  0.22 (anti) compared with typical values of  $\delta$  2-5 for syn, and  $\delta$  1-3 for anti<sup>11</sup>), suggesting that the allyl ligand is unsymmetrically bound, approaching a  $\sigma,\pi$ -coordination mode. The other allyl hydrogens appear in the normal region, at 2.53 (syn) and 0.99 (anti). The possibility of an  $\eta^1$ -allyl is ruled out because all 5 allyl hydrogens show coupling to phosphorus (as shown by the substantial sharpening of all signals in the  $^1\text{H}\{^3\text{P}\}$  spectrum), and the chemical shifts are not consistent with a free olefin moiety;  $\eta^1$ -allyl groups typically appear at  $\delta$  3-5.<sup>12</sup> The  $\eta^1$  mode is also inconsistent with the cis arrangement of the phosphines on Rh; an  $\eta^1$ -allyl compound would be expected to have a structure much like **18** (*vide infra*), and like all other  $[\text{RhOs}(\text{R})(\text{CO})_3(\text{dppm})_2]$  compounds.<sup>1b</sup> Presumably the  $\eta^3$ -allyl coordination requires the cis phosphine arrangement due to its increased steric requirements over the  $\eta^1$  mode. The  $^{13}\text{C}$  NMR spectrum at  $-80^\circ\text{C}$  shows three broad resonances at  $\delta$  188.3, 204.7, and 253.4. Again, the low field resonance is consistent with

a semi-bridging carbonyl, although no coupling to Rh is observed due to the broadness of this signal. Compounds **18** and **19** could not be interconverted by heating.

The reaction of 3-methyl-1,2-butadiene (dimethyl allene) with **1** yields the trimethylvinyl analogue  $[\text{RhOs}(\text{C}(\text{CH}_3)=\text{C}(\text{CH}_3)_2)(\text{CO})_3(\text{dppm})_2]$  (**20**), the  $^1\text{H}$  NMR spectrum of which shows three singlets for the methyl groups of the trimethylvinyl ligand. All other features of the NMR spectra for **20** are nearly identical to those of **18**. The IR spectrum of **20** shows carbonyl stretches at 1924, 1875, and 1707  $\text{cm}^{-1}$ , with the latter suggesting a strong semi-bridging interaction.

An analogous substituted vinyl compound is obtained from the reaction of **1** with dimethyl acetylenedicarboxylate (DMAD). Insertion into the Os-H bond has resulted in a product  $[\text{RhOs}(\text{MeO}_2\text{CC}=\text{C}(\text{H})\text{CO}_2\text{Me})(\text{CO})_3(\text{dppm})_2]$  (**21**), having the resulting vinyl group bound to Rh. The  $^1\text{H}$  NMR spectrum shows two resonances for the two sets of methylene protons, a doublet of triplets for the vinyl proton at  $\delta$  4.12 (showing coupling to Rh of 2 Hz and to the two Rh-bound phosphorus nuclei of 1 Hz) and singlets for the two DMAD methyl groups. All carbonyls are bound to Os, as shown by  $^{13}\text{C}$  NMR, and display no coupling to Rh. The absence of  $^{103}\text{Rh}$ - $^{13}\text{C}$ CO coupling in the  $^{13}\text{C}$  NMR and the absence of a low-frequency carbonyl stretch in the IR spectrum suggest that there is no bridging interaction of the carbonyl groups, although a weak semi-bridging interaction cannot be ruled out. The weaker  $\sigma$ -donor ability of the vinyl group in **21**, compared to those in **18** and **20**, is expected because of the electron-withdrawing

**Scheme 3.2**

carboxylate groups; therefore strong  $\pi$  donation from Rh to an Os-bound carbonyl appears unnecessary.

The X-ray structure of **18**, showing only one of the disordered molecules, appears in Figure 3.3 and confirms the structure proposed for these vinyl compounds. Although the structure was inversion disordered, giving rise to superposition of the vinyl ligand and the axial carbonyl, the disorder was resolved satisfactorily, allowing a meaningful discussion of the key structural features. Important bond lengths and angles are given in Table 3.5. At osmium, the geometry is that of a coordinatively-saturated, trigonal-bipyramidal  $\text{OsL}_2(\text{CO})_3$  moiety, in which the phosphines are essentially trans ( $\text{P}(1)\text{-Os-P}(2') = 171.91(3)^\circ$ ) and the angles between the equatorial carbonyl groups are all close to  $120^\circ$ . Ignoring the semi-bridging carbonyl, the geometry at rhodium is essentially square planar, consistent with a 16e configuration. To achieve a 16e count, a dative bond from Os to Rh is required, yielding a Rh-Os separation of  $2.817(1) \text{ \AA}$ , which is normal for a single bond. As has been observed in a number of related species,<sup>1b,5</sup> the buildup of electron density on rhodium (by virtue of two phosphines and an alkyl or alkenyl group) is alleviated by the semi-bridging interaction with  $\text{C}(3)\text{-O}(2')$ . The resulting Rh-C(3) distance, at  $2.075(8) \text{ \AA}$ , is consistent with a strong interaction with rhodium; however, this carbonyl is significantly more linear with respect to Os ( $\text{Os-C}(3)\text{-O}(2') = 155.2(6)^\circ$ ,  $\text{Rh-C}(3)\text{-O}(2') = 118.0(6)^\circ$ ). Whether the unusually short Rh-C(3) distance is chemically meaningful, and therefore indicative of a strong semi-bridging interaction with Rh, or whether it is merely an artifact of the disorder, is

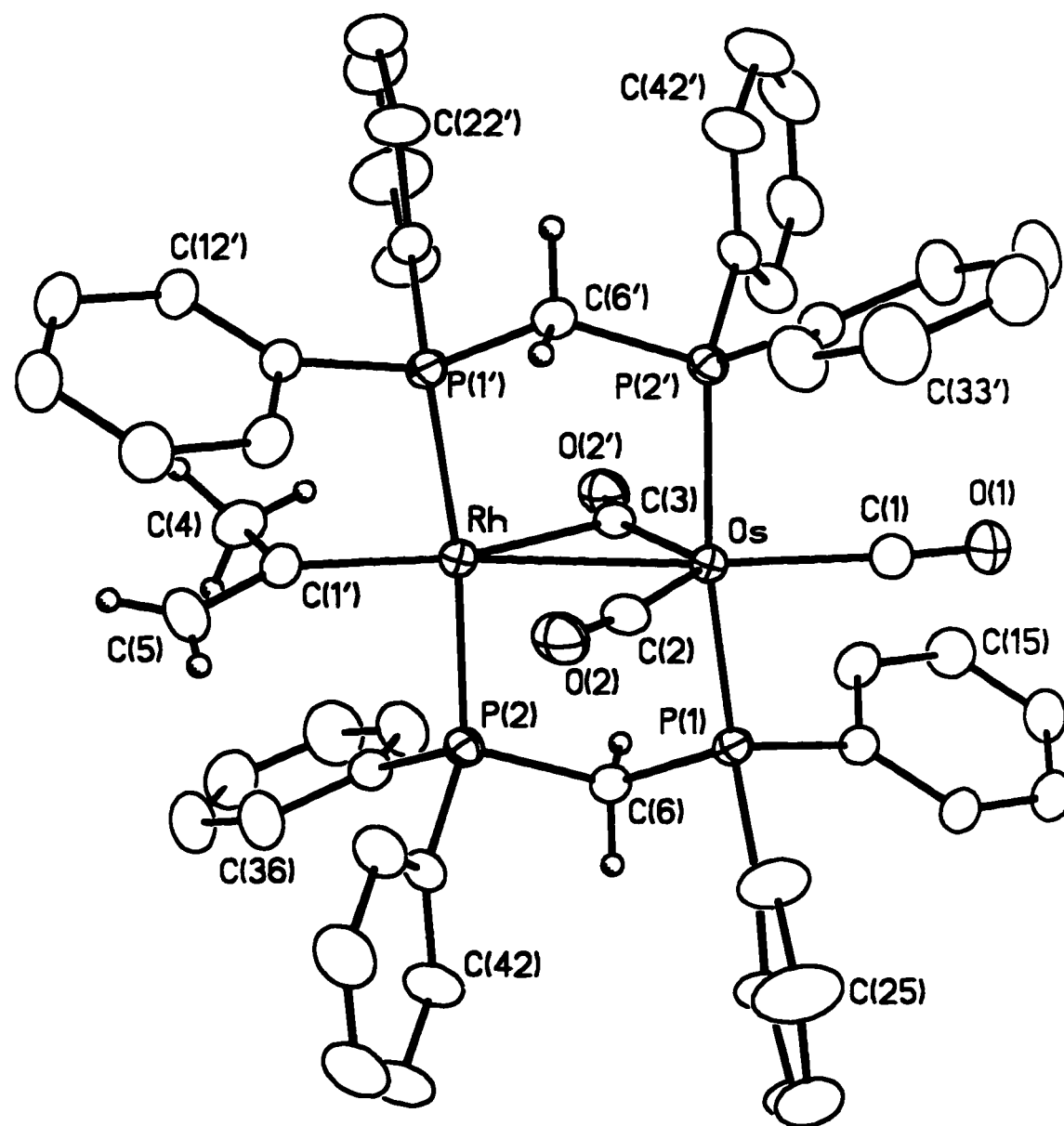


**Figure 3.3.** Perspective view of  $[\text{RhOs}(\text{C}(\text{CH}_3)=\text{CH}_2)(\text{CO})_3(\text{dppm})_2]$  (**18**). Thermal ellipsoids are shown at the 20% probability level, except for hydrogens which are shown arbitrarily small. The dppm phenyl hydrogens have been omitted. Phenyl carbons are numbered sequentially for each phenyl ring beginning with the ipso carbon.

**Table 3.5.** Selected Interatomic Distances (Å) and angles (°) for Compound 18.

Atom1	Atom2	Distance	Atom1	Atom2	Distance		
Os	Rh	2.8165(10)	P1	C(6)	1.827(4)		
Os	P(1)	2.3235(11)	P2	C(6)	1.841(4)		
Os	P(2')	2.3173(11)	O1	C(1)	1.08(2)		
Os	C(1)	1.955(5)	O2	C(2)	1.089(9)		
Os	C(2)	1.874(9)	O2'	C(3)	1.341(8)		
Os	C(3)	2.032(8)	C1'	C(4)	1.635(15)		
Rh	C(1')	1.955(5)	C1'	C(5)	1.33(2)		
Rh	C(3)	2.075(8)					
Atom1	Atom2	Atom3	Angle	Atom1	Atom2	Atom3	Angle
Rh	Os	P(1)	93.12(3)	Os	Rh	P(2)	91.98(3)
Rh	Os	P(2')	91.98(3)	Os	Rh	C(3)	47.3(2)
Rh	Os	C(1)	172.8(2)	P(1')	Rh	C(3)	97.8(2)
Rh	Os	C(2)	73.3(3)	P(2)	Rh	C(3)	90.3(2)
Rh	Os	C(3)	47.3(2)	C(1')	Rh	C(3)	140.9(3)
P(1)	Os	P(2')	171.91(3)	Os	P(1)	C(6)	113.78(13)
P(1)	Os	C(1)	87.5(2)	Rh	P(2)	C(6)	112.51(14)
P(1)	Os	C(2)	98.8(3)	Os	C(1)	O(1)	165.5(11)
P(1)	Os	C(3)	86.4(2)	Rh	C(1')	C(4)	116.6(6)
P(2')	Os	C(1)	86.6(2)	Rh	C(1')	C(5)	132.8(13)
P(2')	Os	C(2)	88.7(3)	C(4)	C(1')	C(5)	109.9(14)
P(2')	Os	C(3)	92.4(2)	Os	C(2)	O(2)	169.7(9)
C(1)	Os	C(2)	113.7(4)	Os	C(3)	Rh	86.6(3)
C(1)	Os	C(3)	125.7(3)	Os	C(3)	O(2')	155.2(6)
C(2)	Os	C(3)	120.7(4)	Rh	C(3)	O(2')	118.0(6)
Os	Rh	P(1)	93.12(3)	P(1)	C(6)	P(2)	111.6(2)

not known.

The vinyl group is bound in an  $\eta^1$ -fashion to rhodium. The Rh-C distance (1.955(5) Å) is shorter than expected, relative to other Rh-vinyl complexes (ca. 2.040 Å),<sup>13</sup> but this is likely a result of the disorder, since the  $\alpha$ -carbon is essentially superimposed on the inversion-disordered carbon of the carbonyl opposite the metal-metal bond. All other distances involving this group are as expected. In particular, the C(1')-C(5) distance of 1.33(2) Å is consistent with a C=C double bond. The angles about C(1) suggest that the vinyl group is bent slightly away from Rh, opening up the Rh-C(1')-C(5) angle to 132.8(13)° and compressing the C(5)-C(1')-C(4) angle to 109.9(14)°. This vinyl-group distortion may be a result of steric interactions with the dppm phenyl groups. Although the non-bonded distance between one of the methyl hydrogens (H(5a)) and one of the phenyl hydrogens (H(46)) (2.43 Å) is an acceptable van der Waals separation, any compression of the Rh-C(1')-C(5) angle would lead to an unfavourable shortening of this distance.

#### **(b) Reactivity of Vinyl Complexes.**

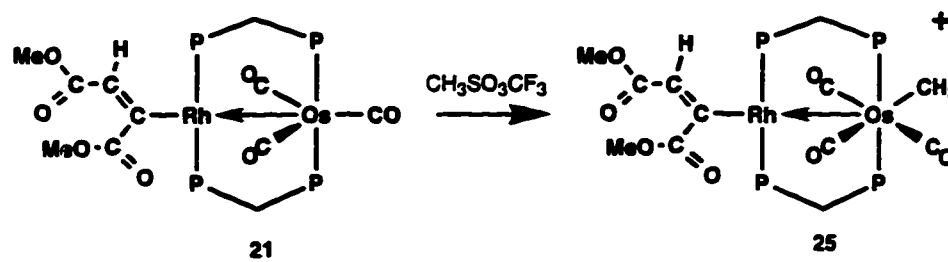
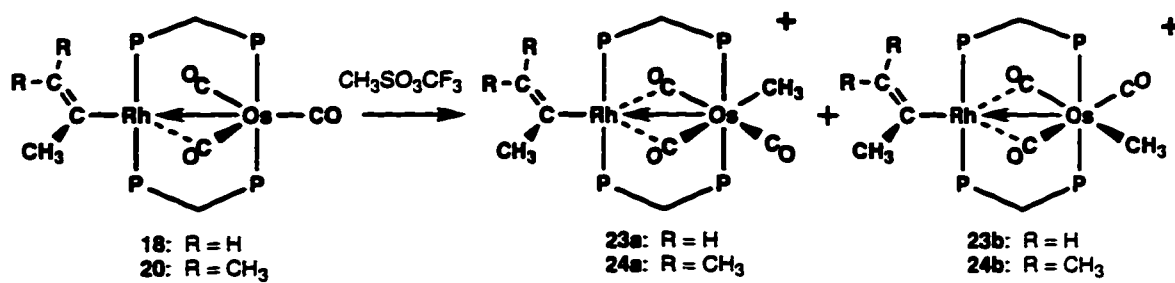
**(i) With CO.** Compound **18** reacts with carbon monoxide to give the migratory-insertion product  $[\text{RhOs}(\text{C}(\text{O})\text{C}(\text{CH}_3)=\text{CH}_2)(\text{CO})_3(\text{dppm})_2]$  (**22**) (see Scheme 3.2), the IR spectrum of which shows bands at 1934 and 1882  $\text{cm}^{-1}$  for the metal-bound carbonyls and at 1720  $\text{cm}^{-1}$  for the acyl group. The C=C stretch is also observed at 1555  $\text{cm}^{-1}$ . The  $^1\text{H}$  NMR spectrum of **22** is similar to that of **18**, showing singlets at  $\delta$  6.07, 5.04, and 0.66 for the two olefinic protons and the methyl group, respectively. In the

$^{13}\text{C}$ -enriched complex, the olefinic protons are split into doublets, with the higher field signal being assigned as trans to the acyl carbonyl on the basis of the larger coupling to  $^{13}\text{C}$  (15 Hz vs. 7 Hz). The  $^{13}\text{C}\{^1\text{H}\}$  NMR spectrum of **22** shows three resonances, at  $\delta$  194.10, 206.38, and 230.47, for the carbonyls on osmium, very similar to those of **18**. As in previous compounds, the high-field resonance shows coupling to the osmium-bound phosphines while the other two resonances are broad. An additional resonance occurs at  $\delta$  271.93 for the acyl carbonyl, and appears as a doublet of triplets with coupling of 31 Hz to rhodium and 5 Hz to the rhodium-bound phosphines. The insertion can be reversed by refluxing **22** in benzene. Whereas refluxing for 1 hour in benzene resulted in decarbonylation of approximately half of the isopropenoyl complex, refluxing in the lower boiling solvent  $\text{CH}_2\text{Cl}_2$  resulted in no reaction. The trimethylvinyl species **20** also reacts with CO, but more slowly than **18**, giving several sparingly soluble products that could not be characterized.

**(ii) With Electrophiles.** One of the goals of this research was to form complexes containing two organic groups or one organic group and a hydride on adjacent metals, with the goal of effecting reductive elimination. Reaction of neutral complexes of the type  $[\text{RhOsR}(\text{CO})_3(\text{dppm})_2]$  with electrophiles to generate dialkyl, alkyl-hydride and related complexes was discussed in Chapter 2, and suggests a parallel route to species containing a vinyl group and either alkyl or hydride ligands. At ambient temperature, reaction of  $[\text{RhOs}(\text{C}(\text{CH}_3)=\text{CH}_2)(\text{CO})_3(\text{dppm})_2]$  (**18**) with methyl triflate leads to a mixture of several products. However, at  $-40^\circ\text{C}$ , the reaction is clean, yielding two

isomers of  $[\text{RhOs}(\text{C}(\text{CH}_3)=\text{CH}_2)(\text{CH}_3)(\text{CO})_3(\text{dppm})_2][\text{CF}_3\text{SO}_3]$  (**23a,b**) in a 1:1 ratio as shown in Scheme 3.3. The  $^1\text{H}$  NMR spectrum of the mixture of isomers shows two sets of resonances that are similar to those of the vinyl group in **18**. In addition, two triplets at  $\delta$  -0.23 and -0.12 correspond to the osmium-bound methyl groups of the two isomers, as shown by  $^{31}\text{P}$ -decoupling experiments. The position of the methyl group on osmium is consistent with previous results described in Chapter 2, in which electrophilic attack was shown to occur at osmium. The  $^{13}\text{C}\{^1\text{H}\}$  NMR spectrum shows three resonances due to osmium-bound carbonyls for each compound, and the IR spectrum of the mixture displays broad, unresolved peaks in the carbonyl region, but a strong peak at  $1805\text{ cm}^{-1}$  suggests the presence of semi-bridging carbonyls. The spectroscopic parameters of the two isomers are nearly identical, suggesting minor differences between the two. Based on this information, we propose that these isomers result from the two possible arrangements of the methyl group, either syn or anti to the vinyl double bond, as shown in Scheme 3.3. Isomers in which the methyl group occupies a site on Os, directed toward rhodium (replacing a semi-bridging CO) are also possible but appear less likely, given the strong tendency for the carbonyls to occupy semi-bridging positions in these complexes. Furthermore, the two isomers proposed are consistent with electrophilic attack at either of the two vacant sites on Os in the precursor **18**. At elevated temperatures, the two isomers of **23** can interconvert, as shown by variable temperature NMR. As the temperature is raised to  $50^\circ\text{C}$ , the peaks in the  $^1\text{H}$  NMR that correspond to the osmium-bound methyl groups of the two isomers broaden, and at  $70^\circ\text{C}$ , the peaks coalesce into a single broad

### Scheme 3.3



peak. The resonances for the methyl groups of the propenyl ligand show similar behavior, but do not quite coalesce at the highest temperature because of their larger chemical shift difference. The olefinic hydrogens are broad and not clearly resolved at the high temperatures. The coalescence appears to result from rotation of the vinyl group, similar to that proposed for **18**.

An alternate route to compound **23** is the reaction of the unstable methyl-hydride complex  $[\text{RhOs}(\text{CH}_3)(\mu\text{-H})(\text{CO})_3(\text{dppm})_2][\text{CF}_3\text{SO}_3]$  (**13**) with allene at  $-40^\circ\text{C}$  to form the two isomers of **23** in the same ratio. Although this hydrido-methyl precursor is susceptible to methane loss at higher temperatures, the reaction with allene at  $-40^\circ\text{C}$  instead gives the migratory insertion product **23**.

Reaction of the trimethylvinyl compound  $[\text{RhOs}(\text{C}(\text{CH}_3)=\text{C}(\text{CH}_3)_2)(\text{CO})_3(\text{dppm})_2]$  (**20**) with methyl triflate at room temperature also yields two isomers of an analogous trimethylvinyl-methyl complex,  $[\text{RhOs}(\text{C}(\text{CH}_3)=\text{C}(\text{CH}_3)_2)(\text{CH}_3)(\text{CO})_3(\text{dppm})_2][\text{CF}_3\text{SO}_3]$  (**24a,b**), in a ratio of 3.8:1.0. The  $^1\text{H}$  NMR spectrum shows six singlets corresponding to the methyl groups of the vinyl ligand of both isomers, and two triplets corresponding to their osmium-bound methyl groups. The  $^{13}\text{C}$  NMR spectrum is similar to that of **23**; however, the IR spectrum is much more clearly resolved than that of **23**, and shows three bands for each isomer. Although the middle frequency bands ( $1860, 1832\text{ cm}^{-1}$ ) are in the same region as terminal bands in the neutral complex ( $1875\text{ cm}^{-1}$  for **20**), they are assigned as bridging carbonyls because they are now on a cationic Os(II) centre, rather than a neutral Os(0) centre. In moving from Os(0) to Os(II), a shift

to higher frequency for  $\nu(\text{CO})$  is expected, and is indeed observed for both the highest (1924  $\text{cm}^{-1}$  in **20** vs. 2041, 2032  $\text{cm}^{-1}$  in **24a,24b**) and the lowest frequency bands (1707  $\text{cm}^{-1}$  in **20** vs. 1808, 1789  $\text{cm}^{-1}$  in **24a,24b**). Since the middle bands shift to slightly lower frequency, rather than higher, they are assigned as bridging carbonyls; therefore two of the carbonyls are involved in semi-bridging interactions in **24a** and **24b**, rather than just one, as in the neutral complexes. It is not possible, on the basis of the spectroscopic data, to identify which structure (**24a** or **24b**) corresponds to the major species. However, on the basis of the X-ray structure determination, which was found to be disordered, containing both isomers superimposed, it has been established that **24a**, having the osmium-bound methyl group syn to the vinyl double bond, is the major isomer (*vide infra*). We assume that this is also the major isomer in solution, since the solubilities of the two isomers are expected to be similar.

The X-ray structure determination of **24**, shown in Figure 3.4, confirms the proposed structure, and although disordered, due to the presence of two isomers in the crystal, this disorder has been resolved satisfactorily as described in the experimental section. Important bond lengths and angles are given in Table 3.6. Although the parameters for both isomers are given in the tables, only those of the major isomer are discussed since they are more reliable, having 70% rather than 30% occupancy. Ignoring the metal-metal interaction, the geometry at osmium is octahedral. The phosphines are essentially mutually trans ( $\text{P}(1)\text{-Os-P}(3) = 177.87(10)^\circ$ ) and the angles between all

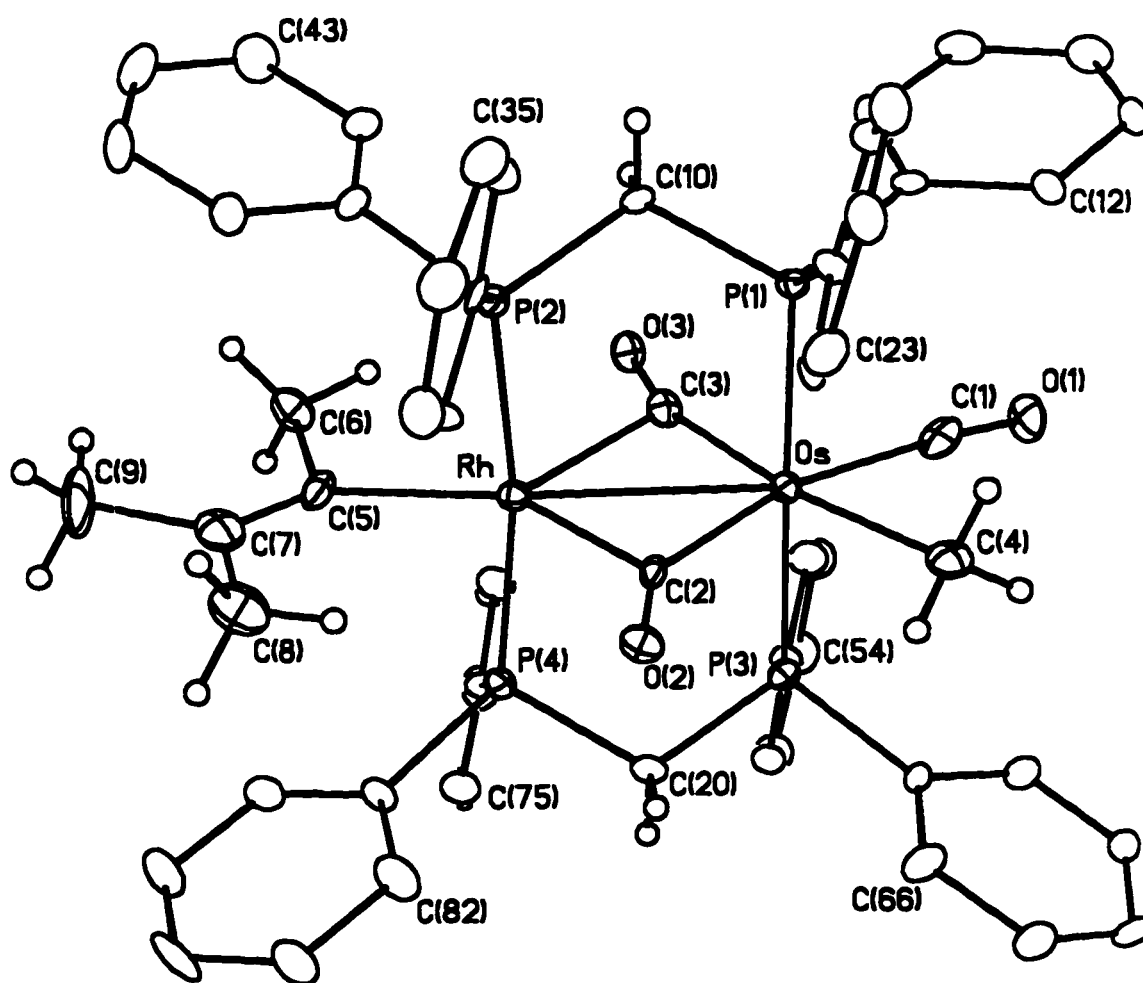


**Figure 3.4.** Perspective view of  $[\text{RhOs}(\text{C}(\text{CH}_3)=\text{C}(\text{CH}_3)_2)(\text{CO})_3(\text{dppm})_2]^+$ , the cation of compound 24, showing only the major isomer. Thermal ellipsoids are shown at the 20% probability level, except for hydrogen atoms which are shown with arbitrarily small thermal parameters. The dppm phenyl hydrogens have been omitted. Phenyl carbons are numbered sequentially for each ring beginning with the ipso carbon. Phenyl hydrogens have the same numbers as the carbons to which they are bound.

**Table 3.6.** Selected Interatomic Distances (Å) and Angles (°) for Compound 24.

Atom1	Atom2	Distance	Atom1	Atom2	Distance
Os	Rh	2.8505(9)	Rh	C(5')	2.05
Os	P(1)	2.390(3)	O(1)	C(1)	1.089(13)
Os	P(3)	2.386(3)	O(2)	C(2)	1.167(13)
Os	C(1)	1.990(13)	C(5)	C(6)	1.65(2)
Os	C(2)	2.094(12)	C(5)	C(7)	1.27(3)
Os	C(3)	1.975(12)	C(7)	C(8)	1.52(3)
Os	C(4)	2.179(12)	C(7)	C(9)	1.53(3)
Rh	P(2)	2.359(3)	C(5')	C(7')	1.37(4)
Rh	P(4)	2.340(3)	C(5')	C(8)	1.68(2)
Rh	C(2)	2.022(11)	C(6)	C(7')	1.50(4)
Rh	C(3)	2.268(11)	C(7')	C(9')	1.73(5)
Rh	C(5)	2.04(2)			

Atom1	Atom2	Atom3	Angle	Atom1	Atom2	Atom3	Angle
Rh	C(2)	Os	87.6(5)	C(4)	Os	P(1)	90.5(3)
Os	C(3)	Rh	84.1(4)	P(3)	Os	P(1)	177.87(10)
C(3)	Os	C(1)	96.8(5)	C(3)	Os	P(3)	94.2(3)
C(3)	Os	C(2)	97.5(4)	C(1)	Os	P(3)	88.9(4)
C(1)	Os	C(2)	165.5(5)	C(2)	Os	P(3)	87.2(3)
C(3)	Os	C(4)	173.3(5)	C(4)	Os	P(3)	89.9(3)
C(1)	Os	C(4)	78.0(5)	C(3)	Os	Rh	52.3(3)
C(2)	Os	C(4)	88.0(4)	C(1)	Os	Rh	148.9(3)
C(3)	Os	P(1)	85.2(3)	C(2)	Os	Rh	45.1(3)
C(1)	Os	P(1)	89.2(4)	C(4)	Os	Rh	133.1(3)
C(2)	Os	P(1)	94.9(3)	P(3)	Os	Rh	90.13(7)

*(Table 3.5 cont.)*

P(1)	Os	Rh	91.12(7)	P(2)	Rh	Os	93.56(7)
C(2)	Rh	C(5)	141.8(7)	P(4)	Rh	Os	94.96(7)
C(2)	Rh	C(3)	90.8(4)	O(1)	C(1)	Os	175.5(12)
C(5)	Rh	C(3)	127.4(6)	O(2)	C(2)	Rh	128.7(8)
C(2)	Rh	C(5')	118.6(3)	O(2)	C(2)	Os	143.5(9)
C(5')	Rh	C(3)	149.1(3)	O(3)	C(3)	Os	159.5(10)
C(2)	Rh	P(2)	94.6(3)	O(3)	C(3)	Rh	116.3(8)
C(5)	Rh	P(2)	87.8(5)	C(7)	C(5)	Rh	132(2)
C(5')	Rh	P(2)	79.30(7)	C(6)	C(5)	Rh	110.2(11)
C(3)	Rh	P(2)	89.7(3)	C(7')	C(5')	Rh	114(2)
C(2)	Rh	P(4)	88.9(3)	C(8)	C(5')	Rh	129.0(5)
C(5)	Rh	P(4)	84.4(5)	C(7)	C(5)	C(6)	117(2)
C(5')	Rh	P(4)	91.70(7)	C(5)	C(7)	C(8)	118(2)
C(3)	Rh	P(4)	98.5(3)	C(5)	C(7)	C(9)	116(3)
P(4)	Rh	P(2)	170.96(10)	C(5)	C(7)	C(9)	124(3)
C(2)	Rh	Os	47.2(3)	C(7')	C(5')	C(8')	109(2)
C(5)	Rh	Os	170.8(6)	C(5')	C(7')	C(6')	119(3)
C(3)	Rh	Os	43.6(3)	C(5')	C(7')	C(9')	122(3)
C(5')	Rh	Os	164.03(2)	C(6)	C(7')	C(9')	118(3)

adjacent groups on Os are close to  $90^\circ$ , giving rise to an 18e configuration at the  $\text{Os}(\text{CH}_3)(\text{CO})_3\text{L}_2^+$  centre. In this bonding model the carbonyls C(2)O(2) and C(3)O(3) are considered as semibridging, donating their electron pairs to Os and functioning as  $\pi$ -acceptors from Rh. An extension of this model has Os donating a pair of electrons from its filled  $d_{xy}$  orbital to Rh, giving it a favoured 16e count, and resulting in a Rh-Os bond length of 2.8505(9) Å, which is consistent with a single bond. The need for the two strong semi-bridging interactions arises from the absence of other  $\pi$ -acid ligands on Rh, coupled with the dative Os-Rh bond and the strong  $\sigma$ -donor trimethylvinyl group. Although both carbonyls are considered as semibridging, C(2)O(2) approaches a symmetrically bridged group. Whereas C(3)O(3) has a short, strong interaction with Os (1.975(12) Å), a weak interaction with Rh (2.268(11) Å), and is much more linear with respect to Os than Rh ( $\text{Os-C(3)-O(3)} = 159.5(10)^\circ$ ,  $\text{Rh-C(3)-O(3)} = 116.3(8)^\circ$ ), carbonyl C(2)O(2) has comparable metal-carbon distances to Os and Rh (2.094(12) and 2.022(11) Å, respectively) and is much less linear with respect to Os ( $\text{Os-C(2)-O(2)} = 143.5(9)^\circ$ ,  $\text{Rh-C(2)-O(2)} = 128.7(8)^\circ$ ). The differing natures of the carbonyls can be rationalized on the basis of the ligands in the trans positions. C(3)O(3) is opposite the strong  $\sigma$ -donor methyl group, so is strongly bound to Os, whereas C(2)O(2) competes for  $\pi$ -electron density with C(1)O(1) opposite it and is less tightly bound to Os, and interacts more strongly with Rh as a consequence. The osmium-methyl bond length (2.179(12) Å) is normal for an  $sp^3$  hybridized carbon.

The arrangement of the carbonyls in compound **24**, which contains two organic fragments, differs from that of the complexes containing one organic fragment. Whereas the mono-alkyl or mono-alkenyl species generally have a single bridging carbonyl, compound **24** has both carbonyls adjacent to Rh in bridging interactions. This may reflect the increased steric crowding at Os, as a consequence of an increase in its coordination number from 5 to 6 upon alkylation, as well as decreased electron density on what is now an Os(II) centre. In support of this idea, the structurally related  $[\text{RhRe}(\text{CH}_3)(\text{CO})_4(\text{dppm})_2]^+$ <sup>5</sup> has a similar octahedral ligand arrangement at Re and again has two semibridging carbonyl groups.

The trimethylvinyl group is bound to Rh in an  $\eta^1$ -fashion, resulting in a normal Rh-C(sp<sup>2</sup>) distance of 2.04(2) Å. All other distances within the vinyl group are as expected, with the possible exception of C(5)-C(7) (1.27(3) Å), which is somewhat shorter than expected for a C-C double bond (1.345 Å);<sup>14</sup> this is likely a result of the disorder. The angles about C(5) reveal a similar distortion of the vinyl group to that seen in compound **18**, with an expanded Rh-C(5)-C(7) angle of 132(2)°, and a compensating small Rh-C(5)-C(6) angle of 110.2(11)°. Again, the distortion is likely caused by steric interactions involving the phenyl groups, with the shortest non-bonded contact involving H(8c) and H(32) (2.16 Å).

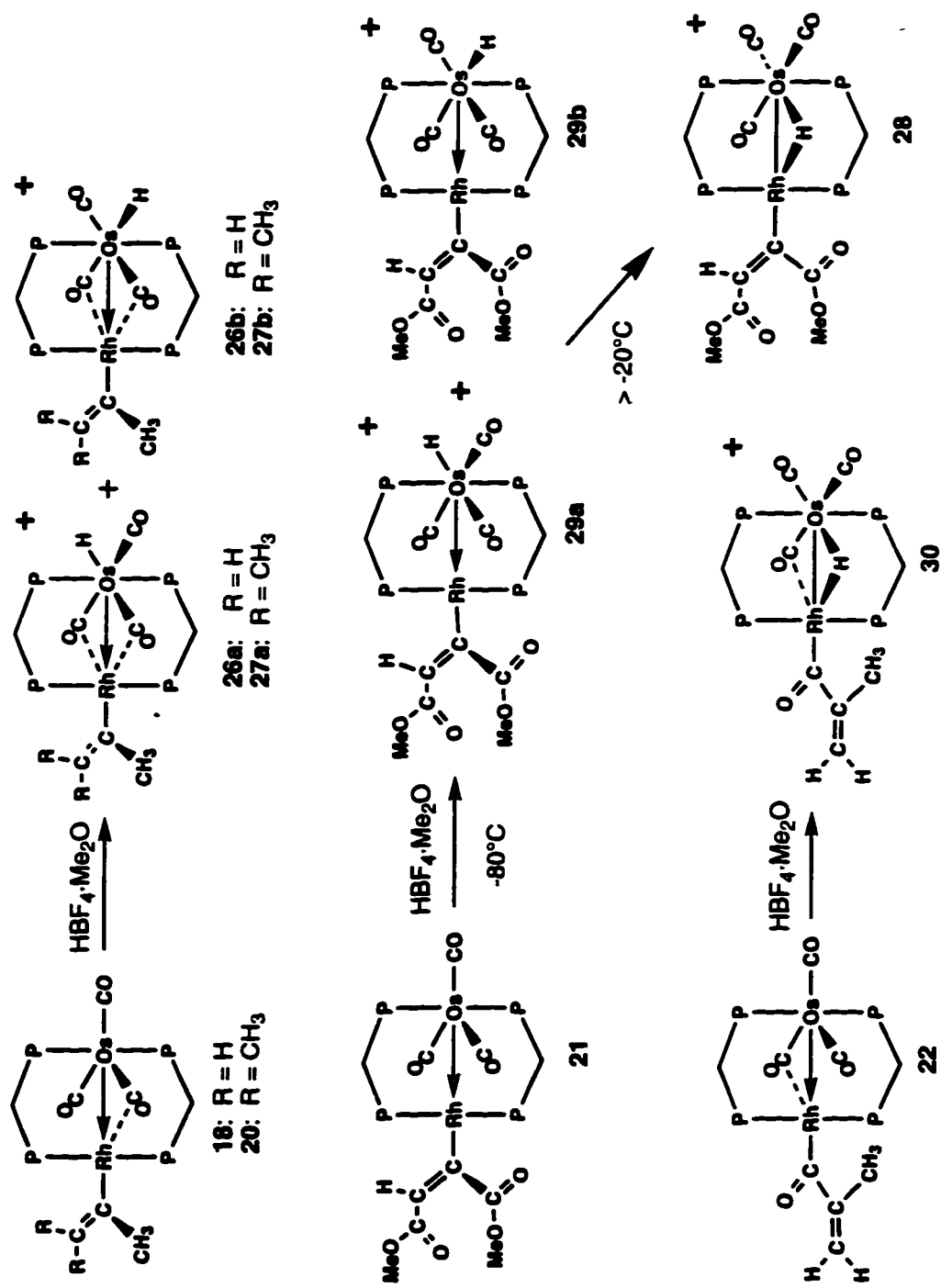
We assume that the very different isomer ratio in **24**, in contrast to the 1:1 isomer ratio in **23**, is a consequence of the greater steric repulsions involving the two additional methyl substituents in the former. Although the trimethylvinyl and the methyl ligands are

on different metals, a consideration of Figure 3.4 shows that a transmission of steric effects between the two groups can occur via the ortho hydrogens (H(32) and H(22)) and the semi-bridging carbonyl C(2)O(2). Relevant non-bonded distances are C(8)-H(32) (2.730 Å), H(32)-O(2) (2.721 Å), O(2)-H(22) (2.641 Å), and H(22)-C(4) (2.859 Å), all of which are within the van der Waals radii for the appropriate groups (3.2 Å for CH<sub>3</sub>-H distances, 3.0 Å for H-O distances<sup>15</sup>). It is not clear, however, which isomer would be favoured by these steric interactions.

Reaction of **21** with methyl triflate yields [RhOs(C(O<sub>2</sub>Me)C=C(H)CO<sub>2</sub>Me)-(CH<sub>3</sub>)(CO)<sub>3</sub>(dppm)<sub>2</sub>][SO<sub>3</sub>CF<sub>3</sub>] (**25**), which is assumed to have a structure similar to compounds **23** and **24**, as shown in Scheme 3.3. The <sup>1</sup>H NMR study shows coupling of the vinylic hydrogen to Rh and coupling of the methyl hydrogens to the Os-bound phosphines, indicating that these groups are bound one to each metal as shown. Unlike **23** and **24**, in which two isomers are obtained, alkylation yields only one isomer of **25**. This likely results from the large carboxylate groups on one side of the vinyl moiety in **21**, while the other side has only a hydrogen directed toward the metal. Another difference between **21** and the other vinyl complexes is the absence of semibridging carbonyls as indicated by the IR stretches (2055, 1955, 1920 cm<sup>-1</sup>) and the absence of Rh coupling in the <sup>13</sup>C NMR.

Protonation of the vinyl complexes leads to the formation of products that are structurally analogous to the vinyl-methyl complexes described, as shown in Scheme 3.4. Compound **18** reacts with one equivalent of HBF<sub>4</sub>·Me<sub>2</sub>O at -40°C to form two isomers of [RhOs(C(CH<sub>3</sub>)=CH<sub>2</sub>)(H)(CO)<sub>3</sub>(dppm)<sub>2</sub>][BF<sub>4</sub>] (**26a,b**), in a ratio of 1.5:1.0. The <sup>1</sup>H NMR

## Scheme 3.4

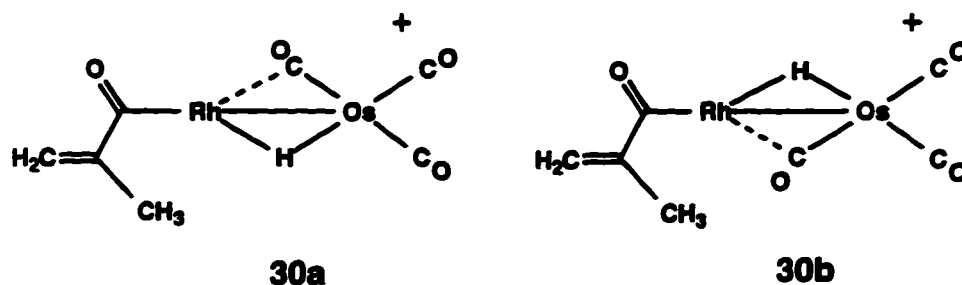


spectrum of this mixture shows two sets of resonances for the isopropenyl groups, as well as hydride resonances at  $\delta$  -6.80 and -6.70, appearing as triplets, with coupling to the Os-bound phosphines.

Protonation of the trimethylvinyl complex **20** occurs cleanly at room temperature to form  $[\text{RhOs}(\text{C}(\text{CH}_3)=\text{C}(\text{CH}_3)_2)(\text{H})(\text{CO}_3)(\text{dppm})_2][\text{BF}_4]$  (**27a,b**) in a ratio of 1.6:1.0. The  $^1\text{H}$  NMR spectrum shows two sets of three methyl groups as expected. In this case, however, one of the methyl groups in each isomer shows a small coupling to the rhodium-bound phosphines. This resonance is assigned to the methyl group on the  $\alpha$ -carbon. The hydride resonances appear as triplets at  $\delta$  -7.02 and -6.55, for the major and minor isomers, respectively, showing coupling to the osmium-bound phosphines, and confirming that the hydrides are terminally bound to this metal. The  $^{13}\text{C}\{^{31}\text{P}\}$  NMR spectrum shows rhodium couplings of 24 and 13 Hz in two of the carbonyls of **27a**, and 29 and 8 Hz for **27b**, consistent with a strong and weak semi-bridging interaction, as confirmed in the structure of **24**.

Protonation of **21**, in contrast, yields the *hydrido-bridged* vinyl complex,  $[\text{RhOs}(\text{MeO}_2\text{CC}=\text{C}(\text{H})\text{CO}_2\text{Me})(\text{CO})_3(\mu\text{-H})(\text{dppm})_2][\text{BF}_4]$  (**28**), as a single isomer. At  $-80^\circ\text{C}$  the protonation results in two intermediate complexes, which are formulated as **29a** and **29b**, isomers of **28** which are structurally analogous to **26** and **27**, having terminal hydride on Os. These isomers persist until *ca.*  $-20^\circ\text{C}$  at which point their conversion to **28** occurs readily.

As with compound **21**, protonation of the isopropenoyl species  $[\text{RhOs}(\text{C}(\text{O})\text{C}(\text{CH}_3)=\text{CH}_2)(\text{CO})_3(\text{dppm})_2]$  (**22**) at  $-80^\circ\text{C}$  with 1 equivalent of  $\text{HBF}_4$  leads to a hydride-bridged complex  $[\text{RhOs}(\text{C}(\text{O})\text{C}(\text{CH}_3)=\text{CH}_2)(\text{CO})_3(\mu\text{-H})(\text{dppm})_2][\text{BF}_4]$  (**30**). No species containing a terminal hydride ligand was seen, even at  $-80^\circ\text{C}$ . Although two isomers (**a** or **b**) are again possible as diagrammed, only one is observed. Presumably



this results from unfavourable interactions between the semi-bridging carbonyl and the methyl substituent of the isopropenoyl group (isomer **30b**); we therefore assume that **30a** is the isomer seen, although we cannot rule out the possibility that **30b** is the observed isomer, and that facile isomerization to isomer **30a** may not be possible. Similarly, compound **28** is thought to exist as isomer **a** as shown in Scheme 3.4, because this isomer avoids unfavourable steric interactions between the osmium bound carbonyl and the carboxylate group. In this case, it seems clear that hydride tunneling is taking place, since **28**, which exists as one isomer, forms from two isomers of **29**.

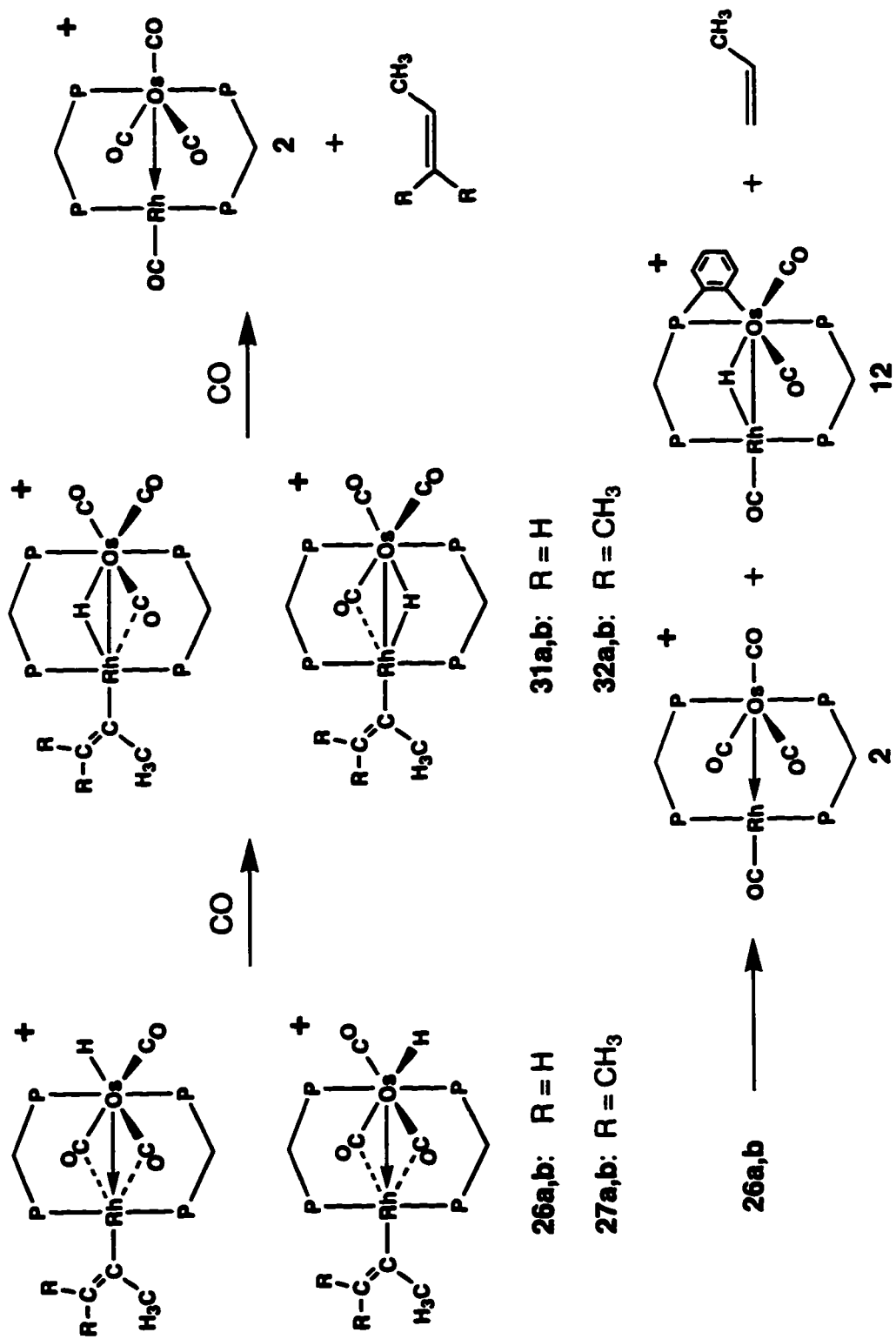
The  $^1\text{H}$  NMR spectrum of **30** shows singlets at  $\delta$  5.88, 4.95 and 0.52 for the isopropenoyl group and a broad multiplet at  $\delta$  -8.82 for the bridging hydride. The  $^{13}\text{C}$  NMR spectrum shows three carbonyls at  $\delta$  174.0, 179.8 and 234.3, with the low field

resonance showing rhodium coupling of 22 Hz, indicating a semi-bridging interaction.

The acyl carbonyl appears as a doublet at  $\delta$  254.05 with rhodium coupling of 31 Hz.

**(iii) Reductive Elimination.** The cationic vinyl-methyl and vinyl-hydride complexes were reacted with CO in an attempt to induce migratory insertion of the CO and methyl or vinyl groups. We had assumed, for example, that compound **26** would yield **30** under CO. However, in no case was insertion to form acyl complexes observed and in fact the vinyl-methyl complexes were unreactive towards CO. The isopropenyl-hydride complex  $[\text{RhOs}(\text{C}(\text{CH}_3)=\text{CH}_2)(\text{H})(\text{CO})_3(\text{dppm})_2][\text{BF}_4]$  (**26 a, b**) reacts rapidly with CO, with isomerization to  $[\text{RhOs}(\text{C}(\text{CH}_3)=\text{CH}_2)(\mu\text{-H})(\text{CO})_3(\text{dppm})_2][\text{BF}_4]$  (**31 a, b**), in which the hydride has moved from a terminal position on Os, to the bridging position (see Scheme 3.5), as confirmed by  $^1\text{H}$ ,  $^{13}\text{C}$ , and  $^{31}\text{P}$  NMR studies. Like compounds **23**, **24**, **26** and **27**, compound **31** has two isomeric forms, resulting from the position of the bridging hydride ligand relative to the vinyl group. These isomers could be distinguished spectroscopically, but could not be unambiguously assigned to the structures shown. Although formation of the hydride-bridged complexes is complete within minutes, they react slowly with subsequent elimination of propene to form the known tetracarbonyl product,  $[\text{RhOs}(\text{CO})_4(\text{dppm})_2][\text{BF}_4]$  (**2**) under CO. The rates of propene elimination from **31 a** and **31 b** are very different. One isomer disappears completely within 1 h, while the other persists for ca. 20 h. If the CO atmosphere is removed under vacuum immediately after conversion to the hydride-bridged intermediate, reductive elimination leads to

### Scheme 3.5



$[\text{RhOs}(\text{CO})_3(\mu\text{-H})(\mu^2\text{-}\eta^3\text{-}o\text{-C}_6\text{H}_4)\text{PhPCH}_2\text{PPh}_2)(\text{dppm})][\text{BF}_4]$  (**1**), along with  $[\text{RhOs}(\text{CO})_4(\text{dppm})_2][\text{BF}_4]$  (**2**) and some unidentified decomposition products. The first product results from orthometalation of a dppm phenyl ring at Os, whereas the second product is presumably a result of CO scavenging from the decomposition products. The trimethylvinyl-hydride complex  $[\text{RhOs}(\text{C}(\text{CH}_3)=\text{C}(\text{CH}_3)_2)(\text{H})(\text{CO})_3(\text{dppm})_2][\text{BF}_4]$  (**27a,b**) reacts in an analogous fashion under CO to form 2-methyl-2-butene and  $[\text{RhOs}(\text{CO})_4(\text{dppm})_2][\text{BF}_4]$ . In this case formation of the intermediate, hydride-bridged complexes is slower, requiring 2 h for complete reaction. The reductive elimination step is also slower, with one isomer disappearing in 2 h, and the other persisting for days.

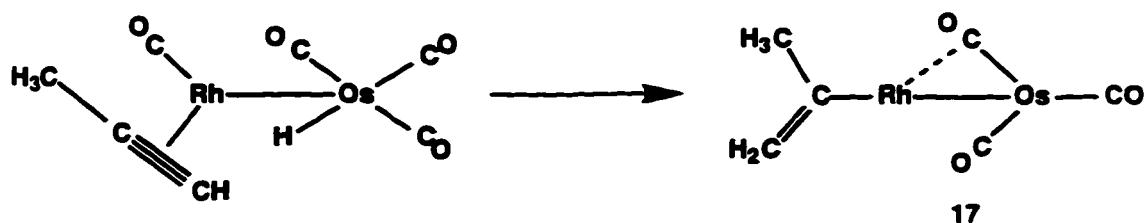
## Discussion

One reason for an interest in binuclear vinyl compounds relates to the proposed involvement of vinyl groups in Fischer-Tropsch chemistry.<sup>2</sup> Not only do these groups undergo migratory insertions with bridging methylene groups more readily than do saturated alkyl groups,<sup>2d</sup> but the intermediacy of the resulting allyl fragments allows an explanation of the small amounts of branched hydrocarbons that result.<sup>2a</sup> The isomerism of allyl to vinyl groups that has been proposed as a key step in alkyl chain growth has been observed in only a few homogeneous systems.<sup>16,17</sup>

We are also interested in the ability of vinyl groups to function as terminal ligands, bound to either Rh or Os, or as bridging ligands, being  $\sigma$ -bound to one metal while  $\pi$ -bonding to the other ( $\eta^1$ ,  $\mu_2\text{-}\eta^2$  mode). The ability of the vinyl moiety to transform from the  $\eta^1$  to the  $\eta^1, \mu_2\text{-}\eta^2$  bonding mode may have a number of effects; it

may influence the reactivity of this group (owing to the additional  $\pi$  involvement), it may facilitate its transfer from one metal to another, or it may stabilize intermediates resulting from ligand loss, owing again to donation of the  $\pi$  electrons. In the chemistry described herein, we see no direct evidence of bridging vinyl coordination modes. All vinyl groups are terminally bound to Rh in the compounds observed, although the rearrangement of the vinyl-hydride compounds leading to the reductive eliminations of the respective olefins presumably occurs via a bridging vinyl group (*vide infra*). It is assumed that the absence of bridging vinyl groups is a function of the steric crowding between the metals by virtue of the dppm phenyl groups.

Formation of a methylvinyl compound from the reaction of  $[\text{RhOsH}(\text{CO})_3(\text{dppm})_2]$  with propyne was predictable, although the isomer obtained,  $[\text{RhOs}(\text{C}(\text{CH}_3)=\text{CH}_2)(\text{CO})_3(\text{dppm})_2]$  (**18**), containing the 1-methylvinyl (isopropenyl) group rather than the 2-methylvinyl product, is of some surprise. The latter species, having the methyl substituent on the  $\beta$ -carbon, should be sterically more favourable than the observed product in which the methyl group is closer to Os. Although we have no mechanistic details about how this migratory insertion occurs (at Rh or Os?), it may be that the propyne is coordinated to Rh such that the bulkier methyl substituent is aimed away from the adjacent Os centre, minimizing steric interactions, as diagrammed below (phosphines omitted).



Hydrogen transfer to the terminal carbon of the alkyne (presumably via the Rh centre) would then yield the observed isomer.

Even more surprising was the formation of the isopropenyl product from the reaction of allene with compound **1**. We had expected that the migratory insertion of allene would occur with transfer of the hydride ligand to the central carbon to give an allyl product, as occurs more often.<sup>18</sup> The present reaction has precedent, however, as a number of examples of allene insertions into metal-hydride bonds to give substituted vinyl ligands have been reported.<sup>19</sup> It is probable that the more familiar tendency to yield allyl products results from the stabilizing influence of the  $\eta^3$ -binding mode of this group. We suggest that when only the  $\eta^1$ -binding mode of these groups is considered, the isopropenyl ligand is actually thermodynamically favoured, owing to the stronger metal-carbon bond involving  $sp^2$  rather than  $sp^3$  hybridization of the  $\alpha$ -carbon. Others have previously suggested a greater stability of the vinyl group.<sup>16</sup> Apparently the  $\eta^3$ -allyl coordination mode is sterically unfavourable in these dppm-bridged complexes in which the phosphines have a trans arrangement at both metals, although when the diphosphines are bent back in a cis-cis arrangement,  $\eta^3$ -allyl bonding has been proposed.<sup>20</sup> Small amounts of an  $\eta^3$ -allyl species (**19**) were obtained as a minor product (ca. 10%), along with the isopropenyl species (**18**) in reactions of **1** with allene. This allyl product was

also synthesized more directly from the reaction of  $[\text{RhOs}(\text{CO})_4(\text{dppm})_2][\text{BF}_4]$  with diallylmagnesium. Coordination of all three allyl carbons, it appears, can only occur with the phosphines on Rh bent back into a cis arrangement, presumably for the steric reasons alluded to above. Attempts to interconvert isomers **18** and **19** by heating resulted only in decomposition.

The allyl complex (**19**) exhibits some interesting features. At ambient temperature, it is highly fluxional. The five hydrogens of the allyl group are not observed in the  $^1\text{H}$  NMR spectrum at ambient temperature, all the dppm methylene hydrogens are equivalent, and the two carbonyls directed towards Rh are equivalent. In addition the two Rh-bound phosphines become equivalent, as do the two Os-bound phosphines in the  $^{31}\text{P}\{^1\text{H}\}$  NMR spectrum. These observations can be explained by a process involving an  $\eta^1$ -allyl intermediate, which is structurally analogous to compounds **18** and **20**. In this intermediate, the phosphines on each metal are equivalent, the two carbonyls can readily exchange, and the opposite end of the allyl can re-coordinate after rotation about the C-C  $\sigma$ -bond. At  $-80^\circ\text{C}$ , the fluxional process is frozen out and the low temperature limiting spectra are observed.

The allyl ligand in the static structure shows unusually highfield chemical shifts for one end of the allyl ligand ( $\delta$  1.30 (syn),  $\delta$  0.22 (anti)).<sup>11</sup> The chemical shifts are, in fact, consistent with the chemical shifts for  $\sigma$ -bound alkyl groups on Rh, suggesting that this end of the allyl ligand is essentially  $\sigma$ -bound, while the other end coordinates as a  $\pi$ -bound olefin. Such unsymmetrical allyl ligands have been described.<sup>21</sup> The reason for

the asymmetry of the allyl ligand may be the position of either end of the ligand relative to the semi-bridging carbonyl. If one end of the allyl ligand is trans to the carbonyl, it will favour strong  $\sigma$ -donation, while the end of the allyl ligand that is cis to the carbonyl will favour  $\pi$ -back donation. However, without X-ray structural characterization, the exact geometry at Rh cannot be determined.

It is notable that, in all compounds characterized herein, the vinyl groups are bound to Rh, although the hydride precursor **1** has the electronically similar hydrido group bound to Os. This parallels a number of studies on related mixed-metal "Rh/M" complexes (M = Ru, Os, Mn,<sup>17</sup> Re,<sup>22</sup> Cr, Mo, W<sup>23</sup>) in which the  $\sigma$ -bound organic group is on Rh, but is in contrast with a number of "Rh/Ir" analogues in which these groups are bound to Ir.<sup>24</sup> It is not clear what factors dictate the favoured binding site of hydrido or  $\sigma$ -bound organic groups on one metal or the other in these systems.

One structural feature common to almost all  $[\text{RhOs}(\text{R})(\text{CO})_3(\text{dppm})_2]$  (R = alkyl, alkenyl) and related compounds is the presence of a semi-bridging carbonyl which is strongly  $\sigma$ -bound to the saturated metal while simultaneously functioning as a  $\pi$ -acceptor from Rh. This appears to arise due to the basicity of Rh, having  $\sigma$ -donor alkyl or alkenyl and phosphine groups attached but having no good  $\pi$ -acceptor ligands terminally bound. The semi-bridging carbonyl removes some of the excess electron density from Rh. This bonding is also consistent with the notion that Os functions as a  $\sigma$ -donor to Rh (*vide supra*), causing an additional electron-density buildup on this metal and further necessitating its removal. Semi-bridging carbonyls seem to commonly accompany M-M'

dative bonds.<sup>25</sup> Consistent with these arguments, the IR stretch of the semibridging carbonyl correlates well with the basicity of the organic group. Therefore, this stretch is lower for **20** ( $R = C(CH_3)=C(CH_3)_2$ ;  $\nu(CO) = 1707\text{ cm}^{-1}$ ) in which two hydrogens have been replaced by better donor methyl groups, than for **18** ( $R = C(CH_3)=CH_2$ ;  $\nu(CO) = 1725\text{ cm}^{-1}$ ). The only compound in this series without a semibridging carbonyl is **21**, which has strongly electron-withdrawing methoxy carbonyl groups on its vinyl ligand. Its lowest metal-bound carbonyl stretch at  $1895\text{ cm}^{-1}$ , suggesting the absence of any substantial bridging interaction.

The reaction of **18** with CO readily yields the isopropenoyl product  $[RhOs(C(O)C(CH_3)=CH_2)(CO)_3(dppm)_2]$  (**22**) via migratory insertion of the isopropenyl and carbonyl groups. There have been surprisingly few examples of carbonyl insertions into metal-alkenyl groups,<sup>26</sup> even though insertions involving other  $\sigma$ -bound organic groups are common.<sup>27</sup> Compound **20** also reacts slowly with CO; however, a number of products were obtained and these were not identified. Attempts to generate methylmethacrylate from **22** by reaction with a sodium methoxide/methanol mix, as previously reported in a related Pt(II) system,<sup>26</sup> failed with no reaction being observed. The failure of **22** to react is not surprising if prior coordination of the alcohol or alkoxide to the metals is required, since these low-valent, electron-rich metals are not expected to be electrophilic.

We were interested in the possible sites of electrophilic attack in the substituted vinyl and isopropenoyl compounds **18**, **20**, **21** and **22**. In addition to attack at either

metal or at the metal-metal bond, attack at the vinyl or the propenoyl group could generate carbene species, as has been previously observed.<sup>28</sup> In the vinyl species **18**, **20** and **21**, the electrophiles ( $\text{H}^+$  and  $\text{CH}_3^+$ ) appear to attack at either of the two available sites on Os, remote from Rh, yielding two isomers. This has been supported by the X-ray structure determination of  $[\text{RhOs}(\text{C}(\text{CH}_3)=\text{C}(\text{CH}_3)_2)(\text{CH}_3)(\text{CO})_3(\text{dppm})_2][\text{SO}_3\text{CF}_3]$  (**24**). In contrast, protonation of the isopropenoyl species (**22**) yields a hydride-bridged complex  $[\text{RhOs}(\text{C}(\text{O})\text{C}(\text{CH}_3)=\text{CH}_2)(\mu\text{-H})(\text{CO})_3(\text{dppm})_2][\text{BF}_4]$  (**30**).

Rearrangement of the terminal-hydride species  $[\text{RhOsH}(\text{C}(\text{CH}_3)=\text{CR}_2)(\text{CO})_3(\text{dppm})_2][\text{BF}_4]$  ( $\text{R} = \text{H}$  (**26**),  $\text{CH}_3$  (**27**)) to the thermodynamically favoured hydride-bridged isomers  $[\text{RhOs}(\text{C}(\text{CH}_3)=\text{CR}_2)(\text{CO})_3(\mu\text{-H})(\text{dppm})_2][\text{BF}_4]$  (**31**, **32**), analogous to the product obtained (**30**) upon protonation of the isopropenoyl compound (**22**), occurs readily upon reaction of these precursors with CO. It is not clear why the isomerization requires the addition of CO. In the analogous compound  $[\text{RhOs}(\text{CH}_3)(\text{H})(\text{CO})_3(\text{dppm})_2][\text{BF}_4]$  (**14**), the rearrangement occurs readily at low temperature without CO addition. However, it may be that the larger size of the vinyl ligands in **31** and **32**, compared to the methyl group of **14**, prevents the rearrangement from occurring via the same mechanism as the rearrangement of **14**.

Rearrangement of the vinyl-hydride species **26** and **27** to the respective hydride-bridged products **31** and **32** is slow in the case of the trimethylvinyl compound **27**, but occurs within minutes with the isopropenyl analogue **26**. It appears that the rate of rearrangement is inversely proportional to the steric bulk of the vinyl groups.

As noted above, protonation of the isopropenoyl compound **22** appears to differ, yielding the hydride-bridged product instead of a terminal hydride species. If the protonation of **22** had occurred at Os, as was the case for **18**, **20**, and **21**, we would have expected to observe an intermediate having a terminal hydride ligand. The absence of such an intermediate, even at low temperature, suggests an alternate site of protonation. We suggest that this may occur at the acyl oxygen, with facile subsequent transfer of the proton to the Rh-Os bond. Although the proposed product (**30a**) is not the isomer expected based on a proton transfer from the acetyl group to the Rh-Os bond, which would have geometry **30b**, conversion of **30b** to **30a** would be facile by tunneling of the hydride between the metals. This rearrangement results in a more favourable arrangement of isopropenoyl and  $\mu$ -CO groups in **30a**.

In the related hydrido-methyl complex  $[\text{RhOs}(\text{CH}_3)(\text{H})(\text{CO})_3(\text{dppm})_2]^+$ , rearrangement to a hydride-bridged species still having the methyl group on Rh (not unlike compounds **31** and **32**) was followed by a transfer of the Rh-bound, terminal methyl group to Os, immediately preceding methane elimination. It therefore appeared that reductive elimination occurred from Os. In the above hydrido-bridged vinyl species reductive elimination again occurs, but at a much slower rate. Based on our data we are not able to unequivocally determine whether elimination occurs from Rh or from Os, but the fact the reductive elimination in the absence of CO leads to orthometalation at Os suggests that the elimination is occurring from Os, as observed for the methyl analogue. The slow rates, compared to those of the methyl/hydride analogue, may be a result of the

larger sizes of the vinyl groups vs. the methyl group, which could inhibit their migration from Rh to Os prior to elimination. Another possibility is that the different rates relate to the different hybridizations of the metal bound carbons ( $sp^2$  in the vinyl groups and  $sp^3$  in the methyl group), and resulting differences in bond enthalpies. Our failure to observe an intermediate in which the vinyl group is bound to Os immediately prior to reductive elimination indicates that reductive elimination is fast compared to the migration.

**References**

1. (a) Hilts, R.W.; Franchuk, R.A.; Cowie, M. *Organometallics* **1991**, *10*, 304.  
(b) Sterenberg, B.T.; Hilts, R.W.; Moro, G.; McDonald, R.; Cowie, M. *J. Am. Chem. Soc.* **1995**, *117*, 245.
2. (a) Saez, I.M.; Meanwell, N.J.; Nutton, A.; Isobe, K.; Vázquez de Miguel, A.; Bruce, D.W.; Okeya, S.; Andrews, D.G.; Ashton, P.R.; Johnstone, I.R.; Maitlis, P.M. *J. Chem. Soc., Dalton Trans.* **1986**, 1565.  
(b) Maitlis, P.M. *Pure Appl. Chem.* **1989**, *61*, 1747.  
(c) Maitlis, P.M.; Saez, I.M.; Meanwell, N.J.; Isobe, K.; Nutton, A.; Vázquez de Miguel, A.; Bruce, D.W.; Okeya, S.; Bailey, P.M.; Andrews, D.G.; Ashton, P.R.; Johnstone, I.R. *New J. Chem.* **1989**, *13*, 419.  
(d) Turner, M.L.; Byers, P.K.; Lary, H.C.; Maitlis, P.M. *J. Am. Chem. Soc.* **1993**, *115*, 4417.  
(e) Turner, M.L.; Lang, H.C.; Shenton, A.; Byers, P.K.; Maitlis, P.M. *Chem. Eur. J.* **1995**, *1*, 549.  
(f) Maitlis, P.M.; Lang, H.C.; Quyoun, R.; Turner, M.L.; Wang, Z.-Q. *Chem. Commun.* **1996**, 1.  
(g) Gibson, V.C.; Parkin, G.; Bercaw, J.E. *Organometallics* **1991**, *10*, 220.
3. Martinez, J.; Gill, J.B.; Adams, H.; Bailey, N.A.; Saez, I.M.; Sunley, G.J.; Maitlis, P.M. *J. Organometal. Chem.* **1990**, *394*, 583.
4. Knox, S.A.R. *J. Organomet. Chem.* **1990**, *400*, 255.

5. Antonelli, D.M.; Cowie, M. *Organometallics* **1990**, *9*, 1818.
6. Sheldrick, G.M. *Acta Crystallogr.* **1990**, *A46*, 467.
7. Sheldrick G.M. SHELXL-93. Program for crystal structure determination. University of Göttingen, Germany, 1993. Refinement on  $F_o^2$  for all reflections (all of these having  $F_o^2 < -3\sigma(F_o^2)$ ). Weighted  $R$ -factors  $wR^2$  and all goodnesses of fit  $S$  are based on  $F_o^2$ ; conventional  $R$ -factors  $R_1$  are based on  $F_o$ , with  $F_o$  set to zero for negative  $F_o^2$ . The observed criterion of  $F_o^2 > 2\sigma(F_o^2)$  is used only for calculating  $R_1$ , and is not relevant to the choice of reflections for refinement.  $R$ -factors based on  $F_o^2$  are statistically about twice as large as those based on  $F_o$ , and  $R$ -factors based on ALL data will be even larger.
8. Walker, N.; Stuart, D. *Acta Crystallogr.* **1983**, *A39*, 158.
9. (a) Collman, J.P.; Hegedus, L.S.; Norton, J.R.; Finke, R.G. *Principles and Applications of Organotransition Metal Chemistry*; University Science Books: Mill Valley, California, 1987, pp. 101-104.  
(b) Elschenbroich, Ch.; Salzer, A. *Organometallics*; VCH Publishers, New York, N.Y., 1989, pp. 206-207.
10. Mann, B.E.; Taylor, B.F. *<sup>13</sup>C NMR Data for Organometallic Compounds*; Academic Press: London, 1981, pp. 88, 140.
11. Collman, J.P.; Hegedus, L.S.; Norton, J.R.; Finke, R.G. *Principles and Applications of Organotransition Metal Chemistry*; University Science Books: Mill Valley, California, 1987, pp. 176-177.

12. (a) Cutler, A.; Ehntholt, D.; Giering, W.P.; Lennon, P.; Raghu, S.; Rosan, A.; Rosenblum, M.; Tancrede, J.; Wells, D.; *J. Am. Chem. Soc.* **1976**, *98*, 3495.  
(b) Numata, S.; Okawara, R.; Kurosawa, H. *Inorganic Chemistry*, **1977**, *16*, 1737.  
(c) Deeming, A.J.; Shaw, B.L.; Stainbank, R.E. *J. Chem. Soc.* **1971**, 374.
13. Orpen, A.G.; Brammer, L.; Allen, F.H.; Kennard, O.; Watson, D.G.; Taylor, R. *J. Chem. Soc., Dalton Trans.* **1989**, 51.
14. Allen, F.H.; Kennard, O.; Watson, D.G.; Brammer, L.; Orpen, A.G.; Taylor, R. *J. Chem. Soc. Perkin Trans. II*, **1987**, 51.
15. Hueey, J. E.; Keiter, E. A.; Keiter, R. L. *Inorganic Chemistry. Principles of Structure and Reactivity*; Harper Collins: New York, 1993, p. 292.
16. Deeming, A.J.; Shaw, B.L.; Stainbank, R.E. *J. Chem. Soc. (A)* **1971**, 374.
17. Wang, L.-S.; Cowie, M. *Can. J. Chem.* **1995**, *73*, 1058.
18. Lobach, M.I.; Kormer, V.A. *Russian Chemical Reviews* **1979**, *48*, 758.
19. (a) Horton, A.D.; Mays, M.J. *J. Chem. Soc., Dalton Trans.* **1990**, 155.  
(b) Hogarth, G.; Lavender, M.H. *J. Chem. Soc., Dalton Trans.* **1992**, 2759.  
(c) Hills, A.; Hughes, D.L.; Jiminez-Tenorio, M.; Leigh, G.J.; McGeary, C.A.; Rowley, A.T.; Bravo, M.; McKenna, C.E.; McKenna, M.-C. *J. Chem. Soc., Chem. Commun.* **1991**, 522.
20. Fryzuk, M.D. *Inorg. Chim. Acta* **1981**, *54*, L265.
21. (a) Shaw, B.L.; Powell, J. *J. Chem. Soc. (A)*, **1968**, 583.

- (b) Mason, R.; Russell, D.R. *J. Chem. Soc., Chem. Commun.* **1966**, 26.
22. Antonelli, D.M.; Cowie, M. *Organometallics* **1991**, *10*, 2550.
23. Graham, T.; Van Gastel, F.; Cowie, M., manuscript in preparation.
24. (a) Antwi-Nsiah, F.; Cowie, M. *Organometallics* **1992**, *11*, 3157.
- (b) Antwi-Nsiah, F.H.; Oke, O.; Cowie, M. *Organometallics* **1996**, *15*, 506.
- (c) Antwi-Nsiah, F.H.; Oke, O.; Cowie, M. *Organometallics* **1996**, *15*, 1042.
25. (a) Hock, A.A.; Mills, O.S. *Acta Crystallogr.* **1961**, *14*, 139.
- (b) Casarin, M.; Ajò, D.; Granozzi, G.; Tanello, E.; Aime, S. *Inorg. Chem.* **1985**, *24*, 1241.
- (c) Iggo, J.A.; Makham, D.P.; Shaw, B.L.; Thornton-Pett, M. *J. Chem. Soc., Chem. Commun.* **1985**, 432.
- (d) Jacobsen, G.B.; Shaw, B.L.; Thornton-Pett, M. *J. Chem. Soc., Chem. Commun.* **1986**, 13.
- (e) Roberts, D.A.; Mercer, W.C.; Geoffroy, G.L.; Pierpont, C.G. *Inorg. Chem.* **1986**, *25*, 1439.
- (f) Zhuang, J.-M.; Batchelor, R.J.; Einstein, F.W.B.; Jones, R.H.; Hader, R.; Sutton, D. *Organometallics* **1990**, 2723.
26. Stang, P.J.; Zhang, Z.; Arif, A.M. *Organometallics* **1992**, *11*, 1017.
27. (a) Anderson, G.K.; Cross, R.J. *Acc. Chem. Res.* **1984**, *17*, 67.
- (b) Kulhmann, E.J.; Alexander, J.J. *Coord. Chem. Rev.* **1980**, *33*, 195.
- (c) Calderazzo, F. *Angew. Chem. Int. Ed. Engl.* **1977**, *16*, 299.

28. (a) Kremer, K. A. M.; Kuo, G.-H.; O'Connor, E. J.; Helquist, P.; Kerber, R. C.  
*J. Am. Chem. Soc.* **1982**, *104*, 6119.
- (b) Wong, W. K.; Tam, W.; Gladysz, J. *J. Am. Chem. Soc.* **1979**, *101*, 5440.
- (c) Grundy, K. R.; Roper, W. R. *J. Organomet. Chem.* **1981**, *216*, 255.

## Chapter 4

### Carbene Complexes of the Rh/Os System

#### Introduction

Transition metal carbene complexes have been the subject of extensive investigation since their discovery in 1964.<sup>1</sup> Carbene complexes have traditionally been divided into two types; electrophilic carbenes, generally having heteroatoms in the  $\beta$  position are known as Fischer carbenes, and nucleophilic carbenes having alkyl substituents are known as Shrock-type carbenes, or alkylidenes.<sup>2</sup> Recently, however, the distinction between these two classes has become blurred, with the discovery of alkyl substituted carbenes that are clearly electrophilic in nature,<sup>3</sup> and carbenes that are intermediate in nature, or that can exhibit both nucleophilic and electrophilic behavior.<sup>4</sup>

Bridging carbenes form a third class that show properties distinct from either of the types of terminal carbenes.<sup>2,5</sup> For example, terminal methylene complexes of late transition metals are extremely rare, while bridging methylenes are common for these metals. The difference in properties is to be expected when the hybridization of the carbene carbon is considered. In terminal carbenes, the carbene carbon is  $sp^2$  hybridized and formally acts as a two electron  $\sigma$ -donor and as a  $\pi$ -acceptor, much like CO. The bridging carbene on the other hand has an  $sp^3$  hybridized carbon, and is more closely related to an alkyl group, and acts as an dianionic four-electron donor, forming  $\sigma$ -bonds to two metals.

Carbene complexes were of particular interest to us because of the importance of surface methylene species in Fischer-Tropsch catalysis.<sup>6</sup> We were particularly interested in combining carbene ligands with vinyl and alkyl ligands because of a recent mechanistic proposal for formation of long-chain hydrocarbons on surfaces through the migration of vinyl groups to surface methylenes.<sup>7</sup> It has been proposed that vinyl groups migrate more readily than alkyl groups.<sup>8</sup> In addition, one part of this proposal involves the isomerization of the allyl group resulting from vinyl-to-methylene migration, to a substituted vinyl group, a step that has little literature precedent.<sup>9</sup> We were interested in testing these proposals in our binuclear systems. This chapter reports our initial attempts at formation of carbene complexes of Rh/Os.

### Experimental Section

**General Comments.** 1-methyl-3-nitro-1-nitosoguanidine (MNNG) and N-methyl-N-nitroso-p-toluenesulfonamide (Diazald) were obtained from Aldrich. Spectroscopic data for all compounds are given in Table 4.1.

### Preparation of Compounds

(a)  $[\text{RhOs}(\text{C}(\text{CH}_3)=\text{CH}_2)(\text{CH}_3)(\text{CO})_3(\text{dppm})(\mu\text{-Ph}_2\text{PCHPh}_2)]$  (33a,b).  $[\text{RhOs}(\text{C}(\text{CH}_3)=\text{CH}_2)(\text{CH}_3)(\text{CO})_3(\text{dppm})_2][\text{CF}_3\text{SO}_3]$  (7a,b, 15 mg, 0.011 mmol) was suspended in 0.5 mL of  $d^8$ -THF. Butyl lithium (2.5 M in hexanes, 4.5  $\mu\text{L}$ , 0.011 mmol) was added, causing the undissolved solid to gradually dissolve over 10 min to form a yellow-orange solution. The product  $[\text{RhOs}(\text{C}(\text{CH}_3)=\text{CH}_2)(\text{CH}_3)(\text{CO})_3(\text{dppm})(\mu\text{-Ph}_2\text{PCHPh}_2)]$  (33a, b) was formed in quantitative yield and was characterized in solution but not isolated.

Table 4.1. Spectroscopic Parameters for the Compounds<sup>a</sup>

compound	IR, <sup>b</sup> cm <sup>-1</sup>	NMR <sup>d</sup>	
		$\delta(^1\text{P}\{\text{H}\})$	$\delta(^1\text{H})$ $\delta(^{13}\text{C}\{\text{H}\})$
[RhOs(C(CH <sub>3</sub> )=CH <sub>2</sub> )(CH <sub>3</sub> )- (CO) <sub>3</sub> (dppm)- ( $\mu$ -Ph <sub>2</sub> PCHPPPh <sub>2</sub> )] (33a)		RhP: 29.30 (dddd), 19.53 (dddd) OsP: -0.78 (ddd), -5.10 (ddd)	PCH <sub>2</sub> P: 3.7 (m, 2H), 3.3 (m, 2H) RhC-CH <sub>3</sub> : <sup>e</sup> RhC=CH <sub>2</sub> : 5.38 (s, 1H), 4.50 (s, 1H) OsCH <sub>3</sub> : -0.45 (dd, 3H <sup>3</sup> J <sub>OsPH</sub> = 9 Hz, 6 Hz)
(33b)		RhP: 30 (dddd), 18 (dddd) OsP: -0.24 (ddd), -7.44 (ddd)	PCH <sub>2</sub> P: 3.6 (m, 2H), 3.4 (m, 2H) RhC-CH <sub>3</sub> : <sup>e</sup> RhC=CH <sub>2</sub> : 5.19 (s, 1H), 4.50 (s, 1H) OsCH <sub>3</sub> : -0.41 (dd, 3H <sup>3</sup> J <sub>OsPH</sub> = 6 Hz, 5 Hz)
[RhOs- ( $\eta^2$ -N(O)N(CH <sub>3</sub> )C(N(H)NO <sub>2</sub> )- (CO) <sub>3</sub> ( $\mu$ -H)(dppm) <sub>2</sub> ][BF <sub>4</sub> ] <sub>2</sub> (34)	2052 (ss), 1981 (ss), 1737 (ss)	RhP: 16.24 ( <sup>1</sup> J <sub>Rh-P</sub> = 99 Hz) OsP: -13.49	PCH <sub>2</sub> P: 3.96 (m, 2H), 3.59 (m, 2H) CH <sub>3</sub> : 1.82 (s, 3H) NH: 9.28 (s, 1H) Rh/Os: -14.92 (bm)
			OsCO: 175.99 (t, <sup>2</sup> J <sub>PC</sub> = 10 Hz), 175.68 (t, <sup>2</sup> J <sub>PC</sub> = 11 Hz), 244.99 (bs)

compound	IR, $\text{cm}^{-1}$	NMR <sup>d</sup>	
		$\delta(^1\text{P}\{\text{H}\})$	$\delta(^{13}\text{C}\{\text{H}\})$
$[\text{RhOs}(\text{CH}_2\text{CH}=\text{CH}_2)(\text{CH}_3)(\text{CO})_3(\text{dppm})_2][\text{BF}_4]$ (35)	2031(ss), 1799 (ms)	RhP: 27.28 ( $^1J_{\text{Rh-P}} = 148$ Hz) OsP: -4.96	OsCO: 179.14 (dt, $^2J_{\text{CC}} = 27$ Hz, $^2J_{\text{PC}} = 9$ Hz), 203.5 (dm, $^1J_{\text{RhC}} = 12$ Hz), 232.57 (ddm, $^1J_{\text{RhC}} = 27$ Hz, $^2J_{\text{CC}} = 27$ Hz)
$[\text{RhOs}(\text{CH}_3)(\text{CO})_3(\mu\text{-Cl})(\text{dppm})_2][\text{BF}_4]$ (36)		PCH <sub>2</sub> P: 3.23 (m, 2H), 3.33 (m, 2H) RhCH <sub>2</sub> : 2.60 (dm, 2H, $^3J_{\text{HH}} = 7$ Hz) CH <sub>2</sub> CH: 5.16 (ddt, $^3J_{\text{trans}} = 16$ Hz, $^3J_{\text{cis}} = 10$ Hz, $^2J_{\text{H-CH}_2} = 7$ Hz) CH=CH <sub>2</sub> : 2.89 (d, $^3J_{\text{HH}} = 16$ Hz), 3.70 (d, $^3J_{\text{HH}} = 10$ Hz) OsCH <sub>3</sub> : -0.26 (t, 3H, $^3J_{\text{PH}} = 7$ Hz)	
$[\text{RhOs}(\text{CH}_3)(\text{CO})_3(\mu\text{-Cl})(\text{dppm})_2][\text{BF}_4]$ (36)		RhP: 19.06 ( $^1J_{\text{Rh-P}} = 111$ Hz) OsP: -6.66	OsCO: 181.7 (s), 177.18 (t, $^2J_{\text{PC}} = 9$ Hz) RhCO: 188.84 (dt, $^1J_{\text{RhC}} = 86$ Hz, $^2J_{\text{PC}} = 15$ Hz)
$[\text{RhOs}(\text{C}(\text{CH}_3)_2(\text{H})(\text{CO}))_3(\text{dppm})_2][\text{BF}_4]_2$ (37)		RhP: 19.0 ( $^1J_{\text{Rh-P}} = 135$ Hz) OsP: -4.80	OsCO: 172.8 (t, $^2J_{\text{P-C}} = 9$ Hz); 193.1 (bs); 204.0 (dt, $^1J_{\text{Rh-C}} = 10$ Hz, $^2J_{\text{P-C}} = 3$ Hz) Rh=C(CH <sub>3</sub> ) <sub>2</sub> : 377.9 (dt, $^1J_{\text{Rh-C}} = 35$ Hz, $^2J_{\text{P-C}} = 5$ Hz) Rh=C(CH <sub>3</sub> ) <sub>2</sub> : 63.6 (s), 60.6 (s)
$[\text{RhOs}(\text{C}(\text{CH}_3)_2)(\text{CH}_3)(\text{CO})_3(\text{dppm})_2][\text{BF}_4][\text{CF}_3\text{SO}_3]$ (38)		RhP: 17.67 ( $^1J_{\text{Rh-P}} = 136$ Hz) OsP: -8.00	

compound	IR, <sup>b</sup> cm <sup>-1</sup>	NMR <sup>d</sup>		
		δ( <sup>31</sup> P{ <sup>1</sup> H})	δ( <sup>1</sup> H)      δ( <sup>13</sup> C{ <sup>1</sup> H})	
[RhOs- (=C(OH)C(CH <sub>3</sub> )=CH <sub>2</sub> )- (μ-H)(CO) <sub>3</sub> (dppm) <sub>2</sub> ][BF <sub>4</sub> ] (39)	2060(ss), 2002(ss), 1756(wb) <sup>e</sup>	RhP: 24.80 ( <sup>1</sup> J <sub>Rh-P</sub> = 115 Hz) OsP: -5.84	PCH <sub>2</sub> P: 4.14 (m, 2H), 3.85(m, 2H) C=CH <sub>2</sub> : 5.61 (s), 4.30 (s) C-CH <sub>3</sub> : 1.06 (s, 3H) OsHRh: -9.85 (bm) OH: 9.56 (s) <sup>f</sup>	OsCO: 172.5 (s); 175.7 (dt, <sup>2</sup> J <sub>C-C</sub> = 27 Hz, <sup>2</sup> J <sub>P-C</sub> = 9 Hz); 234.8 (dd, <sup>1</sup> J <sub>Rh-C</sub> = <sup>2</sup> J <sub>P-C</sub> = 27 Hz) Rh=C: 301.2 (dt, <sup>1</sup> J <sub>Rh-C</sub> = 49 Hz, <sup>2</sup> J <sub>P-C</sub> = 8 Hz)

a. abbreviations used: IR: ss = strong sharp, ms = medium sharp, ws = weak sharp, sb = strong broad, mb = medium broad, sh = shoulder, m = medium, NMR: t = triplet, dt = doublet of triplets, ddt = doublet of doublets of triplets, m = multiplet, bs = broad singlet, dm = doublet of doublets, ddm = doublet of doublets of multiplets, s = singlet, ddd = doublet of doublets of doublets, dddd = doublet of doublets of doublets of doublets, bm = broad multiplet.

b. Nujol mull except as indicated. Values quoted are ν(CO) except as indicated. c. CH<sub>2</sub>Cl<sub>2</sub> solution. d. <sup>31</sup>P{<sup>1</sup>H} chemical shifts are referenced vs. external 85% H<sub>3</sub>PO<sub>4</sub>, while <sup>1</sup>H and <sup>13</sup>C{<sup>1</sup>H} are referenced vs. external TMS. Chemical shifts for the phenyl hydrogens are not given in the <sup>1</sup>H NMR data. e. Propenyl methyl hydrogens were obscured by resonances of butane. f. -40°C.



MNNG (150 mg, 1.02 mmol) in 1 mL of water layered with 15 mL of Et<sub>2</sub>O was reacted in 1 mL of 5 M NaOH. When the reaction was complete, the Et<sub>2</sub>O layer was added to  $[\text{RhOs}(\text{CO})_3(\text{NCMe})(\mu\text{-H})(\text{dppm})_2][\text{BF}_4]_2$  (100 mg, 0.0713 mmol) dissolved in 25 mL of THF. Over 1 h, an orange precipitate formed and was allowed to settle. The pale yellow supernatant was discarded and the residue was washed with 3x5 mL of Et<sub>2</sub>O and dried in vacuo. Yield: 58 mg, 59%.



diazomethane in 10 mL of Et<sub>2</sub>O was generated by decomposition of MNNG (200 mg, 1.36 mmol) with NaOH, using the method of Fales et. al.<sup>10</sup> The Et<sub>2</sub>O solution of diazomethane was added to a stirred slightly cloudy yellow solution of  $[\text{RhOs}(\text{CO})_4(\text{dppm})_2][\text{BF}_4]$  (2, 15 mg, 0.0119 mmol) in 10 mL THF. The mixture was stirred for 2.5 h and the yellow product was allowed to settle. The colourless supernatant solution was removed via canula and the residue was washed with 3x5 mL of Et<sub>2</sub>O and dried in vacuo. The residue was extracted into 3 mL of CH<sub>2</sub>Cl<sub>2</sub>, filtered and the solvent was removed in vacuo. The residue was then recrystallized from CH<sub>2</sub>Cl<sub>2</sub>/Et<sub>2</sub>O, washed with 3x5 mL of Et<sub>2</sub>O and dried in vacuo. Yield: 8 mg, 52%. Anal. calcd. for C<sub>57</sub>H<sub>52</sub>BF<sub>4</sub>O<sub>3</sub>OsP<sub>4</sub>Rh: C, 51.99; H, 3.98. Found: C, 51.46; H, 3.35. Compound 35 can be independently synthesized by reaction of  $[\text{RhOs}(\eta^3\text{-C}_3\text{H}_5)(\text{CO})_3(\text{dppm})_2]$  (19) with methyl triflate.



in CD<sub>2</sub>Cl<sub>2</sub> for three days, complete conversion to  $[\text{RhOs}(\text{CH}_3)(\mu\text{-Cl})(\text{CO})_3(\text{dppm})_2][\text{BF}_4]$  (36) is observed. The solvent was then removed in vacuo, and the residue was

recrystallized from  $\text{CH}_2\text{Cl}_2/\text{Et}_2\text{O}$ , washed with 3x5 mL of  $\text{Et}_2\text{O}$  and dried in vacuo. Anal. calcd. for  $\text{C}_{54}\text{H}_{47}\text{BClF}_4\text{O}_3\text{OsP}_4\text{Rh}$ : C, 50.54; H, 3.69; Cl, 2.76. Found: C, 50.94; H, 3.83; Cl, 2.84.

(d)  $[\text{RhOs}(=\text{C}(\text{CH}_3)_2)(\text{H})(\text{CO})_3(\text{dppm})_2][\text{BF}_4]_2$  (37). The compound  $[\text{RhOs}(\text{C}(\text{CH}_3)=\text{CH}_2)(\text{CO})_3(\text{dppm})_2]$  (3, 13 mg, 0.011 mmol) was dissolved in 0.5 mL of  $\text{CD}_2\text{Cl}_2$  and cooled to  $-80^\circ\text{C}$ .  $\text{HBF}_4 \cdot \text{Me}_2\text{O}$  (3.3  $\mu\text{L}$ , 3.7 mg, 0.027 mmol) was added and NMR spectra at  $-80^\circ\text{C}$  showed quantitative conversion to 36. At temperatures above  $0^\circ\text{C}$  compound 37 was unstable, decomposing into  $[\text{RhOs}(\text{C}(\text{CH}_3)=\text{CH}_2)(\text{H})(\text{CO})_3(\text{dppm})_2][\text{BF}_4]$  (26a,b) and other unidentified products.

(e)  $[\text{RhOs}(=\text{C}(\text{CH}_3)_2)(\text{CH}_3)(\text{CO})_3(\text{dppm})_2][\text{BF}_4][\text{CF}_3\text{SO}_3]$  (38). The compound  $[\text{RhOs}(\text{C}(\text{CH}_3)=\text{CH}_2)(\text{CH}_3)(\text{CO})_3(\text{dppm})_2][\text{CF}_3\text{SO}_3]$  (23a,b, 4 mg, 0.0030 mmol) was dissolved in 0.5 mL of  $\text{CD}_2\text{Cl}_2$  and cooled to  $-40^\circ\text{C}$ .  $\text{HBF}_4 \cdot \text{Me}_2\text{O}$  (2  $\mu\text{L}$ , 2.2 mg, 0.016 mmol) was added and NMR spectra showed quantitative conversion to 37 at  $-40^\circ\text{C}$ . At temperatures above  $0^\circ\text{C}$ , the sample was unstable, decomposing into 23a,b and other unidentified products.

(f)  $[\text{RhOs}(=\text{C}(\text{OH})\text{C}(\text{CH}_3)=\text{CH}_2)(\mu\text{-H})(\text{CO})_3(\text{dppm})_2][\text{BF}_4]_2$  (39). The compound  $[\text{RhOs}(\text{C}(\text{O})\text{C}(\text{CH}_3)=\text{CH}_2)(\text{CO})_3(\text{dppm})_2]$  (22; 20 mg, 0.016 mmol) was dissolved in 0.5 mL of  $\text{CD}_2\text{Cl}_2$  and cooled to  $-80^\circ\text{C}$ .  $\text{HBF}_4 \cdot \text{Me}_2\text{O}$  (4  $\mu\text{L}$ , 4.4 mg, 0.33 mmol) was added and the reaction was monitored by NMR. At  $-80^\circ\text{C}$ , the compound  $[\text{RhOs}(\text{C}(\text{O})\text{C}(\text{CH}_3)=\text{CH}_2)(\mu\text{-H})(\text{CO})_3(\text{dppm})_2][\text{BF}_4]$  (30) formed quantitatively. At temperatures above  $-40^\circ\text{C}$ , 30 transformed into 38, which persisted in solution at ambient temperature for up to 2 hours, but decomposed upon workup.

(g) Reaction of  $[\text{RhOs}(\text{C}(\text{O})\text{C}(\text{CH}_3)=\text{CH}_2)(\text{CO})_3(\text{dppm})_2]$  (22) with  $\text{CH}_3\text{SO}_3\text{CF}_3$ . Compound 22 (20 mg, 0.016 mmol) was dissolved in 0.5 mL of  $\text{CD}_2\text{Cl}_2$  and cooled to  $-80^\circ\text{C}$ . Methyl triflate (1.8  $\mu\text{L}$ , 2.7 mg, 0.016 mmol) was added and the reaction was monitored by NMR. No reaction was observed up to  $-30^\circ\text{C}$ . At this temperature, three products began to form simultaneously and conversion to these products, along with several minor products, was complete at ambient temperature. The mixture of products could not be separated but spectroscopic evidence suggests that a mixture of  $[\text{RhOs}(\text{C}(\text{O})\text{C}(\text{CH}_3)=\text{CH}_2)(\text{CO})_3(\text{dppm})_2][\text{CF}_3\text{SO}_3]$  and two isomers of  $[\text{RhOs}(\text{C}(\text{O})\text{C}(\text{CH}_3)=\text{CH}_2)(\text{CH}_3)(\text{CO})_3(\text{dppm})_2][\text{CF}_3\text{SO}_3]$  were formed.

#### X-ray Data Collection.



Diffusion of benzene into a concentrated  $\text{CH}_2\text{Cl}_2$  solution of complex 34 yielded deep red-orange crystals, which were mounted and flame-sealed in glass capillaries under solvent vapor to minimize solvent loss. Data were collected on an Siemens P4/RA diffractometer using  $\text{Cu K}\alpha$  radiation at  $-60^\circ\text{C}$ . Unit cell parameters were obtained from a least-squares refinement of the setting angles of 45 reflections in the range  $57.6^\circ \leq 2\theta \leq 59.1^\circ$ . The cell parameters indicated a monoclinic space group with  $Z = 4$  and the systematic absences indicated the space group  $\text{P}2_1/\text{n}$ . Intensity data were collected as outlined in Table 4.2. Three reflections were chosen as intensity standards and were remeasured every 200 reflections; no decay was evident.

**Table 4.2.** Crystallographic Experimental Details*A. Crystal Data*

formula	$C_{58}H_{55}BCl_6F_4N_5O_6OsP_4Rh$
formula weight	1634.57
crystal dimensions(mm)	0.12 x 0.22 x 0.33
crystal system	monoclinic
space group	$P2_1/n$ (non-standard setting of $P2_1/c$ (No. 14))
unit cell parameters <sup>a</sup>	
a(Å)	17.7057(8)
b(Å)	19.2528(6)
c(Å)	19.3535(6)
$\beta$ (°)	102.115(4)
V(Å <sup>3</sup> )	6450.4(4)
Z	4
$\rho_{\text{calcd}}$ (g cm <sup>-3</sup> )	1.683
$\mu$ (cm <sup>-1</sup> )	95.02

*B. Data Collection and Refinement Conditions*

diffractometer	Siemens P4/RA <sup>b</sup>
radiation( $\lambda$ (Å))	CuK $\alpha$ (1.54178)
monochromator	incident beam, graphite crystal
temperature(°C)	-60
data collection $2\theta$ limit(°)	113.50
total data collected	8949 ( $0 \leq h \leq 19$ , $0 \leq k \leq 20$ , $-20 \leq l \leq 20$ )
independent reflections	8623
number of observations (NO)	6724
structure solution method	direct methods ( <i>SHELXS-86</i> <sup>c</sup> )
refinement method	full-matrix least-squares on $F^2$ ( <i>SHELXL-93</i> <sup>d</sup> )

(Table 4.2 cont.)

absorption correction method	Gaussian integration (face indexed)	
range of absorption correction factors	0.17603-0.38800	
data/restraints/parameters	8606/0/780	
goodness-of-fit(S) <sup>e</sup>	1.105	
final R indices <sup>f</sup>		
observed data	R <sub>1</sub> = 0.0487	wR <sub>2</sub> = 0.1038
all data	R <sub>1</sub> = 0.0719	wR <sub>2</sub> = 0.1204
largest difference peak and hole	0.851 and -1.819eÅ <sup>-3</sup>	

<sup>a</sup>Obtained from least-squares refinement of 45 reflections with  $57.6^\circ < 2\theta < 59.1^\circ$ .

<sup>b</sup>Programs for diffractometer operation and data collection were those supplied by Siemens.

<sup>c</sup>Sheldrick, G. M. *Acta Crystallogr.* 1990, *A46*, 467.

<sup>d</sup>Sheldrick, G. M. *SHELXL-93*, Program for crystal structure determination. University of Gottingen, 1993. Weighted *R*-factors  $wR_2$  and all goodnesses of fit *S* are based on  $F_o^2$ ; conventional *R*-factors  $R_1$  are based on  $F_o$ , with  $F_o$  set to zero for negative  $F_o^2$ . The observed criterion of  $F_o^2 > 2\sigma(F_o^2)$  is used only for calculating  $R_1$ , and is not relevant to the choice of reflections for refinement. *R*-factors based on  $F_o^2$  are statistically about twice as large as those based on  $F_o$ , and *R*-factors based on ALL data will be even larger.

<sup>e</sup> $S = [\sum w(F_o^2 - F_c^2)^2 / (n - p)]^{1/2}$  ( $n$  = number of data;  $p$  = number of parameters varied;  $w = [\sigma^2(F_o^2) + (a_1 P)^2 + a_2 P]^{-1}$  where  $P = [\text{Max}(F_o^2, 0) + 2F_c^2]/3$ ,  $a_1 = 0.0435$ ,  $a_2 = 34.1834$ ).

<sup>f</sup> $R_1 = \sum ||F_o| - |F_c|| / \sum |F_o|$ ;  $wR_2 = [\sum w(F_o^2 - F_c^2)^2 / \sum w(F_o^4)]^{1/2}$ .

### Structure Solution and Refinement.

The positions of the Os, Rh and P atoms, as well as the dppm methylene and several phenyl carbons, were obtained through use of the direct-methods program *SHELXS-86*.<sup>11</sup> The remaining non-hydrogen atoms were located using successive least-squares refinements and difference Fourier maps. Refinement was completed using the program *SHELXL-93*.<sup>12</sup> The hydride ligand was located using electron density contour plots and its position and isotropic thermal parameter were allowed to refine. The hydrogen bound to N(3) was located in the Fourier map, but was input using an idealized position. All other hydrogen atom positions were calculated by assuming idealized  $sp^2$  or  $sp^3$  geometries about their attached carbons; these hydrogens were given thermal parameters equal to 120% of the equivalent isotropic displacement parameters of their attached carbons. After all atoms had been located and the structure refined to convergence using isotropic displacement parameters, the data were corrected for absorption using Gaussian integration (face indexed) absorption correction. The structure was further refined with all non-hydrogen atoms having anisotropic thermal parameters. The final model for complex **34**, with 780 parameters varied, converged to a value of  $R_1 = 0.0487$ . Atomic coordinates and displacement parameters for the non-hydrogen core atoms are given in Table 4.3.

### Results and Compound Characterization

Initial attempts at forming methylene complexes in the Rh/Os system focused on deprotonation or removal of a hydride from methyl ligands in the appropriate complexes. Reaction of  $[\text{RhOs}(\text{CH}_3)(\text{CO})_3(\text{dppm})_2]$  (11) with  $[\text{Ph}_3\text{C}][\text{PF}_6]$  led to

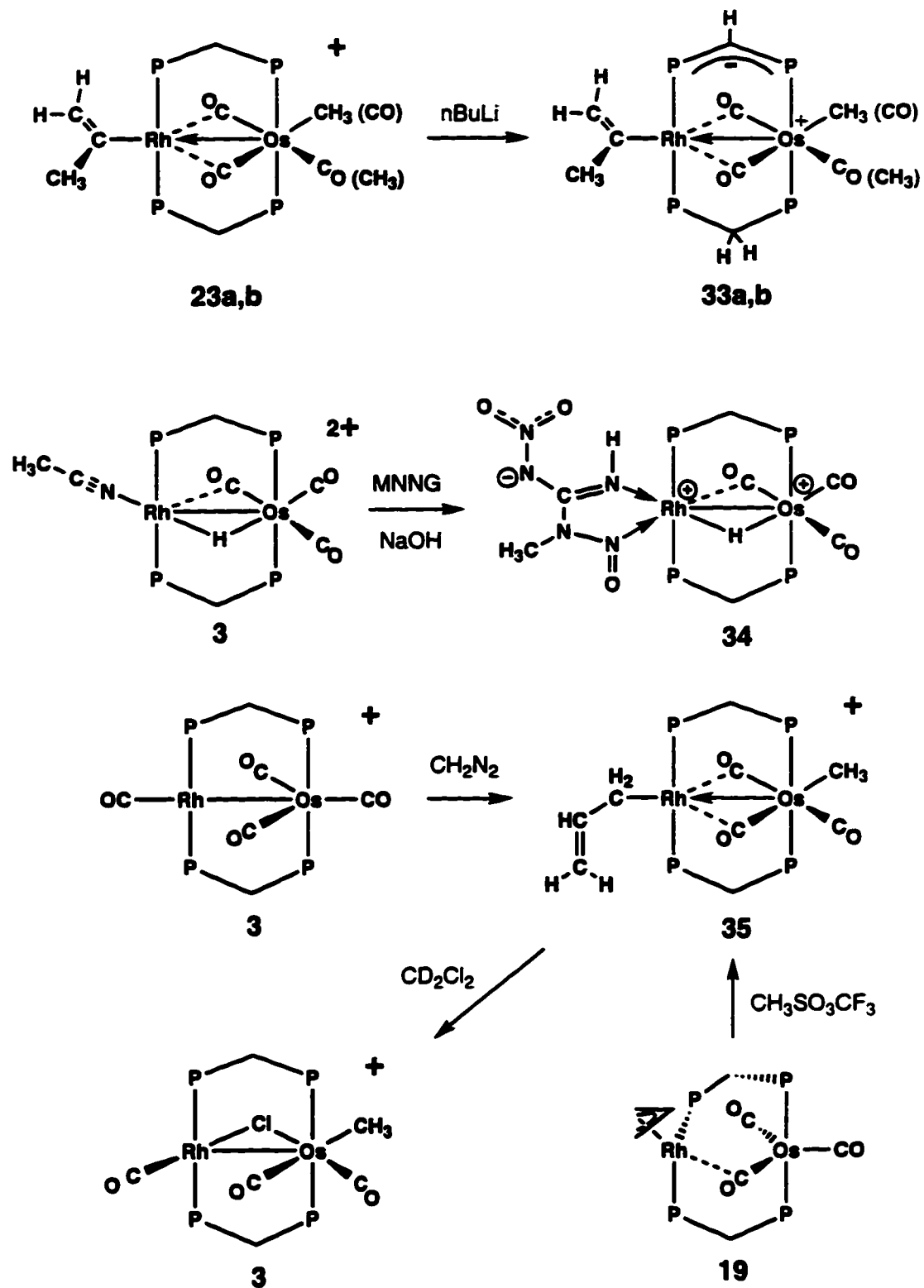
**Table 4.3** Atomic Coordinates and Equivalent Isotropic Displacement Parameters for the Core Atoms of Compound 34.

Atom	x	y	z	U <sub>eq</sub> , Å <sup>2</sup>
Os	0.51740(2)	0.27236(2)	0.14589(2)	0.01895(12)*
Rh	0.61148(3)	0.16189(3)	0.21809(3)	0.0181(2)*
H(1)	0.5871(49)	0.2427(45)	0.1929(45)	0.044(27)
P(1)	0.53788(12)	0.15424(11)	0.30566(11)	0.0217(5)*
P(2)	0.44524(12)	0.27714(12)	0.23697(11)	0.0226(5)*
P(3)	0.69311(12)	0.16251(11)	0.13673(11)	0.0204(5)*
P(4)	0.58972(12)	0.27148(11)	0.05487(11)	0.0209(5)*
O(1)	0.5671(4)	0.4254(3)	0.1751(3)	0.043(2)*
O(2)	0.3711(4)	0.3104(4)	0.0399(3)	0.044(2)*
O(3)	0.4771(3)	0.1179(3)	0.1130(3)	0.0258(13)*
O(4)	0.7496(4)	0.2165(3)	0.3388(3)	0.037(2)*
O(5)	0.6660(4)	-0.0724(3)	0.2239(3)	0.044(2)*
O(6)	0.7582(4)	-0.1249(3)	0.2963(4)	0.046(2)*
N(1)	0.7167(4)	0.1666(4)	0.3064(3)	0.026(2)*
N(2)	0.7466(4)	0.1049(4)	0.3272(4)	0.025(2)*
N(3)	0.6478(3)	0.0606(4)	0.2405(3)	0.020(2)*
N(4)	0.7476(4)	-0.0121(4)	0.3114(4)	0.028(2)*
N(5)	0.7223(4)	-0.0708(4)	0.2757(4)	0.030(2)*
C(1)	0.5504(5)	0.3680(5)	0.1658(5)	0.027(2)*
C(2)	0.4281(5)	0.2954(5)	0.0801(5)	0.030(2)*
C(3)	0.5130(5)	0.1644(5)	0.1419(4)	0.023(2)*
C(4)	0.7085(5)	0.0464(4)	0.2882(4)	0.021(2)*
C(5)	0.8152(5)	0.1004(5)	0.3837(5)	0.044(3)*
C(10)	0.4977(4)	0.2391(4)	0.3197(4)	0.021(2)*
C(20)	0.6883(4)	0.2454(4)	0.0897(4)	0.021(2)*

decomposition over a wide range of temperatures, whereas the cationic dialkyl or vinyl/alkyl complexes were unreactive towards the trityl reagent. Formation of methylene complexes by deprotonation of a methyl group also proved unsuccessful, since the most acidic hydrogens in the cationic dialkyl, or vinyl/alkyl complexes are those of the dppm methylene groups. For example, reaction of  $[\text{RhOs}(\text{C}(\text{CH}_3)=\text{CH}_2)-(\text{CH}_3)(\text{CO})_3(\text{dppm})_2][\text{CF}_3\text{SO}_3]$  (**23**) with BuLi resulted in deprotonation of one of the dppm methylene groups to form  $[\text{RhOs}(\text{C}(\text{CH}_3)=\text{CH}_2)(\text{CH}_3)(\text{CO})_3(\mu\text{-dppm})(\mu\text{-Ph}_2\text{PCHPh}_2)]$  (**31a,b**) which exists as two isomers like the starting compound. (see Scheme 4.1) The spectroscopic data for **31** are as expected. The  $^{31}\text{P}$  NMR spectrum shows two overlapping ABMNX patterns for the two isomers, very similar to the spectrum of  $[\text{RhOs}(\text{CO})_4(\mu\text{-dppm})(\mu\text{-Ph}_2\text{PCHPh}_2)]$  (**9**), which was prepared in an analogous fashion (see Chapter 2). The  $^1\text{H}$  NMR resonances of the vinyl group are analogous to those of **23**, but the methyl groups now appear as doublets of doublets rather than triplets because the phosphines on Os are now inequivalent. The dimethyl complex  $[\text{RhOs}(\text{CH}_3)_2(\text{CO})_3(\text{dppm})_2][\text{CF}_3\text{SO}_3]$  (**17**) also reacts with BuLi with deprotonation of one dppm group.

Another method commonly used to introduce methylene groups onto metal complexes is by reaction with diazomethane.<sup>13</sup> Thus, the reaction of diazomethane with  $[\text{RhOs}(\text{CO})_3(\text{NCMe})(\mu\text{-H})(\text{dppm})_2][\text{BF}_4]_2$  (**3**), was attempted, to determine if diazomethane would displace the acetonitrile. However, in initial attempts, the diazomethane for this reaction was generated by collecting it in Et<sub>2</sub>O layered on top of the aqueous phase containing the precursor, MNNG. This method allowed a deprotonated form of the MNNG to enter the wet Et<sub>2</sub>O phase.

## Scheme 4.1



Instead of reacting with diazomethane, the complex reacted with the deprotonated form of MNNG, to form  $[\text{RhOs}(\eta^2\text{-N}(\text{O})\text{N}(\text{CH}_3)\text{C}(\text{NNO}_2)\text{NH})(\text{CO})_3(\mu\text{-H})(\text{dppm})_2][\text{BF}_4]$  (**34**), as diagrammed in Scheme 4.1. The  $^1\text{H}$  NMR spectrum of **34** shows an AB quartet for the dppm methylenes and a broad multiplet at  $\delta$  -14.92 which is indicative of a bridging hydride, as well as singlets at  $\delta$  1.82 and 9.28, with integrations of 3 and 1, respectively, indicating that the methyl group of MNNG has remained intact and suggesting that one of two N-bound hydrogens has been lost. The  $^{13}\text{C}$  NMR spectrum contains resonances for three carbonyls, appearing as triplets at  $\delta$  175.99 and 175.68, consistent with two terminal carbonyls on Os, and at  $\delta$  244.99, suggesting a bridging or semibridging carbonyl; the bridging carbonyl is also apparent in the IR spectrum, which shows a stretch at  $1737\text{ cm}^{-1}$ , as well as terminal bands at  $1981$  and  $2052\text{ cm}^{-1}$ . Compound **34** has a structure analogous to that of **3**, with a bridging hydride, two terminal carbonyls on Os, and a semibridging carbonyl; however, the coordination mode of the ligand on Rh could not be unambiguously determined from the spectroscopy.

Compound **34** has been characterized by X-ray crystallography and is shown in Figure 4.1. Important bond lengths and angles are given in Table 4.4. Only one  $\text{BF}_4^-$  counterion per cation is observed, confirming the monocationic nature of the complex, consistent with the loss of one proton from the MNNG group. The MNNG-derived ligand is bidentate on Rh, coordinated through the nitroso nitrogen (N(1)) and through the imine nitrogen (N(3)). The imine hydrogen H(3) was located in the Fourier map, supporting its placement on N(3) and indicating that it is the amine nitrogen N(4) which has been deprotonated. It appears counterintuitive that the neutral imine nitrogen coordinates to Rh instead of N(4), which has the negative charge. We assume

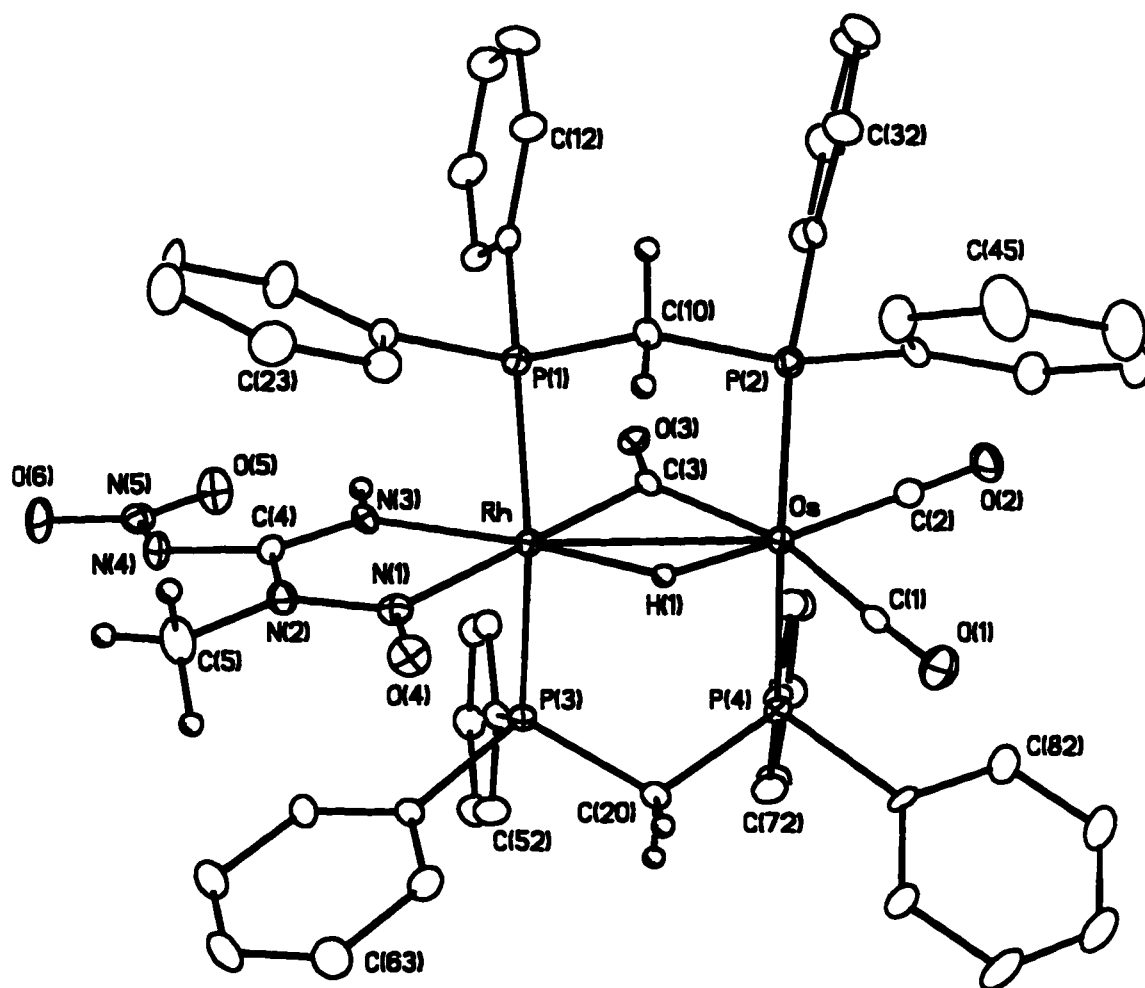


**Figure 4.1.** Perspective view the  $[\text{RhOs}(\eta^2\text{-N}(\text{O})\text{N}(\text{CH}_3)\text{C}(\text{NNO}_2)\text{NH})\text{-(CO)}_3(\mu\text{-H})(\text{dppm})_2]^+$  cation of compound 34. Thermal ellipsoids are shown at the 20% probability level except for hydrogens which are shown arbitrarily small. Phenyl hydrogens have been omitted. Phenyl carbons are numbered sequentially for each phenyl ring, beginning with the ipso carbon.

**Table 4.4.** Selected Distances (Å) and Angles (°) for **34**.

Atom 1	Atom 2	Distance	Atom 1	Atom 2	Distance
Os	Rh	2.8765(7)	P(2)	C(10)	1.827(8)
Os	H(1)	1.48(8)	P(3)	C(20)	1.830(8)
Rh	H(1)	1.66(9)	O(1)	C(1)	1.149(10)
Os	P(2)	2.386(2)	O(2)	C(2)	1.175(10)
Os	P(4)	2.385(2)	O(3)	C(3)	1.171(10)
Os	C(1)	1.945(10)	O(4)	N(1)	1.225(8)
Os	C(2)	1.862(9)	O(5)	N(5)	1.257(9)
Os	C(3)	2.081(9)	O(6)	N(5)	1.241(9)
Rh	P(1)	2.349(2)	N(1)	N(2)	1.329(9)
Rh	P(3)	2.350(2)	N(2)	C(4)	1.442(10)
Rh	N(1)	2.250(7)	N(2)	C(5)	1.456(10)
Rh	N(3)	2.071(7)	N(3)	C(4)	1.290(10)
Rh	C(3)	2.034(8)	N(4)	N(5)	1.351(10)
P(1)	C(10)	1.825(8)	N(4)	C(4)	1.349(10)

Atom 1	Atom 2	Atom 3	Angle	Atom 1	Atom 2	Atom 3	Angle
Rh	Os	P(2)	90.85(5)	H(1)	Os	Rh	25.3(34)
Rh	Os	P(4)	90.43(5)	P(2)	Os	P(4)	178.20(8)
Rh	Os	C(1)	118.9(2)	P(2)	Os	C(1)	90.1(2)
Rh	Os	C(2)	146.1(3)	P(2)	Os	C(2)	89.2(3)
Rh	Os	C(3)	45.0(2)	P(2)	Os	C(3)	92.6(2)
H(1)	Os	C(2)	170.7(33)	P(4)	Os	C(1)	88.1(2)
H(1)	Os	C(1)	93.8(34)	P(4)	Os	C(2)	90.4(3)
H(1)	Os	C(3)	70.0(34)	P(4)	Os	C(3)	89.2(2)
H(1)	Os	P(4)	86.8(33)	C(1)	Os	C(2)	95.0(4)
H(1)	Os	P(2)	93.8(33)	C(1)	Os	C(3)	163.7(3)

*(Table 4.4 cont.)*

C(2)	Os	C(3)	101.1(4)	Os	P(2)	C(41)	113.7(3)
Os	Rh	P(1)	92.55(6)	Rh	P(3)	C(20)	111.5(3)
Os	Rh	P(3)	92.62(6)	Rh	P(3)	C(51)	118.0(3)
Os	Rh	N(1)	129.9(2)	Rh	P(3)	C(61)	112.9(3)
Os	Rh	N(3)	157.0(2)	Os	P(4)	C(20)	110.7(3)
Os	Rh	C(3)	46.3(2)	Os	P(4)	C(71)	118.5(3)
H(1)	Rh	C(3)	68.6(29)	Os	P(4)	C(81)	114.3(3)
H(1)	Rh	N(3)	173.9(30)	Rh	N(1)	O(4)	130.5(6)
H(1)	Rh	N(1)	107.9(29)	Rh	N(1)	N(2)	114.0(5)
H(1)	Rh	P(1)	96.9(30)	O(4)	N(1)	N(2)	115.5(7)
H(1)	Rh	P(3)	87.6(30)	N(1)	N(2)	C(4)	115.3(6)
H(1)	Rh	Os	22.5(29)	N(1)	N(2)	C(5)	119.8(7)
P(1)	Rh	P(3)	174.78(8)	C(4)	N(2)	C(5)	124.9(7)
P(1)	Rh	N(1)	87.2(2)	Rh	N(3)	C(4)	121.6(6)
P(1)	Rh	N(3)	89.1(2)	N(5)	N(4)	C(4)	115.9(7)
P(1)	Rh	C(3)	90.2(2)	O(5)	N(5)	O(6)	120.2(7)
P(3)	Rh	N(1)	88.9(2)	O(5)	N(5)	N(4)	123.4(7)
P(3)	Rh	N(3)	86.4(2)	O(6)	N(5)	N(4)	116.4(7)
P(3)	Rh	C(3)	93.9(2)	Os	C(1)	O(1)	176.8(8)
N(1)	Rh	N(3)	73.0(3)	Os	C(2)	O(2)	178.5(8)
N(1)	Rh	C(3)	175.4(3)	Os	C(3)	Rh	88.7(4)
N(3)	Rh	C(3)	110.8(3)	Os	C(3)	O(3)	142.6(6)
Rh	P(1)	C(10)	110.1(3)	Rh	C(3)	O(3)	128.7(6)
Rh	P(1)	C(11)	118.1(3)	N(2)	C(4)	N(3)	115.9(7)
Rh	P(1)	C(21)	116.0(3)	N(2)	C(4)	N(4)	109.1(7)
Os	P(2)	C(10)	112.3(3)	N(3)	C(4)	N(4)	135.0(8)
Os	P(2)	C(31)	119.0(3)				

that coordination of N(4) is not observed owing to unfavourable interactions between the NO<sub>2</sub> moiety and the dppm phenyl groups that would result if N(4) were coordinated. For the most part the bond distances within the chelate ring correspond to the valence bond representation shown in Scheme 4.1. Thus, the N(3)-C(4) distance of 1.290(10) Å is consistent with a double bond<sup>14</sup>, and can be contrasted to the substantially longer N(2)-C(4) and N(2)-C(5) distances of 1.442 (10) and 1.456 (10) Å, respectively, which correspond to single bonds. Similarly, the N(4)-C(4) and N(4)-N(5) distances of 1.349(10) and 1.351(10) Å appear normal for single bonds involving the respective atoms. Although in the valence bond representation shown we would expect a pyramidal N(2), this atom is trigonal planar with the sum of its angles exactly equaling 360°; presumably the lone pair on this atom is involved in some delocalized bonding over the ligand framework.

The bidentate coordination results in an approximately octahedral Rh centre if the metal-metal bond is ignored, with essentially trans phosphines (P(1)-Rh-P(3) = 174.78(8)°) and ligands in the plane all close to 90° from the phosphines. The N(3)-Rh-N(1) angle is rather acute (73.0(3)°), as a result of the bite angle of the ligand, and the N(3)-Rh-C(3) angle is larger to compensate (110.8(3)°). At Os, the geometry is also octahedral if the metal-metal interaction is ignored, with the phosphines essentially trans (P(4)-Os-P(2) = 178.20(8)°), and the angles between adjacent ligands are all close to 90°. The Rh-Os separation is 2.8765(7) Å, consistent with a single bond, and the bridging hydride ligand was located and refined. Two of the carbonyls are terminal on Os, while the third forms a semi-bridging interaction with Rh. Although the carbonyl is more linear with respect to Os than to Rh (Os-C(3)-O(3) = 142.6(6)°; Rh-C(3)-O(3) = 128.7(6)°), the

bond lengths are similar (Os-C(3) = 2.081(9) Å, Rh-C(3) = 2.034(8) Å), suggesting a strong semi-bridging interaction.

In an effort to eliminate the above reaction involving the deprotonated form of MNNG, the diazomethane was prepared in a more conventional fashion, involving distillation to eliminate contamination. Addition of a diazomethane ether solution to **3** does result in a reaction, however, a complex mixture of products resulted, and these have not been identified.

The related complex  $[\text{RhOs}(\text{CO})_4(\text{dppm})_2][\text{BF}_4]$  (**2**) also reacts with a large excess of diazomethane generated as above, to yield  $[\text{RhOs}(\text{CH}_2\text{CH}=\text{CH}_2)(\text{CH}_3)(\text{dppm})_2][\text{BF}_4]$  (**35**), by incorporation of 4 equiv of methylene units. The  $^1\text{H}$  NMR spectrum of **35** shows a triplet at  $\delta$  -0.26 for the Os-bound methyl group, showing coupling to the Os-bound phosphines. The  $\alpha$  hydrogens of the  $\eta^1$ -allyl group appear as a broad multiplet at  $\delta$  2.60, and are coupled to the  $\beta$ -hydrogen, as well as to the Rh-bound phosphines, although any Rh coupling is presumably masked by the broadness of the peak. The  $\beta$ -hydrogen appears as a multiplet at  $\delta$  5.16, showing coupling to the  $\alpha$  hydrogens as well as typical cis (10 Hz) and trans (16 Hz) couplings to the other olefinic hydrogens, which appear as doublets at  $\delta$  3.70 (cis) and  $\delta$  2.89 (trans). In contrast to the neutral allyl complex  $[\text{RhOs}(\eta^3\text{-C}_3\text{H}_5)(\text{CO})_3(\text{dppm})_2]$  (**19**), which has an  $\eta^3$ -bound allyl group, the allyl/methyl complex **35** has an  $\eta^1$ -bound allyl ligand, as indicated by the chemical shifts and coupling constants involving the allyl hydrogens, and by the lack of  $^{31}\text{P}$  coupling to any but the  $\alpha$ -hydrogens. In addition, the pattern of the  $^{31}\text{P}$  NMR spectrum suggests a trans geometry at Rh which is not consistent with  $\eta^3$  coordination, and no fluxional behavior is observed.

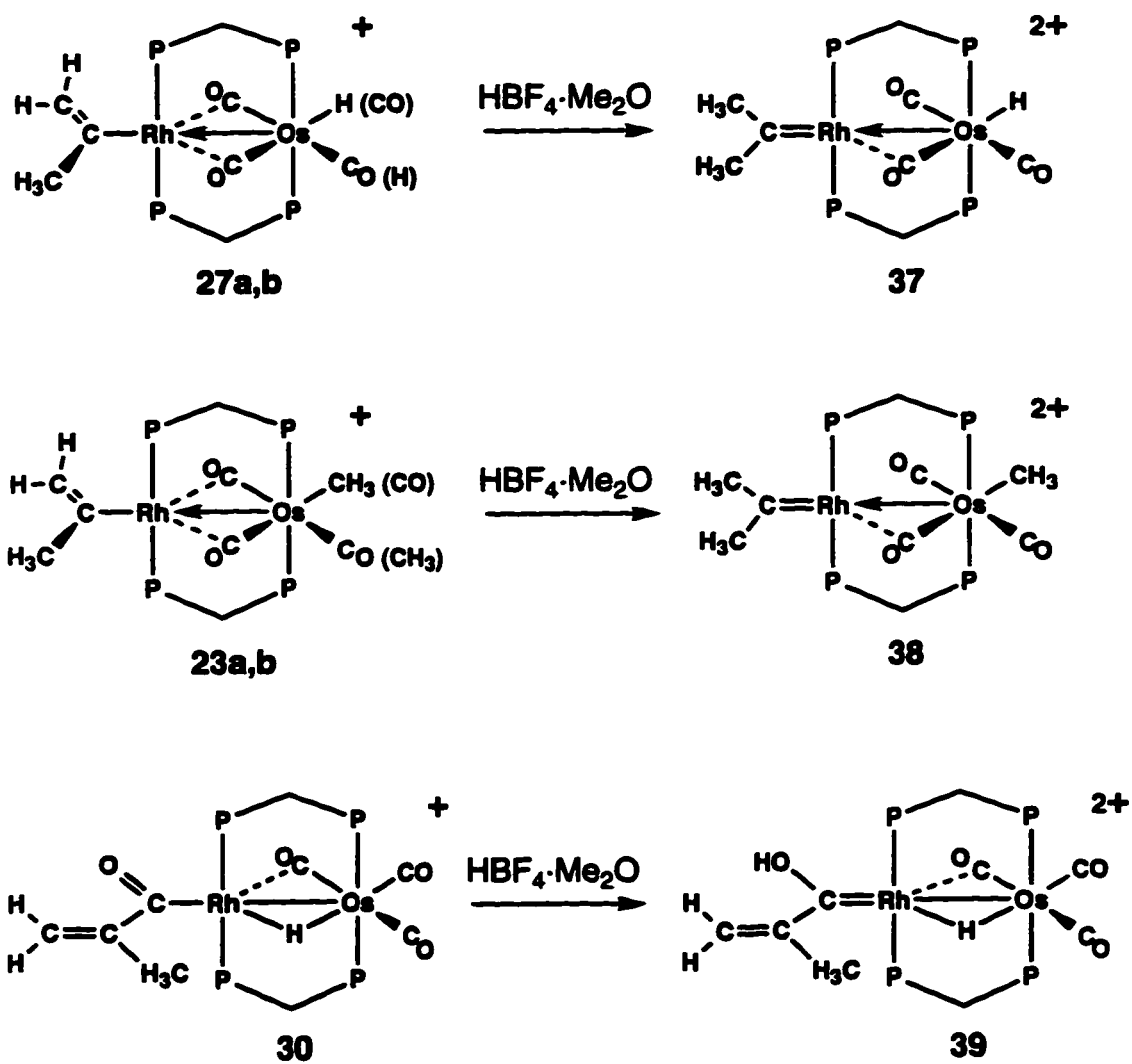
Unlike the vinyl/methyl analogues described in Chapter 3, for which two isomers were observed, compound **35** appears as only one isomer, indicating that the  $\eta^1$ -allyl group rotates freely about the Rh-C bond. The  $^{13}\text{C}$  NMR spectrum of **35** shows resonances for three carbonyls at  $\delta$  179.14, 203.5, and 232.57, with the two low field resonances showing coupling constants to Rh of 12 and 27 Hz, respectively, indicating that two carbonyls form semibridging interactions with Rh, as was observed in several analogous dialkyl and alkyl/vinyl compounds. Compound **35** was independently synthesized by reaction of  $[\text{RhOs}(\eta^3\text{-C}_3\text{H}_5)(\text{CO})_3(\text{dppm})_2]$  (**19**) with methyl triflate, supporting the proposed formulation.

If left to stand in  $\text{CD}_2\text{Cl}_2$  solution, compound **35** slowly transforms into  $[\text{RhOs}(\text{CH}_3)(\mu\text{-Cl})(\text{CO})_3(\text{dppm})_2][\text{BF}_4]$  (**36**) which displays  $^1\text{H}$  NMR resonances for the dppm methylenes as well as a triplet at  $\delta$  -0.39 for the Os-bound methyl group. The  $^{13}\text{C}$  NMR spectrum shows resonances for two terminal carbonyls on Os, and one on Rh. The  $^{31}\text{P}$  NMR spectrum shows the same unusually small coupling constants seen for compound **6** (as discussed in Chapter 2), which suggest the absence of a metal-metal bond and the presence of a bridging chloride. The instability of **35** is noteworthy because all related RhOs dialkyl and vinyl/alkyl complexes described in this thesis show remarkable stability.

### Carbene complexes from Protonation Reactions

Reaction of the isopropenyl complex  $[\text{RhOs}(\text{C}(\text{CH}_3)=\text{CH}_2)(\text{CO})_3(\text{dppm})_2]$  (**18**) with one equivalent of acid yields the vinyl-hydride complex  $[\text{RhOs}(\text{C}(\text{CH}_3)=\text{CH}_2)\text{-}(\text{H})(\text{CO})_3(\text{dppm})_2][\text{BF}_4]$  (**26**) (see Chapter 3). Addition of a second equivalent of acid

results in a subsequent protonation at the  $\beta$ -carbon of the vinyl group to yield the dicationic carbene complex  $[\text{RhOs}(=\text{C}(\text{CH}_3)_2)(\text{H})(\text{CO})_3(\text{dppm})_2][\text{BF}_4]_2$  (**37**) (see Scheme 4.2), which is stable in solution only below  $0^\circ\text{C}$ , in the presence of excess acid. Above  $0^\circ\text{C}$ , deprotonation occurs, reforming **26a,b**, along with some decomposition products. Lowering the temperature results in reformation of **37**. Although two isomers of the monoprotection product are formed, the second protonation yields one isomer, since the carbene ligand is now symmetrical. The  $^1\text{H}$  NMR spectrum of **37** shows singlets at  $\delta$  2.65 and 2.18, for the methyl groups of the carbene moiety, and a triplet at  $\delta$  -6.21 for the hydride, showing coupling of 13 Hz to the osmium-bound phosphines. The  $^{13}\text{C}\{^1\text{H}\}$  NMR spectrum shows three carbonyl resonances at  $\delta$  172.8, 193.1, and 204.0, with the lowfield resonance showing rhodium coupling of 10 Hz, indicating a semi-bridging interaction. The carbene carbon appears as a doublet of triplets at  $\delta$  377.9, with a rhodium coupling of 35 Hz and coupling to the rhodium-bound phosphines of 5 Hz. The rhodium coupling is consistent with that involving an  $\text{sp}^2$  carbon<sup>15</sup> and the lowfield chemical shift is expected for a dicationic carbene complex.<sup>16</sup> In a similar manner, protonation of  $[\text{RhOs}(\text{C}(\text{CH}_3)=\text{CH}_2)(\text{CH}_3)(\text{CO})_3(\text{dppm})_2][\text{CF}_3\text{SO}_3]$  (**23a,b**) with  $\text{HBF}_4 \cdot \text{Me}_2\text{O}$  at  $-40^\circ\text{C}$  leads to  $[\text{RhOs}(=\text{C}(\text{CH}_3)_2)(\text{CH}_3)(\text{CO})_3(\text{dppm})_2][\text{BF}_4][\text{CF}_3\text{SO}_3]$  (**38**). The spectroscopy of **38** is similar to that of **37**, except that, instead of the hydride resonance, a triplet is seen in the  $^1\text{H}$  NMR spectrum for the osmium-bound methyl group at  $\delta$  -0.1, showing 8 Hz coupling to the osmium-bound phosphines.

**Scheme 4.2**

The initial protonation of the isopropenoyl complex  $[\text{RhOs}(\text{C}(\text{O})\text{C}(\text{CH}_3)=\text{CH}_2)(\text{CO})_3(\text{dppm})_2]$  (**22**) resulted in formation of a hydride-bridged complex  $[\text{RhOs}(\text{C}(\text{O})\text{C}(\text{CH}_3)=\text{CH}_2)(\text{CO})_3(\mu\text{-H})(\text{dppm})_2][\text{BF}_4]$  (**30**) (see Chapter 3). The subsequent protonation of **30** occurs at the acyl oxygen, yielding the carbene species  $[\text{RhOs}(=\text{C}(\text{OH})\text{C}(\text{CH}_3)=\text{CH}_2)(\text{CO})_3(\mu\text{-H})(\text{dppm})_2][\text{BF}_4]_2$  (**39**), which has a heteroatom in one of the  $\beta$  positions. The  $^1\text{H}$  NMR spectrum of **39** shows the expected resonances for the propenyl group on the carbene ligand as well as a broad multiplet at  $\delta$  -9.5 for the hydride. In the reaction mixture involving  $\text{HBF}_4$  the hydroxyl proton of **39** was obscured by the broad resonance for the excess  $\text{HBF}_4$  at  $\delta$  9.95. However, if triflic acid is used, the hydroxyl hydrogen becomes obvious as a singlet at  $\delta$  9.56. The carbene resonance in the  $^{13}\text{C}$  NMR spectrum again appears typically lowfield, at  $\delta$  301.2 as a doublet of triplets, showing rhodium coupling of 49 Hz. As expected, the heteroatom stabilized carbene is more stable than the alkyl-substituted carbene complexes,<sup>17</sup> persisting to ambient temperature, but subsequently decomposing upon workup.

## Discussion

Our interest in carbene complexes stems from their importance in the chain growth steps of Fischer-Tropsch reactions.<sup>6</sup> In particular, we were interested in combining vinyl and carbene ligands on our metal complexes because of the proposed involvement of vinyl groups in the chain propagation steps.<sup>7</sup>

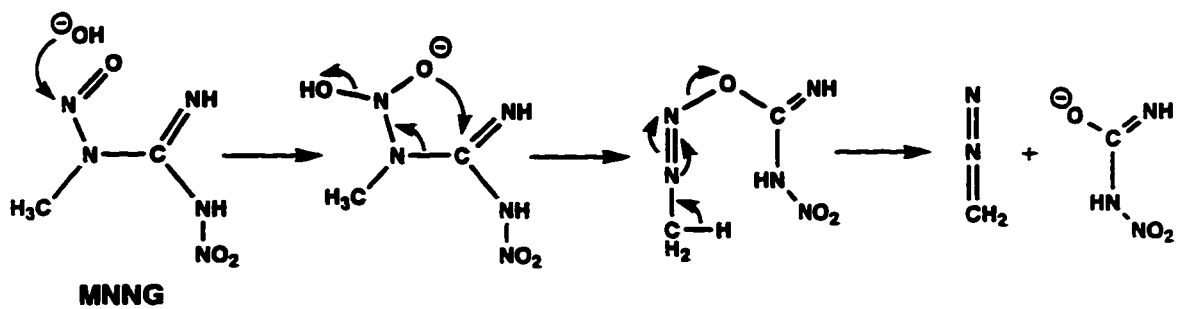
Initial attempts at formation of carbenes by deprotonation were unsuccessful because the acidity of the dppm methylenes resulted in deprotonation at this site. This reactivity was not surprising, since we<sup>18</sup> and other workers<sup>19</sup> have previously

demonstrated facile deprotonation of the dppm methylene hydrogens. The lack of success of the reactions of the neutral alkyl complexes with trityl cation is likely due to oxidation of the complexes by the cation<sup>20</sup> since the neutral Rh(I)/Os(0) complexes are susceptible to oxidation, as evidenced by their air sensitivity. The trityl cation is not strong enough to remove a hydride from the cationic complexes to form dicationic carbenes, although similar complexes have been shown to be accessible by alternate routes.

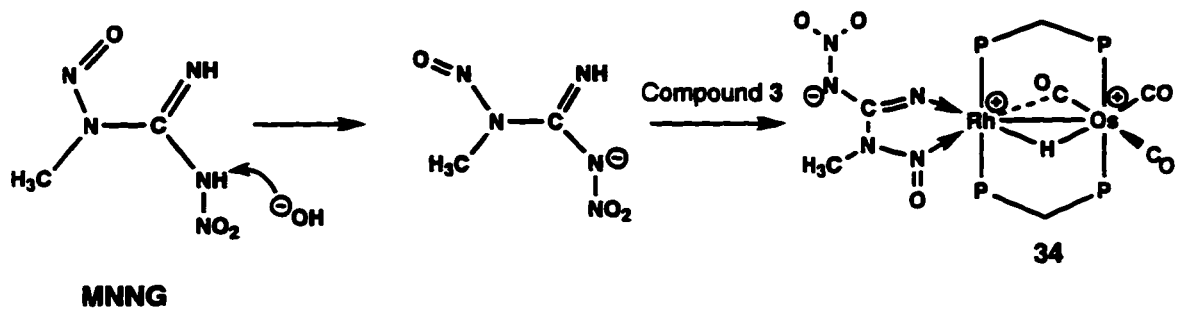
Attempts to form methylene complexes by reaction of diazomethane with  $[\text{RhOs}(\text{NCMe})(\text{CO})_3(\mu\text{-H})(\text{dppm})_2][\text{BF}_4]_2$  (**3**) resulted in an unexpected chelate complex. Instead of reacting with the diazomethane, compound **3** reacted with a deprotonated form of the diazomethane precursor MNNG. In formation of diazomethane from MNNG,<sup>21</sup> the deprotonation occurs from the methyl group of MNNG, as shown in Scheme 4.3. However, in this case it appears that deprotonation instead occurred from the nitro-amine group, which is expected to be acidic since it is adjacent to the electron withdrawing nitro group.<sup>22</sup> The anionic ligand then acts as a nucleophile, displacing acetonitrile from Rh, and although the deprotonated nitrogen does not bind to the metal, this is not surprising since it is adjacent to a strong electron withdrawing nitro group,<sup>22</sup> which stabilizes the negative charge on this nitrogen. Furthermore, it appears that coordination through this site would result in unfavourable interactions between the nitro group and the dppm ligands. The possibility that deprotonation occurred after coordination is ruled out by attempts to induce direct reaction of  $[\text{RhOs}(\text{NCMe})(\text{CO})_3(\mu\text{-H})(\text{dppm})_2][\text{BF}_4]_2$  (**3**) with MNNG; no reaction was observed.

### Scheme 4.3

(a) Diazomethane formation:



(b) Formation of compound 34



Compound **34** is unusual in that it is the only complex in our series of RhOs compounds with a saturated  $\text{Rh}^{+1}$  centre. In the analogous IrOs system, saturated  $\text{Ir}^{-1}$  centres, as in  $[\text{IrOs}(\text{CO})_5(\text{dppm})_2][\text{BF}_4]$ ,<sup>23</sup> have been observed, which is not unexpected based on the greater tendency for Ir to be coordinatively saturated. In the case of compound **34**, the 18e Rh centre is clearly a result of the chelate effect. The resulting increased electron density on Rh is accompanied by an increase in the strength of the semi-bridging carbonyl interaction, as indicated by a substantial reduction in the IR stretching frequency of **34**, compared to that of the precursor **3** (1737 vs 1819  $\text{cm}^{-1}$ ).

The reaction of  $[\text{RhOs}(\text{CO})_4(\text{dppm})_2][\text{BF}_4]$  (**2**) with  $\text{CH}_2\text{N}_2$  (generated by the conventional method involving distillation) led to an unexpected result. Although the intent was to form a mono methylene complex, instead C-C bond formation has occurred, in which with four equivalents of  $\text{CH}_2\text{N}_2$  combined to form a methyl group and an allyl ligand. Reaction with smaller amounts of  $\text{CH}_2\text{N}_2$  does not yield products having fewer “ $\text{CH}_2$ ” groups but simply results in a mixture of the starting material and the observed product **35**. This reaction may have relevance to the “vinyl mechanism” proposed for Fischer Tropsch catalysis.<sup>7</sup> In this mechanism, the chain propagation step involves the migration of a vinyl group onto a methylene to form an allyl group, followed by isomerization of the allyl to form a substituted vinyl group. In formation of **35**, the combination of methylene groups also leads to an allyl fragment. Attempts to elucidate the mechanism of this transformation by forming complexes that could be intermediates in the reaction, such as those containing a single methylene group, have been unsuccessful thus far. Although the details of the mechanism are not known, we can speculate that the transformation involves the migration of a vinyl group onto a

methylene group to form the allyl. The vinyl group could be formed by the combination of two methylenes to form a methyl group and a methine, followed by combination of the methine with another methylene to form the vinyl group. Another possible mechanism for the reaction would be the formation of a metalacyclobutane from three equivalents of  $\text{CH}_2\text{N}_2$ , followed by  $\beta$ -elimination to form an allyl group and a hydride, which then inserts another methylene to form the observed methyl group. Both of these mechanisms are highly speculative at this point and we have no evidence that distinguishes between them. If the individual steps in the transformation to **35** could be observed, the reaction might serve as a useful model for the chain growth steps.

Compound **35** can be synthesized more directly by introduction of a methyl group onto the Os centre of  $[\text{RhOs}(\eta^3\text{-CH}_2\text{CHCH}_2)(\text{CO})_3(\text{dppm})_2]$  (**19**), resulting in a change from an  $\eta^3$  coordination to an  $\eta^1$  coordination of the allyl group. This change is probably a result of the larger steric crowding at the octahedral Os centre, compared to the trigonal bipyramidal Os centre of **19**. In **19**, the phosphines move into a cis orientation at Rh to accommodate  $\eta^3$ -allyl coordination. In **35**, we propose that the phosphines cannot move into a cis orientation forcing the allyl group to an  $\eta^1$  coordination mode.

Attempts to alkylate the isopropenyl compound  $[\text{RhOs}(\text{C}(\text{O})\text{C}(\text{CH}_3)=\text{CH}_2)-(\text{CO})_3(\text{dppm})_2]$  (**22**) to form a compound analogous to the vinyl/alkyl complexes **23** and **24**, resulted in a mixture of products. The  $^{13}\text{C}$  NMR spectrum of the mixture suggested that one of the products resulted from alkylation of the acyl oxygen to form a Rh-bound carbene product, suggesting that conversion of both the isopropenyl (**18**) and the isopropenyl (**22**) complexes to carbenes should be possible. As noted, protonation of **18**

does not occur at the isopropenyl group, but occurs at Os to give  $[\text{RhOs}(\text{C}(\text{CH}_3)=\text{CH}_2)(\text{H})(\text{CO})_3(\text{dppm})_2]^+$  (26), and protonation of 22 yields the hydrido-bridged species  $[\text{RhOs}(\text{C}(\text{O})\text{C}(\text{CH}_3)=\text{CH}_2)(\text{CO})_3(\mu\text{-H})(\text{dppm})_2][\text{BF}_4]$  (30). However, reaction with an additional equivalent of acid in each case yields the dicationic carbene products  $[\text{RhOs}(\text{C}(\text{CH}_3)_2)(\text{H})(\text{CO})_3(\text{dppm})_2]^{2+}$  (37) and  $[\text{RhOs}(\text{C}(\text{OH})\text{C}(\text{CH}_3)=\text{CH}_2)(\text{CO})_3(\mu\text{-H})(\text{dppm})_2]^{2+}$  (39). In addition, the dimethyl carbene/methyl species  $[\text{RhOs}(\text{C}(\text{CH}_3)_2)(\text{CH}_3)(\text{CO})_3(\text{dppm})_2]^{2+}$  (38) is obtained upon protonation of the isopropenyl group in the isopropenyl-methyl complex 23. Although carbene complexes of Rh are well known in which there are heteroatoms in the  $\beta$ -position,<sup>24</sup> complexes containing terminal carbene groups on Rh lacking heteroatoms, such as 37 and 38, are quite rare.<sup>25</sup> In addition, terminal carbene species of Rh are far less common than those containing bridging carbene groups,<sup>26</sup> so it is surprising that the carbene groups do not bridge the metals in compounds 37-39. It may be that such a bridging mode is unfavourable owing to the steric interactions involving the carbene substituents and the dppm phenyl groups. Compounds 37 and 38 are unstable at ambient temperature, being readily deprotonated. As expected, the Fischer carbene (39) had a greater stability owing to delocalization involving the hydroxyl group.<sup>27</sup>

The carbene complexes 37 and 38 are expected to be very electrophilic in nature, owing to the dicationic charge of the complexes. We therefore refer to them as carbenes, as opposed to alkylidenes, for which nucleophilic character is implied.<sup>28</sup> As has been observed in other electrophilic carbenes,<sup>29</sup> the hydrogens  $\alpha$  to the carbene carbons are acidic, as noted above. Similar non-heteroatom stabilized, electrophilic carbene

complexes of W, Fe, Mo, and Ni, some prepared by similar routes, have been shown to display unusual reactivity, including the cyclopropanation of olefin substrates,<sup>29</sup> and insertion reactions of organosilanes.<sup>30</sup> The initial step in the cyclopropanation reactions is generally dissociation of a carbonyl or other ligand, to allow coordination of the olefin. This step may not be necessary in the complexes **37** and **38**, described herein, since the Rh centre is already unsaturated. The potential of these carbene complexes to function as reagents for cyclopropanation and organosilane insertions is currently under study.

**References**

1. (a) Fischer, E. O., Maasböl, A. *Angew. Chem. Int. Ed. Eng.*, **1964**, *3*, 580.  
(b) Fischer, E. O. *Adv. Organomet. Chem.* **1976**, *14*, 1.
2. Collman, J.P.; Hegedus, L.S.; Norton, J.R.; Finke, R.G. *Principles and Applications of Organotransition Metal Chemistry*; University Science Books: Mill Valley, California, 1987, pp. 119-136.
3. Brookhart, M.; Studabaker, W. B. *Chem. Rev.* **1987**, *87*, 411.
4. Gallop, M. A.; Roper, W. R.; *Advances in Organometallic Chemistry* **1986**, *25*, 121.
5. Hermann, W. A. *Advances in Organometallic Chemistry* **1982**, *20*, 159.
6. (a) Muetterties, E. L.; Stein, J. *Chem. Rev.* **1979**, *79*, 479.  
(b) Maitlis, P. M.; Saez, I. M.; Meanwell, N. J.; Isobe, K.; Nutton, A.; Vaquez de Miguel, A.; Bruce, D. W.; Okeya, S.; Bailey, P. M.; Andrews, D. G.; Ashton, P. R.; Johnstone, I. R. *New J. Chem.*, **1989**, *13*, 419.
7. Maitlis, P. M.; Long, H. C.; Quyoum, R.; Turner, M. L.; Wang, Z-Q. *Chem. Commun.* **1996**, 1.
8. Calhorda, M. J. *Organometallics*, **1991**, *10*, 1431.
9. (a) Deeming, A.J.; Shaw, B.L.; Stainbank, R.E. *J. Chem. Soc. (A)* **1971**, 374.  
(b) Wang, L.-S.; Cowie, M. *Can. J. Chem.* **1995**, *73*, 1058.
10. Fales, H. M.; Jaouni, T. M.; Babashuk, J. F. *Anal. Chem.*, **1973**, *45*, 2302.
11. Sheldrick, G.M. *Acta Crystallogr.* **1990**, *A46*, 467.

12. Sheldrick G.M. SHELXL-93. Program for crystal structure determination. University of Göttingen, Germany, 1993. Refinement on  $F_o^2$  for all reflections (all of these having  $F_o^2 < -3\sigma(F_o^2)$ ). Weighted  $R$ -factors  $wR^2$  and all goodnesses of fit  $S$  are based on  $F_o^2$ ; conventional  $R$ -factors  $R_1$  are based on  $F_o$ , with  $F_o$  set to zero for negative  $F_o^2$ . The observed criterion of  $F_o^2 > 2\sigma(F_o^2)$  is used only for calculating  $R_1$ , and is not relevant to the choice of reflections for refinement.  $R$ -factors based on  $F_o^2$  are statistically about twice as large as those based on  $F_o$ , and  $R$ -factors based on ALL data will be even larger.
13. Herrmann, W. A. *Angew. Chem. Int. Ed. Engl.*, **1978**, *17*, 800.
14. Orpen, A.G.; Brammer, L.; Allen, F.H.; Kennard, O.; Watson, D.G.; Taylor, R. J. *Chem. Soc., Dalton Trans.* **1989**, 51.
15. Mann, B.E.; Taylor, B.F. *<sup>13</sup>C NMR Data for Organometallic Compounds*; Academic Press: London, 1981, pp. 88, 140.
16. Gallop, M.A.; Roper, W.R. *Advances in Organometallic Chemistry* **1986**, *25*, 121.
17. Collman, J.P.; Hegedus, L.S.; Norton, J.R.; Finke, R.G. *Principles and Applications of Organotransition Metal Chemistry*; University Science Books: Mill Valley, California, 1987, pp. 127-129.
18. (a) Torkelson, J. R.; Cowie, M. unpublished results.  
(b) Chapter 2 of this thesis.
19. (a) Puddephatt, R. J. *Chem. Soc. Rev.*, **1983**, *12*, 99.  
(b) Sharp, P.R.; Ge, Y.-W. *J. Am. Chem. Soc.* **1987**, *109*, 3796.  
(c) Sharp, P.R.; Ge, Y.-W. *Inorg. Chem.* **1993**, *32*, 94.

20. Collman, J.P.; Hegedus, L.S.; Norton, J.R.; Finke, R.G. *Principles and Applications of Organotransition Metal Chemistry*; University Science Books: Mill Valley, California, 1987, pp. 448-449.
21. March, J. *Advanced Organic Chemistry*; John Wiley & Sons: New York, 1985, p. 936.
22. Ibid. p. 230.
23. Hilts, R.W.; Franchuk, R.A.; Cowie, M. *Organometallics* **1991**, *10*, 1297.
24. Brown, F.J. *Prog. Inorg. Chem.* **1980**, *27*, 1. Cardin, D.J.; Cetinkaya, B.; Lappert, M.F. *Chem. Rev.* **1972**, *72*, 545.
25. Schwab, P.; Werner, H. *J. Chem. Soc., Dalton Trans.* **1994**, 3415. Schwab, P.; Mahr, N.; Wolf, J.; Werner, H. *Angew. Chem., Int. Ed. Engl.* **1994**, *33(1)*, 97.
26. Herrmann, W.A. *Advances in Organometallic Chemistry* **1982**, *20*, 159.
27. Collman, J.P.; Hegedus, L.S.; Norton, J.R.; Finke, R.G. *Principles and Applications of Organotransition Metal Chemistry*; University Science Books: Mill Valley, California, 1987, pp. 127-129.
28. Brookhart, M.; Studabaker, W.B. *Chem. Rev.* **1987**, *87*, 411.
29. Hegedus, L.S. *Transition Metals in the Synthesis of Complex Organic Molecules*; University Science Books: Mill Valley, California, 1994, p.154.
30. Scharrer, E.; Brookhart, M. *J. Organometal. Chem* **1995**, *497*, 61.

## **Chapter 5**

### **Organometallic Chemistry of the Rh/Ru System**

#### **Introduction**

As discussed in earlier chapters, routes to dialkyl, alkyl/vinyl and related alkyl/hydrido and vinyl/hydrido complexes of RhOs were developed. In the case of the hydride complexes, reductive elimination appeared to occur from the Os centre. Unfortunately, reductive elimination of the dialkyl or alkyl/vinyl moieties did not occur under the relatively mild conditions investigated. This is not surprising given the reluctance for elimination of alkanes from the relatively inert Os<sup>+2</sup> centre.<sup>1</sup> In attempts to promote reductive elimination and migratory insertion reactions of catalytic relevance, the Os centre was substituted by the more labile Ru. In addition to the anticipated greater reactivity of the RhRu over the RhOs system<sup>2</sup>, we had further interests in the former metal combination owing to the application of such systems as catalysts. Recently, there has been a great interest in the possibility of synergistic effects in catalysis, where a combination of two different metals leads to increased catalytic activity or improved selectivity.<sup>3</sup> The Rh/Ru combination is one of the most promising, and its use has already been demonstrated in syngas chemistry, where a mixed Rh/Ru catalyst was shown to promote formation of ethylene glycol.<sup>4</sup> In this chapter attempts to form alkyl, alkenyl, dialkyl and related complexes of RhRu, analogues to the complexes that were synthesized in the RhOs system, will be discussed.

## Experimental Section

**General Comments.** Reactions were carried out using standard Schlenk techniques or in a Vacuum Atmospheres glovebox as indicated.  $\text{RuCl}_3$  was purchased from Strem. The compound  $[\text{RhRu}(\text{CO})_3(\mu\text{-H})(\text{dppm})_2]$  (**40**) was prepared by the published procedure<sup>5</sup> and  $[\text{RhRu}(\text{CO})_4(\text{dppm})_2][\text{BF}_4]$  (**41**) was prepared by a route developed by workers in this group, analogous to that used to prepare  $[\text{RhOs}(\text{CO})_4(\text{dppm})_2][\text{BF}_4]$  (**2**).<sup>6</sup>

Infrared spectra were run on a Perkin Elmer 883 spectrophotometer in THF solutions prepared in the glovebox, or as Nujol mulls on a Nicolet Magna 750 FTIR spectrometer. Spectroscopic data for all compounds are given in Table 5.1.

### Preparation of Compounds.

**(a)  $[\text{RhRu}(\text{CH}_3)(\text{CO})_3(\text{dppm})_2]$  (**42**).** This preparation was carried out in the glovebox. The compound  $[\text{RhRu}(\text{CO})_4(\text{dppm})_2][\text{BF}_4]$  (**41**, 50 mg, 0.042 mmol) was dissolved in 50 mL of THF, forming an orange solution. MeLi (5 mL, 0.025 M, 0.13 mmol in THF) was added, causing an immediate colour change to red-orange. After 1 h of stirring, the solvent was removed in vacuo and the residue was washed with 3x5 mL of pentane, and then extracted into 3x2 mL of THF and filtered. The solvent was removed in vacuo and the residue redissolved in 1 mL of THF and precipitated by gradual addition of pentane, forming a dark orange powder which was washed with 3x5 mL of pentane and dried in vacuo. Yield 35 mg, 77%. Satisfactory elemental analysis was not obtained because of difficulty in separating  $\text{LiBF}_4$  from the compound.

**(b)  $[\text{RhRu}(\text{C}(\text{O})\text{CH}_3)(\text{CO})_3(\text{dppm})_2]$  (**43**).** The compound  $[\text{RhRu}(\text{CH}_3)(\text{CO})_3\text{-}$

Table 5.1. Spectroscopic Parameters for the Compounds<sup>a</sup>

Compound	IR, cm <sup>-1b</sup>	NMR <sup>d</sup>	
		$\delta(^1\text{P}\{\text{H}\})$	$\delta(^{13}\text{C}\{\text{H}\})$
[RhRu(CH <sub>3</sub> )(CO) <sub>3</sub> (dppm) <sub>2</sub> (42)	1928 (sb), 1878 (sb), 1762 (sb) <sup>c</sup>	48.14 (RuP) 37.12 (RhP, <sup>1</sup> J <sub>Rh-P</sub> = 150 Hz); Hz, <sup>3</sup> J <sub>Rh-P-H</sub> = 8 Hz	RuCO: 211.63 (t, 1C, <sup>2</sup> J <sub>PC</sub> = 19 Hz); 234.50 (dm, 2C, <sup>1</sup> J <sub>RhC</sub> = 15 Hz)
[RhRu(C(O)CH <sub>3</sub> )(CO) <sub>3</sub> (dppm) <sub>2</sub> (43)		47.01 (RuP) 24.95 (RhP, <sup>1</sup> J <sub>Rh-P</sub> = 150 Hz); PCH <sub>2</sub> P: 3.13 (bm, 4H); RhC(O)CH <sub>3</sub> : 0.85 (s)	
[RhRu(CH <sub>3</sub> ) <sub>2</sub> (CO) <sub>3</sub> (dppm) <sub>2</sub> ]- [CF <sub>3</sub> SO <sub>3</sub> ] (44)	2039ss, 1860m, 1812ss	28.6-31.2 (RuP, RhP, 2nd order multiplet) Hz, <sup>3</sup> J <sub>Rh-P-H</sub> = 8 Hz	PCH <sub>2</sub> P: 3.18 (bm, 4H); RhCH <sub>3</sub> : 0.81 (dt, 1H, <sup>2</sup> J <sub>RhH</sub> = 2 Hz, <sup>3</sup> J <sub>Rh-P-H</sub> = 8 Hz) RuCH <sub>3</sub> : -0.17 (t, <sup>3</sup> J <sub>PH</sub> = 6 Hz)
[RhRu(η <sup>3</sup> -C <sub>3</sub> H <sub>5</sub> )(CO) <sub>3</sub> (dppm) <sub>2</sub> (45) 25°C	1947s, 1894s, 1725s <sup>c</sup>	42.03 (RuP) 23.5 (RhP, vb); P <sub>A</sub> : 45.22; P <sub>B</sub> : 37.87; P <sub>C</sub> : 34.54; P <sub>D</sub> : 5.52 J(P <sub>A</sub> P <sub>B</sub> ) = 255 Hz J(P <sub>A</sub> P <sub>C</sub> ) = 109 Hz J(P <sub>A</sub> P <sub>D</sub> ) = 36 Hz J(P <sub>B</sub> P <sub>C</sub> ) = 34 Hz J(P <sub>B</sub> P <sub>D</sub> ) = 112 Hz J(P <sub>C</sub> P <sub>D</sub> ) = 19 Hz J(RhP <sub>c</sub> ) = 156 Hz J(RhP <sub>d</sub> ) = 130 Hz	PCH <sub>2</sub> P: 3.70 (bs) CH <sub>C</sub> : 5.05 PCH <sub>2</sub> P: 4.32, 4.05, 3.88, 3.11 CH <sub>S</sub> : 2.53, 1.40 CH <sub>A</sub> : 0.96, 0.25
-80°C			

Compound	IR, cm <sup>-1b</sup>	NMR <sup>d</sup>	
		$\delta(^{31}\text{P}\{\text{H}\})$	$\delta(\text{H})$ $\delta(^{13}\text{C}\{\text{H}\})$
[RhRu(CH <sub>2</sub> CH=C(CH <sub>3</sub> ) <sub>2</sub> )(CO) <sub>3</sub> -(dppm) <sub>2</sub> ] (46)	1910sh, 1883sb, 1750sb <sup>c</sup>	46.27 (RuP) 32.96 (RhP, <sup>1</sup> J <sub>Rh-P</sub> = 161 Hz)	PCH <sub>2</sub> P: 3.45 (m, 4H) RhCH <sub>2</sub> : 1.46 (dt, 1H, <sup>3</sup> J <sub>HH</sub> = 9 Hz, <sup>3</sup> J <sub>HP</sub> = 9 Hz) CH <sub>2</sub> CH: 4.80 (t, 1H, <sup>3</sup> J <sub>HH</sub> = 9 Hz) CH <sub>3</sub> : 0.97 (s, 3H), 0.71 (s, 3H) RuCO: 209.73 (t, 1C, <sup>2</sup> J <sub>PC</sub> = 20 Hz); 233.77 (dt, 2C, <sup>1</sup> J <sub>RhC</sub> = 14 Hz, <sup>2</sup> J <sub>PC</sub> = 16 Hz)
[RhRu(C(CH <sub>3</sub> )=CH <sub>2</sub> )(CO) <sub>3</sub> -(dppm) <sub>2</sub> ] (47)	1930sh, 1880sb, 1740sb <sup>c</sup>	45.81 (RuP) 29.18 (RhP, <sup>1</sup> J <sub>Rh-P</sub> = 158 Hz)	PCH <sub>2</sub> P: 3.40 (b, 4H) RhC=CH <sub>2</sub> : 3.83 (bs), 4.72 (bs) RhC-CH <sub>3</sub> : 0.83 (s, 3H)
[RhRu(C(O)C(CH <sub>3</sub> )=CH <sub>2</sub> )(CO) <sub>3</sub> -(dppm) <sub>2</sub> ] (48)		46.16 (RuP) 23.86 (RhP, <sup>1</sup> J <sub>Rh-P</sub> = 166 Hz)	PCH <sub>2</sub> P: 3.60 (b, 4H) RhC=CH <sub>2</sub> : 4.89 (bs), 5.98 (bs) RhC-CH <sub>3</sub> : 0.65 (s, 3H) RuCO: 207.94 (t, <sup>2</sup> J <sub>PC</sub> = 19 Hz); 222.36 (vb); 239.59 (vb) RhCO: 264.99 (dt, <sup>1</sup> J <sub>Rh-C</sub> = 30 Hz, <sup>2</sup> J <sub>P-Rh-C</sub> < 3 Hz)

<sup>a</sup> abbreviations used: IR: ss = strong sharp, ms = medium sharp, ws = weak sharp, sb = strong broad, mb = medium broad, sh = shoulder, m = medium. NMR: t = triplet, dt = doublet of triplets, ddt = doublet of doublets of triplets, m = multiplet, td = triplet of doublets, bs = broad singlet, dd = doublet of doublets, dm = doublet of multiplets, dit = doublet of triplets of triplets, s = singlet, pq = pseudo quintet, ddd = doublet of doublets of quintets, ddd = doublet of doublets of doublets, bm = broad multiplet. <sup>b</sup> nujol mull except as indicated. Values quoted are  $\nu(\text{CO})$  except as indicated. <sup>c</sup> THF solution. <sup>d</sup> <sup>31</sup>P{<sup>1</sup>H} chemical shifts are referenced vs. external 85% H<sub>3</sub>PO<sub>4</sub> while <sup>1</sup>H and <sup>13</sup>C{<sup>1</sup>H} are referenced vs. external TMS. Chemical shifts for the phenyl hydrogens are not given in the <sup>1</sup>H NMR data

(dppm)<sub>2</sub>] (**42**) was dissolved in 0.5 mL of THF-d<sup>8</sup> and placed in a sealed NMR tube inside the glovebox. Outside of the glovebox, CO or <sup>13</sup>CO was used to pressurize the NMR tube to approximately 1.2 atm. <sup>31</sup>P NMR spectrum showed quantitative conversion to [RhRu(C(O)CH<sub>3</sub>)(CO)<sub>3</sub>(dppm)<sub>2</sub>] (**43**). The solvent was removed in vacuo, and the residue was recrystallized from THF/pentane inside the glovebox. The <sup>31</sup>P NMR spectrum of the isolated solid showed that it was a mixture of **43** and **42** (1.5 to 1).

(c) **[RhRu(CH<sub>3</sub>)<sub>2</sub>(CO)<sub>3</sub>(dppm)<sub>2</sub>][CF<sub>3</sub>SO<sub>3</sub>] (**44**).** The compound [RhRu(CH<sub>3</sub>)(CO)<sub>3</sub>(dppm)<sub>2</sub>] (**42**, 30 mg, 0.028 mmol) was dissolved in 10 mL of CH<sub>2</sub>Cl<sub>2</sub> which was immediately degassed with two freeze/pump/thaw cycles. Methyl triflate (3.2 μL, 0.028 mmol) was added causing a colour change from orange to yellow/orange. The solution was allowed to stir for 1 h, the solvent was removed in vacuo and the residue was redissolved in 3 mL of CH<sub>2</sub>Cl<sub>2</sub> and filtered. The solvent was reduced to 1 mL and 10 mL of Et<sub>2</sub>O was slowly added to precipitate a yellow powder, which was washed with 3x5 mL of Et<sub>2</sub>O and dried in vacuo. Yield 26 mg, 75%. Anal. calcd. for C<sub>56</sub>H<sub>50</sub>F<sub>3</sub>O<sub>6</sub>P<sub>4</sub>RhRuS: C, 54.42; H, 4.07. Found: C, 53.74; H, 3.96.

(d) **Reaction of [RhRu(CH<sub>3</sub>)<sub>2</sub>(CO)<sub>3</sub>(dppm)<sub>2</sub>][CF<sub>3</sub>SO<sub>3</sub>] (**44**) with CO.** Compound **44** (28 mg, 0.023 mmol) was dissolved in 0.5 mL of CD<sub>2</sub>Cl<sub>2</sub> in an NMR tube which was then pressurized with 1.4 atm of CO or <sup>13</sup>CO. The reaction was monitored over three days, and the tube was repressurized with CO daily. Compound **44** was gradually transformed over the three days into [RhRu(CO)<sub>4</sub>(dppm)<sub>2</sub>][CF<sub>3</sub>SO<sub>3</sub>] (**2b**) and 1 equiv of acetone.

(e) **[RhRu(η<sup>3</sup>-C<sub>3</sub>H<sub>5</sub>)(CO)<sub>3</sub>(dppm)<sub>2</sub>] (**45**).** The compound [RhRu(CO)<sub>3</sub>(μ-H)-(dppm)<sub>2</sub>] (**40**, 44 mg, 0.042 mmol) was dissolved in 10 mL of THF in the glovebox and

removed from the box in a sealed flask. Outside the glovebox, allene gas was allowed to flow through the flask for 2 min, causing an immediate colour change from brown to bright orange. The solvent was removed in vacuo and the orange residue was recrystallized from THF/Et<sub>2</sub>O inside the glovebox and washed with 3x10 mL of Et<sub>2</sub>O and dried in vacuo yielding an orange powder. Yield: 32 mg, 69%. Anal. calcd. for C<sub>56</sub>H<sub>49</sub>O<sub>3</sub>RhRuP<sub>4</sub>: C, 61.26; H, 4.50. Found: C, 60.97; H, 4.31.

(f) **[RhRu(CH<sub>2</sub>CH=C(CH<sub>3</sub>)<sub>2</sub>)(CO)<sub>3</sub>(dppm)<sub>2</sub>] (46).** [RhRu(CO)<sub>3</sub>(μ-H)(dppm)<sub>2</sub>] (40, 60 mg, 0.057 mmol) was dissolved in 10 mL of THF in the glovebox and removed from the box in a sealed flask. Outside the glovebox, (CH<sub>3</sub>)<sub>2</sub>C=C=CH<sub>2</sub> (6 mL, 0.061 mmol) was added, causing a gradual colour change from brown to orange. After 15 min stirring, the solvent was removed in vacuo and the orange residue was recrystallized from THF/Et<sub>2</sub>O/pentane in the glovebox and washed with 3x10 mL of pentane and dried in vacuo, yielding an orange powder. Yield 26 mg, 41%.

(g) **Reactions of [RhRu(CO)<sub>3</sub>(μ-H)(dppm)<sub>2</sub>] with propyne.** (i) **Formation of [RhRu(η<sup>3</sup>-C<sub>3</sub>H<sub>5</sub>)(CO)<sub>3</sub>(dppm)<sub>2</sub>] (45).** The compound [RhRu(CO)<sub>3</sub>(μ-H)(dppm)<sub>2</sub>] (40, 38 mg, 0.036 mmol) was dissolved in 10 mL of THF in the glovebox. Outside the glovebox, a large excess of propyne was allowed to flow through the flask for 1 min and then the flask was sealed under 1 atm of propyne, causing a gradual colour change, over 5 min from brown to orange. The solvent was removed in vacuo, the flask was returned to the glovebox, and the residue was redissolved in a minimum amount of THF; 15 mL of Et<sub>2</sub>O was added. Over 24 h, a bright orange precipitate formed which was shown by NMR to be pure [RhRu(η<sup>3</sup>-C<sub>3</sub>H<sub>5</sub>)(CO)<sub>3</sub>(dppm)<sub>2</sub>] (45). Yield 21 mg, 53%. If the reaction is carried out in situ in THF-d<sup>8</sup>, 45 is not observed as a product, rather a mixture of two

major products is seen, one of which was identified as  $[\text{RhRu}(\text{C}(\text{CH}_3)=\text{CH}_2)(\text{CO})_3(\text{dppm})_2]$  (**47**).

(ii) **Formation of  $[\text{RhRu}(\text{C}(\text{CH}_3)=\text{CH}_2)(\text{CO})_3(\text{dppm})_2]$  (**47**).** A very concentrated solution of  $[\text{RhRu}(\text{CO})_3(\mu\text{-H})(\text{dppm})_2]$  (**40**) was formed by dissolving 40 mg (0.038 mmol) of the complex in 0.5 mL of THF. A small excess of propyne (5 mL, 0.22 mmol) was added via gastight syringe, resulting in an immediate colour change from brown to orange. The solvent was removed in vacuo and the residue was recrystallized inside the glovebox from THF/Et<sub>2</sub>O, washed with 3x5 mL of Et<sub>2</sub>O and dried in vacuo, yielding  $[\text{RhRu}(\text{C}(\text{CH}_3)=\text{CH}_2)(\text{CO})_3(\text{dppm})_2]$  (**47**). Yield: 18 mg, 43%. Anal. Calc. for C<sub>56</sub>H<sub>49</sub>O<sub>3</sub>RhRuP<sub>4</sub>: C, 61.26; H, 4.50. Found: C, 60.46, H, 4.23. Isolated samples of **47** contained approx. 25%  $[\text{RhRu}(\text{C}(\text{O})\text{C}(\text{CH}_3)=\text{CH}_2)(\text{CO})_3(\text{dppm})_2]$  (**48**), and reaction of the mixture with CO resulted in conversion to **48**, while vacuum reversed the insertion. If the reaction is carried out in situ in the NMR solvent, **47** is the major species present in solution.

#### X-ray Data Collection.

$[\text{RhRu}(\text{CH}_3)_2(\text{CO})_3(\text{dppm})_2][\text{CF}_3\text{SO}_3]$  (**44**). Diffusion of ether into a concentrated CH<sub>2</sub>Cl<sub>2</sub> solution of complex **44** yielded small yellow crystals, which were mounted and flame-sealed in glass capillaries under N<sub>2</sub> and solvent vapor to minimize decomposition and/or solvent loss. Data were collected on an Siemens P4/RA diffractometer using Cu K $\alpha$  radiation at -60°C. Unit cell parameters were obtained from a least-squares refinement of the setting angles of 30 reflections in the range  $55.2^\circ \leq 2\theta \leq 58.2^\circ$ . The cell parameters indicated a monoclinic space group and the systematic

**Table 5.2.** Crystallographic Experimental Details**A. Crystal Data**

formula	$C_{56}H_{50}F_3O_6P_4RhRuS$
formula weight	1235.88
crystal dimensions (mm)	$0.33 \times 0.17 \times 0.14$
crystal system	monoclinic
space group	$P2_1/c$ (No. 14)
unit cell parameters <sup>a</sup>	
$a$ (Å)	10.7661 (6)
$b$ (Å)	21.0548 (10)
$c$ (Å)	23.3957 (5)
$\beta$ (deg)	94.467 (3)
$V$ (Å <sup>3</sup> )	5287.2 (4)
$Z$	4
$\rho_{\text{calcd}}$ (g cm <sup>-3</sup> )	1.553
$\mu$ (mm <sup>-1</sup> )	6.860

**B. Data Collection and Refinement Conditions**

diffractometer	Siemens P4/RA <sup>b</sup>
radiation ( $\lambda$ [Å])	Cu K $\alpha$ (1.54178)
monochromator	incident-beam, graphite crystal
temperature (°C)	-60
scan type	$\theta$ - $2\theta$
data collection $2\theta$ limit (°)	110.0
total data collected	6406 ( $-10 \leq h \leq 10, -2 \leq k \leq 20, -1 \leq l \leq 23$ ) <sup>c</sup>
independent reflections	5480
number of observations ( $NO$ )	4137 ( $F_o^2 > 2\sigma(F_o^2)$ )
structure solution method	direct methods ( <i>SHELXS-86</i> <sup>d</sup> )
refinement method	full-matrix least-squares on $F^2$ ( <i>SHELXL-93</i> <sup>e</sup> )

(Table 5.2 cont.)

absorption correction method	<i>DIFABS</i>
range of absorption correction factors	1.262–0.840
data/restraints/parameters	5466 [ $F_o^2 \geq -3\sigma(F_o^2)$ ]/4 <sup>e</sup> /409
goodness-of-fit ( <i>S</i> ) <sup>h</sup>	1.044 [ $F_o^2 \geq -3\sigma(F_o^2)$ ]
final <i>R</i> indices <sup>i</sup>	
$F_o^2 > 2\sigma(F_o^2)$	$R_1 = 0.0599$ , $wR_2 = 0.1205$
all data	$R_1 = 0.0876$ , $wR_2 = 0.1476$
largest difference peak and hole	0.878 and $-0.607$ e Å <sup>-3</sup>

<sup>e</sup>Obtained from least-squares refinement of 30 reflections with  $55.2^\circ < 2\theta < 58.2^\circ$ .

<sup>h</sup>Programs for diffractometer operation and data collection and reduction were those of the *XSCANS* system supplied by Siemens.

<sup>i</sup>Data in the quadrant  $\pm h + k + l$  were collected except when obstructed by the geometry of the low-temperature apparatus (Siemens LT-2), in which case Friedel equivalent reflections were obtained.

<sup>j</sup>Sheldrick, G. M. *Acta Crystallogr.* 1990, *A46*, 467.

<sup>k</sup>Sheldrick, G. M. *J. Appl. Cryst.*, in preparation. Refinement on  $F_o^2$  for all reflections except for 14 having  $F_o^2 < -3\sigma(F_o^2)$ . Weighted *R*-factors  $wR_2$  and all goodnesses of fit *S* are based on  $F_o^2$ ; conventional *R*-factors  $R_1$  are based on  $F_o$ , with  $F_o$  set to zero for negative  $F_o^2$ . The observed criterion of  $F_o^2 > 2\sigma(F_o^2)$  is used only for calculating  $R_1$ , and is not relevant to the choice of reflections for refinement. *R*-factors based on  $F_o^2$  are statistically about twice as large as those based on  $F_o$ , and *R*-factors based on ALL data will be even larger.

<sup>l</sup>Walker, N.; Stuart, D. *Acta Crystallogr.* 1983, *A39*, 158.

<sup>m</sup>Distance restraints were applied within the triflate anion:  $d(\text{S}-\text{C}) = 1.75$  Å and  $d(\text{F}-\text{C}) = 1.35$  Å.

<sup>n</sup> $S = [\sum w(F_o^2 - F_c^2)^2 / (n - p)]^{1/2}$  ( $n$  = number of data;  $p$  = number of parameters varied;  $w = [\sigma^2(F_o^2) + (0.0248P)^2 + 54.7805P]^{-1}$  where  $P = [\text{Max}(F_o^2, 0) + 2F_c^2]/3$ ).

<sup>o</sup> $R_1 = \sum ||F_o| - |F_c|| / \sum |F_o|$ ;  $wR_2 = [\sum w(F_o^2 - F_c^2)^2 / \sum w(F_o^4)]^{1/2}$ .

absences indicated  $P2_1/c$  with  $Z = 4$ . Intensity data were collected as outlined in Table 5.2. Three reflections were chosen as intensity standards and were remeasured every 200 reflections; no decay was evident.

### **Structure Solution and Refinement.**

The positions of the Rh, Ru and P atoms were obtained through use of the direct-methods program *SHELXS-86*.<sup>7</sup> The remaining non-hydrogen atoms were located using successive cycles of least-squares refinement and difference Fourier syntheses. Refinement of O(4) with full occupancy was unsatisfactory, yielding an unusually large thermal parameter, and a significant residual peak was noted near the methyl carbon atom, in a position that would suggest a carbonyl group, suggesting a disorder of carbonyl C(4)O(4) and the Ru bound methyl carbon C(5). The most satisfactory results were obtained with occupancies of 5:1 for the two rotamers. Refinement was completed using the program *SHELXL-93*.<sup>8</sup> Hydrogen atom positions were calculated by assuming idealized  $sp^2$  or  $sp^3$  geometries about their attached carbons as appropriate; these hydrogens were given thermal parameters equal to 120% of the equivalent isotropic displacement parameters of their attached carbons. After all atoms had been located and the structure refined to convergence using isotropic displacement parameters, the data were corrected for absorption using the method of Walker and Stuart.<sup>9</sup> The structure was further refined with all non-hydrogen atoms having anisotropic thermal parameters. The final model for complex 44, with 409 parameters varied, converged to a value of  $R_1 = 0.0599$  (observed data). Atomic coordinates and displacement parameters for the non-hydrogen core atoms are given in Table 5.2.

**Table 5.2.** Atomic Coordinates and Equivalent Isotropic Displacement Parameters for inner-sphere atoms of **44**.

Atom	<i>x</i>	<i>y</i>	<i>z</i>	<i>U</i> <sub>eq</sub> , Å <sup>2</sup>
Rh	0.43929(7)	0.24180(4)	0.01292(3)	0.0385(3)*
Ru	0.21481(7)	0.30445(4)	0.03350(3)	0.0389(3)*
P(1)	0.3616(3)	0.20084(13)	-0.07560(11)	0.0410(7)*
P(2)	0.1134(2)	0.26190(14)	-0.05101(11)	0.0421(7)*
P(3)	0.5412(2)	0.27579(13)	0.09924(11)	0.0389(7)*
P(4)	0.3005(2)	0.34359(14)	0.12309(11)	0.0414(7)*
O(2)	0.2801(8)	0.1700(5)	0.0835(4)	0.080(3)*
O(3)	0.4035(7)	0.3643(4)	-0.0422(3)	0.054(2)*
O(4) <sup>a</sup>	0.0800(11)	0.4302(6)	0.0132(5)	0.089(4)*
O(5) <sup>a</sup>	-0.0190(52)	0.2755(27)	0.0857(23)	0.049(17)
C(1)	0.6077(12)	0.1956(6)	-0.0014(5)	0.075(4)*
C(2)	0.2843(11)	0.2176(6)	0.0577(5)	0.054(3)*
C(3)	0.3643(10)	0.3283(5)	-0.0114(5)	0.045(3)*
C(4)	0.1330(11)	0.3851(7)	0.0191(5)	0.060(3)*
C(5)	0.0416(16)	0.2889(8)	0.0730(6)	0.091(5)*
C(6)	0.2245(9)	0.2443(5)	-0.1050(4)	0.041(3)*
C(7)	0.4297(9)	0.2946(5)	0.1524(4)	0.042(3)*

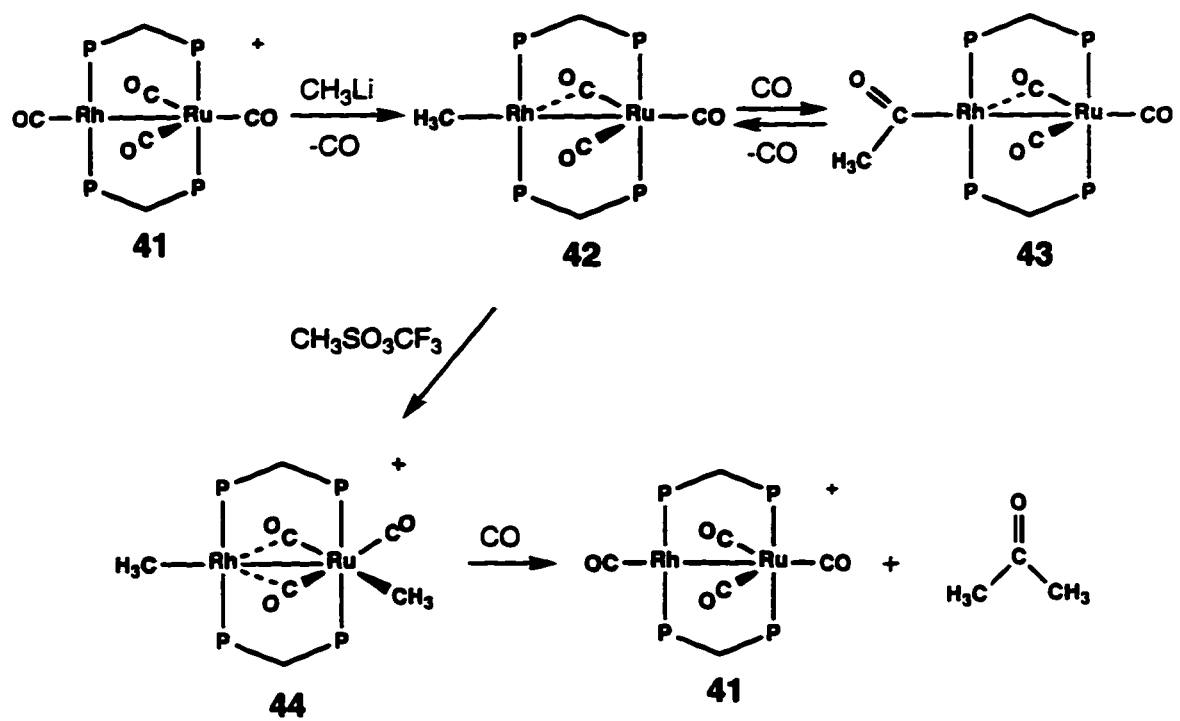
Anisotropically refined atoms are marked with an asterisk (\*). The form of the anisotropic displacement parameter is:  $\exp[-2\pi^2(h^2a^{*2}U_{11} + k^2b^{*2}U_{22} + l^2c^{*2}U_{33} + 2klb^{*c}U_{23} + 2hla^{*c}U_{13} + 2hka^{*b}U_{12})]$ . <sup>a</sup>The carbonyl oxygen atoms O(4) and O(5) were refined with respective occupancy factors of 0.833 and 0.167.

## Results and Compound Characterization.

### (a) Preparation and Reactivity of methyl complexes.

The complex  $[\text{RhRu}(\text{CO})_4(\text{dppm})_2][\text{BF}_4]$  (**41**) reacts readily with MeLi to form  $[\text{RhRu}(\text{CH}_3)(\text{CO})_3(\text{dppm})_2]$  (**42**), much as was observed in the formation of the analogous RhOs species  $[\text{RhOs}(\text{CH}_3)(\text{CO})_3(\text{dppm})_2]$  (**11**) (see Chapter 2). Compound **42** is much more air sensitive than the RhOs analogue; although **11** is air stable for short periods in the solid state, compound **42** decomposes immediately upon exposure to air. The  $^1\text{H}$  NMR spectrum of **42** shows a doublet of triplets at  $\delta$  -0.32 for the methyl group, showing coupling to Rh and to the Rh-bound phosphines, as well as a multiplet for the dppm methylene hydrogens. The  $^{13}\text{C}\{^1\text{H}\}$  NMR spectrum shows two carbonyl resonances at  $\delta$  211.63 and 234.50 in a ratio of 1 to 2. The highfield resonance appears as a triplet, showing coupling to the Ru-bound phosphines, whereas the lowfield resonance is a doublet of multiplets with a 15 Hz Rh coupling, indicating semibridging interactions with these carbonyls. Although two carbonyls appear to bridge, we suggest that only one carbonyl bridges in the solid state, and that in solution the two carbonyls are rapidly exchanging as described for the RhOs analogue. On the basis of these data the structure is assigned as shown in Scheme 5.1, and is analogous to that of the RhOs methyl complex **11**, described in Chapter 2.

Compound **42** reacts with CO, resulting in migratory insertion involving the methyl group to form  $[\text{RhRu}(\text{C}(\text{O})\text{CH}_3)(\text{CO})_3(\text{dppm})_2]$  (**43**). The  $^1\text{H}$  NMR spectrum of **43** shows a singlet for the methyl group at  $\delta$  0.85 and a broad multiplet at  $\delta$  3.13 for the

**Scheme 5.1**

dppm methylene groups. The migratory insertion is reversible; under vacuum, the acyl complex partially reverts to the methyl complex.

Reaction of **42** with methyl triflate results in attack by the electrophile at Ru, to form  $[\text{RhRu}(\text{CH}_3)_2(\text{CO})_3(\text{dppm})_2][\text{CF}_3\text{SO}_3]$  (**44**). As was the case for the analogous Os system, the group 8 metal is the site of electrophilic attack. The  $^1\text{H}$  NMR spectrum of **44** shows resonances for two different methyl groups at  $\delta$  0.81 and -0.17, for which the first resonance appears as a doublet of triplets, showing coupling to Rh and the Rh-bound phosphines, and the second appears as a triplet, displaying coupling to the Ru-bound phosphines. The  $^{31}\text{P}$  NMR spectrum (see Figure 5.1) has a very unusual appearance from strong second order effects due to the proximity of the two resonances. The IR spectrum of **44** shows three bands at 2039, 1860, and  $1812\text{ cm}^{-1}$ , and is very similar to those of the RhOs dialkyl and vinyl/alkyl complexes, which were shown to have two semibridging carbonyls. Compound **44** is assigned the solution structure shown in Scheme 5.1 based on analogies with the RhOs system.

Compound **44** has also been structurally characterized by X-ray crystallography, confirming the structure suggested by the spectroscopic parameters and shown in Figure 5.2. The structure was disordered, resulting in superposition of the Ru-bound methyl group and the adjacent carbonyl; however, the disorder was resolved satisfactorily. Important bond lengths and angles are given in Table 5.3. Ignoring the metal-metal interaction, the geometry at Ru is octahedral, having essentially mutually trans phosphines ( $\text{P}(1)\text{-Os-P}(3) = 174.52(10)^\circ$ ) and angles close to  $90^\circ$  between all adjacent groups on Ru. The result is an 18e configuration at the  $\text{Ru}(\text{CH}_3)(\text{CO})_3\text{L}_2^+$  centre, nearly identical to the Os centre in  $[\text{RhOs}(\text{C}(\text{CH}_3)=\text{C}(\text{CH}_3)_2)(\text{CH}_3)(\text{CO})_3(\text{dppm})_2]\text{-}$

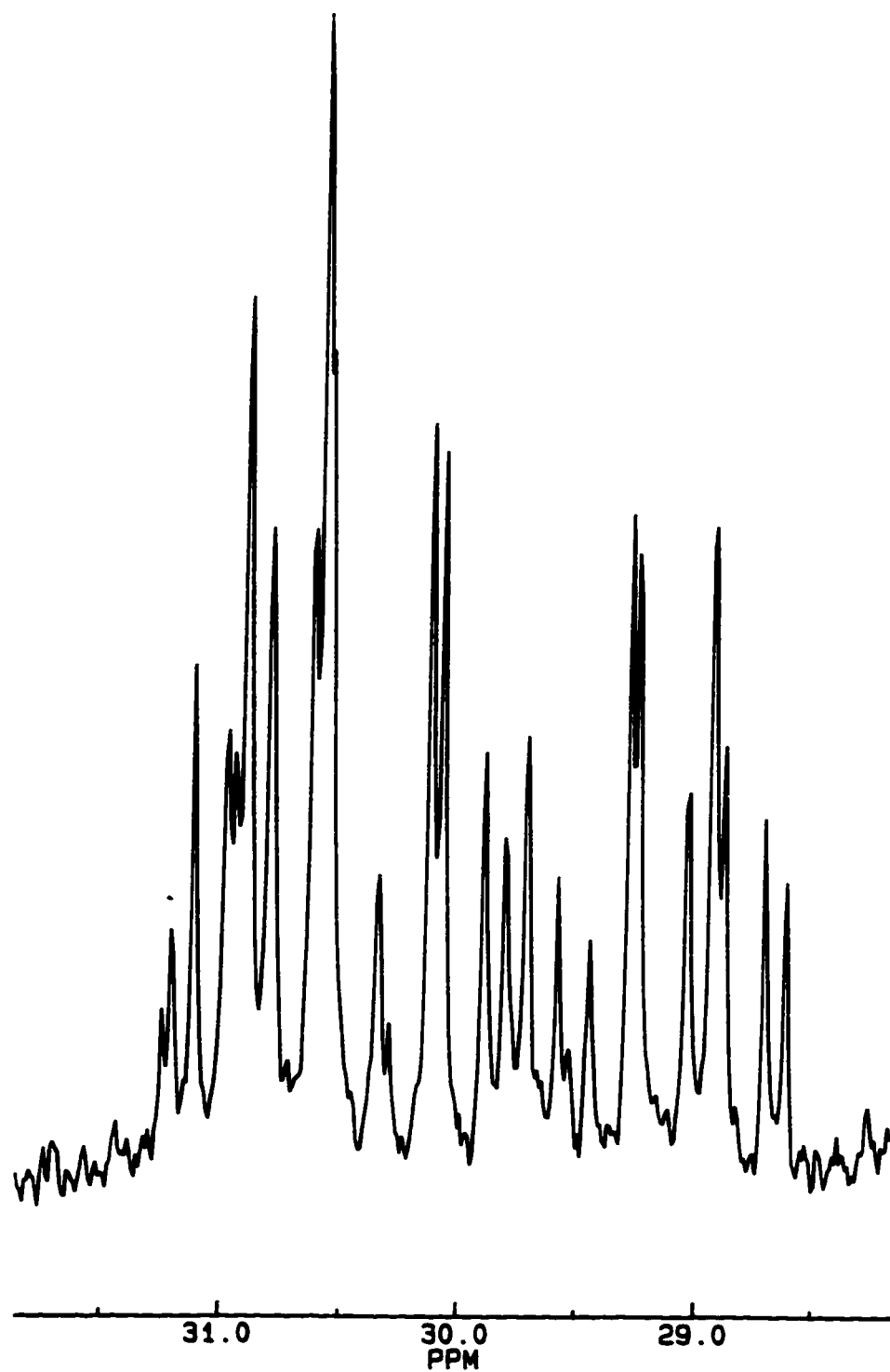


**Figure 5.1.**  $^{31}\text{P}\{^1\text{H}\}$  NMR of **44** showing the strong second order effects that result from the proximity of the two resonances.

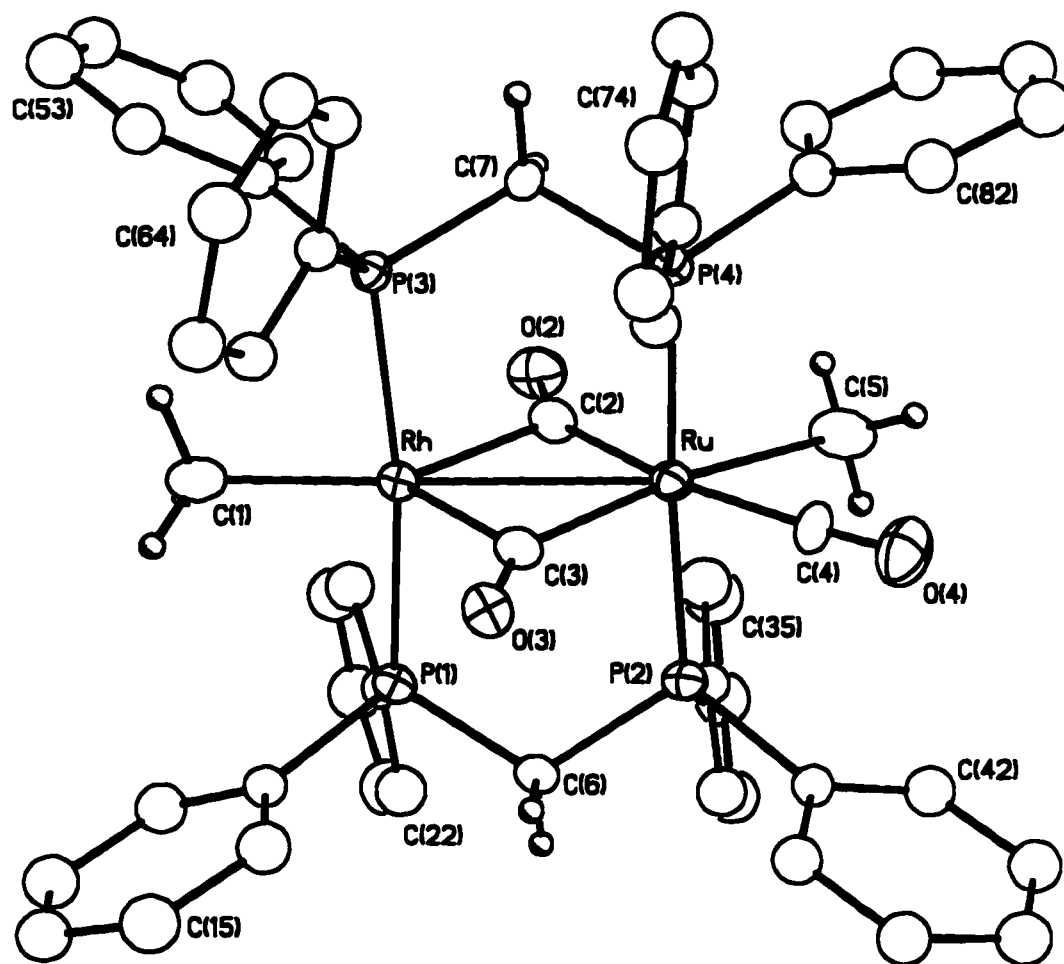


**Figure 5.2.** Perspective view of the cation of  $[\text{RhRu}(\text{CH}_3)_2(\text{CO})_3(\text{dppm})_2][\text{CF}_3\text{SO}_3]$  (**44**). Thermal parameters are shown at the 20% level, except for hydrogens which are shown arbitrarily small. Phenyl hydrogens are omitted. Phenyl carbons are numbered sequentially within each phenyl ring, beginning with the ipso carbon.

**Table 5.4.** Selected Interatomic Distances (Å) and Angles (°) Involving Inner-sphere Atoms of **44**.

Atom1	Atom2	Distance	Atom1	Atom2	Distance
Rh	Ru	2.8274(11)	Ru	C(4)	1.930(13)
Rh	P(1)	2.337(3)	Ru	C(5)	2.17(2)
Rh	P(3)	2.335(3)	P(1)	C(6)	1.826(10)
Rh	C(1)	2.107(12)	P(2)	C(6)	1.844(10)
Rh	C(2)	2.101(12)	P(3)	C(7)	1.838(10)
Rh	C(3)	2.055(12)	P(4)	C(7)	1.822(10)
Ru	P(2)	2.360(3)	O(2)	C(2)	1.173(13)
Ru	P(4)	2.371(3)	O(3)	C(3)	1.149(12)
Ru	C(2)	2.039(13)	O(4)	C(4)	1.112(14)
Ru	C(3)	2.052(12)	O(5)*	C(5)	0.79(5)

Atom1	Atom2	Atom3	Angle	Atom1	Atom2	Atom3	Angle
Ru	Rh	P(1)	94.10(8)	C(1)	Rh	C(3)	133.6(5)
Ru	Rh	P(3)	93.45(7)	C(2)	Rh	C(3)	92.5(5)
Ru	Rh	C(1)	179.2(3)	Rh	Ru	P(2)	91.50(8)
Ru	Rh	C(2)	46.0(4)	Rh	Ru	P(4)	91.95(7)
Ru	Rh	C(3)	46.5(3)	Rh	Ru	C(2)	47.8(3)
P(1)	Rh	P(3)	172.45(10)	Rh	Ru	C(3)	46.5(3)
P(1)	Rh	C(1)	86.7(3)	Rh	Ru	C(4)	139.9(4)
P(1)	Rh	C(2)	96.3(3)	Rh	Ru	C(5)	140.9(5)
P(1)	Rh	C(3)	88.6(3)	P(2)	Ru	P(4)	174.52(10)
P(3)	Rh	C(1)	85.8(3)	P(2)	Ru	C(2)	91.6(3)
P(3)	Rh	C(2)	88.9(3)	P(2)	Ru	C(3)	89.6(3)
P(3)	Rh	C(3)	96.7(3)	P(2)	Ru	C(4)	90.7(3)
C(1)	Rh	C(2)	134.0(5)	P(2)	Ru	C(5)	86.7(4)

*(Table 5.4 cont.)*

P(4)	Ru	C(2)	87.5(3)	Rh	P(3)	C(7)	111.3(3)
P(4)	Ru	C(3)	95.8(3)	Ru	P(4)	C(7)	111.7(3)
P(4)	Ru	C(4)	89.4(3)	Rh	C(2)	Ru	86.1(5)
P(4)	Ru	C(5)	88.0(4)	Rh	C(2)	O(2)	121.8(10)
C(2)	Ru	C(3)	94.4(5)	Ru	C(2)	O(2)	151.8(10)
C(2)	Ru	C(4)	171.8(5)	Rh	C(3)	O(3)	127.1(9)
C(2)	Ru	C(5)	93.2(6)	Ru	C(3)	O(3)	145.5(9)
C(3)	Ru	C(4)	93.5(5)	Rh	C(3)	Ru	87.0(5)
C(3)	Ru	C(5)	171.7(5)	Ru	C(4)	O(4)	175.3(13)
C(4)	Ru	C(5)	79.1(6)	Ru	C(5)	O(5)*	167.7(47)
Rh	P(1)	C(6)	111.9(3)	P(1)	C(6)	P(2)	113.0(5)
Ru	P(2)	C(6)	111.6(3)	P(3)	C(7)	P(4)	112.8(5)

\*Atom O(5) is the oxygen of the terminal carbonyl in the minor rotamer (occupancy 0.167).

[CF<sub>3</sub>SO<sub>3</sub>] (**24a,b**). As in **24**, two of the carbonyls form semi-bridging interactions with the Rh. The two semibridging carbonyls in **44** are slightly different, with the carbonyl trans to the Ru-bound methyl group (C(3)-O(3)) having a slightly stronger semi-bridging interaction with Rh than does C(2)-O(2). Whereas the C(2)-Ru distance is significantly shorter than the C(2)-Rh distance (2.039(13) Å vs. 2.101(12) Å), the C(3)-Ru and C(3)-Rh distances are nearly equal (2.052(12) Å and 2.055(12) Å). The C(2)-O(2) carbonyl is also somewhat more linear with respect to Ru (Ru-C(2)-O(2) = 151.8(10)°, Ru-C(3)-O(3) = 145.5(9)°). One methyl group (C(1)H<sub>3</sub>) is terminally bound to Rh, along with the two phosphines, resulting in a 14-electron Rh centre, necessitating a Ru to Rh dative bond resulting in a metal-metal separation of 2.8274(11) Å which is consistent with a single bond. If the semibridging carbonyls are ignored, the geometry at Rh is essentially square planar, with trans phosphines and the methyl group opposite the metal-metal bond.

The dimethyl complex **44** reacts slowly with CO over several days, resulting in the formation of [RhRu(CO)<sub>4</sub>(dppm)<sub>2</sub>][CF<sub>3</sub>SO<sub>3</sub>] (**41**), along with acetone. If <sup>13</sup>CO is used in the reaction, the resulting acetone contains mostly <sup>12</sup>CO, particularly in the early stages of the reaction. Two intermediates which were observed in the transformation of **44** to **41** are currently under study.

#### **(b) Preparation and Reactivity of Allyl and Vinyl Complexes.**

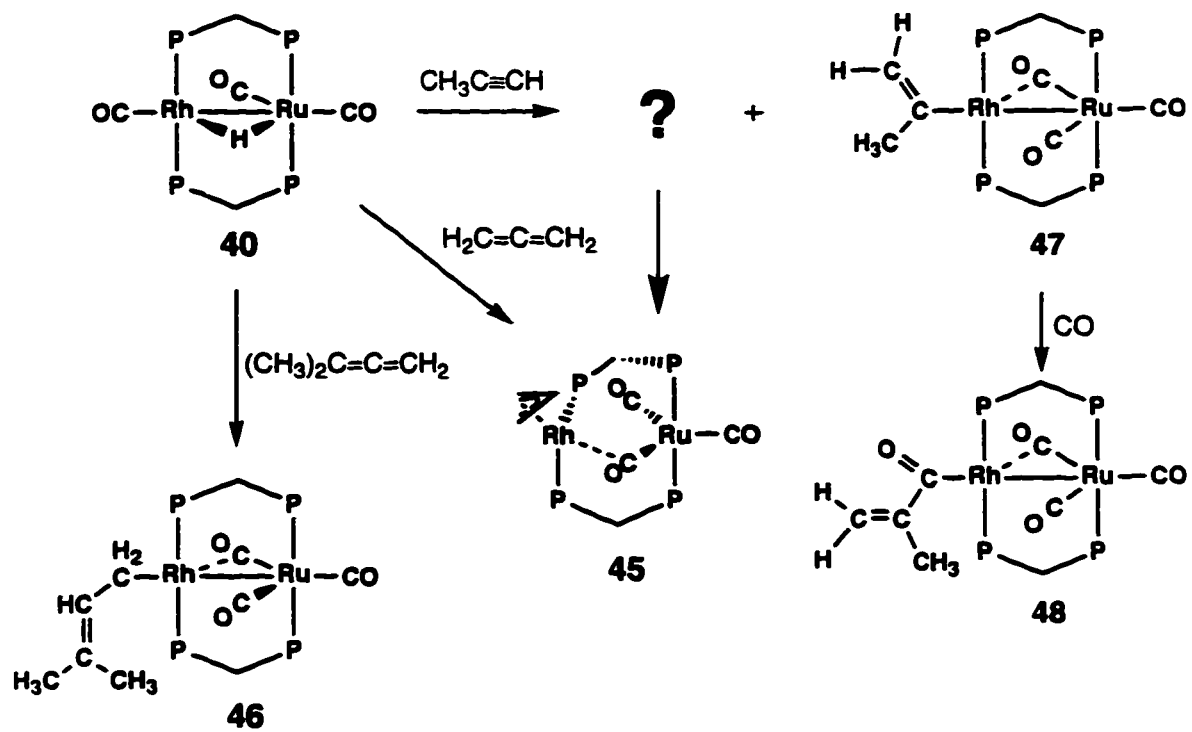
The reaction of [RhOsH(CO)<sub>3</sub>(dppm)<sub>2</sub>] with allene and propyne yielded mainly the isopropenyl complex [RhOs(C(CH<sub>3</sub>)=CH<sub>2</sub>)(CO)<sub>3</sub>(dppm)<sub>2</sub>] (**18**), with small amounts of the isomeric allyl complex [RhOs(η<sup>3</sup>-C<sub>3</sub>H<sub>5</sub>)(CO)<sub>3</sub>(dppm)<sub>2</sub>] (**19**) in the former reaction. Owing to the structural differences between the RhOs hydride and the RuRh analogue

[RhRu(CO)<sub>3</sub>(μ-H)(dppm)<sub>2</sub>] (i.e. terminal or bridging hydride ligand), the allene and propyne reactions were repeated with this RhRu complex. It was anticipated that subtle differences in the two systems may result in differences, either in the products obtained or in the product distributions.

The reaction of [RhRu(CO)<sub>3</sub>(μ-H)(dppm)<sub>2</sub>] (**40**) with allene yielded only [RhRu(η<sup>3</sup>-C<sub>3</sub>H<sub>5</sub>)(CO)<sub>3</sub>(dppm)<sub>2</sub>] (**45**), analogous to the minor product in the RhOs hydride reaction (see Scheme 5.2). No evidence of the isopropenyl species analogous to **18** was observed. The spectroscopy of **45** is very similar to that of **19**. At room temperature, the molecule is highly fluxional. The <sup>31</sup>P{<sup>1</sup>H} NMR spectrum shows a multiplet at δ 42.03 for the Ru phosphines and a very broad resonance for the Rh-bound phosphines at δ 23.5, and the <sup>1</sup>H NMR spectrum shows a broad singlet for the dppm methylenes but no signal for the allyl group. At -80°C, the <sup>31</sup>P{<sup>1</sup>H} NMR spectrum shows 4 inequivalent phosphorus resonances. The coupling constant between the two Rh-bound phosphines is only 19 Hz, indicating a cis arrangement of the phosphines, whereas the P-P coupling constant for the Ru-bound phosphines is 255 Hz, indicating a trans arrangement at this metal. The <sup>1</sup>H NMR spectrum at -80°C shows nine unique resonances, four for the dppm methylene hydrogens, and five for the allyl group. The resonances for one end of the allyl group are unusually high field (1.40 (syn), 0.25 (anti) compared with typical values of δ 2-5 for syn, and δ 1-3 for anti<sup>10</sup>), suggesting that the allyl group is very unsymmetrically bound, approaching σ-π coordination.

If a more sterically hindered allene, H<sub>2</sub>C=C=C(CH<sub>3</sub>)<sub>2</sub>, is used, an η<sup>3</sup>-allyl is not observed and instead the product is the η<sup>1</sup>-allyl [RhRu(CH<sub>2</sub>CH=C(CH<sub>3</sub>)<sub>2</sub>)(CO)<sub>3</sub>(dppm)<sub>2</sub>] (**46**). It is interesting that no evidence of a trimethylvinyl compound, as was found

## Scheme 5.2



exclusively in the RhOs system, was observed. In the  $^1\text{H}$  NMR spectrum of **46**, the  $\alpha$  hydrogens of the allyl fragment appear as a doublet of triplets, coupling to the  $\beta$  hydrogen as well as the Rh-bound phosphines, while the resonance for the  $\beta$  hydrogen is a triplet due to coupling to the  $\alpha$  hydrogens, and the two methyl groups appear as singlets. Although no Rh coupling to the  $\alpha$  hydrogens is observed, this coupling is expected to be small (1-2 Hz) and may be masked by the broadness of the peak. The dppm methylene hydrogens are all equivalent, indicating that the molecule has front-back symmetry, and that the allyl fragment rotates freely. The  $^{13}\text{C}\{^1\text{H}\}$  NMR spectrum shows two unique carbonyls at  $\delta$  209.73 and 233.77, with the highfield resonance appearing as a triplet showing coupling to the Ru bound phosphines, and the lowfield resonance appearing as a doublet of triplets, coupling to the Ru-bound phosphines and to Rh. The 14 Hz Rh coupling is consistent with a semi-bridging interaction, and the IR spectrum also indicates the presence of a semi-bridging carbonyl, with bands at 1910, 1883, 1750  $\text{cm}^{-1}$ . Although both carbonyls are equivalent in the  $^{13}\text{C}\{^1\text{H}\}$  NMR spectrum, it is likely that only one is semibridging in the solid state and that the two positions are rapidly exchanging in solution, as discussed for  $[\text{RhOs}(\text{CH}_3)(\text{CO})_3(\text{dppm})_2]$  (**11**) in Chapter 2.

Reaction of concentrated solutions of **40** with a small excess of propyne results in the formation of the isopropenyl complex  $[\text{RhRu}(\text{C}(\text{CH}_3)=\text{CH}_2)(\text{CO})_3(\text{dppm})_2]$  (**47**). The spectroscopy of **47** is almost identical to that of the RhOs analogue **18**, showing a singlet for the methyl group and singlets for each of the olefinic hydrogens of the isopropenyl group. The IR spectrum has three bands at 1930, 1880, and 1740  $\text{cm}^{-1}$ , indicating a semibridging carbonyl. Samples of **47** were found to be contaminated with approx. 25%  $[\text{RhRu}(\text{C}(\text{O})\text{C}(\text{CH}_3)=\text{CH}_2)(\text{CO})_3(\text{dppm})_2]$  (**48**), which is the product that results from CO

insertion. The identity of this impurity was confirmed by reaction of the mixture with CO, resulting in complete conversion of **47** to **48**. If the reaction with propyne is carried out in situ in the NMR solvent,  $^{31}\text{P}\{^1\text{H}\}$  NMR spectroscopy reveals the presence of decomposition products in addition to **47**. Formation of **48** probably results from scavenging of CO from these decomposition products by **47**.

Reaction of **40** with a large excess of propyne followed by workup yields the  $\eta^3$ -allyl complex **45** in moderate yields. Complex **45** is not the initial product in the reaction. If the reaction is carried out in situ in the NMR solvent, **45** is not initially observed, but a mixture of two major and several minor products is observed. Complex **45** forms slowly and selectively precipitates from THF/Et<sub>2</sub>O solutions of the mixture. The main component of the remaining supernatant solution is compound **47**, so it appears that the other unknown major product is being converted to **45**. Unfortunately, this product could not be characterized in the mixture, and it could not be isolated because it converts to **45**. However, the  $^{31}\text{P}\{^1\text{H}\}$  NMR chemical shifts ( $\delta$  35.37 (RhP), 27.33 (RuP) vs.  $\delta$  45.81 (RuP), 29.18 (RhP) for **47**) are very different from those of the previous complexes with the organic fragment on Rh (note that the RuP resonance is now *downfield* of that due to RhP). This may indicate that the organic group is on Ru in this compound.

## Discussion

The complex  $[\text{RhRu}(\text{CH}_3)(\text{CO})_3(\text{dppm})_2]$  (**42**) is formed readily by displacement of a carbonyl from  $[\text{RhRu}(\text{CO})_4(\text{dppm})_2][\text{BF}_4]$  (**41**) by MeLi, as was observed in the

RhOs system. Substitution of Os by the more labile Ru centre results in this reaction occurring more readily and requiring a smaller excess of MeLi. It is not clear, however, what the function of the group 8 metal is in this reaction, since the final product has the methyl group on Rh. Whether initial attack is at Ru (or at the Ru-bound CO) or whether attack occurs at Rh, with Ru exerting a labilizing effect, is not known. The increased lability of the Ru complexes is seen in their increased air sensitivity; while the Os analogues can be handled briefly in air, the neutral Ru complexes decompose within seconds upon exposure to air in the solid state. The cationic complexes in both systems, which generally have the group 8 metal in the +2 oxidation state, are relatively air stable.

As in the RhOs system, the neutral methyl complex reacts with methyl triflate to form the cationic dimethyl complex  $[\text{RhRu}(\text{CH}_3)_2(\text{CO})_3(\text{dppm})_2][\text{CF}_3\text{SO}_3]$  (44); again, the site of electrophilic attack is apparently the group 8 metal. While the RhOs dimethyl complex was unreactive, the RhRu dimethyl complex reacted slowly with CO to eliminate acetone. The formation of acetone from the dimethyl complex suggests that migratory insertion to give an acyl group occurs at only one metal. The insertion reaction is followed by either methyl or acyl migration to the adjacent metal, and reductive elimination from that metal. It appears that migratory insertion at Rh can be ruled out since the addition of methyl triflate to  $[\text{RhRu}(\text{C}(\text{O})\text{CH}_3)(\text{CO})_3(\text{dppm})_2]$  (43), in which the acyl group is known to be on Rh, leads only to decomposition, with no evidence of acetone formation. This assumes that the group 8 metal is the most nucleophilic site in the molecule; the acyl carbonyl may be site of  $\text{CH}_3^+$  attack, with the resulting carbene complex decomposing. Supporting the proposal that migratory insertion is occurring at Ru is the fact that CO insertion is never observed on Rh in cationic complexes in the

RhOs system. In the reaction of the RhOs vinyl/hydride complexes with CO the result is elimination of the alkene, with no aldehyde formation, and all the dialkyl and vinyl/alkyl complexes are unreactive towards CO. In addition, carbonyl insertions are well known on  $\text{Ru}^{+2}$  centres.<sup>11</sup> In the RhOs system, the reductive elimination of methane was shown to occur only from the octahedral  $\text{Os}^{+2}$  centre, not from the square planar  $\text{Rh}^{+1}$  centre, even if significant rearrangement was required to bring the appropriate ligands to that metal. This suggests that elimination of acetone in the RhRu system may occur from the Ru(II) centre, necessitating migration of the Rh-bound methyl group to Ru. If the CO insertion reaction is occurring at Ru, the resulting 16e Ru centre should readily accept the methyl group from Rh, while the incoming CO could coordinate to Rh, resulting in the appropriate arrangement of ligands for the reductive elimination.

Insertion reactions of the RhRu hydride complex with allenes result in regioselectivity that is opposite to that observed in the RhOs system. While the RhOs hydride  $[\text{RhOs}(\text{H})(\text{CO})_3(\text{dppm})_2]$  inserts allenes so that the metal ends up on the internal carbon in the major product, insertion of allenes into metal-hydride bond of  $[\text{RhRu}(\text{CO})_3(\mu\text{-H})(\text{dppm})_2]$  (40) results in the metal adding to the terminal carbon, as is more commonly observed.<sup>12</sup> The product observed in the reaction with allene is the  $\eta^3$ -allyl complex  $[\text{RhRu}(\eta^3\text{-C}_3\text{H}_5)(\text{CO})_3(\text{dppm})_2]$  (45), which is analogous to the minor product observed in the same reaction with the RhOs hydride. With dimethylallene, the  $\eta^3$ -allyl cannot form, presumably due to the steric influence of the methyl groups, and the observed product is the  $\eta^1$ -allyl complex  $[\text{RhRu}(\eta^1\text{-CH}_2\text{CH}=\text{C}(\text{CH}_3)_2)(\text{CO})_3(\text{dppm})_2]$  (46).

The reasons for the different regioselectivities of the two systems are not completely clear, but may be related to the structural differences of the starting hydride

complexes. While the RhOs hydride complex has a terminal hydride ligand bound to Os, and is thought to have cis phosphines at Os, the RhRu analogue has a bridged hydride and trans phosphines at Ru.

As in the RhOs system, the phosphines on Rh in the allyl compound **45** move into a cis configuration to accommodate the  $\eta^3$ -coordination mode of the allyl group. This complex shows the same fluxional behavior as the RhOs analogue discussed in Chapter 3. At ambient temperature the five allyl hydrogens are not observed in the  $^1\text{H}$  NMR spectrum, and the four dppm methylene hydrogens are equivalent. At this temperature, the two Rh-bound phosphines are equivalent, as are the two Ru-bound phosphines in the  $^{31}\text{P}\{^1\text{H}\}$  NMR spectrum. At  $-80^\circ\text{C}$ , the fluxional process is frozen out, and four inequivalent phosphorus resonances are observed, as well as five unique resonances for the allyl hydrogens. These observations can be explained by a process involving an  $\eta^1$ -allyl intermediate, which is structurally analogous to compound **46**. In this intermediate, the phosphines on each metal would become equivalent, and the opposite end of the allyl can re-coordinate after rotation about the Rh-C  $\sigma$ -bond.

As in the RhOs analogue **19**, the allyl ligand in **45** is very unsymmetrical, showing unusually high field chemical shifts for one end of the allyl ligand ( $\delta$  1.30 (syn),  $\delta$  0.22 (anti)).<sup>11</sup> The chemical shifts are consistent with the chemical shifts for  $\sigma$ -bound alkyl groups on Rh, suggesting that this end of the allyl ligand is essentially  $\sigma$ -bound, while the other end coordinates as a  $\pi$ -bound olefin. This asymmetry likely results from the position of either end of the ligand relative to the semi-bridging carbonyl. The end of

the allyl ligand trans to the carbonyl will favour strong  $\sigma$ -donation, while the end of the allyl ligand cis to the carbonyl will favour  $\pi$ -back donation.

The reaction of **40** with propyne led to unexpected results. Based on the reactions with allenes, in which the metal ended up on the terminal carbon, we would have expected propyne to show similar regioselectivity. However, if the reaction is carried out with a high concentration of **40**, and a small excess of propyne is added, the major product is  $[\text{RhRu}(\text{C}(\text{CH}_3)=\text{CH}_2)(\text{CO})_3(\text{dppm})_2]$  (**47**), arising from hydride migration to the terminal carbon. It is not clear why the propyne reaction does not occur with the same regioselectivity as reactions with the allenes. An even more unusual result is obtained when the same reaction is carried out under different conditions. With low concentrations of **40** and a large excess of propyne the isolated product is  $[\text{RhRu}(\eta^3\text{-C}_3\text{H}_5)(\text{CO})_3(\text{dppm})_2]$  (**45**). If the reaction is carried out in situ in the NMR solvent, two major products are observed, one of which is the isopropenyl complex  $[\text{RhRu}(\text{C}(\text{CH}_3)=\text{CH}_2)(\text{CO})_3(\text{dppm})_2]$  (**47**) and the other of which could not be characterized in solution but converts to **45** upon workup. Although the intermediate complex could not be characterized, the  $^{31}\text{P}$  chemical shifts suggest that the organic fragment in this intermediate may be on Ru. Insertions of alkynes into metal hydride bonds of coordinatively saturated Ru complexes are known.<sup>13</sup> This reaction warrants further investigation to determine the nature of this interesting transformation.

## References

- (a) Carter, W. J.; Kelland, J. W.; Okrasinski, S. J.; Warner, K. E.; Norton, J. R. *Inorg. Chem.* **1982**, *21*, 3955.

(b) Carter, W. J.; Okrasinski, S. J.; Norton, J. R. *Organometallics*, **1985**, *4*, 1377.
- (a) Hartwig, J. F.; Anderson, R. A.; Bergman, R. G. *Organometallics*, **1991**, *6*, 1710.

(b) Hartwig, J. F.; Anderson, R. A.; Bergman, R. G. *J. Am. Chem. Soc.* **1991**, *113*, 6492.
- Braunstein, P.; Rose, J in *Comprehensive Organometallic Chemistry II* Abel, E. W.; Stone, F. G. A.; Wilkinson, G. eds; Pergamon: Oxford, 1995; Vol 10, Chp 7, pp. 351-352.
- Dombek, B. D. *Organometallics*, **1985**, *4*, 1707.
- Antonelli, D. M.; Cowie, M. *Organometallics*, **1990**, *9*, 1818.
- Hilts, R.W.; Franchuk, R.A.; Cowie, M. *Organometallics* **1991**, *10*, 304.
- Sheldrick, G.M. *Acta Crystallogr.* **1990**, *A46*, 467.
- Sheldrick G.M. SHELXL-93. Program for crystal structure determination. University of Göttingen, Germany, 1993. Refinement on  $F_o^2$  for all reflections (all of these having  $F_o^2 < -3\sigma(F_o^2)$ ). Weighted  $R$ -factors  $wR^2$  and all goodnesses of fit  $S$  are based on  $F_o^2$ ; conventional  $R$ -factors  $R_1$  are based on  $F_o$ , with  $F_o$  set to zero for negative  $F_o^2$ . The observed criterion of  $F_o^2 > 2\sigma(F_o^2)$  is used only for calculating  $R_1$ , and is not relevant to the choice of reflections for refinement.

*R*-factors based on  $F_o^2$  are statistically about twice as large as those based on  $F_o$ , and *R*-factors based on ALL data will be even larger.

9. Walker, N.; Stuart, D. *Acta Crystallogr.* **1983**, *A39*, 158.
10. Collman, J.P.; Hegedus, L.S.; Norton, J.R.; Finke, R.G. *Principles and Applications of Organotransition Metal Chemistry*; University Science Books: Mill Valley, California, 1987, pp. 176-177.
11. (a) Grundy, K. R.; Jenkins, J. *J. Organomet. Chem.* **1984**, *265*, 77.  
(b) McCooey, K. M.; Probitts, E. J.; Mawby, R. J. *J. Chem. Soc., Dalton Trans.* **1987**, 1713.  
(c) Barnard, C. F. J.; Daniels, A. J.; Mawby, R. J. *J. Chem. Soc., Dalton Trans.* **1979**, 1331.
12. Lobach, M.I.; Kormer, V.A. *Russian Chemical Reviews* **1979**, *48*, 758.
13. Torres, M. R.; Vegas, A.; Santos, A.; Ros, J. *J. Organomet. Chem.*, **1986**, *309*, 169.

## Chapter 6

### Conclusions

The goal of this thesis was to develop the organometallic chemistry of the dppm bridged RhOs system in order to attempt to gain an understanding of the roles of adjacent metals in transformations involving organic fragments. In addition, we were interested in extending this chemistry to the related RhRu system, not only to compare the two systems, but also because of expectations that the more labile Ru centre would more readily undergo carbon-carbon bond formation reactions. Our interest in binuclear chemistry stemmed from the possible importance of cooperativity between adjacent metals on a catalyst surface in organic transformations. We were particularly interested in alkyl, alkenyl, allyl, and carbene complexes, because all of these fragments are thought to be important surface species in Fischer-Tropsch catalysis.

Several neutral monoalkyl and related complexes of the form  $[\text{RhMR}(\text{CO})_3(\text{dppm})_2]$  ( $\text{M} = \text{Os}, \text{Ru}$ ;  $\text{R} = \text{CH}_3, \text{vinyl}, \text{acyl}, \text{C}\equiv\text{CH}, \text{CH}_2\text{CN}$ ) were successfully synthesized by a variety of routes. In all cases (with the exception of the  $\eta^3$ -allyl complexes) the R group occupies a terminal position on the square planar 16e Rh. This arrangement parallels that seen in several analogous systems involving the metal pairs, RhW,<sup>1</sup> RhMo,<sup>2</sup> RhMn,<sup>3</sup> and RhRe<sup>4</sup>. The only exception appears to be in the RhIr series where, for example,  $[\text{RhIr}(\text{CH}_3)(\text{CO})_3(\text{dppm})_2]^+$  has the methyl group bound to the 18e Ir centre, although in this case simple substitution of one carbonyl for ethylene results in a transfer of the methyl group to Rh.<sup>5</sup> Clearly there are very subtle differences between the two possible arrangements, and the factors which favour binding

of the organic ligand to one metal or the other are not fully understood. Such factors are clearly of interest if the functions of the different metals in the reactivity of such groups is to be understood. It could be argued that in the RhOs and RhRu compounds, the observed arrangement, with the alkyl group on Rh, results in a favourable  $\text{Rh}^{-1}/\text{M}^0$  formulation, as opposed to  $\text{Rh}^0/\text{M}^{+1}$ . However, this cannot be the only factor involved since in the analogous RhOs hydride  $[\text{RhOs}(\text{H})(\text{CO})_3(\text{dppm})_2]$  (1), the hydride ligand is on Os, giving an apparent  $\text{Rh}^0/\text{Os}^{+1}$  configuration. The observed arrangement may be sterically more favourable. Placing the small hydride ligand on the more crowded Os centre may alleviate some of the steric interactions involving the dppm ligands and the carbonyls at this metal.

A feature common to all of the alkyl and related complexes is the presence of a semibridging carbonyl interaction between Rh and one of three carbonyls on the group 8 metal. This semibridging carbonyl does not function as an electron pair donor to Rh, but acts as a  $\pi$ -acceptor from this metal; this appears to be necessary in order to alleviate the buildup of electron density on Rh resulting from the presence of three strong  $\sigma$  donors (phosphines and alkyl group) and of the dative bond from Os, and the absence of other  $\pi$  acceptors on Rh. This idea is supported by the spectroscopic data which demonstrate that the strength of the semibridging interaction (as indicated by the frequency of the IR stretch of the semibridging carbonyl and the Rh-C coupling constant) correlates very well with the  $\sigma$ -donor ability of the R group. Strong  $\sigma$  donors such as a methyl group on Rh lead to substantial bridging interactions, while weaker  $\sigma$  donors, such as an acetylide group lead to a much weaker  $\pi$ -back donation and a weaker semi-bridging interaction.

These semibridging carbonyl interactions illustrate the ability of bridging modes to “fine tune” the electron density in this system.

Protonation of the RhOs methyl complex  $[\text{RhOs}(\text{CH}_3)(\text{CO})_3(\text{dppm})_2]$  (11), or methylation of the hydride complex **1**, results in a site specific elimination of methane, in which reductive elimination occurs from the octahedral  $\text{Os}^{+2}$  centre and not from the square planar  $\text{Rh}^{+1}$  centre. Elimination occurs from Os regardless of the original location of the methyl and hydride ligands. Although the preference for elimination from the octahedral  $\text{Os}^{+2}$  centre is certainly not surprising considering its higher oxidation state and the cis orientation of the methyl and hydride groups on this metal, this reaction illustrates the high mobility of the ligands in this system which allows them to be readily transferred from metal to metal, from terminal to bridging modes, and finally to the appropriate arrangement for the reductive elimination. Once the ligands are in position on Os for elimination, it appears that the adjacent Rh centre makes reductive elimination from Os more favourable, since analogous mononuclear  $\text{Os}^{+2}$  methyl/hydride complexes do not undergo reductive elimination as readily as this binuclear complex.<sup>7</sup> It may be that the Rh centre acts to stabilize the unsaturated intermediate by donating electron density to Os. While the methyl/hydride complex spontaneously rearranges and eliminates at low temperatures, the analogous alkenyl/hydride complexes are stable at room temperature, and only rearrange and reductively eliminate in the presence of CO. This reactivity difference is thought to result from the large size of the vinyl ligands compared to the methyl group. The crystal structure of the closely related trimethylvinyl/methyl complex reveals significant interactions between the vinyl group, the dppm phenyl hydrogens, and the carbonyls. These steric interactions prevent the kind of facile rearrangement seen in

the methyl/hydride system. Dialkyl and vinyl/alkyl complexes of the RhOs system have also been synthesized, but, unlike the alkyl/hydride or alkenyl/hydride complexes, they are unreactive toward reductive elimination. In the RhRu system, however, the dimethyl complex,  $[\text{RhRu}(\text{CH}_3)_2(\text{CO})_3(\text{dppm})_2]^+$  reacts with CO, leading to reductive elimination of acetone. The CO insertion reaction that precedes this elimination is proposed to occur at Ru, since the Os analog is unreactive owing to stronger Os-C bonds.

The structures of the dialkyl, alkenyl/alkyl and alkyl/hydride or alkenyl/hydride complexes are all very similar, with one organic group terminal on Rh and one alkyl group or hydride in a terminal position on Os. Again, the buildup of electron density on Rh is alleviated by semibridging carbonyl interactions, but in these cases two carbonyls bridge, rather than just one as in the monoalkyl complexes. The reason for this appears to be that the octahedral geometry at Os allows two carbonyls to bridge without large distortions, and in fact, the octahedral geometry places the two carbonyls in ideal positions to bridge. In the monoalkyl complexes, bridging of two carbonyls would require significant distortions of the trigonal bipyramidal geometry at Os or Ru.

Insertion reactions into metal-hydride bonds played a key role in the formation of the vinyl and allyl complexes described in this thesis, and these reactions show some interesting features. In the RhOs system, the regioselectivity is such that the metal ends up on the internal carbon of the allene or alkyne, while the hydrogen ends up on the terminal carbon, although the opposite regioselectivity is usually sterically more favourable.<sup>8</sup> In the RhRu system, the regioselectivity is generally the opposite to that of the RhOs system. The regioselectivity in the RhOs system is attributed to steric interactions in the intermediate alkyne/hydride or allene/hydride complexes with the

phosphines on Os, which are believed to be bent towards the hydride ligand. It is notable that the regioselectivity is determined by the geometry at the metal centre adjacent to the metal at which the insertion takes place.

As alluded to above, the chemistry in this system is strongly influenced by the steric effects of the dppm phenyl groups, which essentially restrict the chemistry to the equatorial plane perpendicular to the metal-phosphine vectors. The steric restrictions are likely the reason that certain binding modes were not observed in this system. For example, in no case was a bridging vinyl group observed, although this binding mode is common in related binuclear complexes not bridged by dppm.<sup>9</sup> In addition, the carbene complexes  $[\text{RhOs}(\text{C}(\text{CH}_3)_2)(\text{R})(\text{CO})_3(\text{dppm})_2][\text{BF}_4]_2$  (R=H, **37**; R=CH<sub>3</sub>, **38**) contain terminal carbene groups on Rh, which are much less common than bridging carbenes. The preference for terminal vs. bridging carbenes in this system may be due to steric interactions of the methyl substituents, which in the bridged geometry would be aimed into the region of the dppm phenyl groups. The restriction of the chemistry to a plane may limit the utility of these complexes as model systems for catalysis, by inhibiting some ligand binding modes that may be important on a metal surface. It would therefore be of interest to extend this chemistry to systems in which the steric influences of the bridging diphosphine groups is not as dominant. One obvious solution would be to replace the phenyl groups by smaller methyl groups by using bis(dimethylphosphino)methane (dmpm). Bis dmpm-bridged complexes have much more room in the equatorial plane by virtue of lower steric bulk of the dmpm groups. Another solution would be to use binuclear systems bridged by only one dppm group, again with the effect of cutting down on the steric constraints at the metals.

Our attempts to form methylene complexes of these systems have so far been unsuccessful, although preliminary work suggests that bridging methylene complexes should be accessible. One interesting reaction that came about while attempting to form methylene complexes was the reaction of  $[\text{RhOs}(\text{CO})_4(\text{dppm})_2][\text{BF}_4]$  (**2**) with diazomethane to form  $[\text{RhOs}(\text{CH}_2\text{CH}=\text{CH}_2)(\text{CH}_3)(\text{CO})_3(\text{dppm})_2][\text{BF}_4]$  (**35**). One of the key steps of the Maitlis vinyl mechanism for Fischer Tropsch catalysis is the formation of an allyl group by migration of a vinyl fragment onto a methylene group,<sup>10</sup> and although we have no mechanistic details, the observed reaction could involve such a migration in the final step to form the allyl group. It would be of interest to form unsubstituted vinyl complexes to see if insertion reactions with diazomethane occur, since no reactions with diazomethane were observed for our substituted vinyl complexes. The next step in this Fischer Tropsch mechanism is an allyl-to-vinyl rearrangement, which clearly does not take place in this reaction, since the chain growth stops with the allyl group. Again, it would be of interest to attempt to induce this rearrangement with, for example, acid or dihydrogen. The formation of **35** demonstrates the tremendous potential of these complexes as model systems for catalysis, in that it appears to mimic reactions thought to be taking place on the heterogeneous catalyst. If the individual steps of the reaction could be observed, the reaction could provide insight into the mechanism of the catalytic cycle.

Although bridging methylene complexes were not observed, a series of electrophilic terminal carbenes complexes has been formed by protonation of vinyl and acyl groups. The dimethylcarbene complexes formed by protonation of isopropenyl groups are particularly interesting because carbenes on Rh without heteroatom stabilization are extremely rare.<sup>11</sup> In addition, the carbenes are on unsaturated  $\text{Rh}^{\text{I}}$

centres, which suggests tremendous potential for these complexes, since there is a vacant coordination site available for an incoming substrate such as an alkene. This method of forming carbene complexes by protonating vinyl groups has already been extended to the RhMo system,<sup>2</sup> suggesting possible general applicability of this reaction in forming  $\text{Rh}^{\text{I}}$  carbenes.

This study has demonstrated the great diversity of chemistry possible in a heterobinuclear system. Examples of metal-metal cooperativity have been observed, such as an adjacent  $\text{Os}^{\text{+2}}$  centre allowing elimination of organic fragments from a  $\text{Rh}^{\text{+1}}$  centre, which would be unlikely to undergo reductive elimination on its own, and the  $\text{Rh}^{\text{+1}}$  centre in turn acting to assist the reductive elimination from the Os centre. The different functions of the two different metals have demonstrated, with Rh serving as the site of attack by incoming nucleophiles, while the group 8 metal is the site of reductive elimination, as well as the site attacked by incoming electrophiles. The ability of the bimetallic complexes to use bridging modes to stabilize the metal centres has been demonstrated and ligand movement around the bimetallic core has been shown to be facile. Carbon-carbon bond formation reactions which have relevance to catalysis have been observed in the formation of acetone by CO insertion and reductive elimination in the RhRu system, as well as in the formation of an allyl group from diazomethane in the RhOs system.

The RhRu system has tremendous potential for allowing the elucidation of the functions of the adjacent metals in various processes that are of interest to us, particularly migratory insertion and reductive elimination reactions. We already have preliminary evidence that migratory insertion takes place at Ru, since reacting

$[\text{RhRu}(\text{CH}_3)_2(\text{CO})_3(\text{dppm})_2]^+$  with  $^{13}\text{CO}$  yields acetone with only a small amount of  $^{13}\text{CO}$  incorporation; this suggests (but doesn't prove) that migratory insertion occurs on the metal (Ru) having the carbonyl ligand already bound. It should be relatively straightforward to gain additional mechanistic information on this process through synthesis of the  $[\text{RhRu}(\text{CH}_3)(^{13}\text{CH}_3)(\text{CO})_3(\text{dppm})_2]^+$  species having the  $^{13}\text{CH}_3$  group on Ru. Observation of the intermediate species should yield information about which methyl group undergoes migratory insertion of CO.

The observation of reductive elimination reactions from the group 8 metal centre in these mixed group 8/group 9 mixed metal complexes is probably the most significant discovery of this project, and more work needs to be done to confirm the proposed mechanisms. These studies may ultimately prove to be of great importance in understanding the involvement of the two metals in the formation of ethylene glycol catalyzed by mixtures of Rh and Ru complexes.<sup>12</sup> Furthermore, BP Chemicals has recently reported a process, now in use, by which methanol carbonylation utilizes an Ir catalyst and Ru promoters.<sup>13</sup> It is tempting, based on the results of this thesis, to suggest that similar alkyl migrations from Ir to Ru occur in this system, followed by elimination from Ru. Work within this group will soon turn to analogous dppm-bridged IrRu systems.

Unfortunately, my part in this project must come to an end with many questions left unanswered. Much of the most interesting work was done near the end of my time here, and it seems like the project has just begun. The chemistry was at times very frustrating, but it was certainly never boring. I wish luck to those who will follow the trail I've blazed and who will open up new, unexplored territory. Watch out for the bears.

**References**

1. Graham, T.; Cowie, M. unpublished results.
2. Graham, T.; Van Gastel, F.; Cowie, M., manuscript in preparation.
3. Wang, L.-S., Cowie, M. *Can. J. Chem.*, **1995**, *73*, 1058.
4. Antonelli, D. M.; Cowie, M. *Organometallics*, **1992**, *10*, 1297.
5. Antwi-Nsiah, F. H.; Oke, O.; Cowie, M. *Organometallics*, **1996**, *15*, 1042.
7. (a) Carter, W. J.; Kelland, J. W.; Okrasinski, S. J.; Warner, K. E.; Norton, J. R. *Inorg. Chem.* **1982**, *21*, 3955.  
(b) Carter, W. J.; Okrasinski, S. J.; Norton, J. R. *Organometallics*, **1985**, *4*, 1377.
8. Lobach, M.I.; Kormer, V.A. *Russian Chemical Reviews* **1979**, *48*, 758.
9. (a) Knox, S. A. R. *J. Organomet. Chem.* **1990**, *400*, 255.
10. Maitlis, P. M.; Long, H. C.; Quyoum, R.; Turner, M. L.; Wang, Z-Q. *Chem. Commun.* **1996**, 1.
11. (a) Schwab, P.; Werner, H. *J. Chem. Soc., Dalton Trans.* **1994**, 3415. Schwab, P.;  
(b) Mahr, N.; Wolf, J.; Werner, H. *Angew. Chem., Int. Ed. Engl.* **1994**, *33(1)*, 97.
12. Dombek, B. D. *Organometallics*, **1985**, *4*, 1707.
13. Garland, C. S.; Giles, M. F.; Sunley, J. G. (BP Chemicals Ltd.) Eur. Pat. Appl. EP 643, 034.